UTS UNIVERSITY OF TECHNOLOGY SYDNEY

A Multi-trait Approach To Evaluate Success In Coral Restoration Efforts On The Great Barrier Reef

by Carmela Isabel Nuñez Lendo

Thesis submitted in fulfilment of the requirements for the degree of

PhD by Research

under the supervision of Prof. David Suggett and Dr. Emma Camp

University of Technology Sydney
Faculty of Science

February 2024

Certificate of original authorship

I, Carmela Isabel Nuñez Lendo, declare that this thesis, is submitted in fulfilment of the requirements for the award of Doctor of Philosophy, in the Faculty of Science at the University of Technology Sydney.

This thesis is wholly my own work unless otherwise referenced or acknowledged. In addition, I certify that all information sources and literature used are indicated in the thesis.

This document has not been submitted for qualifications at any other academic institution.

This research is supported by the Australian Government Research Training Program.

Signature:

Production Note:
Signature removed prior to publication.

Carmela Isabel Nuñez Lendo

Date: 27th of February 2024

Thesis Acknowledgements

My PhD journey has been a very enriching experience for which I am incredibly grateful. I have been fortunate to work in unique places and interact with very passionate people. In doing this, I had the opportunity to know more about myself, understand who I am, and define the vision of myself that I want to achieve.

During this time, I have been so lucky to have knowledgeable supervisors who are world leaders in coral research. Firstly, I would like to thank Prof. David Suggett for trusting me and giving me the chance to embark on a PhD under his supervision. I still remember the excitement from our first online meeting; he was in Port Douglas (Australia), and I was, at the time, in Mo'orea (French Polynesia). We both were very much looking forward to working together. I am also grateful to my other supervisor, Dr. Emma Camp, who gave me a warm welcome to the team the first time I met her. Thanks for showing me how to run on-site experiments 55 km offshore on the Great Barrier Reef on a very tight schedule with all the stress this takes. These learnings reinforced my confidence; I consider those experiences as life presents.

I wish to thank the past, present, and emerging Gadigal of the Eora Nation, Yidinji, Gunggandji, Yirrganydji, and Kuku Yalanji Traditional Owners of the land and sea country where my research took place. Also, to the past and current members of the Future Reefs Research Group, it has been so inspiring to see the diversity of people who share a common passion; #lovecoral. Thank you to Dr. Dave Hughes (great mentor with great humour), Dr. Trent Haydon (so funny and knowledgeable), Dr. Chloë Boote (best fieldwork "wife"), Dr. Matthew Nitschke (so clever!), Dr. Samantha Goyen (doing science with you is so much fun), Dr. Jennifer Matthews, Dr. Unnikrishnan Kuzhiumparambil, Dr. Mickael Ros, Dr. Rachel Alderdice, Dr. David Clases, Dr. Raquel Gonzalez de Vega, Caitlin Younis (thank

you for being yourself!), Amanda Grima (the kindest in the field!), Paige Strudwick, Sage Fitzgerald; Wavelength crew including John and Jenny Edmondson, Lorna Howlett, Christine Roper, Tahn Miller, and Daniela Berenice. Also, thanks to Alicia McArdle and Freda Nicholson (Mars Sustainable Solutions); Eric Fisher, Tessa Concannon, and Justin Bovery-Spencer (from Reef Magic and GBR Biology), and Climate Change Cluster and Faculty technical staff; Paul Brooks, Erin Lockhart, Scott Allchin, Kun Xiao, Helen Price, Rachel Keeys, Susan Fenech, Herbert Yuan, Taya Lapshina, Penny McCracken, and Alexander Angeloski.

A huge thank you to my family. Mum, you are the first one who believed in me and supported me to keep my light on. Thanks for all your prays and patience. Dad, thank you for inspiring me with your “ocean life” memories. A special thank you to my “mirror sister”, Susana, the one who has been my confidant and life coach and has been and is always available for my “SOS call”. To my little sister (not so little now), I am truly grateful to you, Laura — you came all the way from Spain to be with me in the final countdown just before submitting my PhD thesis. You brought the Spanish sunlight with you these days. My warmest gratitude to Maria Luisa for all her prayers in this last sprint before submission, and Joaquín (my brother-in-law) and Han for all their unconditional support in my ups and downs. Thank you to my best friend and personal cheerleader in Australia, Francisco Presas, and remotely from Spain, my best friend, Cristina Mestre. Thanks also to Eva Fernandez for all the advice on navigating the PhD journey and to my bestie in Australia, my dear Katy Horan, who taught me how to enjoy “Les petits plaisirs de la vie”.

Lastly, I would like to quote Snoop Dogg’s speech, as it describes how I feel: “Last but not least, I want to thank me; I want to thank me for believing in me; I want to thank me for doing all this hard work, I want to thank me for having no days off; I want to thank me for

never quitting; I want to thank me for always being a giver, and trying to give more than I receive; I want to thank me for trying to do more right than wrong; I want to thank me for just being me at all times".

Table of Contents

List of Figures

density (I-K, µg cm^{-2}), and chlorophylls ratio (L) of the initial wild colonies (WT0) and wild and nursery corals from 12 months propagation (WT12 and NT12). All data are fragments of *Acropora* cf. *hyacinthus* (n = 6 for all groups except for E-L WT0, n = 4). Means were compared by RM-ANOVA (A-D), ANOVA (E-L, except for H), and Kruskal-Wallis (H) with *post hoc* tests (see main text) where ns indicates no statistical significance, and * and ** indicates $p \leq 0.05$ and 0.01, respectively.

Figure 2.4 Mean (± SEM) of metabolic traits for wild and nursery corals. (A) gross and (B) net photosynthesis, and (C) respiration rates (P_G, P_N, and R, respectively; µmol O_2 cm^{-2} h^{-1}), (D) P_G:R ratio, (E) light and (F) dark calcification rates (G_L and G_D, respectively; µmol $CaCO_3$ cm^{-2} h^{-1}), and (G) G_L:G_D ratio of the initial wild colonies (WT0) and wild and nursery corals from 12 months propagation (WT12 and NT12). All data are fragments of *Acropora* cf. *hyacinthus* (n = 6 for each group). Means were compared by one-way (repeated measures) analysis of variance (ANOVA) with *post hoc* Tukey tests, except for (G) (Kruskal-Wallis's test followed by Dunn's test) (see main text) where ns indicates no statistical significance, and * and ** indicates $p \leq 0.05$ and 0.01, respectively.

Figure 2.5 Mean (± SEM) of energetic traits for wild and nursery corals. (A) carbohydrates, (B) soluble proteins, and (C) total lipids (mg per dry mass), (D) total energy reserves (J per dry mass), (E) dry weight and (F) ash-free dry weight biomass (mg DW and mg AFDW per surface area, respectively) of the initial wild colonies (WT0) and wild and nursery corals from 12 months propagation (WT12 and NT12). All data are fragments of *Acropora* cf. *hyacinthus* (n = 4, 6, and 6 for WT0, WT12, and NT12, respectively). Means were compared by analysis of variance (ANOVA) with *post hoc* Tukey tests (see main text) where ns indicates no statistical significance, and * and ** indicates $p \leq 0.05$ and 0.01, respectively.

Figure 2.6 Mean (± SEM) of elemental traits for wild and nursery corals. (A) C:N, (B) C:P, and (C) N:P ratios (C, carbon; N, nitrogen, and P, phosphorus; atomic values) of the initial wild colonies (WT0) and wild and nursery corals from 12 months propagation (WT12 and NT12). All data are fragments of *Acropora* cf. *hyacinthus* (n = 4, 6, and 6 for WT0, WT12, and NT12, respectively). Means were compared by analysis of variance (ANOVA) with *post hoc* Tukey tests (see main text) where ns indicates no statistical significance, and * and ** indicates $p \leq 0.05$ and 0.01, respectively.

Figure 2.7 Mean (± SEM) of skeletal traits for wild and nursery corals. (A) bulk volume (cm^3), (B) bulk density (g cm^{-3}), (C) biomineral density (g cm^{-3}), (D) pore volume (cm^3), (E) apparent (internal) porosity (%), (F) hardness (HD), and (G) colony mass per area (g cm^{-2}) of the initial wild colonies (WT0) and wild and nursery corals from 12 months propagation (WT12 and NT12). All data are fragments of *Acropora* cf. *hyacinthus* (n = 6 for each group). Means were compared by one-way (repeated measures) analysis of variance

(ANOVA) with *post hoc* Tukey tests (see main text) where ns indicates no statistical significance, and * indicates $p \leq 0.05$.

Figure 2.8 Principal Component Analysis (PCA) of 14 (out of 90) coral traits comparing initial wild colonies (W0; triangles in orange) and wild and nursery corals from 12 months propagation (W12 and N12; squares and circles in pink and green, respectively). PCA biplot, including a cut-off for the cos2 = 0.5, where > 0.5 (in solid line) indicates a good representation of the variable on the PC. As opposed, < 0.5 (dashed line) indicates that the variable is not perfectly represented by the PCs. BD and MM refer to biomineral density and methyl arachidat, respectively.

Figure 3.1 Map of study site on Mojo, Opal Reef, Great Barrier Reef, Australia. Corals were collected from the reef patch adjacent to the coral nursery at 5-6 m in depth. Coral fragments were held on the coral nursery, which is located on the sand patch, suspended at 4–5 m in depth. Delineation of the management zones for Opal Reef is shown. Satellite image: Landsat 8 OLI, bathymetric composite RBG bands 431, acquired September 5th, 2021. Source: NASA/USGS/Pearce, S. 2021.

Figure 3.2 Schematic experimental setup for the Coral Bleaching Automated Stress System (CBASS). A) Fragments of six coral colonies from two coral groups (donor and their nursery-derived corals) were subjected to an 18 h short-term acute heat stress assay (CBASS), run at control (31 °C), medium (34 °C) and high (37 °C) temperatures. To note, fragments from each coral colony were exposed to each temperature treatment. B) Targeted temperature profiles for the acute heat stress assay (CBASS). The graph shows the ambient temperature (31 °C) in February 2021 before exposing the corals to target experimental temperatures of 34 °C and 37 °C. Asterisk indicates the time point (T_{end}) of dark-adapted photosynthetic efficiency measurements together with coral sampling. Additionally, photosynthetic efficiency measurements were taken before starting the experiment (T_0) and after 4.5 h as a check control to ensure the corals held in the CBASS were still alive. Dashed vertical lines designate the start and end of the heating hold.

Figure 3.3 Thermal tolerances of donor (wild) and 12-months-propagated *Acropora* cf. *hyacinthus* (nursery) in Opal Reef (the northern Great Barrier Reef). Maximum quantum yield of photosystem II (F_v/F_m) at the final time point (T_{end}) fitted to log-logistic, dose response curves. Curve fits were used to determine the F_v/F_m ED50 for each coral group (vertical lines), which represent the x-value (in temperature) at the inflection point of the curve where F_v/F_m values in the model fit were 50% lower in comparison to the initial values of the model.

Figure 3.4 Photobiological performance under heat stress of donor (wild) and 12-months-propagated *Acropora* cf. *hyacinthus* (nursery). Mean (± SEM) (A) dark-adapted photosynthetic efficiency (F_v/F_m), (B) symbiont cell density (cells x 10^6 cm^{-2}), (C) total pigments, (D) chlorophyll *a* and (E) *c2* density (C-E, µg cm^{-2}), and chlorophylls ratio (F) of donor (wild, in blue) and 12-months propagated *Acropora* cf. *hyacinthus* (nursery, in yellow)

at different heat stress temperatures. All data are fragments of *Acropora* cf. *hyacinthus* (n = 6 for each coral group and temperature treatment). Means were compared by RM-ANOVA (A-F), ANOVA with *post hoc* tests (see main text) where ns indicates no statistical significance.

Figure 4.1 Moore Reef study sites. In February 2021, (A) Natural healthy-looking representative neighbouring reef with high coral cover (positive control, 'PC') (B) View of a 11-year-old rubble field, created by Cyclone Yasi without rehabilitation (negative control, 'NC') (C) Stabilisation reef plot, showing the Reef Stars structures holding corals of opportunity (4 months post-installation). Approximately 11 months later (December 2021), same reef sites 'PC', 'NC', and 'E' (D-F). Note the high coral cover observed on the Reef Stars in the intervened rubble site 'E'. Credits: Nuñez Lendo, C.I., and Mars Sustainable Solutions.

Figure 4.2 Schematic view of the methodology used to estimate coral reef carbonate budgets on the three studied Moore Reef sites. Our study was based on the Reef Budget methodology from Perry et al., (2012). Positive and negative contributions to reef accretion (production and erosion, respectively) are visualised. Specifically, net carbonate production [**Equation 1**], gross carbonate production [**Equation 2**], and gross bioerosion [**Equation 3**], and the main contributors to production and erosion processes,. Credits: Nuñez Lendo, C.I.

Figure 4.3 Average hard coral cover and rugosity. (A) Hard coral cover (%) and (B) rugosity index were estimated following the Reef Budget methodology (Perry et al., 2012) at the three studied sites, (i) Reef Stars (Experimental, 'E'), (ii) a rubble patch (negative control, 'NC'), and (iii) a non-intervened healthy-looking representative neighbouring reef zone (positive control, 'PC') in February 2022 (16 months post-deployment of the Reef Stars). Means (n = 3 per reef site) (± SEM; standard error of the mean) were compared by analysis of variance (ANOVA) with *post hoc* Tukey tests (see main text) where **, ***, and **** indicate $p \leq 0.01$, 0.001, and 0.0001, respectively.

Figure 4.4 Average (A) net and (B) gross carbonate production, and (C) gross bioerosion expressed in kg $CaCO_3\ m^{-2}\ yr^{-1}$ (following the Reef Budget methodology, Perry et al., 2012) across Moore Reef studied sites, (i) Reef Stars (Experimental site, 'E'), (ii) the negative control 'NC' constituted of unconsolidated coral rubble substrate, and (iii) the positive control 'PC' represented by a natural healthy-looking neighbouring reef area, in February 2022 (16 months post-installation of the Reef Stars). Means (n = 3 per site) were compared by analysis of variance (ANOVA) with *post hoc* Tukey tests (see main text) where ns indicates no statistical significance, and **, ***, and **** indicate $p \leq 0.01$, 0.001, and 0.0001, respectively.

Figure 4.5 Mean (± SEM) skeletal (A) bulk volume (cm^3), (B) bulk density ($g\ cm^{-3}$), (C) biomineral density ($g\ cm^{-3}$), (D) pore volume (cm^3), (E) apparent (internal) porosity (%), and (F) hardness (HD) of three dominant coral classes (*Acropora intermedia*, *Acropora* rubble, and *Pocillopora damicornis*) across sites: E, NC, and PC). All data are fragments (n = 5 for each group). Means (n = 3 per reef site) were compared by one-way

analysis of variance (ANOVA) with *post hoc* Tukey tests (see main text) where ns indicates no statistical significance, and *, **, and **** indicate $p \leq 0.05$, $p \leq 0.01$, and $p \leq 0.0001$.

Figure 5.1 Schematic representation of some knowledge gaps regarding the impacts of coral reef restoration practices. Continuous arrows indicate traits or metrics that are acknowledged to inform coral reef restoration practices. Dotted arrows accompanied by violet text in capitals show aspects of coral restoration found in minimal studies (or even not considered yet) that have been addressed in the three Chapters of this PhD thesis.

Figure 5.2 Framework to link coral (reef) traits to ecosystem service value. Ecosystem service values are diverse, but they all depend on the healthy functioning and resilience of the coral (reef), which are, in turn, informed through metrics related to coral (reef) functioning and resilience (left side), but also through already identified metrics that relate to ecosystem services (right side). In orange are the metrics studied in this thesis that inform coral (reef) functioning, resilience, and services. Ecosystem service values were initially defined by Woodhead et al., 2019, and expanded through the learnings of this thesis. OA = Ocean Acidification.

Figure 5.3 Emergent properties that define the coral "fitness triangle". Survival ("maintenance"), growth, and reproduction are emergent properties that are underpinned by complex biological machinery formed by functional traits. On the right side, various reproductive metrics for different coral life stages (adult, larva, and juvenile) are shown to be considered for initial screening to reduce the trait space and identify key reproductive metrics for restoration goals.

List of Tables

List of supplementary figures

Figure S2.1 Map of study site on Mojo, Opal Reef, Great Barrier Reef, Australia. Corals were collected from the reef patch adjacent to the coral nursery at 5-6 m in depth. Coral fragments were held on the coral nursery, which is located on the sand patch, suspended at 4-5 m in depth. Delineation of the management zones for Opal Reef is shown. Satellite image: Landsat 8 OLI, bathymetric composite RBG bands 431, acquired September 5th, 2021. Source: NASA/USGS/Pearce, S. 2021.

Figure S2.2 Sea Surface Temperatures (SST, °C) for Opal Reef and Mojo nursery (mean ± SEM, n = 13 and 9 months, respectively). Satellite-derived data (MODIS-aqua) was extracted from the GIOVANNI online system maintained by NASA (https://giovanni.gsfc.nasa.gov/giovanni/). SST were obtained using monthly area-averaging bounded to 145° 53' 53.8''E, 16°12' 23.4''S between February 2020 and February 2021 (encompassing the entire Opal Reef of ca. 30 km^2 for a year); black line. Imposed onto the SST are the mean monthly SST recorded by the HOBO logger (every 1 h) from February to September 2021 at the Mojo nursery; dashed line.

Figure S2.3 A) Mean (± SEM) relative linear growth rate (% growth in cm yr^{-1}) of wild and nursery corals from 12 months propagation. All data are fragments of *Acropora* cf. *hyacinthus* (n = 6 for both groups). Means were compared by paired Student's t-tests (see main text) where ** indicates a statistical significance of $p \leq 0.01$. B) Nursery-grown coral derived from colony #1 with an initial area of 64.3 cm^2 in February 2020 (B) and 12 months post-fragmentation the same nursery coral was six times higher (394.8 cm^2) compared to its initial size (C).

Figure S2.4 Bio-physical colouration of wild and nursery corals. Traits encompass (a) red (R), b) green (G), (c) blue (B), (d) hue, (e) saturation, (f) brightness, and bleaching state. Significant differences in the RGB values among coral groups were revealed by a one-way RM ANOVA ($F_{(1.9,9.5)} = 7.5$, $p = 0.0114$ for R; $F_{(1.8,8.8)} = 7.6$, $p = 0.0137$ for G; and $F_{(1.3,6.7)} = 21.0$, $p = 0.0021$ for B). Tukey's test revealed significant differences between WT12 and NT12 ($p = 0.0247$, 0.0126, and 0.0215 for R, G, and B, respectively), suggesting a different colouration between these two coral groups. Additional differences in B values among WT0 vs WT12, and WT0 vs NT12 ($p = 0.0317$ and 0.0077, respectively) were also found. Hue values were approximately doubled for WT0 (85.2 ± 44.4, n = 6) compared to WT12 (34.8 ± 1.2, n = 6) and NT12 (39.5 ± 6.5, n = 6). However, no significant differences in hue levels were detected among coral groups (one-way RM ANOVA, $F_{(1.5,7.7)} = 0.2$, $p = 0.7972$). Regarding the saturation levels, they approximately halved in WT0 (33.3 ± 4.4, n = 6) compared to WT12 and NT12 (70.0 ± 4.6, and 64.7 ± 3.6, respectively; n = 6), and significant differences were found among coral groups (one-way RM ANOVA, $F_{(1.9,9.3)} = 19.0$, $p = 0.0006$). Tukey's test showed significant differences for WT0 vs WT12 ($p = 0.0029$) and WT0 vs NT12 ($p = 0.0113$). In general, brightness values were low among coral groups 41.7 ± 3.7, 54.5 ± 2.4, and 38.0 ± 2.2 for WT0, WT12, and NT12, respectively (n = 6 for each

coral group). Significant differences in brightness levels were found (one-way RM ANOVA, $F_{(2.0,9.9)} = 8.0$, $p = 0.0087$), and Tukey's test revealed to be between WT12 vs NT12 ($p = 0.0257$). Statistical significance is shown as ns (no statistical significance), * and ** ($p \leq 0.05$ and 0.01, respectively).

Figure S2.5 Predicted ITS2 type profiles for wild and nursery corals. Corresponding samples are visualised as a stacked bar chart with a single column representing a sample. The relative abundance of predicted ITS2 type profiles is plotted for each column in the stacked bar plots. All data are fragments of *Acropora* cf. *hyacinthus* (n = 4, 6, and 6 for W0, W12, and N12, respectively).

Figure S2.6 Mean (± SEM) (a) carbohydrates, (b) soluble proteins, and (c) total lipids (mg per ash-free dry mass), and same biomolecule content normalised to mg per surface area (d-f) of the initial wild colonies (WT0) and wild and nursery corals from 12 months propagation (WT12 and NT12). All data are fragments of *Acropora* cf. *hyacinthus* (n = 4, 6, and 6 for WT0, WT12, and NT12, respectively). Means were compared by analysis of variance (ANOVA) with post hoc Tukey tests (see main text) where ns indicates no statistical significance, and * and ** indicates $p \leq 0.05$ and 0.01, respectively.

Figure S2.7 Mean (± SEM) of 19 fatty acid methyl esters (mg per dry mass) (A-S) of the initial wild colonies (WT0) and wild and nursery corals from 12 months propagation (WT12 and NT12). All data are fragments of *Acropora* cf. *hyacinthus* (n = 4, 6, and 6 for WT0, WT12, and NT12, respectively). Means were compared by analysis of variance (ANOVA) with post hoc Tukey tests (see main text) where ns indicates no statistical significance, and *, ** and *** indicates $p \leq 0.05$, 0.01 and 0.001, respectively.

Figure S2.8 Mean (± SEM) of (a) saturated fatty acids (SFA), (b) mono- and (c) poly-unsaturated fatty acids (MUFA and PUFA, respectively) (µg per dry mass) of the initial wild colonies (WT0) and wild and nursery corals from 12 months propagation (WT12 and NT12). All data are fragments of *Acropora* cf. *hyacinthus* (n = 4, 6, and 6 for WT0, WT12, and NT12, respectively). No significant differences in SFA were found (one-way ANOVA, $F_{(2,13)} = 3.8$, $p = 0.0501$), however, differences in MUFA and PUFA were detected among coral groups ($p = 0.0324$ and 0.0099, respectively). Tukey's test revealed significant differences between WT0 and NT12 ($p = 0.0287$ and 0.0080, respectively). Statistical significance is shown as ns (no statistical significance), * and ** ($p \leq 0.05$ and 0.01, respectively).

Figure S2.9 Mean (± SEM) of 18 elements, (A) Carbon [C], (B) Nitrogen [N], (C) Magnesium [Mg], (D) Phosphorus [P], (E) Sulphur [S], (F) Potassium [K], (G) Calcium [Ca], (H) Vanadium [V], (I) Manganese [Mn], (J) Iron [Fe], (K) Nickel [Ni], (L) Copper [Cu], (M) Zinc [Zn], (N) Strontium [Sr], (O) Molybdenum [Mo], (P) Cadmium [Cd], (Q) Tim [Sn], and (R) Lead [Pb] — macronutrients (A-G) and micronutrients (H-R) in mmol or µmol (element) per dry mass, respectively; absolute values — of the initial wild

colonies (WT0) and wild and nursery corals from 12 months propagation (WT12 and NT12). All data are fragments of *Acropora* cf. *hyacinthus* (n = 4, 6, and 6 for WT0, WT12, and NT12, respectively). Means were compared by analysis of variance (ANOVA) with post hoc Tukey tests, except for Cd and Pb (Kruskal-Wallis's test followed by Dunn's test) where ns indicates no statistical significance, and * and ** indicates $p \leq 0.05$ and 0.01, respectively. Cobalt [Co] and Selenium [Se] values were negligible and hence not shown here.

Figure S2.10 Examination of the traits per biological property. 1) Principal Component Analysis (PCA) biplot, including a cut-off for the cos2 = 0.5, and 2) the contribution of variables to dimensions (principal components, PC) 1 and 2, for the following seven biological properties: (A) physical appearance (tissue colouration), (B) photobiology, (C) metabolism, (D) energy reserves, (E) fatty acid methyl esters (FAME), (F) elementome, and (G) skeletal properties. In regard to the cut-off for the cos2 = 0.5, a good representation of the variable on the PC is indicated in solid line (> 0.5). As opposed, < 0.5 (dashed line) indicates that the variable is not perfectly represented by the PCs. (H) Contribution plot for the 14 (out of 90) selected traits used in the final PCA (the so-called multitraits).

Figure S3.1 Sea Surface Temperatures (SST, °C) for A) Opal Reef and Mojo nursery (mean ± SEM, n = 13 and 9 months, respectively) and for B) the Northern Great Barrier Reef (GBR), and C) physical parameters during the 2020 bleaching event on the GBR. A) Satellite-derived data (MODIS-aqua) was extracted from the GIOVANNI online system maintained by NASA (https://giovanni.gsfc.nasa.gov/giovanni/). SST were obtained using monthly area-averaging bounded to 145° 53' 53.8''E, 16°12' 23.4''S between February 2020 and February 2021 (encompassing the entire Opal Reef of ca. 30 km^2 for a year); black line. Imposed onto the SST are the mean monthly SST recorded by the HOBO logger (every 1 h) from February to September 2021 at the Mojo nursery; dashed line. B) Temperature, wind, salinity and ocean currents on the GBR for the month of March 2020 when the mass bleaching event occurred (based on the 4 km eReefs Hydrodynamic model https://ereefs.aims.gov.au/. C) Two-year time series graphic of the 5 km product of SST, Degree Heating Week (DHW) and bleaching alert from NOAA Coral Reef Watch (CRW) (https://coralreefwatch.noaa.gov/).

Figure S3.2 Maximum quantum yield of photosystem II (F_v/F_m) measurements in response to temperature treatment for each coral individual (1-6) across coral groups. Measurements were taken at at the initial, middle, and final time points (T_0, T_{mid}, and T_{end}, respectively). Circles refer to nursery corals and triangles to their wild donors. Individual measurements (corresponding to each coral individual) are plotted according to the colour legend. Donor and 12-months-propagated *A.* cf. *hyacinthus* are referred as wild and nursery, respectively, in the graph. The mean ± the standard error of the mean (SEM) of each coral individual is represented by a black circle (nursery) or triangle (wild) in each time point and temperature treatment.

Figure S3.3 Thermal tolerances of donor and 12-months-propagated *Acropora* cf. *hyacinthus* in Opal Reef (the northern Great Barrier Reef). Maximum quantum yield of photosystem II (F_v/F_m) measurements at the final time point (T_{end}) fitted to log-logistic dose-

response curves. Dotted lines represent 95% confidence intervals. Curve fits were used to determine the Fv/Fm ED50 for each coral group (vertical lines), which represent the x-value (in temperature) at the inflexion point of the curve where F_v/F_m values in the model fit were 50% lower in comparison to the initial values of the model. Donor and 12-months-propagated *A.* cf. *hyacinthus* are referred as wild and nursery, respectively, in the graph.

Figure S3.4 Bio-physical colouration of donor and 12-months-propagated *A.* cf. *hyacinthus* during the Coral bleaching automated stress systems (CBASS). Traits encompass (a) red (R), b) green (G), (c) blue (B), (d) brightness, (e) hue, (f) saturation, and (g) bleaching state. Donor and 12-months-propagated *A.* cf. *hyacinthus* are referred as wild (ib blue) and nursery (in yellow), respectively (n = 6 for each coral group). Graphs show only the two-way RM ANOVA test of environment (i.e., coral group). See **Table S3.4** for the results of the two-way RM ANOVA test of temperature and interaction. No significant differences in the RGB values among coral groups were revealed by a two-way RM ANOVA test of environment ($F_{(1.0,5.0)}$ = 1.280, p = 0.3093 for R; $F_{(1.0,5.0)}$ = 0.6242, p = 0.4653 for G; and $F_{(1.0,5.0)}$ = 0.6265, p = 0.4645 for B). Furthermore, no significant differences in brightness, hue, and saturarion levels, and bleaching state were detected among coral groups (two-way RM ANOVA test of environment ($F_{(1.0,5.0)}$ = 1.486, p = 0.2773 for brightness; $F_{(1.0,5.0)}$ = 0.03441, p = 0.8601 for hue; $F_{(1.0,5.0)}$ = 0.03441, p = 0.8601 for saturation; and ($F_{(1.0,5.0)}$ = 0.6897, p = 0.4441 for bleaching state). Statistical significance is shown as ns (no statistical significance).

Figure S4.1 Diagram of a Mars Assisted Reef Restoration System (MARRS) Reef Star. The Reef Stars are hexagonal-shaped structures made of reinforcing steel rod and rust-protected with a double coating (first fibreglass resin and then coarse beach sand or limestone). The perimeter of the Reef Star's hexagon is 216 cm, covering an area of 0.337 m^2. The Reef Star is elevated by six 'legs' (each 15.6 cm), and the highest point above the reef substrate is 28 cm (in the middle of the Reef Star). Extracted from Williams et al., (2019).

Figure S4.2 Map of MARRS study site on Moore Reef, Great Barrier Reef, Australia. The location (~ 2,000 m^2) targeted for restoration is an area divided into three zones (30 x 20 m), and each site is marked with star pickets at the corners, which correspond to a stabilised substrate section using the MARRS Reef Stars (Experimental, E). Two nearby sites, a rubble patch where no Reef Stars were deployed and that act as a negative control (NC), and a non-intervened healthy-looking neighbouring reef area that has not been influenced by cyclones and possesses high coral cover and diversity (positive control, PC). Extracted from the Operational Procedure for Reef Star installation, maintenance and monitoring (GBR Biology, 2021).

Figure S4.3 Sea Surface Temperatures (SST, °C) for Moore Reef (mean ± SEM; standard error of the mean, n = 13 and 8 months, respectively). Satellite-derived data (MODIS-aqua) was extracted from the GIOVANNI online system maintained by NASA (https://giovanni.gsfc.nasa.gov/giovanni/). SST were obtained using monthly area-averaging bounded to 146° 14' 40.9''E, 16°51' 59.0''S between February 2021 (Reef Stars' first

monitoring) and February 2022 (16 months post-deployment of the Reef Stars), encompassing the entire Moore Reef of ca. 30 km^2 for a year; black line. Imposed onto the SST are the mean monthly SST recorded by the HOBO logger (every 1 h) from February 2021 to February 2022 at the Moore Reef; dashed line.

Figure S4.4 Average benthic cover (%). Benthic cover of major functional categories, including hard coral, crustose coralline algae (CCA), sediment producers, soft corals, macroalgae, turf, rubble, rock, limestone pavement, sand, and others, was estimated following the Reef Budget (Perry et al., 2012) at the three studied sites, (i) Reef Stars (Experimental, 'E'), (ii) a rubble patch (negative control, 'NC'), and (iii) a non-intervened healthy-looking representative neighbouring reef zone (positive control, 'PC') in February 2022 (16 months post-deployment of the Reef Stars).

Figure S4.5 Mean (± SEM) (A) survivorship (%), relative linear and areal growth rate (% growth in cm and cm^2 yr^{-1}, respectively), and relative increase in area covered by coral tissue (%) of coral fragments held on the Reef Stars (experimental site, E) for a 12-month period. All data are fragments of *Acropora* spp. (n = 15). Reef Stars' corals derived from star #15 with an initial averaged area of 77.3 cm^2 in February 2021 (B) and 12 months after on the same Reef Star, corals were on average 1.4 times higher (106.4 cm^2) compared to its initial size (C). Note that fragment #9 was three times higher (from 27.6 to 78.6 cm^2) in the same period.

Figure S4.6 Mean (± SEM) (A) macro- and microbierosion, (B) macrobioerosion, (C) microbioerosion, parrotfish (D) bioerosion, (E) density and (F) biomass across Moore Reef studied sites. The three studied sites were (i) the restored site using Reef Stars (Experimental, 'E'), (ii) a rubble field (negative control, 'NC'), and (iii) a non-intervened healthy-looking representative neighbouring reef site (positive control, 'PC') in February 2022 (16 months post-installation of the Reef Stars). Bioerosion rates are expressed in kg $CaCO_3$ m^{-2} yr^{-1}, and density and biomass as abundance or kg $hectacte^{-1}$, respectively. Urchins were not present across sites (0.0 individual/m^2); hence, their bioerosion contribution is not plotted. Means (n = 3 per reef site) were compared by analysis of variance (ANOVA) with post hoc Tukey tests (see main text) where ns indicates no statistical significance, and *, **, ***, and **** indicate $p \leq 0.05$, 0.01, 0.001, and 0.0001, respectively.

List of supplementary tables

Table S2.1 A total of 90 traits were selected for this study. Survival and growth are considered emergent properties. Seven biological properties were investigated to unveil the biological machinery underpinning coral survival and growth: physical appearance (tissue colouration), photobiology, metabolism, energy reserves, fatty acid methyl esters (FAME), elementome, and skeletal properties.

Table S2.2 (A) Contributions of traits to the first (PC1) and second (PC2) principal components (dimensions, Dim.), and (B) cumulative variance percent of PC1 and PC2 of the Principal Component Analysis (PCA) for all coral groups (WT0, WT12, and NT12) for the following seven biological properties: (1) physical appearance (tissue colouration), (2) photobiology, (3) metabolism, (4) energy reserves, (5) fatty acid methyl esters (FAME), (6) elementome, and (7) skeletal properties. Variables not considered in the PCA, followed by a brief rationale, are written in italic font.

Table S2.3 (A) Contributions of traits in the first (PC1) and second (PC2) principal components, and (B) cumulative variance percent of PC1 and PC2 of the Principal Component Analysis (PCA) for all coral groups (WT0, WT12, and NT12) for the following 14 traits: brightness, blue, symbiont cell density, maximum photochemical efficiency of PSII [$F_q'/F_m'_{MAX}$], dark and light calcifications [G_D and G_L, respectively) , total energy reserves, ash-free dry weight biomass (AFDW), methyl arachidate, methyl myristoleate, potassium [K], strontium [Sr], pore volume, and biomineral density (the so-called multitraits).

Table S2.4 Analysis of variance (ANOVA) and post hoc Tukey HSD to compare the extracted ordination axes (A) PC1 and (B) PC2 of **Fig. 8** across coral groups, WT0, WT12, and NT12. Data were assessed for normality. Means were compared by one-way (repeated measures) analysis of variance (ANOVA) with post hoc Tukey tests, where ns indicates no statistical significance, and * indicates $p \leq 0.05$.

Table S2.5 PERMANOVA using Bray-Curtis dissimilarity to compare differences between coral groups (WT0, WT12, and NT12) at "Mojo" site at Opal reef on the Great Barrier Reef.

Table S3.1 Pairwise permutational multivariate analysis of variance (PERMANOVA; perm = 999) on Euclidian distances using the "*vegan*" R package (time point and temperature as fixed variables) for maximum quantum yield of photosystem II (F_v/F_m) measurements. Post hoc pairwise comparisons were conducted using "*pairwiseAdonis*" R package with Bonferroni adjusted p-values. The effects of time point and temperature on F_v/F_m response variable for the start of the experiment (T_0), halfway down the assay (4.5 h, T_{mid}), and after 7 h (T_{end}) for each target temperature (31 °C, 34 °C, and 37 °C) were analysed (e.g., Evensen et al., 2021).

Table S3.2 PERMANOVA for maximum quantum yield of photosystem II (F_v/F_m) measurements (perm = 999) on Euclidian distances using the "*vegan*" R package (coral group as fixed variable) was performed within each time point (T_0, T_{mid}, and T_{end}) to detect differences in F_v/F_m among coral groups and temperature treatments (31 °C, 34 °C, and 37 °C) to (a) record initial photosynthetic efficiencies (T_0) (i.e., to detect any coral group effect on F_v/F_m within their native seawater of 31 °C before starting the CBASS experiment), (b) monitor photosynthetic efficiencies halfway down the experiment (T_{mid}) (i.e., checkpoint control to ensure the continuation of the experiment), and (c) record final F_v/F_m values (T_{end}) (i.e., to report values as per Voolstra et al., (2020) and to calculate the F_v/F_m ED50 metric as a proxy for the thermal tolerance of coral, Evensen et al., (2021). Post hoc pairwise comparisons were conducted using "*pairwiseAdonis*" R package with Bonferroni adjusted p-values.

Table S3.3 Linear mixed-effects models (LME) were used to analyse iindividual response variables, with coral group and temperature as fixed effects, and genotype and tank replicate as random effects to account for any potential genotype or tank effects.

Table S3.4 Statistical analysis for bio-physical colouration and photobiological performance of donor and 12-months-propagated *A.* cf. *hyacinthus* during the CBASS. Mean ± the standard error of the mean (SEM) and N (sample size) alongside a two-way RM ANOVA is reported for (a) red (R), (b) green (G), (c) blue (B), (d) brightness, (e) hue, (f) saturation, (g) bleaching state, (h) maximum photochemical efficiency [F_v/F_m], (i) symbiont density, (j) pigment density (k) chlorophyll *a* and *c2* density. Values were obtained at the end of the 18-h heat stress assay (a-g) and at T_{end} (7 h after the onset of the experiment).

Table S3.5 Statistical comparison of relative potencies between the ED50 dose-response curves. Log-logistic dose-response curves of the donor (wild) and 12-month-propagated *A.* cf. *hyacinthus* (nursery) were compared through the R function "*EDcomp*".

Table S4.1 Coral individuals collected in February 2022 to study their skeletal properties. *Acropora intermedia*, *Acropora* spp. rubble, and *Pocillopora damicornis* are represented in light blue, mid-blue, and orange, respectively. The reef site where the corals were collected from is also provided in the table. Moore Reef studied sites consisted of (i) Reef Stars (Experimental site, 'E'), (ii) the negative control 'NC' constituted of unconsolidated coral rubble mat, and (iii) the positive control 'PC' represented by a natural healthy-looking neighbouring reef area. In detail, fragments (< 5 cm in length) of *A. intermedia*, *P. damicornis* and rubble were collected at each site (n = 5 each) as follows: *A. intermedia* at the E and PC sites, *P. damicornis* at the E, PC, NC sites, and *Acropora* rubble only from the rubble patch (NC site), in February 2022 (16 months post-deployment of the Reef Stars).

Thesis Abstract

Accelerating reef health declines from local and global stressors has catalysed widespread interest in coral reef restoration practices as an active management tool to boost coral reef recovery, and so ensure the persistence of reef ecosystem services. Active interventions have focussed towards coral and/or reef rehabilitation to repopulate endangered coral species and recover coral cover via in-water coral propagation at increasing scale. Coral nursery and out-planting practices have been pioneered throughout the Caribbean, Indo-Pacific, and the Red Sea over the last two decades. In contrast, such practices have only more recently been considered for Australian coral reefs in 2017, following the back-to-back coral bleaching events in 2016–17. In all cases, coral nursery and out-planting practices continue to almost exclusively evaluate "success" from measurements of coral growth and survival over time, metrics that together are fundamental for determining the return-on-effort of any restoration initiative. However, growth and survivorship measurements, in fact, carry limited value to describe "success", notably where other metrics may regulate – and hence better reflect – ecosystem service values of interest. Such a basic appraisal of success has limited our understanding of the impact of coral restoration activities on reef performance, functioning, associated services, and resilience. Consequently, metrics of biological and ecological success are not typically included in restoration efforts studies.

Restoration goals are often centred on maintaining or recovering a functionally healthy and self-sustaining reef ecosystem and its associated service values. Consequently, there remains a vast mismatch between restoration success metrics and goals, as well as uncertainty surrounding how restoration activities may impact coral reefs. To overcome this fundamental gap in knowledge, my thesis was integrated into current Great Barrier Reef (GBR) restoration

activities of the (i) “Coral Nurture Program” (CNP) — the novel tourism-researcher site-stewardship program to up-scale coral propagation and outplanting at high-value tourism sites — and (ii) Mars Incorporated “Mars Assisted Reef Restoration System (MARRS)”, a global organisation that targets the stabilisation of large areas of unconsolidated rubble to locally enhance reef accretion. In the first “multi-trait assessment” of coral nursery propagation success, I demonstrated how coral nurseries are highly effective at rapidly increasing coral biomass, but without potentially impacting traits indicative of essential ecosystem services – notably, biogeochemical cycling and wave attenuation. Further biological and energetic traits that are critical for coral reef functioning (such as trophic transfer or productivity) were well-sustained by nursery propagation. My approach was critical in revealing the biological machinery (and thus functional traits) supporting fast-tracked coral growth through nursery propagation. I subsequently demonstrated that the same nursery corals displayed similar thermal tolerance to their wild donor colonies; as such, bleaching susceptibility was not impacted during nursery propagation despite enhanced energetic investment previously observed into metabolism and growth. Specifically, I consider metrics related to thermal resilience — measured through bio-physical and photo-physiological metrics that inform how thermal stress affects coral performance, functioning, and resilience — to yield a more complete picture of how nursery propagation positively or negatively changes coral fitness. In considering metrics related to traits indicative of an essential ecosystem service, attenuation (i.e., coastal protection), I subsequently demonstrated that MARRS resulted in remarkably enhanced reef accretion (i.e., high net carbonate budget) in a reef with an otherwise poor recovery trajectory over a short period of time (16 months). Moreover, by integrating other metrics related to skeletal properties, I confirmed that species-specific trade-offs in functional traits (e.g., decreased skeletal hardness) could occur when selecting different coral species in restoration activities.

Throughout my thesis, I have therefore resolved the biological and ecological "success" of novel coral restoration efforts on the GBR by developing a holistic multi-trait measurement approach based on a broader range of coral traits beyond survival and growth. I have identified key traits that better describe "success" during coral reef restoration techniques that more meaningfully contribute to desired ecosystem service outcomes. I demonstrate the value of employing a multi-trait-based approach to understand the effectiveness of coral and/or reef restoration practices on coral performance, reef functioning, and the supported services inherent to restoration success. My findings carry widespread applicability to restoration programs aspiring to implement more diverse measures that are ultimately more meaningful descriptors of restoration outcomes.

Chapter 1. General Introduction

1.1. Ecosystem restoration and management

The observed detrimental impacts of anthropogenic climate change on Earth's natural systems and its biodiversity are evident (e.g., Bellard et al., 2012; Foden et al., 2007; Pecl et al., 2017), and current model projections forecast that the magnitude of human impacts across ecosystems is likely to continue to grow over the coming century (Habibullah et al., 2022; Trew and Maclean, 2021). The alteration of biodiversity and functioning of ecosystems through human-driven impacts relate to not only climate change effects, but also pollution, habitat loss, overexploitation and biological invasions (IPCC, 2019a; Ruckelshaus et al., 2020).

In 2019, the Intergovernmental Panel on Climate Change (IPCC) and the Intergovernmental Science-Policy Platform on Biodiversity and Ecosystem Services (IPBES) developed global assessment reports on the current status and direction of the natural world (IPBES, 2019; IPCC, 2019b). Both reports concluded that climate change is a direct and substantial driver of changes in nature, which can interact with and intensify the impacts of other drivers, such as land use, overexploitation, pollution, and invasive species (Bellard et al., 2012; Shin et al., 2019). It also acknowledged that human activity is behind the increase in global temperatures by 1.0 °C compared to pre-industrial levels (Gillett et al., 2021). This shift towards increased temperature has led to a rise in the frequency and intensity of extreme weather events in the past 50 years (including floods, cyclones, and mass coral bleaching events) (Frame et al., 2020; Perkins-Kirkpatrick et al., 2022) as well as a rise in sea level by over 3 mm a year for the last 20 years (Nicholls et al., 2021). These disturbances and changes have heavily altered

species distributions, population and community structure and dynamics, and ecosystem functioning (e.g., Hastings et al., 2020; Jeger, 2022; Peters et al., 2019). Alarmingly, these modifications in natural systems are predicted to accelerate in coming years with climate change, worsening the current status of biodiversity and ecosystem functioning (Nunez et al., 2019; Staudinger et al., 2013; Weiskopf et al., 2020). Among the most impacted regions will be the tropics; their ecosystems, particularly, will face significant declines in biodiversity as a combination of climate change with land use and fisheries exploitation (Das et al., 2022; Kayitesi et al., 2022; Lam et al., 2020). The projected global increase of 1.5-2.0 °C (i.e., the most optimistic shared socioeconomic pathways for emission trajectories SSP1-1.9 and SSP1-2.6, respectively; Riahi et al., 2017) will cause a reduction in the distribution range for most species, including corals, which will increase their likelihood of extinction (i.e., the number of threatened species will increase) (Arneth et al., 2020; Hoegh-Guldberg et al., 2019; Nunez et al., 2019). Attaining low emissions of 1.5 °C is particularly important for the Great Barrier Reef (GBR) as this will translate into a drastic reduction of bleaching events (i.e., 3 events per decade) instead of 5 events per decade under SSP1-2.6 or annually under intensifying emissions (SSP5-8.5) (McWhorter et al., 2022b). However, limiting warming to 1.5-2.0 °C will be extremely difficult, and most of the climatologically identified refugia on the GBR are predicted to be lost after the mid-century when global warming exceeds 3 °C irrespective of emissions scenario (McWhorter et al., 2022a). Local population extinctions have already been reported, and the extinction rate will depend on species' ability to respond to climate change (e.g., abilities to disperse, move to favorable conditions, evolve or adapt; McFadden et al., 2022).

In the face of massive global degradation and destruction of ecosystems, ecological management — and, more recently, restoration — are practised globally as a direct response

(Kleypas et al., 2021). Restorative-based culture has evolved during the past century, as evidenced by increasingly proactive and bold interventions in natural systems (Anthony et al., 2017; van Oppen et al., 2017, 2015) that have been more traditionally managed by (marine) protected areas (Naidoo et al., 2019) and pollution mitigation (Cooper et al., 2019) — how well these traditional approaches work is dependent upon active and dynamic strategies (e.g., Anthony et al., 2017, 2020), including enforcement. The restoration of natural ecosystems is also directly related to achieving several Sustainable Development Goals (SDGs) set by United Nations, such as (i) no poverty, (ii) zero hunger, (iii) good health and well-being, (iv) life below water, (v) life on land, (vi) clean water and sanitation, (vii) responsible consumption and production, and (viii) climate action among others (www.un.org).

Ecological impacts of restoration efforts have enormous potential to improve population health and socio-economic well-being (Aronson et al., 2006; Camp et al., 2020b; Perring et al., 2018). In recognition of the key role of restoration in ecosystem health, on 1 March 2019, the United Nations (UN) General Assembly declared 2021–2030 the "UN Decade of Ecosystem Restoration". This call to action has the mission of recognising the urgent need to up-scale and accelerate global restoration of degraded ecosystems, to counteract the effects of the climate crisis, enhance food security, provide clean water and protect biodiversity on the planet, reinforce food security, provide access to clean water and protect Earth's biodiversity (Waltham et al., 2020). The UN Decade of Ecosystem Restoration also coincides with the "UN Decade of Ocean Science for Sustainable Development", which aims to overturn degradation in ocean health. My PhD thesis is particularly timely, with the UN Ocean Conference (Portugal, 2022) flagging the need for the rapid scientific development of coral restoration activity as we progress through the UN Decade of Ecosystem Restoration Decade

(2021-2030) and the UN Decade of Ocean Science for Sustainable Development (2021-2030).

1.2. Coral reefs at risk

Coral reefs represent one of the most biologically diverse communities on Earth (Reaka-Kudla, 2005), and so provide wide-ranging ecosystem goods and services, from food and resource security to coastal protection and nutrient cycling (Toth et al., 2023; Webb et al., 2023; Woodhead et al., 2019) — but are degrading rapidly at their fastest in history due to cumulative local and global anthropogenic pressures (Cramer et al., 2020; Dietzel et al., 2020). Whilst local stressors such as nutrient run-off (Silbiger et al., 2018) are exacerbated by chronic ocean warming, deoxygenation and acidification under climate change (Suggett and Smith, 2020), of particular concern has been the rise of more frequent and intense tropical cyclones (Cheal et al., 2017; Moon et al., 2019) and "marine heatwaves" that induce mass coral bleaching events (Frölicher et al., 2018; Hughes et al., 2017b). In 2016 and 2017, back-to-back mass bleaching occurred on the GBR, leading to drastic declines in coral cover and an unprecedented shift in coral assemblages (Eakin et al., 2019; Hughes et al., 2018), as well as rapid "reef decay" (Leggat et al., 2019). The GBR experienced the most widespread mass bleaching ever recorded in 2020, with at least 60% of reefs across all three GBR regions affected (GBRMPA, April 7, 2020), and notably the first documented mass bleaching event under La Niña cool conditions in 2022, and so four major events between 2016 and 2022 (AIMS, 2022; Pratchett et al., 2021), driving coral cover to all-time lows (e.g., Hughes et al., 2021, 2017). Even so, such disturbances have changed reef landscapes that, in turn, have impacted their ability to function as healthy ecosystems (Harborne et al., 2017; Williams and

Graham, 2019) and have lowered their resilience (Bahr et al., 2017; Good and Bahr, 2021; Hughes et al., 2003; Montefalcone et al., 2020; Stuart-Smith et al., 2018).

Mitigating the loss of coral reefs by reducing greenhouse gas emissions is imperative; however, projected climate change, in combination with local stressors, will continue to pose a significant threat to tropical coral reefs. Given the poor projected trajectory of coral reefs in the face of climate change, and the potential consequences for the millions of people who depend on them, novel, immediate and more aggressive interventions to "buy reefs time" are being urgently considered and/or implemented (Anthony et al., 2017, 2015; Suggett and Smith, 2020). Until CO_2 emissions can be reduced, stemming the rate of loss via accelerating coral repopulation may ensure the persistence of reef ecosystems and associated ecosystem services (Hein et al., 2021; Hughes et al., 2017a; Kleypas et al., 2021). Despite some succesful cases, conventional conservation approaches such as marine protected areas (MPAs) (Bates et al., 2019; Steneck et al., 2018) and water quality management (Sith et al., 2019) have proven to be insufficient to cope with the reef degradation momentum and maintain reef structure and functionality impacted by climate change stressors (e.g., Hughes et al., 2017b). Thus, past and current management approaches alone simply will not be enough to secure the future of coral reefs (Anthony et al., 2017). A key factor now recently acknowledged by the GBR Marine Park Authority (i.e., the primary management agency for the GBR, GBRMPA) *Reef BluePrint for Resilience*, which has highlighted the need for new adaptive management approaches on the GBR in response to the rapid reef degradation, including "reef restoration" to secure coral biomass, maintain reef functioning, and build reef resilience to the future climate scenario (Great Barrier Reef Marine Park Authority, 2021, 2017). Such recognition aligns with the need to rebuild marine life-support systems, such as coral reefs, and secure their biomass to achieve a more sustainable relationship with nature as

global populations continue to grow (e.g., Duarte et al., 2020); which is the central premise underpinning the UN's Decade of Ecosystem Restoration (2021-2030) (United Nations, 2020).

1.3. Coral reef restoration tools

Reef restoration has increased in both need and popularity in response to the drastic decline in global coral populations (De'Ath et al., 2012; Edmunds and Elahi, 2007; Gardner et al., 2003), and the acknowledgement that, without human intervention, reef recovery will not be possible (Anthony et al., 2017; Suggett and Smith, 2020; van Oppen et al., 2017). Reef restoration can include both proactive and reactive interventions (**Fig. 1.1**). Proactive restoration implies the protection of coral reef habitat to enable natural reef recovery and ameliorate ecological functioning of the coral reef through management actions such as MPAs (Martínez-Rendis et al., 2020; Topor et al., 2019). Conversely, reactive restoration approaches consist of direct interventions to either mitigate a particular stressor that reduces coral survival (e.g., land-based run-off and pollution; Butler et al., 2013) or accelerate repopulation of corals and hence rebuild coral biomass, targeting particular coral traits and processes (e.g., coral cover and growth, coral recruitment; Boström-Einarsson et al., 2020). The last is commonly known as coral restoration, and it is the process of reef restoration that focuses on establishing resilient coral communities (Boström-Einarsson et al., 2020, 2018).

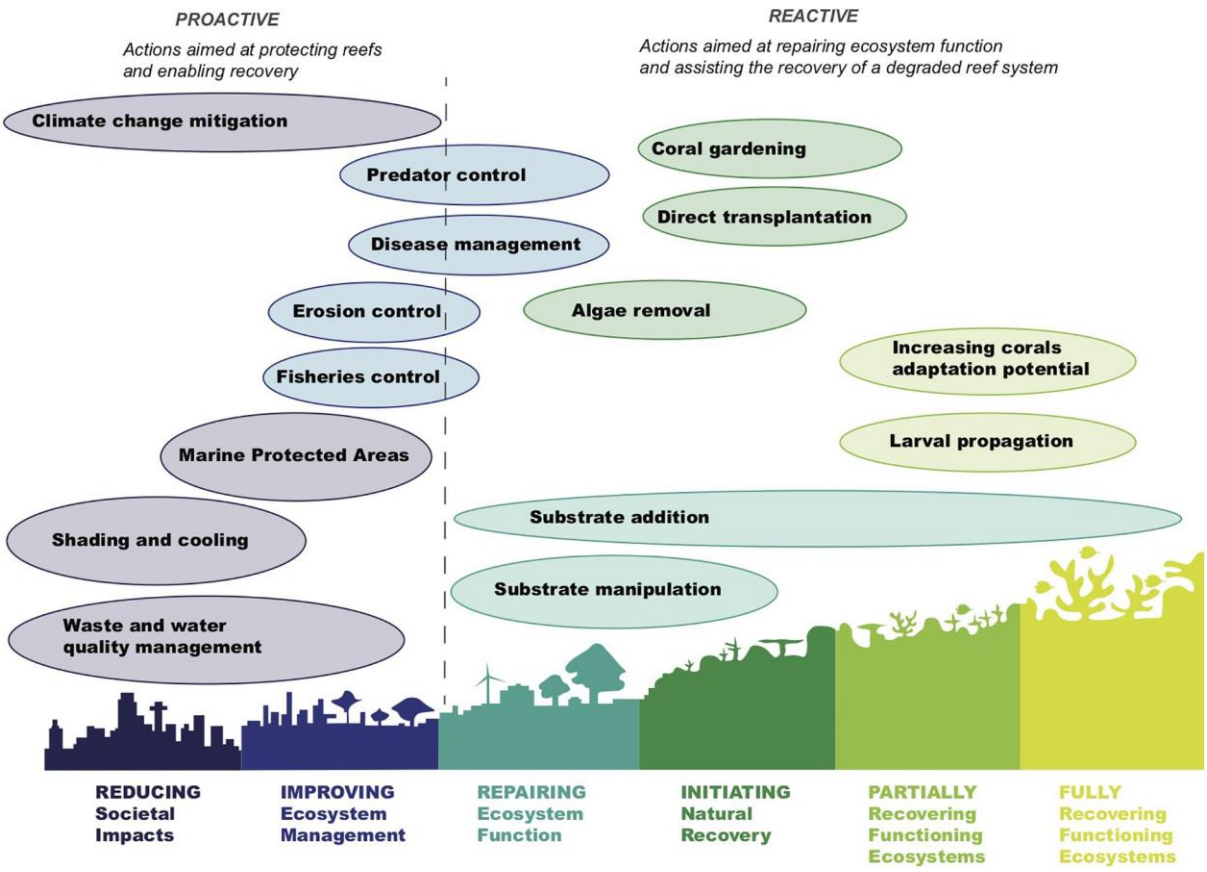

Figure 1.1 Continuum of proactive and reactive actions for coral reef conservation and restoration. Adapted from Society for Ecological Restoration (SER) guidelines (Gann et al., 2019) and extracted from Hein et al., 2021.

Other interventions have focused on substrate stabilisation, such as artificial reefs (Ceccarelli et al., 2020). For example, in Indonesia, following physical damage caused by blast fishing, hexagonal structures made from steel ("Reef Stars") were developed by Mars, Incorporated to stabilise the substrata, resulting in one of the world's largest restored reef efforts, extending over three hectares (Williams et al., 2019). The use of artificial reefs is generally accompanied by direct coral transplantation (Fadli et al., 2012; Ferse, 2008). This is the most common method of coral restoration and consists of the direct transplantation of coral fragments derived from a donor colony to a restoration site. Globally, an average coral survival of 64% was achieved in direct transplantation studies (Boström-Einarsson et al., 2020). Other work has focused on boosting coral growth by electrolysis, where mineral

precipitation on the substratum is facilitated via electricity, and thereby, coral calcification is also promoted (Goreau and Hilbertz, 2012). Interventions have been devised to boost the rate of coral recruitment by directly inoculating coral larvae onto natural substrates ("Larval enhancement"; dela Cruz, 2019) and/or transplanting sexually produced recruits (Chamberland et al., 2015, 2013). In recent years, the development of an innovative approach to increase coral reef resilience by accelerating the natural evolutionary processes ("Assisted evolution"; van Oppen et al., 2017; Van Oppen et al., 2015) has also attracted increasing attention among scientists and practitioners in coral reef conservation. Such interventions are aimed at bioengineering heat-tolerant corals that can face climate change. In 2020, the first coral stock with enhanced thermal resilience was developed through heat-evolved microalgal symbionts (Buerger et al., 2020).

Whilst valid views claim that restoration-based interventions carry limited benefits due to its limited spatial scale (Bruno and Valdivia, 2016; Hughes et al., 2017b), the need by many coastal communities to locally secure coral biomass in the face of climate change has led to many innovative and low-cost — and hence increasingly scalable — methods. For example, improved local coral recovery after a bleaching event by removal of coral predators, such as crown-of-thorns sea stars (COTS) (Birkeland and Lucas, 1990; Muhando and Lanshammar, 2008) or the corallivorous snail *Coralliophila abbreviata* (Shaver et al., 2018). Also, more informed decision-making of coral nurseries (reef sites and species grown) to yield higher coral growth and survival (Suggett et al., 2019), including selection of more "stress-tolerant" coral genotypes (Morikawa et al., 2019). Most of the above-mentioned methods of reef restoration are currently in various stages of development and implementation (Suggett and van Oppen, 2022); most remain in trial "research and development" phases due to their low cost-effectiveness and unlikely deployable for the next five years (Anthony et al., 2019;

Mead et al., 2019). Instead, asexual coral propagation is expanding at local scales and rapidly becoming an approach that can be adopted worldwide and with relatively low-cost effort compared to sexual coral propagation. However, despite many years of coral reef restoration work (Levy et al., 2010; Rinkevich, 2000, 1995; Shafir et al., 2006), many unknowns exist in optimising this process and scaling up to larger reef areas (Suggett and van Oppen, 2022).

1.4. Coral propagation and out-planting

At present, coral propagation and out-planting — historically referred to as "coral gardening" — is the most commonly used coral propagation and restoration method to increase coral cover at individual reef sites (Bowden-Kerby, 2001; B. Rinkevich, 2015; Rinkevich, 1995; Young et al., 2012). It consists of collecting small pieces of coral from healthy wild coral colonies and propagating this collection on *ex situ* (land-based) or *in situ* (field-based) coral nurseries (Epstein et al., 2003, 2001). Once the reared coral fragments have reached a certain size, they can then be transplanted to degraded reefs and serve as a sustainable coral stock for future transplantations (Rinkevich, 2005, 1995).

Coral nurseries and out-planting practices, pioneered throughout the Caribbean, Indo-Pacific, and the Red Sea over the last two decades (e.g., Boström-Einarsson et al., 2018; Clark and Edwards, 1995; Omori et al., 2008; Rinkevich, 2000), have grown into worldwide practices for the restoration of degraded reefs, and recovery of threatened coral species. As such, reef restoration activities in the Caribbean have historically but also continue to focus on relatively few coral species (Greer et al., 2020; Lirman et al., 2010; O'Donnell et al., 2017), but importantly a number of different genetic variants of these species (Calle-Triviño et al., 2020; Lirman et al., 2014; Ware et al., 2020). However, decline in coral cover has been

particularly devastating for Caribbean key reef-builders such as *Acropora cervicornis*, and *A. palmata* (Crabbe et al., 2022; Gardner et al., 2003; Miller et al., 2022). For example, *A. cervicornis* populations have declined by > 95% (Aronson and Precht, 2001; Bruckner, 2002), which has led to low densities and genetic diversity of these coral populations, and hence a reduction in genetic connectivity (Baums, 2008; Vollmer and Palumbi, 2007). In contrast, coral species loss throughout the Indo-Pacific has impacted more complex coral communities, thereby requiring different considerations on how to restore these coral assemblages (Hein et al., 2020a).

Return-on-effort for coral restoration activities (i.e., cost-effectiveness and viability of restoration programs) has been optimised based mainly on the successes and failures from past efforts, in particular, those in the Caribbean (Johnson et al., 2011; Suggett et al., 2019; Young et al., 2012). Undoubtedly, these restoration efforts have generated a wealth of data that can potentially guide future propagation and out-planting practices (Boström-Einarsson et al., 2018). Whilst Indo-Pacific coral propagation has been conducted for over 20 years in various forms (e.g., Fadli et al., 2012; Fox et al., 2003; Shaish et al., 2010; Villanueva et al., 2012), much of the knowledge is unreported in the scientific literature despite other valid reporting methods of knowledge sharing (e.g., Razak et al., 2022). Therefore, many Indo-Pacific locations, such as the GBR, are in their infancy for coral nursery-based reef restoration where no historical data of restoration initiatives exist to tailor practices (e.g., propagation and out-planting efforts) to the local coral taxa and/or reefs (Ladd et al., 2018; Shaver and Silliman, 2017), and hence past and current methods are not directly transferable, creating a large knowledge gap.

Great Barrier Reef coral restoration

The GBR is the world's largest coral reef stretching > 2,000 km comprised of > 2,900 reefs, encompassing a diverse ecosystem with environmental, Indigenous, social, and economic values and uses, such as fishing, tourism, and research (Great Barrier Reef Marine Park Authority, 2019). Such diversity of values and uses, marine landscapes and life (including more than half of the worldwide species of hard corals) make this region one of the most complex natural systems on Earth. Hence, many challenges arise when managing this vast multiple-use area with different features and environments. Historically, coral reef management has focused on decreasing local and regional stressors, such as overfishing, oil and gas mining, coastal development, and poor water quality (e.g., in Beher et al., 2016; MacNeil et al., 2019). A decade ago, COTs control has also become a critical management action on the GBR (Westcott et al., 2020). However, reactive intervention, including coral reef restoration had not been considered as part of Australian coral reef management actions until 2017, following the back-to-back coral bleaching events in 2016–17 and the increase in frequency and intensity of tropical cyclones and COTs outbreaks (Cheal et al., 2017; De'Ath et al., 2012; Hughes et al., 2017b).

Tourism sustains > 90% of the GBR economic value (Great Barrier Reef Marine Park Authority, 2019; Spalding et al., 2017) and therefore represents key stakeholders. In the context of rapidly deteriorating reef health under climate change (Dietzel et al., 2020; Hughes et al., 2019, 2018), and in order to preserve this economy whilst capacity building the tourism industry as better "reef stewards", many operators have turned their interests towards coral propagation at their sites (Suggett et al., 2020, 2019) — and several *in situ* coral nurseries have now been established. The first multi-species coral nursery was approved by the

GBRMPA and installed successfully on Opal Reef, GBR (50–60 km from the mainland) in February 2018 (Suggett et al., 2019) as part of the Coral Nurture Program (www.coralnurtureprogram.org). These underwater structures consist of platforms (2.0 × 1.2 m) deployed at 1–2 m above sand (5–6 m depth) at several reef sites (**Fig. 1.2a**) housing multiple coral species (e.g., Suggett et al., 2019). As of January 2023, over 120 platforms propagating > 2,200 corals (37 species) across 30 key tourism sites are operating alongside already outplanted > 76,600 corals encompassing 68 species. Another type of coral nursery (Coral Tree Nursery©) — commonly used in the Caribbean (Nedimyer et al., 2011; O'Donnell et al., 2017) (**Fig. 1.2b**) was also established in December 2019 (Reef Restoration Foundation, April 19, 2020). However, this technology originally conceived in the Caribbean for propagating branching species of *Acropora* (Nedimyer et al., 2011; O'Donnell et al., 2017) and hence propagates fewer species on the GBR. In 2021, this nursery structure has been deployed at few sites and consists of 20 coral trees (capable of housing around 1,500 coral fragments) (Cook et al., 2022).

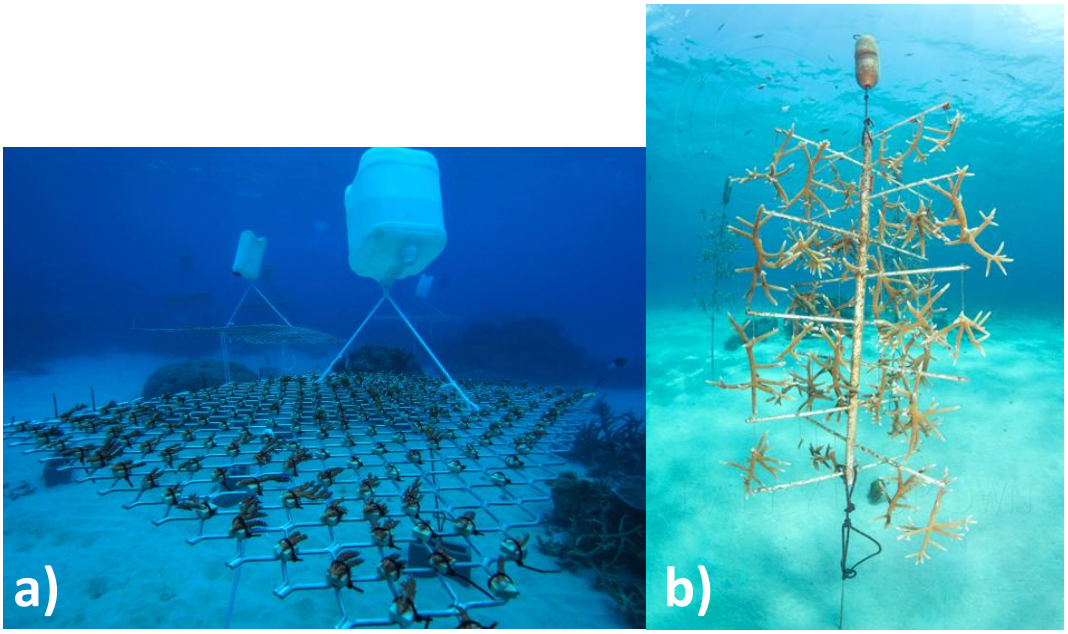

Figure 1.2 a) Opal reef coral nursery (GBR). Novel platform design harbouring 11 coral species from five genera (Suggett et al., 2019). b) Coral Tree Nursery© in the Caribbean holding fragments of one branching coral species, *Acropora cervicornis* (Nedimyer et al., 2011).

Coral nursery and out-planting practices to date almost exclusively evaluate "success" from measurements of coral growth and survival over time (e.g., Hein et al., 2017; Lirman and Schopmeyer, 2016), metrics that together are fundamental for determining the return-on-effort of the restoration initiative (Suggett et al., 2019). However, several studies (Bayraktarov et al., 2017, 2016; Hein et al., 2017; Rinkevich, 2017) have discussed that growth and survivorship carry limited value to describe "success", notably where other factors may affect ecosystem services with a high value of interest. For example, a coral may grow quickly (and therefore be seen to have high "success") but have limited value to coastal protection if the fast growth was underpinned by a weak/porous skeleton.

1.5. Ultimate goals of coral reef restoration

Reactive coral restoration currently aims to establish self-sustaining coral populations that are functionally (genetically and/or phenotypically) diverse to maintain or restore functionality and derived ecosystem services and build resilience in the face of persistent environmental stressors and, notably, climate change (Baums, 2008; Hein et al., 2021). Maintaining desirable features such as high coral cover and diversity, structural complexity, and fish biomass are common restoration goals (Bayraktarov et al., 2019; Seraphim et al., 2020; Yanovski et al., 2017). Less considered goals are nutrient or biogeochemical cycling, trophic interactions, and calcium carbonate ($CaCO_3$) dynamics which are still poorly defined and understood (Brandl et al., 2019). These processes underpin the provision of food and services such as coral reef fisheries and coastal protection to approximately six million people (Ferrario et al., 2014; Seraphim et al., 2020; Teh et al., 2013). Coral reefs' value goes beyond the ecological and economic aspects, and they are also greatly appreciated for their aesthetics and spiritual importance for the coastal communities (Cinner and Aswani, 2007; Hicks et al., 2009). Given coral reefs are foundational systems, it is important to include other coral traits (metrics) more aligned to reef functionality and services to evaluate the success of coral restoration efforts (Hein et al., 2021), as highlighted by the many reports from the Intergovernmental Platform on Biodiversity and Ecosystem Services (IPBES) that focus on the urgent need of assessing the state of the Earth's biodiversity, its ecosystems, and the vital services they provide to society (www.ipbes.net).

Few studies to date have reported increases in hard coral cover and structural complexity on restored sites compared to non-intervened nearby reef areas (Hein et al., 2020a; Ladd et al., 2019; Roper et al., 2022). Despite the evident success of restoring reef functionality and

associated service value, the outcomes of current restoration practices still need to be determined whether they will persist in the projected warming future and hence ensure reef resilience (Ladd et al., 2019). If the end goal is to restore (where lost) or maintain reef functionality and associated services, and build reef resilience, it seems reasonable to include metrics that encompass these desired attributes when evaluating the success of coral reef restoration projects (Boström-Einarsson et al., 2018; Hein et al., 2021; Vardi et al., 2021). Lastly, these metrics are needed to improve cost-efficiency and return-on-effort of coral reef restoration techniques in order to up-scale restoration efforts (Stewart-Sinclair et al., 2021; Suggett et al., 2019; Suggett and van Oppen, 2022; Vardi et al., 2021).

Despite the growing and diverse portfolio of interventions for coral reef restoration, few restoration programs are currently incorporating appropriate methods in project design and practice, highlighting a critical mismatch in regard to the convenient selection of methods towards the project's goal (Hein et al., 2021). Methods suitability and selection should be driven by the identified goals that coral restoration efforts aim to achieve (Edwards et al., 2010; Hein et al., 2020c). **Fig. 1.3** shows a matrix elaborated to identify the suitability of a particular method in regard to a targeted goal. For example, when aiming to mitigate population decline and preserve biodiversity, approaches that focus on larval release and the deployment of seeded substrates are considered most appropriate since these two methods will enhance genetic diversity at the restored site. Methods selection should be based on location and project-specific characteristics (Shaver et al., 2020). However, when it comes to targeting maintenance or recovery of specific ecosystem services such as shoreline protection or fisheries production, none of the current methods are considered as "most appropriate", which evidences a critical gap between current coral reef restoration methods and the

ultimate goal of establishing self-sustaining coral populations that are functionally diverse to maintain or restore reef functionality and derived ecosystem services.

Moreover, as coral reefs are one of the most vulnerable ecosystems to climate change, actions that enhance reef resilience are critical to ensure restoration efforts have a greater chance of success in a warming world. Therefore, including metrics that evaluate how restoration interventions impact or build climate reef resilience is essential in restoration projects. Not only are appropriately chosen methods that target specific goals missing in most restoration programs (from project design and implementation to monitoring), but also identified coral traits (metrics) that inform the success of the targeted goals. Including suitable, climate- and goal-oriented metrics in restoration programs will help identify (i) the impacts of coral restoration efforts on reef structure and community, (ii) whether coral reef restoration is recovering key ecological processes and services, and (iii) whether coral reef interventions are building reef resilience to climate stress, which overall will translate in a more accurate evaluation of the success of a specific restoration intervention, and will help obtain critical information on return-on-effort for the much-needed up-scale of reef restoration under a warming climate. In this context, this PhD thesis investigates other coral (reef) traits (metrics), including some aligned to ecosystem services and reef heat resilience, through a trait-based approach to better inform on the impact of recent coral propagation and outplanting efforts on the GBR and their success.

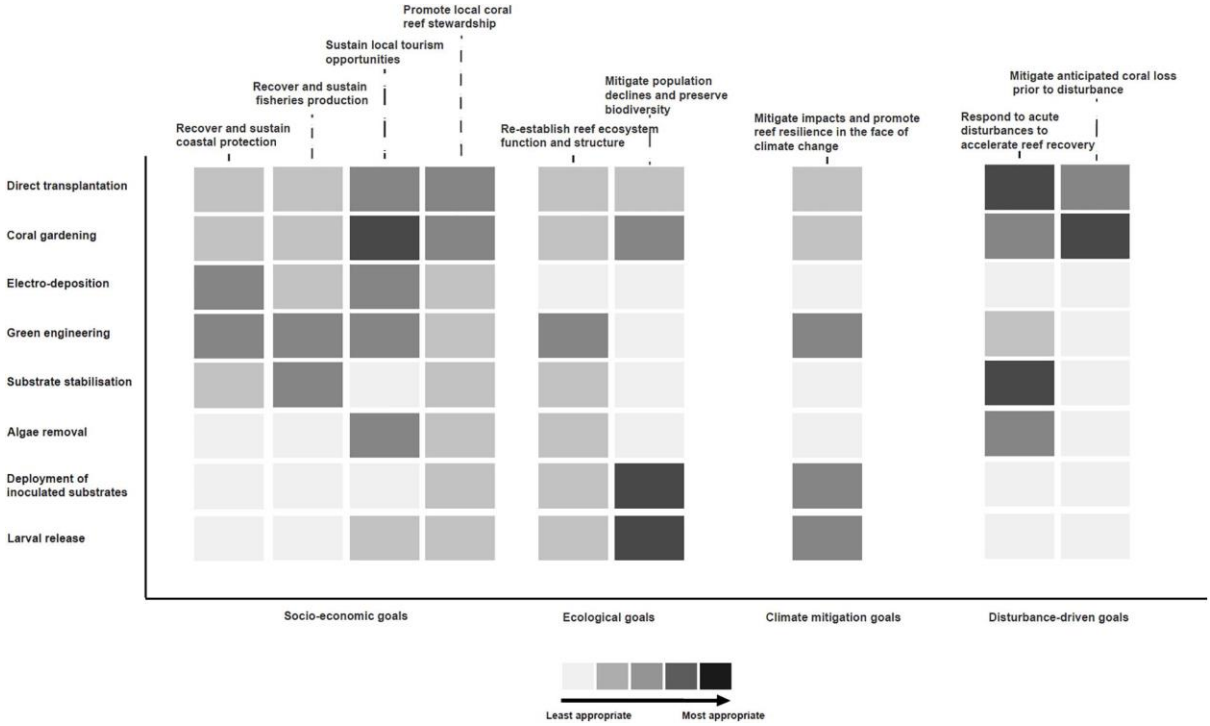

Figure 1.3 Goals-and-methods matrix for coral reef restoration. Four main goals have been identified: socio-economic, ecological, climate mitigation, and disturbance-driven goals, alongside the most appropriate method to achieve them (in a darker colour). Several interventions might be suitable to restore multiple goals. Extracted from Hein et al., 2021.

1.6. Developing a "deeper trait" perspective to restoration "success"

Documenting and understanding the vast array of functional traits in ecosystems has been tremendously useful in understanding organismal and ecosystem processes, functionality, productivity, and resilience (Brown et al., 2004; Finegan et al., 2015; Kunstler et al., 2016) in past and present environmental regimes. As a result, trait-based approaches have been largely used in evolution and ecology because it facilitates quantitative comparisons of biological form and function. Also, the use of traits allows the systematic linking of organismal responses to the environment, which nowadays is more critical than ever under a changing climate, by relatively easy-to-measure traits on large numbers of individuals (Gallagher et al., 2020).

Appropriately chosen and defined traits can help identify organismal response or life-history strategy for a given environment. For example, leaf mass per area (LMA, leaf photosynthesising surface area per unit leaf dry mass) was identified decades ago as a "supertrait". This measurable trait synthesises the energy-acquiring part of the plant, or photosynthetic capacity, which is highly associated with other biological traits and ecological processes such as relative growth rate (defined as weight increment per unit weight present per unit of time), mass-based leaf nitrogen, and leaf longevity (Westoby, 1998; Wright et al., 2004). Traits such as coral growth and survivorship have been commonly measured in coral restoration studies because of the ease of collecting data (e.g., Boström-Einarsson et al., 2020). Whilst these two traits provide a measure of coral biomass and complexity changes via relatively fast and convenient methods, these traits alone may not be informative enough to capture how corals perform under nursery or out-planting practices. For example, considering trade-offs in resource partitioning that potentially govern coral health, and therefore how these practices may impact other ecosystem services metrics such as biogeochemical cycling. Sole reliance on these traits may, thus, not fully capture how coral restoration initiatives impact — positively or negatively — reef health.

Other potential supertraits critical for future climate scenarios have been suggested as those supporting thermal tolerance (Howells et al., 2021) since oceans are projected to warm up to 1-2 °C in the next century (Frieler et al., 2013). Reef-building corals live in a symbiotic relationship with microalgae of the family *Symbiodineacea*. The algae live within the coral's tissue, giving them their characteristic colouration, and through photosynthesis, produce compounds that are the primary food source of the coral. However, this intimate relationship breaks down following stress (e.g., changes in salinity, intense solar radiation, exposure to air

by low tides or low sea level, sedimentation, or chemical pollutants such as herbicides and oil; Reaser et al., 2000), resulting in the loss of symbionts from the coral tissues, and showing their white calcium carbonate skeleton (the so-called coral bleaching). Corals can withstand for longer periods on heterotrophic feeding instead of the photosynthetic pathway and hence survive bleaching periods by recovering their lost symbionts. However, heat tolerance may not confer resistance to the many other stressors impacting reefs under climate change (Hughes et al., 2020; Pendleton et al., 2016).

Alternatively, traits such as coral morphology (also referred to as growth morph or growth form) support reef structural complexity and biodiversity (Darling et al., 2012; Madin et al., 2016a), and considered a good predictor of recovery after disturbances (Darling et al., 2012) including bleaching events (Graham et al., 2015). However, morphology alone does not account for how biochemical signals may moderate species interactions and recovery trajectories (Williams et al., 2017). To overcome these limitations of individual traits, an alternative approach is proposed to simultaneously examine multiple traits and how they affect coral performance and impact desired ecosystem service outcomes. For example, **Table 1.1** provides a summary of literature highlighting possible traits of interest to better describe coral performance beyond growth and survival. It is clear that mining "deeper traits" is currently needed to best inform how additional key measurements can aid descriptions of "success" across the rapidly growing volume of coral restoration efforts worldwide.

Table 1.1 Potential traits relevant to restoration to understand coral biology. (A) Physical, (B) physiological, and (C) molecular coral traits commonly used in coral research and/or restoration are listed below. The details on how to measure a specific trait are classified in technique (the most common methodology); level (which part of the coral holobiont is targeted); type of replicates (minimum number of replicates, and information about if the destruction of the sample is required); and equipment (the most common equipment). Additionally, we added the feasibility for measuring a specific trait (in terms of costs, expertise, and time); and the type of trait (according to being desirable and measurable; desirable and less measurable; and measurable and less desirable). In italic, an alternative methodology to assess the same coral trait. From one to 17, some of the coral traits that have been selected for the multi-trait assessment approach.

A)

Physical Trait	**Technique**	**Level**	**Type of replicates. Are they destructive: Yes (Y) or No (N)**	**Equipment**	**Feasibility (from more feasible (+) to less feasible (+++)**	**Type of trait: Desirable and measurable (DM), desirable and less measurable (DL), or measurable and less desirable (ML)**	**References**
Survival (Survivorship) (1)	Underwater visual survey by taking photographs.	Coral colony and fragment	1–2 photographs/colony or fragment – N	Underwater digital camera.	Cost + Expertise + Time +	DM	(Lirman, 2000; Putchim et al., 2008; Wright et al., 2019)
Growth rate (as linear extension rate) (2)	Underwater visual survey by taking photographs using a ruler for calibration.	Coral colony and fragment	1–2 photographs/colony or fragment – N	Underwater digital camera and ruler. Image analysis using a specific software.	Cost + Expertise + Time ++	DM	(Hughes, 1987; Lirman, 2000; Lizcano-Sandoval et al., 2018)
Growth rate (as 3D reconstruction)	*Underwater visual survey by taking photographs using a ruler for calibration.*	*Coral colony and fragment*	*50-100 photographs/colony or fragment – N*	*Underwater digital camera and ruler. Image analysis using a specific software.*	*Cost ++ Expertise ++ Time +++*	*DL*	(Gutierrez-Heredia et al., 2016; Gutiérrez-Heredia et al., 2015)
Growth rate (as weight gain)	*Scale to obtain the buoyant weigh*[1]*, wet*	*Coral fragment*	*1 measurement/fragment – N*	*Scale.*	*Cost + Expertise + Time +++*	*DL*	(Spencer Davies, 1989; Wright et al.,

[1] Also called buoyant weight growth rate.

	weight or dry weight.						2019)
Coral colour / Tissue colouration (a proxy for symbiont density) (3)	Underwater visual survey by taking photographs with a colour reference card. Quantification of RGB (R, red; G, green; B, blue) values.	Coral colony and fragment	1–2 photographs/colony or fragment – N	Underwater digital camera and colour reference card[2]. Image analysis using a software (optional).	Cost + Expertise ++ Time +++	ML	(Siebeck et al., 2006; Wright et al., 2019)
Bleaching state (4)	Underwater visual survey by taking photographs with the Coral Health Chart. Manual categorisation[3].	Coral colony and fragment	1–2 photographs/colony or fragment – N	Underwater digital camera and Coral Health Chart.	Cost + Expertise + Time +	ML	(Siebeck et al., 2006; Wright et al., 2019)
Lesion progression / Tissue loss / Dead coral tissue	Photographs using a ruler for calibration and quantify or categorise % of tissue loss.	Coral colony and fragment	1–2 photographs/colony or fragment – N	Underwater digital camera and ruler.	Cost + Expertise + Time ++	ML	(Wright et al., 2019)
Skeletal surface (surface area, SA) (5)	Single paraffin wax dipping method.	Coral fragment	1 measurement/fragment – Y	Paraffin wax.	Cost + Expertise ++ Time ++	DL	(Veal et al., 2010)
Skeletal volume	Water displacement in a graduated cylinder.	Coral fragment	1 measurement/fragment – N	Graduated cylinder.	Cost + Expertise + Time ++	ML	(Lavy et al., 2015)
(Skeletal) – bulk volume, biomineral density, bulk density, pore volume,	Hydrostatic weight measurement.	Coral fragment	1 measurement/fragment – Y	Sodium hypochlorite solution (1%), deionised water,	Cost + Expertise ++ Time +++	DL	(Fantazzini et al., 2015)

[2] Also called colour standard, which consists of five coloured areas (black, white, red, green, and blue).

[3] E.g., Either score from one to six or assign categories: (1) unbleached (normal colouration), (2) pale (lighter colour than usual for the time of year), (3) 0-20% of the surface bleached, (4) 20-50% bleached, (5) 50-80% bleached, and (6) 80-100% bleached.

apparent (internal) porosity (6)				oven, glass vessel in a 50 °C water bath under vacuum, and paraffin wax.			
Skeletal hardness (7)	Shore D Hardness Tester (TE-271).	Coral fragment	1 measurement/fragment – Y	Sodium hypochlorite solution (1%), deionised water, oven, and hardness tester.	Cost + Expertise + Time +	DM	(Leggat et al., 2019)
Colony mass per area, CMA (8)	Scale and single paraffin wax dipping method to obtain weight and SA, respectively.	Coral fragment	1 measurement/fragment – Y	Paraffin wax.	Cost + Expertise ++ Time ++	DL	(Madin et al., 2016b)
(Skeletal) – interseptal volume fraction, (macro, micro and nano-) porosity, (micro and nano-) structure, stiffness, and hardness	µCT[4], TD-NMR[5], SAXS[6], SEM[7], AFM[8], and Nanoindentation Tester.	Coral fragment	1–2 measurements/fragment – Y	Sodium hypochlorite solution (1%), deionised water, oven, microscope, mounting substrate, and specific equipment.	Cost +++ Expertise +++ Time +++	DL	(Fantazzini et al., 2015)
***(Skeletal)* – crystallographic vital effects (CVE) (a proxy of physiological processes controlling biomineralisation)**	SEM, EBSD[9], XRPD[10], and TGA[11].	Coral fragment	1–2 measurements/fragment – Y	Sodium hypochlorite (4%) solution, deionised water, diamond saw; mounting substrate (stain and	Cost +++ Expertise +++ Time +++	DL	(Coronado et al., 2019)

[4] Micro computed tomography.
[5] Time-domain nuclear magnetic resonance.
[6] Small-angle X-ray scattering.
[7] Scanning electron microscopy.
[8] Atomic force microscopy.
[9] Electron backscatter diffraction.
[10] X-ray powder diffraction (non-destructive).
[11] Thermal gravimetric analysis.

				epoxy resin), and specific equipment.			
Skeletal growth rate	Calcein dying or Calcein-Alizarin dying.	Coral fragment	1–2 measurements/fragment – Y	Stain and electronic microscope.	Cost +++ Expertise +++ Time +++	DL	(Holcomb et al., 2013)

B)

Physiological Trait	**Technique**	**Level**	**Type of replicates. Are they destructive: Yes (Y) or No (N)**	**Equipment**	**Feasibility (from more feasible (+) to less feasible (+++)**	**Type of trait: Desirable and measurable (DM), desirable and less measurable (DL), or measurable and less desirable (ML)**	**References**
Photosynthesis – Net O_2 production (indicator of photosynthetic rate) (9a)	Photosynthesis vs Respiration ratio.	Coral fragment	1 measurement/fragment – N (5 cm)	Incubation chamber and O_2 logger.	Cost ++ Expertise +++ Time +++	DL	(Camp et al., 2019, 2017, 2015; Gardner et al., 2017; Strahl et al., 2015; Wright et al., 2019)
Respiration – Net O_2 consumption (indicator of respiratory rate) (9b)	Photosynthesis vs Respiration ratio.	Coral fragment	1 measurement/fragment – N (5 cm)	Incubation chamber and O_2 logger.	Cost ++ Expertise +++ Time +++	DL	(Camp et al., 2019, 2017, 2015; Gardner et al., 2017; Strahl et al., 2015; Wright et al., 2019)
Calcification – Total alkalinity (indicator of net calcification rate) (10)	Rates of light and dark calcification.	Coral fragment	1 measurement/fragment – N (5 cm)	Incubation chamber and mercuric chloride (0.05% by volume) to fix the water samples.	Cost ++ Expertise +++ Time +++	DL	(Camp et al., 2019, 2017, 2015; Gardner et al., 2017; Strahl et al., 2015; Wright et

							al., 2019)
Chlorophyll *a* fluorescence – (Non)photobiological traits (11)	E_K (light saturation coefficient), $F_q'/F_m'_{MAX}$ (derived maximum photochemical efficiency), [1-C] (photochemical quenching), [1-Q] (non-photochemical quenching) $_{MAX}$, F_v/F_m (maximum quantum yield of photosystem II).	Coral fragment	1 fragment/colony – N (2 cm)	PAM fluorometer.	Cost ++ Expertise +++ Time ++	DL	(Camp et al., 2019, 2017, 2015; Gardner et al., 2017; Strahl et al., 2015; Suggett et al., 2012; Wright et al., 2019)
Symbiont cell density (12)	Number of symbiont cells/coral surface area (cells cm^{-2}).	Symbiont fraction	1-cm fragment – Y	Haemocytometer and microscope.	Cost + Expertise ++ Time +++	DL	(Camp et al., 2016a; Gardner et al., 2017; Hoogenboom et al., 2010)
Total pigment (Chlorophyll *a* and *c2*) content and ratio (13)	Identification and quantification.	Symbiont fraction	1-cm fragment – Y	Stored in liquid nitrogen and then in -80 °C, extraction of pigments and quantification by spectrophotometry.	Cost + Expertise ++ Time +++	DL	(Gardner et al., 2017; Wright et al., 2019)
Total protein content (14)	Identification and quantification.	Host and symbiont fractions	1-cm fragment – Y	Stored in liquid nitrogen and then in -80 °C, bicinchoninic method with bovine serum albumin as a	Cost ++ Expertise +++ Time +++	DL	(Gardner et al., 2017; Grottoli et al., 2018; Wright et al., 2019)

				standard.			
Total carbohydrate content (15)	Identification and quantification.	Host and symbiont fractions	1-cm fragment – Y	Stored in liquid nitrogen and then in -80 °C, phenol-sulfuric acid method with glucose as a standard.	Cost ++ Expertise +++ Time +++	DL	(Grottoli et al., 2018; Wright et al., 2019)
Total lipid content (16)	Identification and quantification.	Host and symbiont fractions	1-cm fragment – Y	Stored in liquid nitrogen and then in -80 °C, 2:1 chloroform:methanol solution followed by washing steps.	Cost ++ Expertise +++ Time +++	DL	(Grottoli et al., 2018, 2004; Padilla-Gamiño et al., 2013)
Catalase activity (CAT, a proxy for coral innate immune response)	Identification and quantification.	Host fraction	1-cm fragment – Y	Stored in liquid nitrogen and then in -80 °C, antioxidant assay, microplate reader.	Cost ++ Expertise +++ Time +++	DL	(Gardner et al., 2017; Wright et al., 2019)
Non-fluorescent chromoprotein content[12] (a proxy for coral innate immune response)	Identification and quantification.	Host fraction	1-cm fragment – Y	Stored in liquid nitrogen and then in -80 °C, extraction of chromoproteins and quantification by spectrophotometry.	Cost ++ Expertise +++ Time +++	DL	(Gardner et al., 2017; Wright et al., 2019)
Other antioxidant and enzyme activity (SOD[13], GSx[14], and CAT-like activity)	Identification and quantification.	Host fraction	1-cm fragment – Y	Stored in liquid nitrogen and then in -80 °C, antioxidant assay,	Cost ++ Expertise +++ Time +++	DL	(Gardner et al., 2017; Wright et al., 2019)

[12] Thought to play a role in photoprotection of the coral's resident symbiont microalgal photosystems from photoinhibition caused by high light levels found near the surface of coral reefs.
[13] Superoxide dismutase enzyme.
[14] Glutathione enzyme.

				microplate reader.			
N_2 fixation (related to nutrition)	Rates of light and dark calcification.	Coral fragment	1 measurement/fragment – N (5 cm)	Incubation chamber and acetylene (C_2H_2) reduction assay.	Cost ++ Expertise +++ Time +++	DL	(Bednarz et al., 2018, 2015)
Carbon acquisition (related to nutrition)	Identification and quantification.	Coral fragment	1 measurement/fragment – Y (5 cm)	$NaH_{13}CO_3$ incubations followed by mass spectrometry coupled to a C/N analyser.	Cost +++ Expertise +++ Time +++	DL	(Pupier et al., 2019)
Photoautotrophy vs heterotrophy (related to nutrition)	Identification and quantification.	Coral host	1 measurement/fragment – Y (5 cm)	Photoautotrophic labelling (DI-^{13}C pulse-chase), and heterotrophic labelling (^{13}C-rotifer pulse-chase).	Cost +++ Expertise +++ Time +++	DL	(Baumann et al., 2014; Grottoli et al., 2006; Hughes et al., 2010)

C)

Molecular trait	Technique	Level	Type of replicates. Are they destructive: Yes (Y) or No (N)	Equipment	Feasibility (from more feasible (+) to less feasible (+++)	Type of trait: Desirable and measurable (DM), desirable and less measurable (DL), or measurable and less desirable (ML)	References
Symbiont diversity (17)	ITS2 sequencing.	Symbiont fraction	1-cm fragment – Y	Stored in liquid nitrogen and then in -80 °C. DNA extraction protocol, and sequencing facility.	Cost +++ Expertise +++ Time +++	DL	(Howe-Kerr et al., 2020)
Coral diversity	Single nucleotide polymorphisms (SNP) markers (genotype).	Coral host	1-cm fragment – Y	Stored in liquid nitrogen and then in -80 °C, DNA extraction protocol, and sequencing facility.	Cost +++ Expertise +++ Time +++	DL	(Kitchen et al., 2020)
Gene expression (including heat shock protein gene expression, and other gene markers)	RNA sequencing.	Coral host	1 fragment (1–2 cm) – Y	Stored in RNAlater, RNA extraction protocol, and sequencing facility.	Cost +++ Expertise +++ Time +++	DL	(Venn et al., 2009)
Microbial composition (diversity), relative abundance and function	16S sequencing.	Coral fragment	1 fragment (1–2 cm) – Y	Stored in RNAlater, DNA extraction protocol, and sequencing facility.	Cost +++ Expertise +++ Time +++	DL	(Wegley et al., 2007)
DMSP / DMSO concentrations	Identification and quantification.	Coral fragment		Store in methanol at -20 °C, determination by	Cost +++ Expertise +++	DL	(Deschaseaux et al., 2014; Gardner et al.,

				qNMR[15] or GC[16].	Time +++		2017)

[15] Quantitative ^{1}H nuclear magnetic resonance spectroscopy.

[16] Gas-chromatography.

1.7. Thesis Roadmap, Aims and Objectives

In 2018, the "Coral Nurture Program" (CNP) was successfully established on the Northern Great Barrier Reef (Cairns-Port Douglas region of Queensland, Australia) as a unique partnership between tourism operators and scientists to up-scale coral restoration practices (e.g., coral propagation and out-planting, and substrate stabilisation), and identify high-value reef sites that can be managed by local stewardship (Howlett et al., 2022). Similarly, other approaches such as Mars Assisted Reef Restoration System (MARRS, or "Reef Stars"), which are applied on reef sites to contribute toward rubble stabilisation or larval-based restoration (also called larval enhancement) that focus on boosting coral recruitment, emerged on the GBR (McLeod et al., 2022). Despite the difference among employed methods and, hence, the different potential impacts on the reef, their success evaluation mainly relies on survival and growth rates. In turn, such basic appraisal of success has limited our understanding of the impact of coral restoration activities on coral (reef) performance, functioning, associated services, and resilience (**Fig. 1.4**).

The overall goal of this PhD is to evaluate the biological and ecological "success" of innovative coral restoration efforts on the Great Barrier Reef. This will be achieved through developing a holistic multi-trait measurement approach — based on a broader range of coral traits, apart from only survival and growth. Development of a multi-trait approach will facilitate identification of other potential key traits that better describe "success" during coral propagation and out-planting activities and more meaningfully contribute to desired ecosystem service outcomes, which are the ultimate goal of the restoration initiatives. Activities of this project are directly aligned to the GBR tourism industry to identify optimum

approaches (including appropriate data metrics) needed to propagate coral and rehabilitate degraded reef sites.

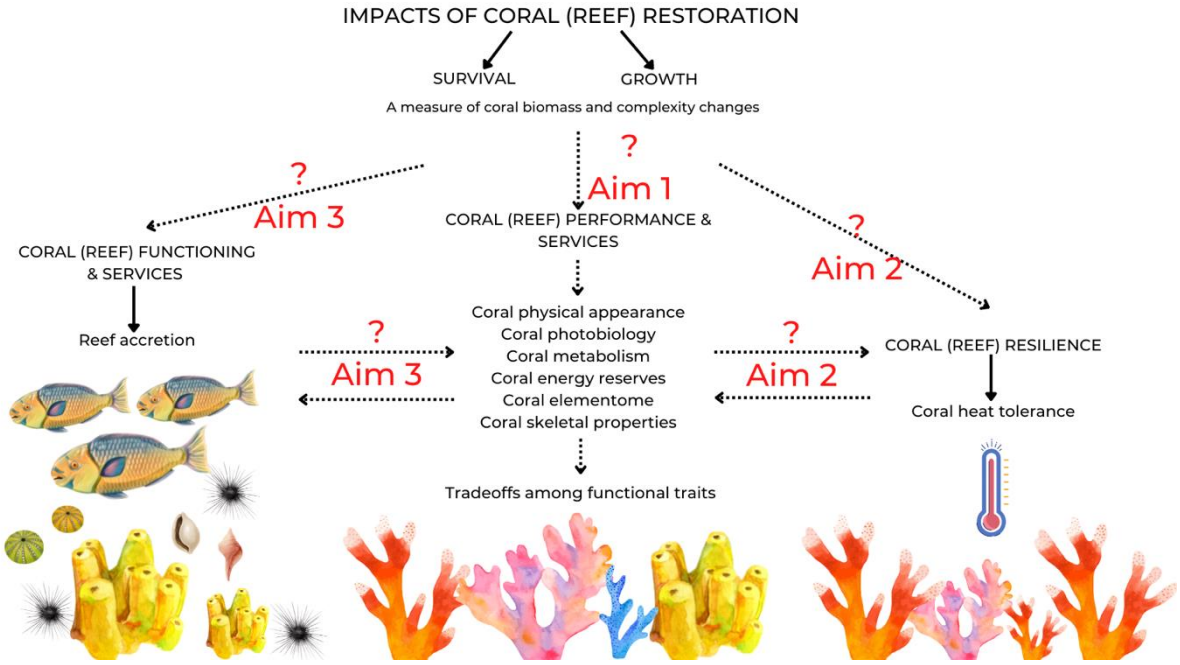

Figure 1.4 Schematic representation of some knowledge gaps that exist regarding the impacts of coral reef restoration practices. Continuous arrows indicate traits or metrics that are acknowledged to inform coral reef restoration practices. Dotted arrows accompanied by interrogation marks show aspects of coral restoration found in minimal studies (or even not considered yet) and addressed in the three aims of this PhD thesis.

This thesis is comprised of three research Aims (**Chapters 2-4**), where **Chapters 2** and **3** are connected around a common experimental design using coral nurseries (Opal Reef, northern GBR), and **Chapter 4** is centred on reef stabilisation methodologies (Moore Reef, central GBR). All studies have been presented in the form of a journal manuscript. At the time this thesis was finalised, **Chapter 2** had been submitted in a peer-reviewed journal (and published as a preprint), **Chapter 4** had been published, and **Chapter 3** was fully drafted for submission.

The specific aims of this research are to:

Aim 1 (Chapter 2) – Evaluate coral performance by exploring resource allocation across a diverse array of functional traits in natural versus nursery-reared colonies.

Hypothesis 1*: Nursery-based corals will display a different resource allocation in functional traits than their conspecifics from natural reefs because the coral nursery provides different environmental conditions.*

This Chapter has been submitted to *Scientific Reports* and is available as a Preprint: **Nuñez Lendo, C.I.**, Camp, E.F., Edmondson, J., Hughes, D.J., Kuzhiumparambil, U. Clases, D., Gonzalez de Vega, R., Suggett D.J., 2023. Multiple trait approach to inform ecosystem service value of corals propagated for restoration on the Great Barrier Reef. Res. Sq. PREPRINT. https://doi.org/10.21203/rs.3.rs-2030847/v1

Aim 2 (Chapter 3) – Identify whether there are differences in coral heat tolerance among coral groups (i.e., donor colonies and nursery-reared fragments) under heat stress- exposure.

Hypothesis 2*: Differences in thermal tolerance will be genotype-specific. However, nursery corals will exhibit a different thermal tolerance than their conspecifics in the reef because the coral nursery offer a different environment.*

Aim 3 (Chapter 4) – Assessment of Mars Assisted Reef Restoration System (MARRS) on reef accretion by evaluating carbonate budgets.

Hypothesis 3*: Direct transplantation of underwater structures harbouring nursery corals with higher structural complexity will exhibit a higher increase in ecosystem services than designs with lower complexity or unamended (control) soft bottom areas subjected to natural recovery.*

This Chapter has been published: **Nuñez Lendo, C.I.**, Suggett, D.J., Boote, C., McArdle, A., Nicholson, F., Fisher, E.E., Smith, D., Camp, E.F., 2024. Carbonate budgets induced by coral restoration of a Great Barrier Reef site following cyclone damage. *Front. Mar. Sci.* 10:1298411. doi: 10.3389/fmars.2023.1298411

Chapter 2

Multiple trait approach to inform ecosystem service value of corals propagated for restoration on the Great Barrier Reef

C. Isabel Nuñez Lendo[1]*, Emma F. Camp[1], John Edmondson[2], David J. Hughes[1], Unnikrishnan Kuzhiumparambil[1], David Clases[1,3], Raquel Gonzalez de Vega[1,3], David J. Suggett[1,4]

[1]Climate Change Cluster, University of Technology Sydney, Ultimo, NSW 2007, Australia

[2]Wavelength Reef Cruises, Port Douglas, QLD, Australia

[3]TESLA-Analytical Chemistry, Institute of Chemistry, University of Graz, Austria

[4]KAUST Reefscape Restoration Initiative (KRRI) and Red Sea Research Centre (RSRC),

King Abdullah University of Science and Technology, Thuwal, 23955, Saudi Arabia

Author contributions: CINL, DJS, and EFC designed the experiment, and alongside JE conducted the field-based experimental set up and sample collection. CINL analysed the bio-physical, metabolic, photobiological, bio-elemental, and skeletal samples, and DH, UK, DC, and RGV contributed to the analysis of photobiological, and bio-elemental samples. CINL conducted the statistical analysis and prepared the figures with guidance from DJS and EFC. CINL wrote the manuscript with editorial support from DJS and EFC, and with all authors contributing their relevant expertise in methods reporting and evaluation, and overall manuscript editing.

C. Isabel Nuñez Lendo

Emma F. Camp — Production Note: Signature removed prior to publication.

John Edmondson — Production Note: Signature removed prior to publication.

David J. Hughes — Production Note: Signature removed prior to publication.

Unnikrishnan Kuzhiumparambil — Production Note: Signature removed prior to publication.

David Clases — Production Note: Signature removed prior to publication.

Raquel Gonzalez de Vega — Production Note: Signature removed prior to publication.

David J. Suggett — Production Note: Signature removed prior to publication.

2. Abstract

Coral propagation- and planting-based reef restoration practices are accelerating globally, yet short-term "success" continues to be measured as broad metrics of coral survival and growth, even though goals are often centred on recovering broad ecosystem service values. As such, how restoration activities may impact healthy reef functioning remains uncertain. For example, trade-offs in resource acquisition and partitioning that potentially regulate growth vs survival may yield very different outcomes towards factors governing reef biogeochemical cycles. Here we considered a proof-of-concept "multi-trait" approach to capture how a broader range of functional traits reflect the expression of growth and survival for a key coral species (*Acropora* cf. *hyacinthus*) — impacted by recent mass bleaching events — propagated for restoration activities on the Great Barrier Reef (GBR), Australia. We examined a diverse array of bio-physical, bio-chemical, and skeletal traits (n = 90 traits) for wild (donor) colonies and their nursery-derived fragments from a 12-month growth period (Opal Reef, northern GBR). Nursery corals grew 20-25 times faster than their donor (wild) colonies, but both exhibited similar survivorship. Faster growth within nurseries was accompanied by more pigmented colonies (darker-coloured and with more symbionts), and higher respiration and dark calcification rates. However, despite these metabolic changes, biogeochemical properties of the nursery and reef corals (carbohydrates, lipids, proteins, elemental stoichiometry, and skeletal properties) remained largely the same after 12 months, suggesting the bio-energetic value to trophic transfer as well as the structural rigour of corals was unaltered by nursery propagation. Thus, a "multi-trait" approach enables more informed evaluation as to how propagation activities impact diverse ecosystem service values, highlighting the immense importance of this knowledge in choosing coral individuals for restoration. Our example provides confidence to practitioners that key ecosystem service

attributes of native corals are largely retained through an intermediate nursery growth phase that can accelerate coral biomass gains.

2.1 Introduction

Coral reefs sustain immense biodiversity and essential ecosystem services to almost a billion people but are deteriorating rapidly under relentless anthropogenic pressures (Hughes et al., 2017a) transforming coral reefs into highly altered assemblages (Heron et al., 2016; Hughes et al., 2020, 2003; Pandolfi et al., 2003). In response, coral propagation and re-planting initiatives have grown over the past 5-10 years in attempts to restore coral populations (e.g., Boström-Einarsson et al., 2020; Hein et al., 2021, 2020b) and offset further losses as local and global stressors continue to grow (Hein et al., 2020b, 2020a; van Woesik et al., 2020). Cost-effectiveness and efficacy of coral propagation and re-planting activities to date has improved largely through collective learning of localised success and failures as more activity has established (e.g., Boström-Einarsson et al., 2020; Fox et al., 2019; Johnson et al., 2011; Omori, 2019; Schopmeyer et al., 2017; Suggett et al., 2019; Young et al., 2012). For restoration efforts to be considered successful, the repaired habitat needs to have sufficient biotic and abiotic resources to sustain its structure and function (e.g., Calle-Triviño et al., 2021; Hein et al., 2021), but other more specific measures of success may also be needed, such as increasing abundance of a specific species (Williams et al., 2017).

Coral restoration success itself remains almost universally gauged in terms of two key traits — coral growth and survivorship — because of the relative ease of collecting associated data (e.g., Boström-Einarsson et al., 2020; Hein et al., 2017; Lirman and Schopmeyer, 2016; Suggett et al., 2019), but also given that growth and survivorship fundamentally govern coral

competitive fitness over space and time (e.g., Madin et al., 2016b; Suggett et al., 2019). However, these two traits alone may not (always) be informative enough to capture how coral health and reef functioning, and hence ecosystem service contributions are impacted during coral propagation and re-planting. For example, photosynthesis is a key measure of metabolic energy generation for growth vs survivorship, but also regulates biogeochemical transformation of key elements available to other reef taxa (Owen et al., 2021; Pawlik and Mcmurray, 2019), including CO_2 drawdown from the atmosphere (Ciais et al., 2013). Similarly, coral morphology (and in turn, structural complexity) is central to sustaining reef biodiversity (Darling et al., 2012; Graham et al., 2015), but does not account for how biochemical signals may moderate species interactions and recovery trajectories post disturbance (Williams et al., 2017). Therefore, whilst many functional coral traits (i.e., biological attributes or characteristics of a coral individual that impact its performance and thus fitness; Bellwood et al., 2019) can individually be considered central metrics of reef health, they can carry different weighting to the perception of success depending on the ecosystem service value goals for any restoration effort (Hein et al., 2021).

Trait-based approaches have been widely used in ecology (and evolutionary studies) to facilitate quantitative comparisons of biological form and function (Gallagher et al., 2020). Accounting for expression and trade-offs of functional traits has been particularly critical for understanding organism and ecosystem processes, functionality, productivity, and resilience (Brown et al., 2004; Finegan et al., 2015; Kunstler et al., 2016) in both past and present environmental regimes needed to forecast future ecosystem function. As a result, many studies have focussed on the expression of "supertraits" — measurable properties that capture a large amount of variation for a broad range of biological, ecological, and evolutionary processes (*sensu* Madin et al., 2016b), such as leaf mass per area in plants (Westoby, 1998;

Wright et al., 2004) and body mass in animals (White et al., 2007; Woodward et al., 2005). In corals, colony mass per unit tissue surface area (CMA, the relationship between coral weight and area) has similarly been proposed as a supertrait where CMA likely captures long-term colony investment of resource allocation and growth (Madin et al., 2016b). Whilst such metrics are powerfully informative, they remain proxies of function for the major biological properties of interest, and thus problematic for reef restoration where specific functional indicators are often required to support decision making, such as heat tolerance (Camp, 2022; Morikawa et al., 2019; Parkinson et al., 2020). Intriguingly, Cornwell et al., (2021) recently demonstrated that variation in heat tolerance of the coral species *Acropora hyacinthus* could in fact, to some extent, be explained by trade-offs amongst inherent endosymbiont load (and growth rate) — but nonetheless noted caution in unilateral use of this single trait for restoration.

Coral studies have increasingly moved towards multi-trait assessments of function to better resolve the major biological properties regulating fitness outcomes, both in terms of inherent gene expression (e.g., Dixon and Matz, 2021) and emergent measurable physiological outcomes (e.g., Gardner et al., 2017). However, such approaches have yet to be applied in the context of coral restoration, and it remains unclear whether and how deeper mining of traits beyond growth and survival could better inform descriptions of success across the rapidly growing volume of coral restoration efforts worldwide. We therefore implemented a proof-of-concept, multi-trait approach to evaluate collective trait expression for *A.* cf. *hyacinthus* propagated in coral nurseries (vs wild parent established on the reef) over 12 months on the Great Barrier Reef (GBR). Whilst many traits can conceivably be used to describe coral performance (summarised in **Table 1.1** in **Chapter 1**), we selected well-established, eco-physiological traits (**Fig. 2.1**). We examine how these various traits — and the "trait space"

they collectively reveal — reflect trade-offs in resource partitioning underpinning differences in growth and/or survival potential for corals propagated in nurseries compared to the reef (see selected traits in **Table S2.1**).

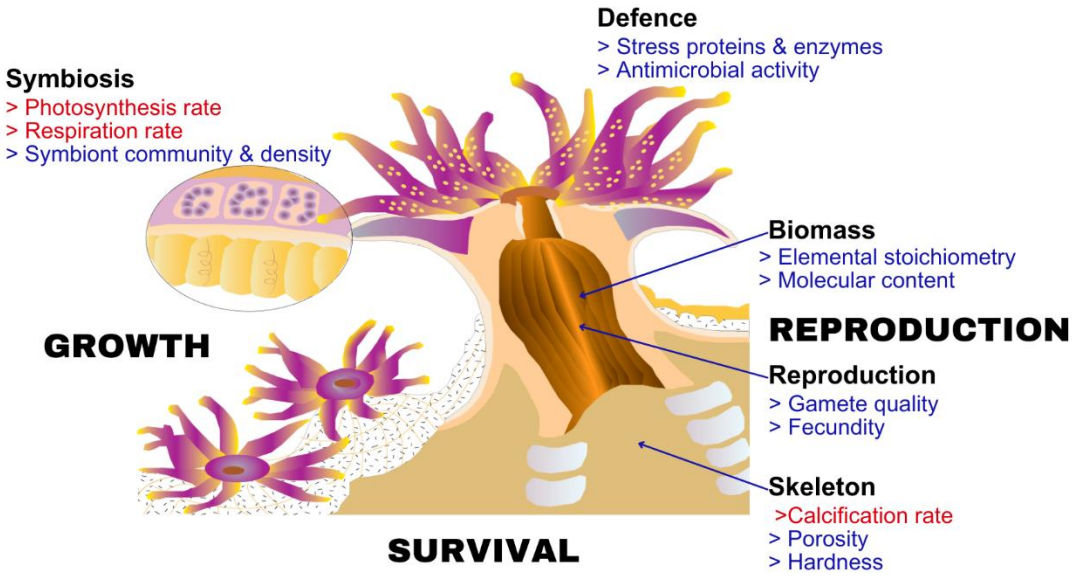

Figure 2.1 Visual representation of biological properties regulating coral fitness outcomes. Resource allocation within an individual could potentially be reflected in a particular trait or a set of traits that underpin the vital processes of survival (maintenance), growth (development), and reproduction. The figure shows some of the components (or functional traits and processes; in red those related to rates) of the biological machinery of the coral that potentially govern their functioning. Modified from Kris Beckert (Integration & Application Network; Kruczynski and Fletcher, 2012).

2.2 Materials and Methods

2.2.1 Sampling location and experimental design

Our multi-trait assessment focussed on a key coral species for the northern Great Barrier Reef (GBR), Australia, *Acropora hyacinthus* (Ortiz et al., 2021). We tentatively identified all source colonies as *A. hyacinthus* in the field, but subsequent examination (Sage Rassmussen, Pers. Comm.) indicated that one colony exhibited a slightly different radial corallite

appearance (colony #1) less consistent with this species. As such, we refer to the taxon studied throughout as *A.* cf. *hyacinthus*. Colonies (average initial area: 8290.4 ± 2422.0 cm^2) of *A.* cf. *hyacinthus* (n = 6) were selected, tagged, and sampled from "Mojo" site at Opal reef (5–6 m depth, collected a minimum of 10 m apart), 50–60 km from Port Douglas, Queensland (145° 53' 50.3''E, 16°12' 30.4''S) (**Fig. S2.1**), February 2020. A maximum of 10% of each wild colony was removed using a hammer and a chisel, and from each partial colony 6 fragments were made. Three of these fragments (i.e., n = 3 replicates of each colony; with an average initial area of 127.1 ± 8.2 cm^2 per fragment) were moved to a nearby coral nursery facility consisting of two aluminium diamond-mesh frames (2.0 x 1.2 m) placed 1–2 m above the sand by means of 2 × 9 kg Besser blocks and a 20-L float (Howlett et al., 2021; Suggett et al., 2019) so that corals were suspended at 4–5 m depth. Both aluminium frames were conditioned *in situ* for at least two weeks prior to holding any coral fragment. The additional set of fragments (n = 3 per colony; 1 for incubation, 1 for laboratory analysis, and 1 for skeleton assessment) were also originated from the same initial partial parent colony — referred to hereafter as "Wild" — for all initial laboratory trait measurements (time zero; WT0) alongside taking pictures of the wild colonies for assessment of physical traits. Both the wild colonies and nursery retained fragments (or clones) were then all re-sampled after 12 months (February 2021; WT12 and NT12) to evaluate potential trait expression variation from propagation on the nursery vs reef. All traits were therefore measured at WT0, WT12, and NT12, with the exception of growth and survivorship which were calculated from the difference in size and total colonies/fragments remaining between time points (i.e., WT12-WT0 or NT12-WT0).

Due to technical failure environmental data were extracted from GIOVANNI online system for satellite-derived data maintained by NASA (https://giovanni.gsfc.nasa.gov/giovanni/). Sea

surface temperature (SST) was obtained using monthly area-averaging bounded to 145° 53' 50.3''E, 16°12' 30.4''S (Opal Reef) between the beginning of February 2020 and the end of February 2021. We also obtained 9-month HOBO SST data from the nursery at Mojo, which was overlaid with Giovanni SST data for Opal Reef (**Fig. S2.2**). It should be noted that at the onset of the experiment — i.e., March 2020 — the GBR experienced its third (and most widespread) mass bleaching event in five years. Coral mortality from this event was relatively low throughout the GBR compared to 2016/17 (AIMS, 2021), and whilst *A.* cf. *hyacinthus* colonies and fragments at Opal Reef visibly paled (including on the nurseries, JE, Pers. Comm.) in the second month of the experiment no mortality of our experimental coral material was observed.

On site data were collected and consisted of measuring several metabolic traits as previously described in Camp et al., (2017), notably endosymbiont photophysiological performance, photosynthesis, respiration, and calcification rates. Additional samples were snap-frozen in liquid N_2 for further analysis in the laboratory including symbiont cell density and pigment content (chlorophyll *a* and *c2*) (Baghdasarian et al., 2017), ITS2 symbiont identity (Camp et al., 2020a), bio-molecular content (carbohydrates, lipids, proteins, and fatty acid methyl esters [FAME]) (Conlan et al., 2017; Grottoli et al., 2018, 2017) and elemental composition — C:N, referring to C (Carbon), N (Nitrogen), and trace elements — of the coral holobiont (host + symbiont fractions) as per Grima et al., (2022). Data on physical traits were obtained by underwater photographs (Lirman et al., 2014; Siebeck et al., 2006) and by storing additional sub-samples in sodium hypochlorite for later analysis of skeletal properties (e.g., bulk volume, biomineral density, bulk density, pore volume, apparent (internal) porosity, hardness, and colony mass per area) (Fantazzini et al., 2015; Leggat et al., 2019; Madin et al., 2016b). All samples for the incubations (n = 6) and the skeletal assessment (n = 6) were

collected for WT0. Unfortunately, two samples (designated for laboratory analysis only) were lost for this coral group (n = 4). During the second field campaign, all samples were successfully collected for NT12 and NT12 (n = 6 per each analysis).

2.2.2 Survival and growth

Corals were photographed using an Olympus Stylus TOUGH TG-4 digital camera together with a ruler by SCUBA. Growth rates were determined as the change in size (areal and linear extension) over time (ΔG; $cm^2\ y^{-1}$ and $cm\ y^{-1}$) and survival rate as the proportion of all initial coral individuals remaining over time (%). To compare growth amongst coral groups, we determined the relative growth rate as % growth y^{-1} (i.e., $[\Delta G/G_I] \times 100$), where G_I corresponds to the initial size (area or diameter). Normalising ΔG to G_I in this way enables comparison of growth from other studies where corals with different initial sizes have been used (e.g., Suggett et al., 2019).

2.2.3 Physical appearance

Each coral colony or fragment was photographed (excluding the pale growing tip) at exposure 0 and a fixed distance of 20 cm with an Olympus Stylus TOUGH TG-4 digital camera, together with two underwater colour reference cards — a black and white card (Chow et al., 2016) and the Coral Watch bleaching card (Siebeck et al., 2006). Manual settings were used to ensure the gain and white balance settings remained constant. Photographs were subsequently analysed in Adobe Photoshop (version 20.013.20074) using the histogram function to determine the hue (reflected colour, with values of 0-360°), saturation (proportion of grey in the hue), and brightness (relative lightness and darkness,

both having values of 0-255, where 0 and 255 are absolute white and black, respectively) from ten selected sampling points on the coral, which were then averaged (with the black and white card as a reference). Red, green, and blue (RGB) values (values from 0 to 255 corresponding to standard white and black, respectively) were also extracted using the same card. Coral tissue colouration was further categorised according to the bleaching state by use of the Coral Watch bleaching card as per Siebeck et al., (2006), where a colour score difference > 2 is considered indicative of a significant change in symbiont density and chlorophyll *a* concentration, and thus bleaching state.

2.2.4 Photosynthesis, respiration and calcification rates, and photobiology

Light and dark calcification, net photosynthesis, and respiration rates were performed on the operations vessel (*Wavelength 5*). Visible non-live coral tissue such as coral skeleton or attached rock/substrate were removed from each fragment (~5 cm) from each coral group (n = 6 fragments per group) prior to incubation as per Camp et al., (2017) (to prevent biological alteration of incubated seawater). Fragments were then incubated for 2 h in the light followed by 2 h in the dark (covered in a blackout material) within 470 mL custom-made sealable acrylic chambers filled with ambient seawater (30 °C) continuously mixed via a magnetic stir plate. All chambers were positioned in a temperature-controlled water bath (ambient temperature of 30 ± 0.5 °C) to maintain the same temperature across chambers. Light intensity for incubations was set to 300 µmol photons m^{-2} s^{-1}, corresponding to the average light saturation coefficient (E_K, mmol photons m^{-2} s^{-1}) — a measure of the long-term light acclimation state (e.g., Suggett et al., 2012) — as determined via rapid light curves (RLCs) assessed by Pulse Amplitude-Modulated (PAM) fluorometer (Walz) (instrument settings detailed below). Incubation irradiance was supplied via white LED aquarium lights (Hydra

52, Aqua Illuminations, Illinois, USA) positioned directly above the chambers, and measured using a PAR meter equipped with a 4π sensor (Li-Cor LI-250A). Oxygen optodes were connected to a FireSting O_2 logger and data were acquired using the FireSting software (PyroScience GmbH, Aachen, Germany). Each optode was calibrated prior to measurements using a freshly prepared sodium thiosulfate solution (10% w/w) and air-bubbled ambient seawater at experimental temperatures for 0% and 100% air saturation values, respectively.

Oxygen concentration was measured at the beginning, during, and after 2 h (for both light and then dark phases) in each chamber until a linear change in rate was recorded for each replicate. Net photosynthesis and respiration rates (P_N, R) were calculated based on the changes in O_2 concentration over time during the light and dark incubations, respectively, corrected for any changes in parallel water-only controls (n = 2) (Camp et al., 2017). Gross photosynthesis (P_G) was subsequently determined from net photosynthesis adjusted for respiration (i.e., $P_G = P_N - R$). Rates of light and dark calcification were determined by the alkalinity anomaly technique (Smith and Kinsey, 1976) corrected for any changes in total alkalinity (A_T) of the controls (n = 3). All rates were normalised to the incubation volume, time, and coral surface area, which was determined by the single wax dipping technique (Stimson and Kinzie, 1991; Veal et al., 2010).

RLCs were used to obtain the following photobiological traits: light saturation coefficient (E_K, µmol photons m^{-2} s^{-1}), derived maximum photochemical efficiency of PSII ($F_q'/F_m'_{MAX}$), photochemical quenching ([1-C]), and non-photochemical quenching (1-Q) as per Suggett et al., (2015) of the coral-associated *Symbiodiniaceae* (Nitschke et al., 2018; Suggett et al., 2012). The PAM fluorometer was programmed as Measurement intensity: 12;

Gain: 4; Saturating intensity: 10; Saturation width: 0.8s; Damping: 2; Light curve interval: 3. For each RLC, an initial dark measurement and 8 actinic light steps were applied, whereby each light intensity was applied for 20 s. The actinic light levels (verified against a factory-calibrated LI-192 quantum sensor, Li-Cor) of the RLC were 0, 117, 149, 212, 302, 434, 600, 847 and 1304 and 0, 115, 195, 265, 350, 500, 710, 1020, 1400 µmol photons m^{-2} s^{-1} in February 2020 and 2021, respectively. All coral material was low-light acclimated for at least 20 min prior to the RLC as per Suggett et al., (2022). Values for [1-Q] and [1-C] were only evaluated at the maximum RLC light intensity for the purposes of comparing trait expression.

2.2.5 *Symbiodiniaceae* cell density and pigment content

Coral tissue was removed from the coral fragments with an air-gun (Deschaseaux et al., 2013) in a small Ziplock bag containing 4 mL of 0.2 µm filtered seawater (FSW) (Minisart NML 16534 syringe filters, Sartorius, Germany). An aliquot of the resulting coral slurry (1 mL) was used for cell counts. The symbiont fraction was isolated from the host tissue via centrifugation (4 °C at 3500 RPM for 5 min), and the symbiont pellet resuspended in 1 mL FSW. The algal suspension was preserved with 20 µL of 2% glutaraldehyde, and cell counts were later performed using a hemacytometer under a Nikon Ti microscope at 10x magnification. Cell density was obtained by standardising the values to volume and fragment surface area (wax dipping method).

A second 1 mL aliquot of the slurry was then used to determined chlorophylls *a* and *c2* concentration. Host and symbiont fractions were again separated via centrifugation (as described above) and the pellet resuspended in 1 mL FSW. The 1 mL-algal suspension was pelleted and the cells lysed with 3 mL of 100% acetone in a scintillation vial placed on an ice

bath and sonicated for 10 min. Samples were covered with aluminium foil throughout to minimise any chlorophyll degradation. After sonication, samples were stored at -4 °C to allow pigment extraction. After 24 h, samples were centrifuged to remove cellular debris and measured on a spectrophotometer (Cary 60 UV-Vis, Agilent Technologies, Santa Clara, CA, USA); λ = 630, 663 and 750 nm in a 4 mL-glass cuvette. Chlorophyll *a* and *c2* were derived from the spectrophotometric equations of Jeffrey and Humphrey (1975) by standardising values to cell concentration and fragment surface area (pg $cell^{-1}$ and pg cm^{-2}), in addition to calculating chlorophylls ratio (*a*:*c2*).

2.2.6 *Symbiodiniaceae* ITS2 identity

Small sub-samples of each fragment (~1 cm^2) were air-picked with 2 mL of 0.2 µm-FSW into small Ziplock bags. The resulting slurry was then centrifuged (4 °C at 3500 RPM for 5 min) to retrieve a pellet of the endosymbionts. DNA extraction of the pellet was performed using the Qiagen Dneasy Plant Mini Kit (Qiagen, Hilden, Germany), where cells were disrupted with glass beads (BioSpec). Extracted DNA quality and quantity were checked using a NanoDrop 2000C spectrophotometer (Thermo Fisher Scientific, MA, USA). Amplification of the ITS2 region was performed by PCR where ITS2-reverse and ITSintfor2 primer pairs were used (LaJeunesse et al., 2019), following PCR conditions from Arif et al., (2014). Sequencing of the amplicons was achieved using Illumina Miseq (2 × 300 bp) at the Ramaciotti Centre for Genomics (University of New South Wales, Australia). Output files of the Illumina sequencing were submitted to SymPortal (Hume et al., 2019) to identify *Symbiodiniaceae* taxa (LaJeunesse et al., 2018) from the ITS2 marker.

2.2.7 Energy reserves and tissue biomass

Coral tissue was air-brushed from fragment sub-samples (~10 cm) in medium Ziplock bags containing 20-30 mL of 10% Tris buffer (Sigma-Aldrich), and the resulting 10-15 mL slurry was freeze-dried. A minimum of 15 g of dry coral mass was used to determine carbohydrates, lipids, and proteins content. Soluble lipids were extracted using chloroform:methanol method as per Grottoli et al., (2018, 2017). Briefly, the coral slurry was submerged in a 2:1 chloroform:methanol solution for 1 h, washed in 0.88% NaCl followed by 100% chloroform, and washed again with 0.88% KCl. Following lipid extraction, fatty acids were esterified into methyl esters following the acid catalysed methylation method (Christie and Han, 2010) and detected through gas chromatography (GCMS-QP2020 equipped with an AOC-20is autosampler, Shimadzu Corporation) (methodology adapted from Conlan et al., 2017)).

Soluble proteins were extracted using the bicinchoninic acid method (Smith et al., 1985) with bovine serum albumin as a standard (Pierce BCA Protein Assay Kit). Soluble carbohydrates were quantified via the phenol-sulfuric acid method (DuBois et al., 1956) with glucose as a standard. Soluble holobiont carbohydrate, protein, and lipid concentrations were then standardised to dry and ash-free dry weights and surface area. Total energy reserves were calculated as the sum of lipids, protein, and carbohydrate values converted into Joules (Gnaiger and Bitterlich, 1984). Tissue biomass was measured by drying a whole coral sample (skeleton, animal tissue, and algal endosymbiont) to constant dry weight (48 h, 60 °C) and burning for 6 h (450 °C). The difference between dry and burned weight was the ash-free dry weight. Both dry and ash-free dry weights were standardised to the surface area of that coral fragment.

2.2.8 Elementome

Coral tissue was air-picked in a trace-clean laminar flow hood from small sub-samples of each fragment (< 5 cm) in previously acid-washed Ziplock bags, containing 2 mL of 10% Tris buffer (Sigma-Aldrich). The resulting coral slurry consisted of host tissue and symbiont was freeze-dried. Total dry weight material was divided into a minimum of 30 mg and 5 mg for C:N and trace elements analysis, respectively. Total elemental C and N was determined using a Leco Total Carbon and Nitrogen Analyser (Purcell, 1996) following manufacturer methods for soil and plant material with a furnace temperature at 1200 °C and a soil calibration standard. Major and trace elements (Phosphorus [P], Magnesium [Mg], Sulphur [S], Potassium [K], Calcium [Ca], Vanadium [V], Manganese [Mn], Iron [Fe], Nickel [Ni], Copper [Cu], Zinc [Zn], Strontium [Sr], Molybdenum [Mo], Cadmium [Cd], Tin (Sn), Lead (Pb), Cobalt [Co], and Selenium [Se]) were determined by acid digestion of each freeze-dried sample (Grima et al., 2022; Pettersson and Olsson, 1998). Digestion and filtration steps were conducted as per Grima et al., (2022). Quantitative analysis of elements was carried out using flow injection analysis (FIA) employing an Agilent 1200 Series HPLC system coupled with an 8900 series ICP-MS/MS instrument (Agilent Technologies, Santa Clara, CA, USA) according to a method developed by Grima et al., (2022). The interface was equipped with s-lenses and Pt sampler and skimmer cones. The ICP-MS/MS instrument was operated in MS/MS mode using oxygen as cell gas (99.995%, grade 4.5, BOC, North Ryde, NSW, Australia) for mass shifting of S and P. The remaining elements were acquired on mass. Quantification was performed in an external calibration approach using diluted, matrix-matched element standards for ICP-MS obtained from Choice Analytical Pty Ltd (Thornleigh, NSW, Australia). The performance of the ICP-MS instrument was tuned daily with a solution containing 1 μg L^{-1} Li, Y, Tl and 100 μg L^{-1} P and S.

2.2.9 Skeletal properties

The buoyant method applied for corals (adapted from Bucher et al., 1998) and Jokiel et al., (1978), combined with the Archimedes principles, were used to test bulk volume, biomineral density, bulk density, pore volume, apparent (internal) porosity, hardness, and colony mass per area on previously cleaned and dried coral skeletons (< 2 cm) (Fantazzini et al., 2015). Colony mass per area (considered a supertrait; Madin et al., 2016b) was also estimated. Briefly, the fragment was previously weighed to obtain the dry weight (m or DW; g) before being inserted in a glass vessel in a 50 °C water bath for two h under vacuum. The vessel was filled with Milli-Q water to obtain the saturated weight (m_s or SW; g) of the coral followed by the measurement of the buoyant weight (m_h or BW; g). Lastly, surface area (SA) was extracted following the wax technique. Skeletal properties were extracted using the previous calculations and the density of water (ρH_2O) at 20 °C (0.9982 g cm^{-3}) as per the following equations:

[Eq. 1] $V_A = (m_s - m) / \rho H_2O$; the pore volume connected to the external surface (V_A)

[Eq. 2] $V_B = (m_s - m_h) / \rho H_2O$; the total volume occupied by the coral skeleton (called bulk volume)

[Eq 3] $P_A = V_A / V_B = (m_s - m) / (m_s - m_h)$; the apparent porosity (or effective or connected porosity, P_A) (ratio of the pore volume connected to the external surface (V_A) to V_B)

[Eq 4] $d_b = m / V_B$; the bulk density (ratio of the mass to V_B)

[Eq 5] $d_r = m / (V_B - V_A)$; the biomineral density (ratio of the biomineral mass to biomineral volume, excluding pore volume connected to the external surface, also called real density or micro-density)

Hardness testing was conducted using a Shore D Hardness Tester (TE-271) as per Leggat et al., (2019) on a second coral fragment (< 2 cm), calibrated using reference material as per the manufacturer's recommendation (Vander Voort, 1999). Hardness was consistently determined on the base of the branch for all fragments, with 10 measurements performed for each.

2.2.10 Statistical analysis

Data analyses were performed using R (version R-4.3.2) and GraphPad Prism (version 9.1.2). To conduct and visualise the Principal Component Analysis (PCA), the "FactoMineR" and "factoextra" R packages were used (Kassambara and Mundt, 2020; Lê et al., 2008). Assumptions of normality were assessed visually via QQ plots and a Shapiro-Wilk's test, and equal variances were assessed using Brown-Forsythe test (Shapiro and Wilk, 1965). Data were transformed to meet normality assumptions where required. In particular, arcsine (Y/100) for percentages (1-100%) such as survivorship, saturation, and brightness; log transformation was carried for % data above 100% such as relative growth rate (log(Y)) and for negative values (log (Y+a)); and sin (Y) for degree data such as hue. Paired student's t-test (normal distributions with equal variances, or its non-parametric homolog, Wilcoxon rank-sum test) were used to evaluate differences in survival and growth rates for wild and nursery corals (WT12 and NT12) over a year. Significance was set at $p < 0.05$ (for all tests) and the mean ± the standard error of the mean (SEM) was reported unless specifically noted.

A series of (repeated measures) analysis of variance (ANOVA) (or its non-parametric homolog, Friedman or Kruskal-Wallis tests, respectively) with post hoc tests (Tukey or Dunn) were undertaken to compare among coral groups ("control" WT0, WT12, and NT12) for the rest of the coral traits. Additionally, a PCA biplot, including a cut-off for the cos2 = 0.5, was built for each following biological section: (a) photobiology, (b) physical appearance, (c) elementome, (d) metabolism, (e) energy reserves, (f) fatty acid methyl esters (FAME), and (g) skeletal properties, in order to identify the main drivers of the variation during propagation alongside the redundant traits to construct the final multi-trait PCAs (with main drivers). Lastly, differences in coral groups ("control" WT0, WT12, and NT12) were tested for significance with pairwise permutational multivariate analysis of variance (PERMANOVA; perm = 999) of Bray–Curtis dissimilarities using the "vegan" R package (Oksanen et al., 2008).

2.3 Results

2.3.1 Survivorship and growth

A. cf. *hyacinthus* survivorship after 12 months was not statistically different amongst coral groups (wild vs nursery grown corals, 100.0 ± 0.0 vs 77.8 ± 11.1 %, respectively; n = 6 for each coral group) (Wilcoxon rank-sum test, p = 0.2500; **Fig. 2.2A**). However, higher relative areal growth rate (ΔG_A; % growth in cm^2 y^{-1}) over 12 months was evident for the nursery corals (308.9 ± 52.8) compared to the wild corals (12.4 ± 11.5) ($t_{(5.0)}$ = 4.2, p = 0.0083; **Fig. 2.2B**). This outcome was also observed in the relative increase in area covered by coral tissue (%) (112.4 ± 11.5 vs 309.0 ± 54.0 %, for wild vs nursery corals, respectively; n = 6 for each coral group) (**Fig. 2.2C**; $t_{(5.0)}$ = 4.7, p = 0.0055). Similarly, relative linear growth rate (ΔG_L; % growth in cm y^{-1}) was higher for nursery compared to wild corals (84.4 ± 11.2 vs 4.5 ± 5.0,

$t_{(5.0)} = 4.3$, $p = 0.0076$; **Fig. S2.3A**). Amongst the six colonies examined, highest areal growth rates in wild and nursery corals were consistently observed for colony #1 (50.7 and 432.0 cm^2 y^{-1}, respectively; see example in **Fig. S2.3B-C**). Overall, areal and linear growth rates observed for nursery corals were ~20-25 times higher compared against wild corals.

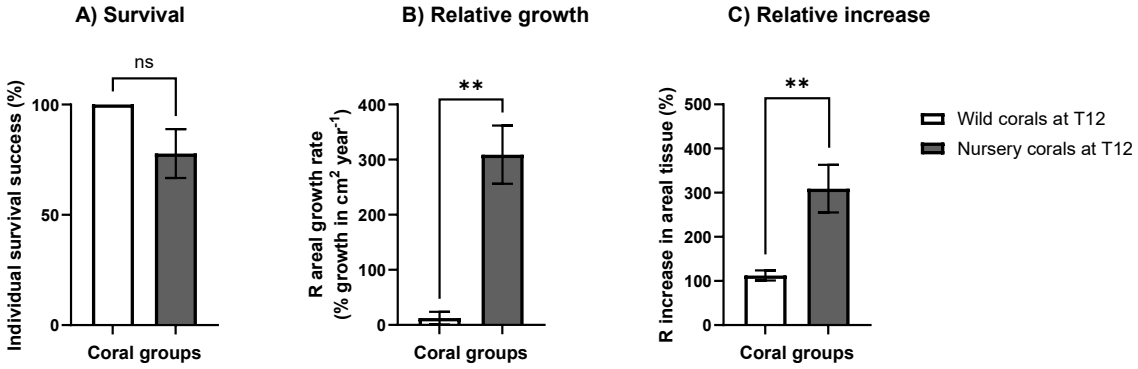

Figure 2.2 Mean (± SEM; standard error of the mean) (A) survivorship (%), (B) relative areal growth rate (% growth in cm^2 yr^{-1}), and (C) relative increase in area covered by coral tissue (%) of wild and nursery corals from 12 months propagation. All data are fragments of *Acropora* cf. *hyacinthus* (n = 6 for both groups). Statistical significance was indicated by ns (no statistical significance) and ** ($p \leq 0.01$).

2.3.2 Physical appearance

Multiple traits were examined to describe bio-physical colouration (red [R], green [G], blue [B], hue, saturation, brightness, and bleaching state; **Fig. S2.4**). Initial RGB values for wild corals (WT0) were 103.2 ± 10.0, 89.0 ± 8.5, and 68.0 ± 9.8 for RGB, respectively (n = 6). Higher RGB and brightness values correspond to a paler colouration (i.e., closer to white). R and G values were slightly increased (138.5 ± 6.0 and 97.8 ± 3.4), and B values significantly decreased (42.2 ± 3.9) in wild corals (n = 6) after 12 months (WT12) compared to initial wild colonies (WT0); Tukey's test WT0 vs WT12, p = 0.0317. In contrast, the nursery corals (NT12) became darker after 12 months (RGB of 98.5 ± 5.1, 67.3 ± 4.6, and 27.8 ± 2.6, respectively; n = 6) compared to the other two coral groups. Tukey's test revealed significant

differences for WT12 vs NT12, p = 0.0247, 0.0126 and 0.0215 for RGB, respectively; and for WT0 vs NT12 (p = 0.0077) for B values.

Apart from significant differences in the RGB, differences in brightness values among NT12 and WT12 coral groups were also evident (Tukey's test WT12 vs NT12, p = 0.0257; **Fig. S2.4A-D**) indicating different colouration between these two coral groups. We also observed similar saturation and hue levels among WT12 and NT12 (significant differences were only detected in saturation levels for WT0-WT12 and WT0-NT12, p = 0.0029 and 0.0113, respectively; **Fig. S2.4E-F**). All coral groups were in a non-bleached stage (average score of 6.0 ± 0.0 for all three coral groups) based on the coral colour reference card (Siebeck et al., 2006) (see **Fig. S2.4G**). In summary, at 12 months post-fragmentation, corals propagated within the nursery (NT12) were darker than those retained in the wild (WT12) compared to the start (WT0).

2.3.3 Photobiology

Whilst nursery-propagation resulted in darker colonies after 12 months, photobiological traits for NT12 vs WT12 were generally similar; of note, however, photobiological characteristics varied as a function of time whereby both NT12 and WT12 were largely different compared to WT0 for 8 out of 12 photobiological traits. Specifically, the light saturation coefficient (E_K, μmol photons m^{-2} s^{-1}) was higher for WT12 and NT12 (292.8 ± 64.4 and 328.2 ± 49.7, respectively) compared to WT0 (126.4 ± 16.9) (**Fig. 2.3A**; one-way RM ANOVA, $F_{(1.4,7.2)}$ = 6.2, p = 0.0337; Tukey's test WT0 vs WT12, and WT0 vs NT12; p = 0.0447, and 0.0310, respectively). Maximum photochemical efficiency of PSII ($F_q'/F_m'_{MAX}$, dimensionless) was lower for WT12 and NT12 (0.6412 ± 0.0130 and 0.6368 ± 0.0162) compared to WT0 (0.7043

± 0.0118) (**Fig. 2.3B**; one-way RM ANOVA, $F_{(1.3,6.5)} = 12.2$, $p = 0.0091$; Tukey's test WT0 vs WT12, and WT0 vs NT12, $p = 0.0134$, and 0.0438, respectively). When examining the fluorescence quenching parameters, photochemical quenching capacity was reduced (i.e., $[1\text{-}C]_{MAX}$ values were higher) for WT12 and NT12 (0.2330 ± 0.0422 and 0.3037 ± 0.0342) compared to WT0 (0.1214 ± 0.0198) (one-way RM ANOVA, $F_{(2.0,9.8)} = 16.8$, $p = 0.0007$; Tukey's test WT0 vs WT12 ($p = 0.0350$) and WT0 vs NT12 ($p = 0.0070$); **Fig. 2.3C**). Similarly, non-photochemical quenching capacity was also reduced ($[1\text{-}Q]_{MAX}$ values were higher) for WT12 and NT12 (0.8539 ± 0.0345 and 0.8123 ± 0.0387) vs WT0 (0.6879 ± 0.0255) (**Fig. 2.3D**; one-way RM ANOVA, $F_{(1.7,8.6)} = 7.1$, $p = 0.0169$; Tukey's test WT0 vs WT12, $p = 0.0488$).

Symbiont cell densities (cells x 10^6 cm^{-2}) were higher for WT12 and NT12 (0.5600 ± 0.1037 and 0.7317 ± 0.1224, n = 6, respectively) compared to the initial wild colonies (WT0) (0.2525 ± 0.0368, n = 4) (**Fig. 2.3E**; one-way ANOVA, $F_{(2,13)} = 2.5$, $p = 0.0331$; Tukey's test WT0 vs NT12; $p = 0.0264$). No differences were found among coral groups for total pigment per cell, although lowest values were observed for NT12 (8.7 ± 1.1), followed by WT12 (10.5 ± 2.2) and highest values for WT0 (13.4 ± 2.2) (**Fig. 2.3F-H**; one-way ANOVA, $F_{(2,13)} = 1.3$, $p = 0.2945$; one-way ANOVA, $F_{(2,13)} = 1.7$, $p = 0.2945$; and Kruskal-Wallis, $H = 3.6$, $p = 0.1655$, respectively), consistent with higher light-acclimated symbiont photobiology (above). However, pigment per coral surface area demonstrated that NT12 (but not WT12) *A.* cf. *hyacinthus* was more pigmented than WT0 (**Fig. 2.3I-K**; one-way ANOVA, $F_{(2,13)} = 5.9$, $p = 0.0152$; one-way ANOVA, $F_{(2,13)} = 4.5$, $p = 0.0333$; and one-way ANOVA, $F_{(2,13)} = 8.1$, $p = 0.0051$), consistent with the darker colouration observed for the NT12 corals (**Fig. S2.4**). Specifically, total pigment, and Chl *a* and Chl c_2 densities (per coral surface area) were higher for NT12 (5.9 ± 0.7, 4.2 ± 0.6, and 1.7 ± 0.2, respectively) vs WT0 (3.2 ± 0.3, 2.2 ±

0.2, and 1.0 ± 0.1, respectively; Tukey's test, p = 0.0117, 0.0275, and 0.0046, respectively). Intriguingly, the chlorophyll ratio (*a*:*c2*) remained similar over time and environments (WT0 (2.3 ± 0.2), WT12 (2.8 ±0.2) and NT12 (2.6 ± 0.3); one-way ANOVA, $F_{(2,13)} = 1.1$, p = 0.3543, **Fig. 2.3L**). In summary, after 12 months of growth, colonies on both the nursery and reef contained more symbiont cells (and more pigments) (typical of lower-light adapted corals) but were counterintuitively acclimated to higher light intensities.

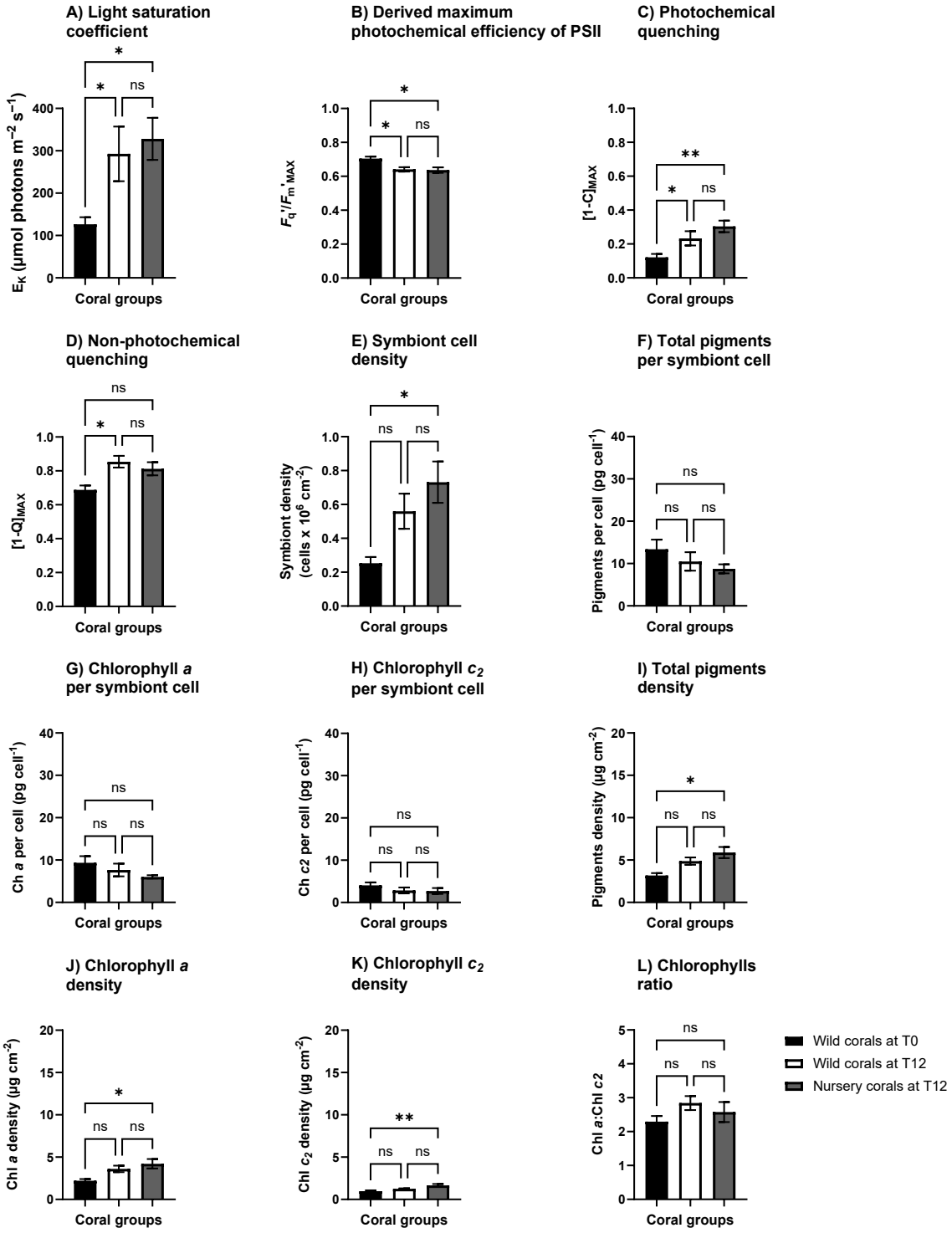
A) Light saturation coefficient
B) Derived maximum photochemical efficiency of PSII
C) Photochemical quenching
D) Non-photochemical quenching
E) Symbiont cell density
F) Total pigments per symbiont cell
G) Chlorophyll a per symbiont cell
H) Chlorophyll c2 per symbiont cell
I) Total pigments density
J) Chlorophyll a density
K) Chlorophyll c2 density
L) Chlorophylls ratio
Coral groups
Wild corals at T0
Wild corals at T12
Nursery corals at T12

Figure 2.3 Mean (± SEM) of photobiological traits for wild and nursery corals. (A) light saturation coefficient (µmol photons m^{-2} s^{-1}), (B) derived maximum photochemical efficiency of PSII, (C) photochemical quenching, (D) non-photochemical quenching, (E) symbiont cell density (cells x 10^6 cm^{-2}), (F) total pigments, (G) chlorophyll *a* and (H) *c2* per symbiont cell (F-H; pg $cell^{-1}$), and (I) total pigment, (J) chlorophyll *a* and (K) *c2* density (I-K, µg cm^{-2}), and chlorophylls ratio (L) of the initial wild colonies (WT0) and wild and nursery corals from 12 months propagation (WT12 and NT12). All data are fragments of *Acropora* cf. *hyacinthus* (n = 6 for all groups except for E-L WT0, n = 4). Means were compared by RM-ANOVA (A-D), ANOVA (E-L, except for H), and Kruskal-Wallis (H) with post hoc tests (see main text) where ns indicates no statistical significance, and * and ** indicates $p \leq 0.05$ and 0.01, respectively.

2.3.4 *Symbiodiniaceae* ITS2 identity

All samples showed an association with *Cladocopium*; however, the major ITS2 type profiles were highly variable across all groups (WT0, WT12, and NT12; see **Fig. S2.5**), with only one major ITS2 type profile (C50a/C3k/C50c/C3-C3b-C50f) present in all three groups. All four initial samples had unique major ITS2 type profiles that included C21/C3, C40/3, C3-C21-C3k-C3at-C3b-C3av-C3dp, and C50a/C3k/C50c/C3-C3b-C50f. The wild colonies after 12 months also all had distinct major ITS2 type profiles. The highest association of WT12 (3 out of 6 samples) was with *Cladocopium* of the C3k radiation, albeit three distinct C3k ITS2-type profiles observed (representative of different genotypes). Of all groups, the nursery corals had the most consistent major ITS2 type profiles, with 5 of the 6 samples associating with *Cladocopium* of the C3k radiation (4 unique type profiles). In summary, after 12 months of growth, both the wild and nursery colonies had distinct major ITS2 profiles relative to the initial wild colony major ITS2 type profiles.

2.3.5 Metabolism

Surface area-normalised gross photosynthesis rate (P_G, µmol O_2 cm^{-2} h^{-1}) of NT12 (932.5 ± 73.8) was similar to WT0 (932.4 ± 108.8) and ~35% higher than WT12 (690.0 ± 57.5) but

overall not statistically different across groups (one-way RM ANOVA, $F_{(1.6,7.9)} = 3.4$, $p = 0.0941$; note Tukey's test failed to detect differences for NT12-WT12 ($p = 0.0530$); **Fig. 2.4A**). Similarly, no differences were found in net photosynthesis (P_N, μmol O_2 cm^{-2} h^{-1}) among coral groups (one-way RM ANOVA, $F_{(1.1,5.6)} = 1.9$, $p = 0.2277$; **Fig. 2.4B**), where P_N of NT12 (278.5 ± 51.1) was slightly lower than WT0 and WT12 (442.2 ± 93.8 and 332.4 ± 33.1, respectively). In contrast to P_G and P_N, respiration rates (R, μmol O_2 cm^{-2} h^{-1}) were higher for NT12 (654.0 ± 35.4) than both WT0 and WT12 (490.2 ± 24.5 and 357.6 ± 50.6, respectively) (one-way RM ANOVA, $F_{(1.5,7.4)} = 19.3$, $p = 0.0017$; Tukey's test, $p = 0.0107$ for WT0 vs NT12 and, $p = 0.0092$ for WT12 vs NT12; **Fig. 2.4C**). Consequently, the P_G:R ratio was lower for NT12 (~1.4) than WT0 (~1.9) or WT12 (~2.1) but not statistically distinguishable between coral groups (one-way RM ANOVA, $F_{(1.5,7.6)} = 4.2$, $p = 0.0674$; **Fig. 2.4D**). Light-dependent calcification rate (G_L, μmol $CaCO_3$ cm^{-2} h^{-1}) for NT12 (0.3704 ± 0.0811; n = 4) was lower than WT0 (0.6726 ± 0.1347) and higher than WT12 (0.1112 ± 0.0411; n = 4) (**Fig. 2.4E**; one-way ANOVA, $F_{(2,11)} = 6.6$, $p = 0.0130$; note Tukey's test detected differences only for WT0 vs WT12, $p = 0.0108$). Significant differences were observed for corresponding dark calcification (G_D, μmol $CaCO_3$ cm^{-2} h^{-1}) across groups. In descending order, WT12, NT12, and WT0 were -0.3876 ± 0.1178, 0.1010 ± 0.1043, and 0.2250 ± 0.0654, respectively; **Fig. 2.4F**; one-way RM ANOVA, $F_{(1.2,5.9)} = 11.9$, $p = 0.0124$), particularly Tukey's test detected differences between WT12 vs WT0 and NT12, $p = 0.0393$ and 0.0022, respectively. The G_L:G_D ratio remained constant for all coral groups (**Fig. 2.4G**; Kruskal-Wallis, $H = 6.3$, $p = 0.0327$), and Dunn's test revealed differences between WT0 and WT12 ($p = 0.0373$).

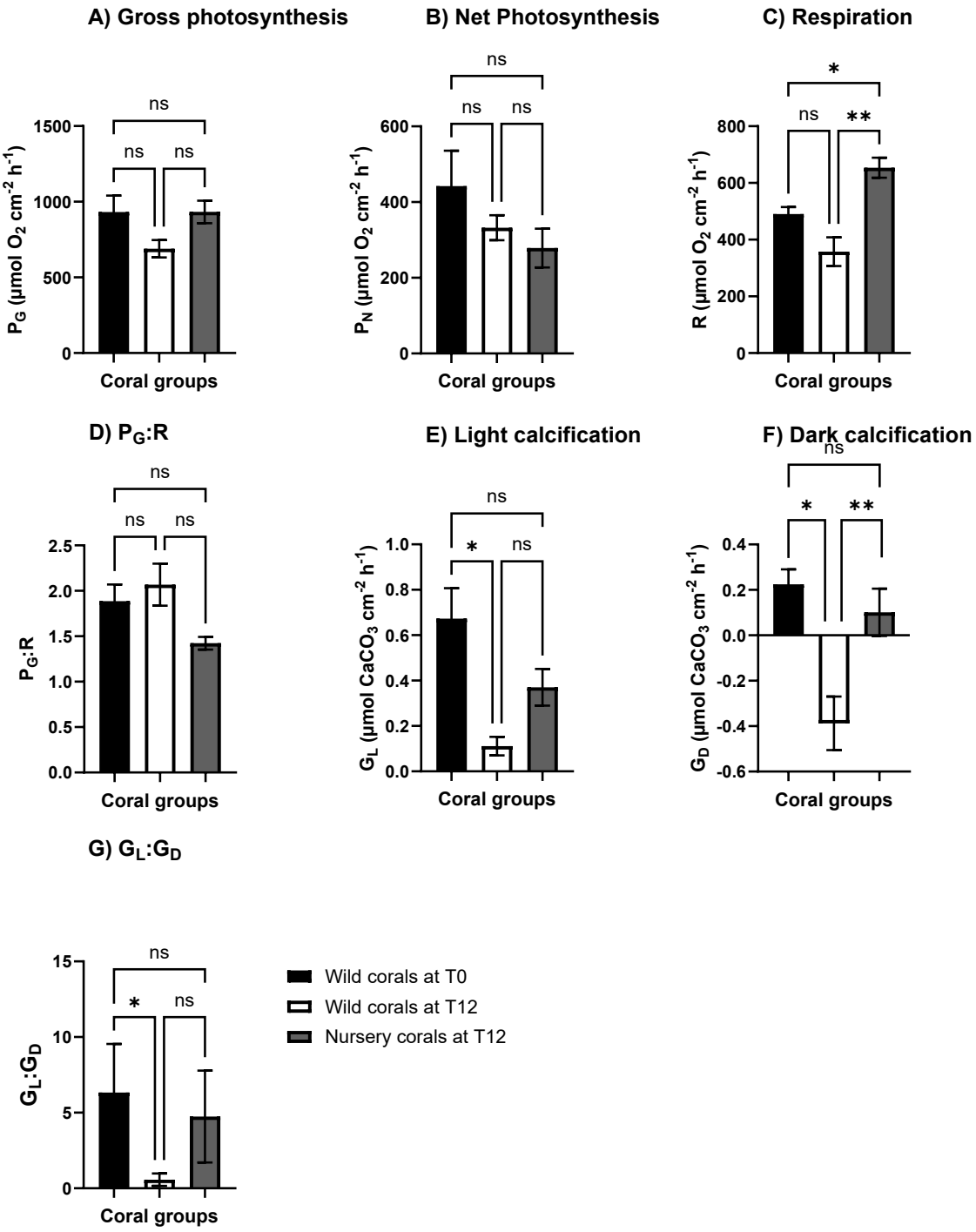
A) Gross photosynthesis
B) Net Photosynthesis
C) Respiration
D) P_G:R
E) Light calcification
F) Dark calcification
G) G_L:G_D
P_G (µmol O_2 cm^{-2} h^{-1})
P_N (µmol O_2 cm^{-2} h^{-1})
R (µmol O_2 cm^{-2} h^{-1})
G_L (µmol $CaCO_3$ cm^{-2} h^{-1})
G_D (µmol $CaCO_3$ cm^{-2} h^{-1})
G_L:G_D
Coral groups
ns
*
**
Wild corals at T0
Wild corals at T12
Nursery corals at T12

Figure 2.4 Mean (± SEM) of metabolic traits for wild and nursery corals. (A) gross and (B) net photosynthesis, and (C) respiration rates (P_G, P_N, and R, respectively; µmol O_2 cm^{-2} h^{-1}), (D) P_G:R ratio, (E) light and (F) dark calcification rates (G_L and G_D, respectively; µmol $CaCO_3$ cm^{-2} h^{-1}), and (G) G_L:G_D ratio of the initial wild colonies (WT0) and wild and nursery corals from 12 months propagation (WT12 and NT12). All data are fragments of *Acropora* cf. *hyacinthus* (n = 6 for each group). Means were compared by one-way (repeated measures) analysis of variance (ANOVA) with post hoc Tukey tests, except for (G) (Kruskal-Wallis's test followed by Dunn's test) (see main text) where ns indicates no statistical significance, and * and ** indicates $p \leq 0.05$ and 0.01, respectively.

2.3.6 Energy reserves and tissue biomass

No differences were found for any of the 28 energetic characteristics when nursery-propagating corals were compared to their wild counterparts (NT12 vs WT12) (**Fig. 2.5**, **Fig. S2.7** and **Fig. S2.8**). However, a time effect was observed for carbohydrate, lipid, and protein content (mg:mg dry weight [DW]) and total energy reserves (J:g DW), whereby wild corals at T12 exhibited more energetic reserves to total tissue biomass compared to WT0 (**Fig. 2.5A-D**). Specifically, carbohydrate concentrations for WT0, WT12, and NT12 were 0.0101 ± 0.0022, 0.0252 ± 0.0023, 0.0293 ± 0.0058, respectively; lipid content was 0.0984 ± 0.0107, 0.1356 ± 0.0098, and 0.1339 ± 0.0071; and protein content 0.0254 ± 0.0034, 0.0407 ± 0.0035, and 0.0415 ± 0.0019, respectively. Energy reserves determined from the carbohydrate, lipid, and protein contents were lower for WT0 (4671.0 ± 468.5) compared to WT12 and NT12 (6770.0 ± 414.9, and 6794 ± 222.3, respectively). Carbohydrate concentrations were significantly different between WT0 and NT12 ($p = 0.0222$), while soluble proteins, total energy reserves and dry weight biomass from WT12 and NT12 were significantly different from WT0 (Tukey's test WT12 vs WT0; $p = 0.0110$, 0.0053 and 0.0011, respectively, and Tukey's test NT12 vs WT0; $p = 0.0079$, 0.0049, 0.0101, respectively), but not from each other, while lipid content was significantly higher for WT12 than WT0 (Tukey's test, $p = 0.0421$), but not for NT12. Note for comparability, **Fig. S2.6A-D** presents the same data normalised to ash-free dry weight and surface area, but where no

differences were detected amongst coral groups (except for soluble proteins, Tukey's test WT0 vs NT12; p = 0.0460). Surface area-normalised total dry weight tissue biomass (mg DW cm^{-2}; **Fig. 2.5E**) — but not the ash-free total dry weight biomass (mg DW cm^{-2}; **Fig. 2.5F**) — was significantly greater for WT0 (21.4 ± 2.3) than WT12 and NT12 (12.1 ± 1.0, and 14.5 ± 1.0) (Tukey's test; p = 0.0011 and 0.0101, respectively). Thus, despite the greater growth of *A.* cf. *hyacinthus* for nursery compared to reef colonies over 12 months, all colonies exhibited less tissue biomass (but more energy reserves) at 12 months compared to initial samples. A strong time effect (but not location effect) was also observed when profiling lipids in more detail via 19 fatty acid molecules (**Fig. S2.7**). In general, differences in MUFA and PUFA (mono- and poly-unsaturated fatty acids) (one-way ANOVA, $F_{(2,13)}$ = 4.5, p = 0.0324, and one-way ANOVA, $F_{(2,13)}$ = 6.7, 0.0099, respectively) but not in SFA (saturated fatty acids; one-way ANOVA, F(2,13) = 3.8, but note p = 0.0501) were found for both nursery and reef corals at T12 compared to T0 (**Fig. S2.8**).

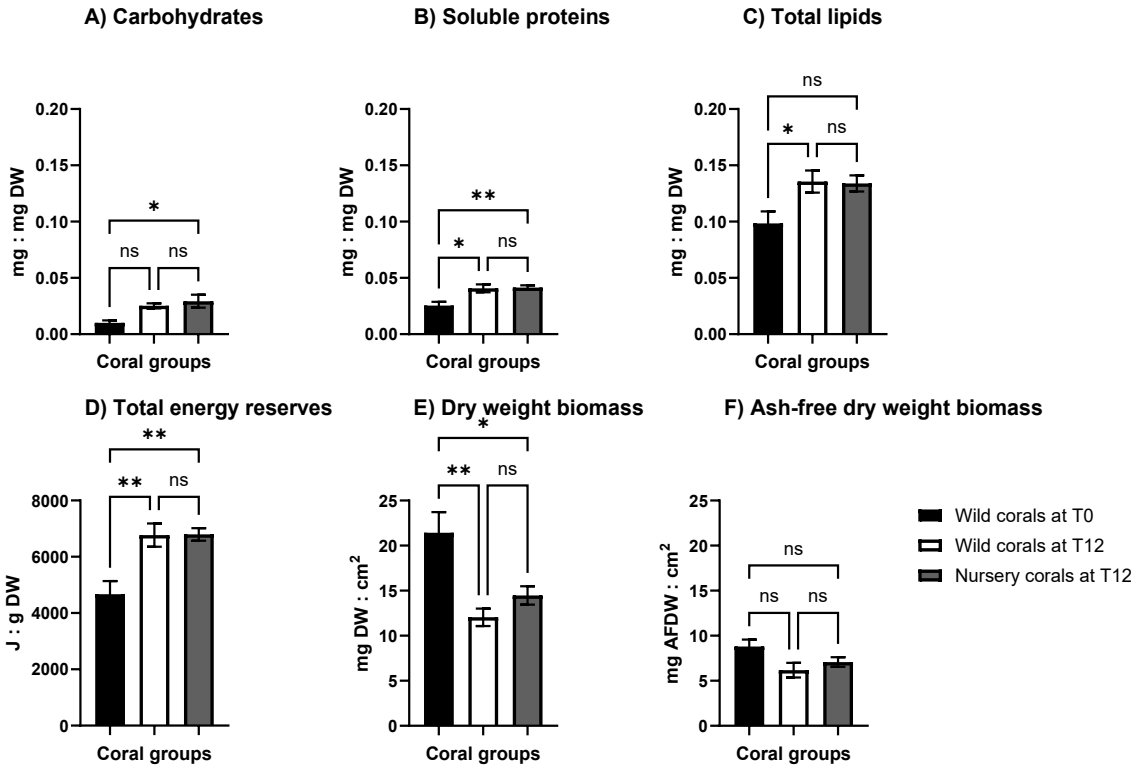

Figure 2.5 Mean (± SEM) of energetic traits for wild and nursery corals. (A) carbohydrates, (B) soluble proteins, and (C) total lipids (mg per dry mass), (D) total energy reserves (J per dry mass), (E) dry weight and (F) ash-free dry weight biomass (mg DW and mg AFDW per surface area, respectively) of the initial wild colonies (WT0) and wild and nursery corals from 12 months propagation (WT12 and NT12). All data are fragments of *Acropora* cf. *hyacinthus* (n = 4, 6, and 6 for WT0, WT12, and NT12, respectively). Means were compared by analysis of variance (ANOVA) with post hoc Tukey tests (see main text) where ns indicates no statistical significance, and * and ** indicates $p \leq 0.05$ and 0.01, respectively.

2.3.7 Elemental content

After 12 months propagation, carbon-to-nitrogen ratios (C:N) for WT0, WT12, and NT12 were similar (7.11 ± 0.18, 7.02 ± 0.24, and 6.98 ± 0.54, respectively) (**Fig. 2.6A**; ANOVA, $F_{(2,12)} = 0.0238$, $p = 0.9765$). In contrast, carbon-to-phosphorus (C:P) and nitrogen-to-phosphorus (N:P) ratios for WT0 (1332.9 ± 223.5, and 189.9 ± 35.7) were 100% significantly greater than WT12 (679.6 ± 72.0, and 94.8 ± 7.6; n = 5) and NT12 (604.7 ± 95.9, and 84.4 ± 8.55), respectively (one-way ANOVA, $F_{(2,12)} = 8.8$, $p = 0.0045$, and one-way ANOVA, $F_{(2,13)}$

= 10.3, p = 0.0021; **Fig. 2.6B-C**). This change over time appeared driven by lower P content in WT0 (0.0208 ± 0.0028 mmol P g sample^{-1}; **Fig. S2.9D**). Furthermore, C:N:P was highest for WT0 (1333:190:1) compared to W12 and NT12 (680:95:1 and 605:84:1, respectively), and all were significantly higher than the Redfield ratio of 106:16:1 (Redfield, 1934).

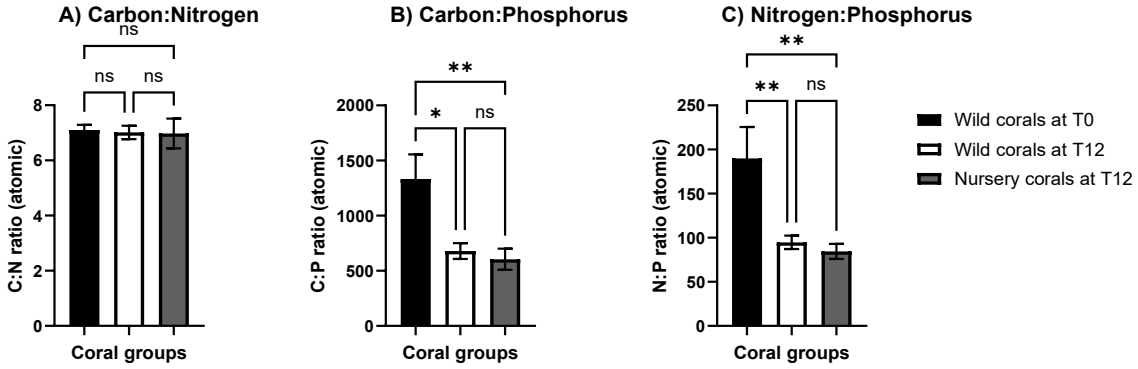

Figure 2.6 Mean (± SEM) of elemental traits for wild and nursery corals. (A) C:N, (B) C:P, and (C) N:P ratios (C, carbon; N, nitrogen, and P, phosphorus; atomic values) of the initial wild colonies (WT0) and wild and nursery corals from 12 months propagation (WT12 and NT12). All data are fragments of *Acropora* cf. *hyacinthus* (n = 4, 6, and 6 for WT0, WT12, and NT12, respectively). Means were compared by analysis of variance (ANOVA) with post hoc Tukey tests (see main text) where ns indicates no statistical significance, and * and ** indicates $p \leq 0.05$ and 0.01, respectively.

In general, no differences were detected over time (WT0 vs WT12) or at 12 months post-propagation (WT12 vs NT12) for C, N, P, and 17 major and trace elements (**Fig. S2.9**), except for magnesium, phosphorus, sulphur, and potassium (WT0 vs NT12, Tukey's test; p = 0.0294, 0.0083, 0.0197, and 0.0130, respectively; **Fig. S2.9C-F**). Significant differences were also found for Cu content, where NT12 (0.8836 ± 0.1097) was similar to WT0 (0.9543 ± 0.0624) and higher than WT12 (0.5567 ± 0.0434); one-way ANOVA, $F_{(2,13)} = 6.8$, p = 0.0096; Tukey's test WT0 vs WT12, and WT12 vs NT12; p = 0.0159, and 0.0260, respectively; **Fig. S2.9L**.

2.3.8 Skeletal properties

Skeletal traits appeared largely unchanged after 12-months of propagation (WT12 vs NT12) (bulk volume, bulk density, biomineral density, pore volume, apparent (internal) porosity, hardness, and colony mass per area; **Fig. 2.7A-G**). The only exception was hardness (HD) (**Fig. 2.7F**; one-way RM ANOVA, $F_{(1.4,7.2)} = 8.2$, $p = 0.0182$, Tukey's test WT0 vs WT12, $p = 0.0488$) where values were higher for WT0 (38.8 ± 1.5) than both WT12 or NT12 after 12 months (31.5 ± 1.1, and 35.3 ± 0.9, respectively). Also, significant differences in biomineral density were found for WT0 vs NT12 (Tukey's test, $p = 0.0387$). Thus, overall, propagation in nurseries compared to the reef did not result in a difference in skeletal properties despite the greater growth rates observed for nursery colonies (**Fig. 2.2B**).

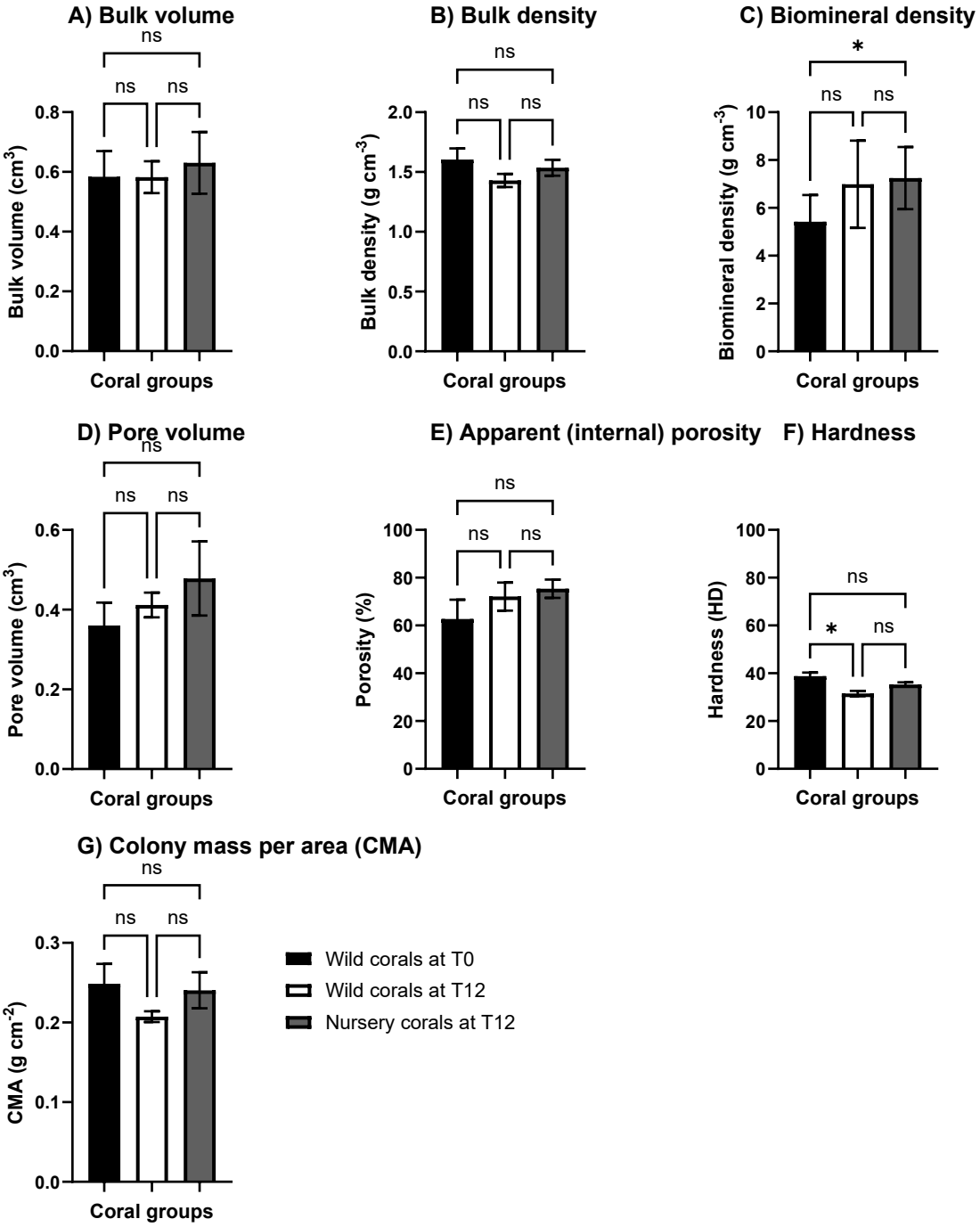

Figure 2.7 Mean (± SEM) of skeletal traits for wild and nursery corals. (A) bulk volume (cm^3), (B) bulk density (g cm^{-3}), (C) biomineral density (g cm^{-3}), (D) pore volume (cm^3), (E) apparent (internal) porosity (%), (F) hardness (HD), and (G) colony mass per area (g cm^{-2}) of the initial wild colonies (WT0) and wild and nursery corals from 12 months propagation (WT12 and NT12). All data are fragments of *Acropora* cf. *hyacinthus* (n = 6 for each group). Means were compared by one-way (repeated measures) analysis of variance (ANOVA) with post hoc Tukey tests (see main text) where ns indicates no statistical significance, and * indicates $p \leq 0.05$.

2.3.9 Multi-trait assessment and "trait redundancy"

We finally performed a series of principal components analysis (PCA) to reduce the trait space and identify the main drivers of variance from amongst the 90 traits examined (**Table S2.1**). Specifically, a PCA was first conducted for each of the following seven biological properties: physical appearance, photobiology, metabolism, energy reserves, FAME, elementome, and skeletal traits; to identify the two main contributing traits to the variation (**Table S2.2A**) beyond survivorship and growth, and in doing so where "trait redundancy" (i.e., traits that have similar contribution to the separation of coral groups) existed within biological properties. This was observed via overlapped trait-based vectors and correlated variables in **Fig. S2.10** and **Table S2.2A**, respectively. A total of 14 (of 90) traits (brightness, blue, symbiont cell density, maximum photochemical efficiency of PSII [$F_q'/F_m'_{MAX}$], dark and light calcifications [G_D and G_L, respectively], total energy reserves, ash-free dry weight biomass, methyl arachidate, methyl myristoleate, potassium [K], strontium [Sr], pore volume, and biomineral density) were identified as the strongest drivers of variation from the individual PCAs (**Table S2.3**), and were therefore subsequently selected for the final PCA (the so-called multitraits; **Fig. 2.8**). We observed spatial separation between the three groups (WT0, WT12, and NT12), despite some overlap; and where WT0 was somewhat separated from WT12 and NT12 (**Fig. 2.8**). Overall, 51.6% of the coral trait variance between coral groups was accounted by the first and second principal components collectively (PC1 and PC2, respectively; **Table S2.3B**). PC1 accounted for 34.5% of the total trait variance of the coral holobiont, with the following top 4 loadings: methyl arachidate (15.41%), total energy reserves (14.49%), blue (11.47%), and K (10.47%) (see **Table S2.3A** for contributions by the rest of the traits) contributing the largest loadings to this vector (**Fig. 2.8**). A further 17.1% of the total trait variance was accounted for by PC2, with brightness (25.77%), dark calcification

(15.80%), ash-free dry weight biomass (11.51%), and symbiont cell density (8.23%) followed by other traits (see **Table S2.3A**) contributing the largest loadings to this vector (**Fig. 2.8**). Differences between coral groups were dependent on both PC1 and PC2, with PC resolving separation between all three coral groups. Here, WT0 separated from NT12 by PC1 ($p = 0.0237$; **Table S2.4A**), whilst all three coral groups were separated from each other by PC2 (WT0-WT12, WT0-NT12, and WT12-NT12; $p = 0.025$, 0.027, and 0.0067, respectively). However, the one-way PERMANOVA between coral groups for the main 14 traits did not return differences between coral groups ($p = 0.3706$; **Table S2.5**).

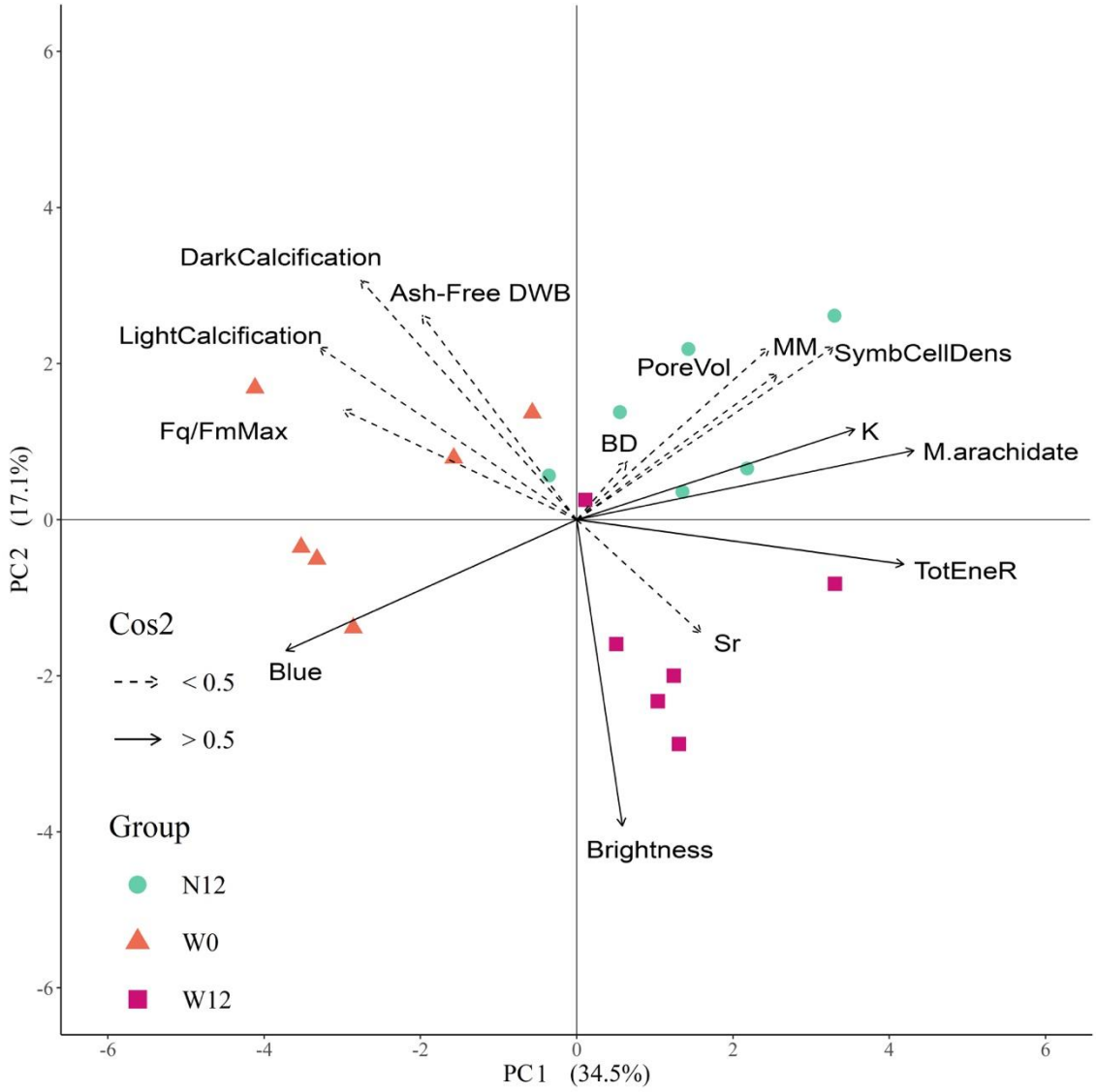

Figure 2.8 Principal Component Analysis (PCA) of 14 (out of 90) coral traits comparing initial wild colonies (W0; triangles in orange) and wild and nursery corals from 12 months propagation (W12 and N12; squares and circles in pink and green, respectively). PCA biplot, including a cut-off for the cos2 = 0.5, where > 0.5 (in solid line) indicates a good representation of the variable on the PC. As opposed, < 0.5 (dashed line) indicates that the variable is not perfectly represented by the PCs. BD and MM refer to biomineral density and methyl arachidat, respectively.

2.4 Discussion

Most coral reef restoration project goals focus on recovery of a functionally healthy and self-sustaining reef ecosystem. However, evaluations of success towards this goal to date have largely rested on few ecological (Hein et al., 2020b, 2020a; Nuñez Lendo et al., 2024) or

biological metrics (e.g., coral growth and survival; Boström-Einarsson et al., 2020; Rinkevich, 2019) rather than more specific metrics that inform ecosystem services outcomes (Boström-Einarsson et al., 2020; Hein et al., 2021, 2017). We therefore examined how deeper mining of coral biological multi-trait expression encompassing bio-physical, and bio-chemical properties, can potentially provide more meaningful descriptions of success beyond growth and survival alone. Our observations — using *Acropora* cf. *hyacinthus* grown over 12 months on the Great Barrier Reef (GBR) — demonstrated higher relative growth rates (but comparable survivorship) for nursery compared to wild grown colonies. However, these higher growth rates were underpinned by higher respiration and dark calcification rates, as well as more pigmented — darker-coloured, more symbiont cells and pigments per surface area — colonies. Intriguingly, this "nursery effect" occurred against a backdrop of a different dominant symbiont ITS2 type profile with overall higher light acclimation (E_K, more quenching capacity) and more symbiont cells and pigments (per surface area), hosted by the corals after 12 months of growth for both nursery and wild colonies. Other key properties, including elemental and bio-molecular content (carbohydrates, lipids, proteins, and fatty acid methyl esters) and skeletal properties — appeared less affected by nursery propagation over 12 months. Thus collectively, compared to growth and survivorship, the multi-trait evaluation yields insight into potential changes in colony performance and reef functioning, and hence factors governing overall ecological success.

2.4.1 Biological responses to nursery propagation

High survivorship and relative growth rates of *A.* cf. *hyacinthus* in nurseries of our study site (Mojo, Opal Reef) are consistent with previous observations from the same nursery approach at different sites of the same reef (Howlett et al., 2021; Suggett et al., 2019). Specifically, Howlett et al., (2021) reported *A. hyacinthus* areal growth rates of 1-2 cm^2 $month^{-1}$

(equivalent to 14.4 cm^2 y^{-1}; RayBan) to 10.8 cm^2 $month^{-1}$ (129.6 cm^2 y^{-1}; Blue Lagoon), where the latter site is close to our study site (Mojo, ca. 200 m away) that yielded areal growth of 30 cm^2 $month^{-1}$ (equivalent to > 300 cm^2 y^{-1}). In water, light availability generally appears lower at RayBan than Mojo/Blue Lagoon (Howlett et al., 2021), where these lower areal growth rates are consistent with those measured for *A. hyacinthus* in more turbid environments (e.g., Singapore reefs, Bongiorni et al., 2011).

Most intriguing was the higher growth (20-25 times greater) observed for our nursery grown compared to reef grown *A.* cf. *hyacinthus*. Few studies to date have evaluated the growth performance of corals in nurseries compared to their respective source colonies retained on the reef; for example, linear growth of the branching coral *Acropora formosa* was previously shown to be ~5-50% faster in nurseries than in the natural neighbouring reef (Malaysia; Xin et al., 2016). Such higher growth rates in nurseries have been proposed to reflect more favourable biological and physical conditions where nurseries are often located away from the reef; these include improved light availability (lower sedimentation), increased water flow, enhanced planktonic supply, reduced intra- and interspecific competition, and controlled corallivory (Bongiorni et al., 2011; Levy et al., 2010; Rinkevich, 2005; Shafir and Rinkevich, 2010, 2008). Whilst we cannot currently verify the specific nature of our higher nursery growth rates, our nursery design is conducive to coral growth via a low surface area and reduced drag to enable relatively unimpeded water flow (e.g., Howlett et al., 2021), which is essential for coral metabolism (Nakamura and Van Woesik, 2001; West and Salm, 2003), and supply of planktonic food for heterotrophic feeding (Borell et al., 2008). Corals on our nurseries are typically observed with their polyps out during the day, and also fish-associated nursery communities comprise few (if any) persistently present corallivore fish (All authors, Pers. Obs.). However, it is also possible that higher growth gains for nursery

corals — which start as relatively small fragment sizes of 64.3-191.7 cm^2 — in part reflect more rapid growth compared to established adult colonies (e.g., Warne et al., 2022). When a sexually mature coral colony is fragmented below a certain size, it redirects resources towards regrowth rather than reproduction (Lirman, 2000; Zakai et al., 2000). Consequently, the size and life stage (age) of corals employed in restoration efforts inevitably affect their performance, as freshly fragmented coral exhibits higher growth and regeneration rates (i.e., following trauma, corals undergo rapid tissue and skeletal repair; Bak, 1983; Chadwick and Loya, 1990; Loya, 1976; Meesters et al., 1994) compared to well-established adult colonies, which above a size threshold, shift resources from growth to sexual reproduction (Babcock, 1991; Kojis and Quinn, 2001; Soong, 1993).

Both bio-optical and metabolic traits were observed to change for nursery compared to wild-grown corals. Photographic-based traits revealed colonies became darker in the nursery over 12 months (compared to on the reef) (**Fig. S2.4**), accompanied by more pigmentation per colony surface area (**Fig. 2.3 I-K**). At face value, this darker colouration might appear indicative of acclimation to lower light intensities, as increases in coral pigmentation often occur via low-light acclimation (Falkowski and Dubinsky, 1981; Hennige et al., 2009; Iglesias-Prieto and Trench, 1994). However, the photophysiology, in fact, indicated that both nursery and wild colonies had become high-light acclimated over the growth period, as indicated by a two-fold higher E_K in these coral groups (Lohr et al., 2019; Nitschke et al., 2018; Suggett et al., 2012), while symbiont cells also generally contained less photosynthetic pigments (Hennige et al., 2009) (**Fig. 2.3 A** and **F-H**). Despite the high variance in major ITS2 type profiles (**Fig. S2.5**) and consequent unique genotypes, such acclimation over time might reflect that both reef and nursery major symbiont type moved to C3k predominantly over 12 months. Presumably, host-symbiont metabolic compatibility changed to match a

change in the prevailing resources available (e.g., light; Suggett et al., 2017) — but where specific nursery growth conditions were further fundamentally altered compared to the reef. For example, lower symbiont densities have been observed under higher temperatures (e.g., Brown et al., 1999; Fagoonee et al., 1999; Fitt, 2000; Scheufen et al., 2017)) and lower inorganic nutrient supply (Brown et al., 1999; Dubinsky et al., 1990; Ferrier-Pagès et al., 2001; Stimson and Kinzie, 1991). Ultimately however, the exact nature of increased symbiont density cannot be verified without further detailed assessments of specific environmental histories in the reef compared to adjacent nursery habitats.

The high ITS2 type profile variance found across all coral groups was perhaps somewhat surprising, assuming a highly connected population (Hock et al., 2017). Future work expanding the number of samples taken per colony would help resolve whether any intra-colony variance in major ITS2 type profiles explain the variance found here (Lewis et al., 2022). In contrast, high homogeneity in major ITS2 type profiles was reported on the same species in the same location (Mojo reef) in February 2020 (i.e., sampling time of our donor colonies; T0) by Grima et al., (2022). However, Kriefall et al., (2022) recently reported a high profile variance for *A. hyacinthus* sampled across dynamic Mo'orean reef habitats. As such, the shifts we observed over 12 months are likely indicative of a change in the prevailing local environmental conditions inherent to both reef and nursery habitats at Opal Reef. Interestingly, the nursery corals exhibited the most consistent ITS2 type profiles, with most samples associated with C3k. This type is considered a host-specific symbiont type in the genus *Acropora* (Tonk et al., 2013) and is associated with strongly performing holobiont colonies when exposed to sub-optimum environmental conditions (Howe-Kerr et al., 2020). However, careful consideration should be taken when considering the dominant symbiont type shift to be the cause of acclimation as there are many distinct ITS2 predicted profiles not

previously reported in *A. hyacinthus* that could yield different photophysiologies given they are predicted unique genotypes (Camp et al., 2020c).

More symbionts per surface area for nursery-grown corals after 12 months were accompanied by almost 50% higher respiration rates (R) in nursery coral compared to wild corals after 12 months growth. Higher R indicates higher basal metabolic traits (Bruno and Edmunds, 1998; Szmant-Froelieh and Pilson, 1984) associated with greater heterotrophic activity (Levy et al., 2006; Wooldridge, 2014) of either stored energy or acquisition of new energy, which in the latter case for corals may occur through enhanced feeding (Levy et al., 2006; Wooldridge, 2014). Indeed, corals have previously been suggested to grow faster through enhanced capacity to feed in higher flow waters compared to the reef (Borell et al., 2008). We, therefore, propose that greater respiratory rates may be due to higher rates of heterotrophic activity, which may be a critical feature supporting higher growth rates possibly through enhanced feeding in our nurseries. However, future studies should verify this hypothesis with targeted feeding studies.

All coral groups had higher C:N:P values than 106:16:1 (typically from phytoplankton; Ptacnik et al., 2010; Redfield, 1934), and might be explained by the coral-symbiont relationship and their nutrient cycling and uptake (Dubinsky and Jokiel, 1994; Rahav et al., 1989). All coral groups exhibited similar C:N (values of ~7), which is consistent with recent studies (Blanckaert et al., 2020; Grima et al., 2022), highlighting the conservative nature of this feature in corals, but also across other taxa, e.g., phytoplankton (Garcia et al., 2018). Higher C:N is indicative of elevated carbon-rich storage materials (Szmant et al., 1990), so the stability of C:N despite the increase in total lipids compared to carbohydrates measured

over time (**Fig. 2.5AC** and **Fig. 2.6**) could be considered surprising. However, in marine phytoplankton under N limitation, species that accumulated lipids over carbohydrates saw small changes in their C:N (Liefer et al., 2019), which could perhaps explain the results observed here but clearly requires further targeted investigation in future. Our data demonstrated similar C:P and N:P for both the wild and nursery corals at the end of the experiment, despite the marked differences in their growth rates. Intriguingly, the Growth Rate Hypothesis (GRH) predicts a positive relationship between phosphorus (P) content and growth rate in invertebrates, where P content decreases due to allocation to RNA synthesis during the organism's growth (Main et al., 1997). Thus our observations for corals here add to the growing body of evidence refuting the GRH when P is not limiting and can be stored in excess (Camp et al., 2022; Norici et al., 2011; Sterner and Elser, 2003).

Of the coral elemental profiles (n = 20) in our study, corals grown in their (non-native) nursery environments exhibited higher growth but no change in elemental content suggesting that the "biochemical niche" (*sensu* Grima et al., 2022) largely did not differ from neighbouring reef (**Fig. S2.9**). As such, biogeochemical service provision — e.g., elemental quotas available for trophic transfer — was unaltered through nursery growth. The one exception was the higher Cu for nursery corals compared to the wild colonies after 12 months. Given the higher respiration rates for nursery grown corals, it is plausible to propose that this higher Cu reflects higher metabolic requirements where Cu is an essential cofactor for aerobic respiration (it acts as a redox cofactor in the Cytochrome *c* Oxidase) (Llases et al., 2019). In *Chlamydomonas*, the "Cu economy" involves substituting copper-containing plastocyanin with heme-containing cytochrome; in turn, the Cu that is saved by this replacement is used instead for COX biosynthesis, prioritizing allocation and reallocation of copper to respiration vs. photosynthesis (Kropat et al., 2015). Verifying this hypothesis

warrants further investigation (e.g., the presence of transcripts encoding proteins belonging to COX).

Finally, greater metabolic potential to support enhanced growth is important to ensure that coral skeletal properties are retained, i.e., more resources to ensure faster growth does not result in a weaker skeleton. We observed lower light and dark calcification rates per coral surface area for nursery and wild corals after 12 months compared to initial wild colonies (but differences were only detected in WT12-WT0 light and dark calcification rates and WT12-NT12 dark calcification rates; **Fig. 2.4E-F**). Based on our current data available, it is not clear why calcification rates lower after 12 months, however this reduction might reflect that environmental conditions have changed over time. Importantly, we observed that dark calcification rates per coral surface area were, in fact, > 5 times higher for nursery compared to wild corals after 12 months, aligning with the higher growth rates for nursery corals (20-25 times higher). Such an outcome is perhaps expected since higher growth is accompanied by higher calcification (Kuffner et al., 2017; Lizcano-Sandoval et al., 2018) in other coral species reared in nurseries. Further analysis of skeletal properties (bulk volume, biomineral density, bulk density, pore volume, apparent (internal) porosity, hardness, and colony mass per area; **Fig. 2.7**) did not reveal differences between nursery and wild grown corals that overall did not impact on skeletal strength. In particular, Lizcano-Sandoval et al., (2018) showed that skeletal density was maintained despite an increase in growth and calcification, as the opposite of another study (Kuffner et al., 2017) where there were trade-offs between skeletal density and growth, while calcification rate was conserved, depending on the nursery environment.

2.4.2 Towards a multi-trait approach to evaluate benefits of coral propagation

In evaluating 90 traits spread across multiple properties (bio-optics, metabolism, energy, lipid diversity, elementome, and skeleton), we demonstrate that faster-growing corals in nurseries undertake a significant change in metabolism and resource partitioning compared to wild grown corals, which could conceivably impact the interpretation of ecosystem service value beyond just areal gain in coral cover (see also Hein et al., 2021). Specifically, higher respiration and dark calcification can inherently alter ecosystem metabolic balance (Cyronak et al., 2018) and, in turn, biogeochemical cycling of key elements that underpin CO_2 and O_2 inventories (Camp et al., 2019, 2016b). Similarly, lower calcification may reduce skeletal strength (Crook et al., 2013; Fantazzini et al., 2015) that is critical for dissipating wave energy. Based on our nursery observations, the gains observed in areal coverage (growth rate) clearly need to be balanced in terms of costs (or additional benefits) to other ecosystem services, highlighting the need to introduce multi-trait assessments to robustly determine how nursery growth may aid reef ecosystem service value(s). In our study the enhanced growth of nursery corals did not come at a cost to skeletal integrity/strength, likely as a result of the greater metabolic activity, thus ensuring corals locally re-planted are likely of a similar robustness as the original source colonies.

Whilst we used a multi-trait approach here as a proof-of-concept for a deeper examination of biological attributes, it is clear that broad examination of many traits (initially 90 but reduced to 14 in our case) is neither routinely feasible nor often warranted. The final PCA (**Fig. 2.8**). showed multiple components that are driving the variation among coral groups. Whilst these provide a diagnostic of key factors that stand out in the biological processes of this specific case (i.e., *Acropora* cf. *hyacinthus* in an optimal nursery environment in the Northern GBR), in isolation, it is hard to resolve the collective process, although it might also indicate where

greater investigation of specific properties is required to unlock the underlying mechanisms at play. Therefore, deeper diving into the various properties is initially needed to understand why and how this final PCA emerges. In this regard, the individual PCAs (**Fig. S2.10**) showed how several key traits were instrumental in driving differences amongst nursery and wild grown corals, whereas other traits could be considered redundant. For example, vectors of surface area-normalised chlorophyll *a* and *c2* and total pigments all closely aligned (as were those for the various symbiont cell density normalised pigment contents), suggesting one descriptor of pigmentation is likely sufficient to differentiate coral groups. Similarly, in the case of the PAM-based photobiology, $F_q'/F_m'_{MAX}$ (derived maximum photochemical efficiency) separated the coral groups along an opposite vector to all of E_K, [1-Q], and [1-C], suggesting that $F_q'/F_m'_{MAX}$ and E_K may be adequate to retain these coral groups since [1-Q] and [1-C] often (but not always) reflect strategies underpinning changes to E_K (e.g., Camp et al., 2019; Nitschke et al., 2018).

Overall, fewer traits are likely sufficient to retain groupings. However, our data demonstrate that most traits provide meaningful descriptors at play (operating along different vectors). Despite the challenges of reconciling actual processes from distilling 90 traits down to 14, a multi-trait approach clearly generates deeper insight to enable more informed decision making for restoration; for example, to select species (Madin et al., 2023), stress tolerance (Gardner et al., 2017; Hoadley et al., 2021; Nitschke et al., 2018), growth factors (Suggett et al., 2022), and genetic and microbiome dynamics (Wright et al., 2019). So, practices that quantify success based on wider traits are more likely to inform how restoration may retain or alter diverse ecosystem service values. This also extends to measuring the success of nursery-grown corals once outplanted in the reef, as this is crucial to ensure the long-term future of restored corals (Boström-Einarsson et al., 2020), since the performance of coral fragments

can vary from the nursery stage to the outplanting (O'Donnell et al., 2018), and ecological success (Nuñez Lendo et al., 2024, **Chapter 4**), may only be temporary in the absence of self-sustaining coral populations.

2.5 Conclusion

In conclusion, by using a multi-trait proof-of-concept, we have shown how changes in the biological machinery underpin enhanced coral growth through nursery-based propagation compared to original donor wild corals. Our diverse trait-based observations collectively evidence an enhanced metabolism (photosynthetic, respiratory, and calcifying activity) and pigmentation, likely through heterotrophic feeding under nursery conditions. As such, we show that nursery grown corals carry attributes that may impact the perceived ecosystem value beyond simply addition of new coral biomass to the reef; for example, changes in the biogeochemical cycling of key elements that underpin CO_2 and O_2 inventories (through respiration and dark calcification). Our findings strongly support the notion of the need for coral restoration practices to move beyond a few "simple" metrics of growth and survivorship (e.g., Hein et al., 2021) as measures of success, where goals are to improve (or retain) the ecosystem service value(s).

2.6 Acknowledgements

We wish to thank the past, present, and emerging Gadigal of the Eora Nation, Yidinji, Gunggandji, Yirrganydji, and Kuku Yalanji Traditional Owners of the land and sea country where our research took place. Also, to Dr. Matthew Nitschke, Dr. Samantha Goyen, Dr. Jennifer Matthews, Dr. Unnikrishnan Kuzhiumparambil, Dr. Trent Haydon, Dr. Mickael Ros, Paige Strudwick, Amanda Grima, Sage Fitzgerald, Rachel Alderdice; Wavelength crew

including Jenny Edmondson, Lorna Howlett, Christine Roper, Tahn Miller, and Climate Change Cluster and Faculty technical staff, Paul Brooks, Erin Lockhart, Scott Allchin, Kun Xiao, Helen Price, Rachel Keeys, Susan Fenech, Herbert Yuan, Taya Lapshina, Penny McCracken, and Dr Alexander Angeloski. This research was supported by an International Research Scholarship (IRS) and UTS President's Scholarship (UTSP) to CINL. Access to sites and coral material, as well as contributions of DJS, EC and JE to writing and manuscript preparation, was facilitated through funding to the Coral Nurture Program from the Australian & Queensland Governments “Solving the bottleneck of reef rehabilitation through boosting coral abundance: Miniaturising and mechanising coral out-planting” in 2020; and the partnership between the Australian Government’s Reef Trust and the Great Barrier Reef Foundation in 2021; also, the many in kind contributions from Wavelength Reef Cruises crew who have tirelessly supported the work at Opal Reef since 2018. Contribution of EFC was through the University of Technology Sydney Chancellor’s Postdoctoral Research Fellowship and ARC Discovery Early Career Research Award (DE190100142). All material was collected under permit G20/43740.1 and G21/45224.1 (2020, and 2021, respectively) from the Great Barrier Reef Marine Park Authority.

2.7 Supplementary Material

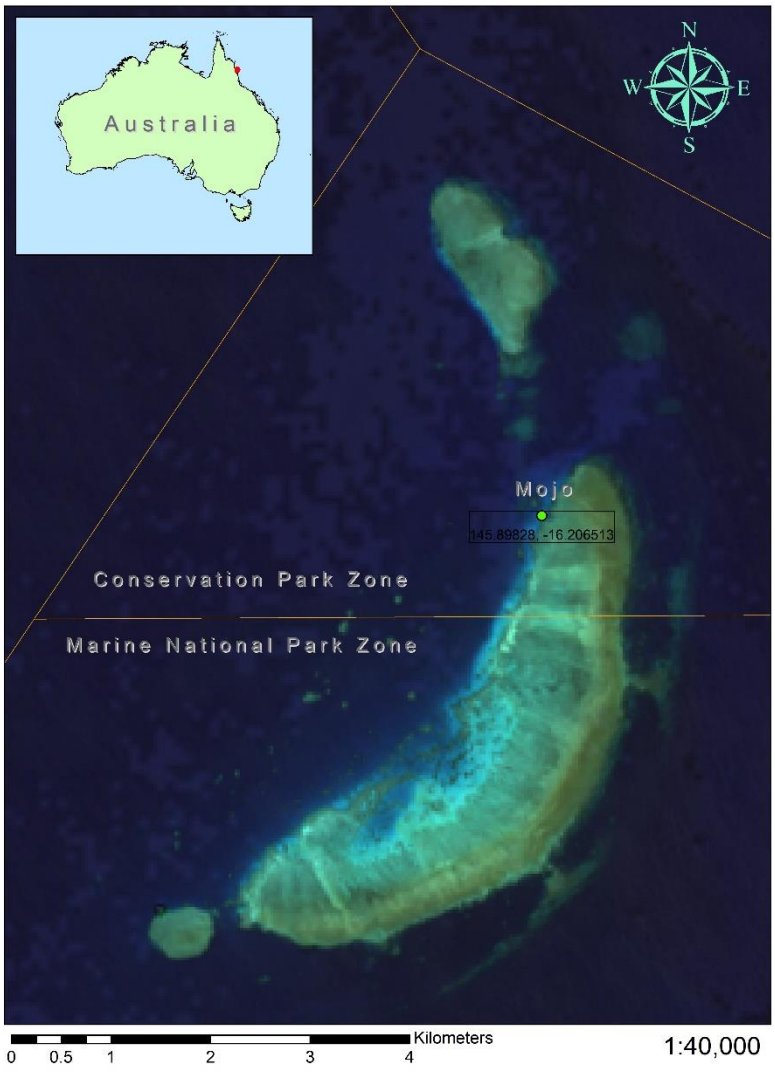

Figure S2.1 Map of study site on Mojo, Opal Reef, Great Barrier Reef, Australia. Corals were collected from the reef patch adjacent to the coral nursery at 5–6 m in depth. Coral fragments were held on the coral nursery, which is located on the sand patch, suspended at 4-5 m in depth. Delineation of the management zones for Opal Reef is shown. Satellite image: Landsat 8 OLI, bathymetric composite RBG bands 431, acquired September 5th, 2021. Source: NASA/USGS/Pearce, S. 2021.

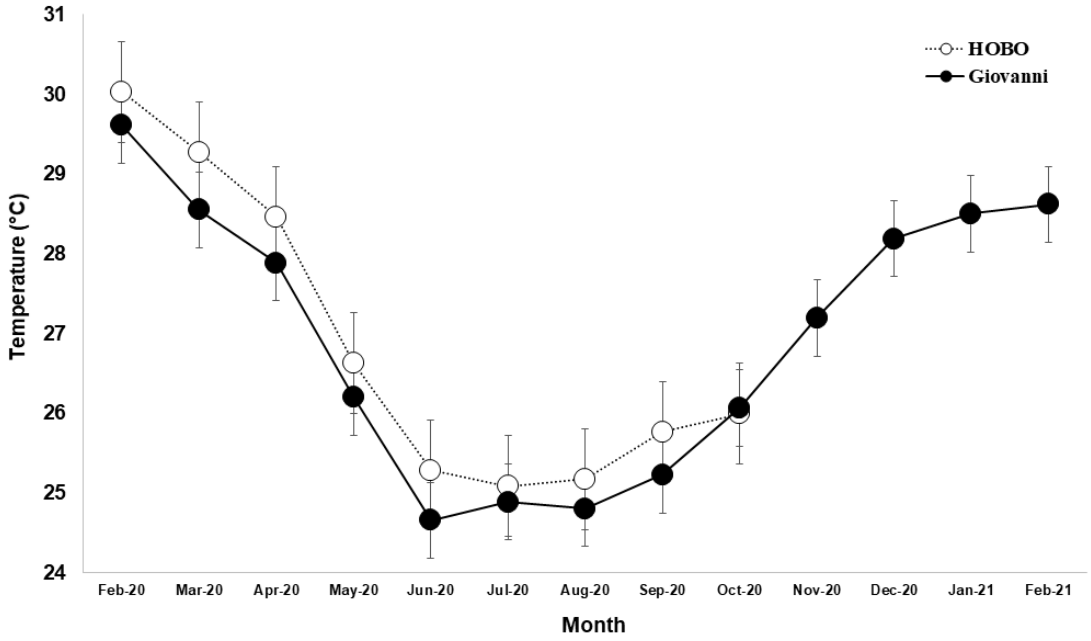

Figure S2.2 Sea Surface Temperatures (SST, °C) for Opal Reef and Mojo nursery (mean ± SEM, n = 13 and 9 months, respectively). Satellite-derived data (MODIS-aqua) was extracted from the GIOVANNI online system maintained by NASA (https://giovanni.gsfc.nasa.gov/giovanni/). SST were obtained using monthly area-averaging bounded to 145° 53' 53.8''E, 16°12' 23.4''S between February 2020 and February 2021 (encompassing the entire Opal Reef of ca. 30 km^2 for a year); black line. Imposed onto the SST are the mean monthly SST recorded by the HOBO logger (every 1 h) from February to September 2021 at the Mojo nursery; dashed line.

A)

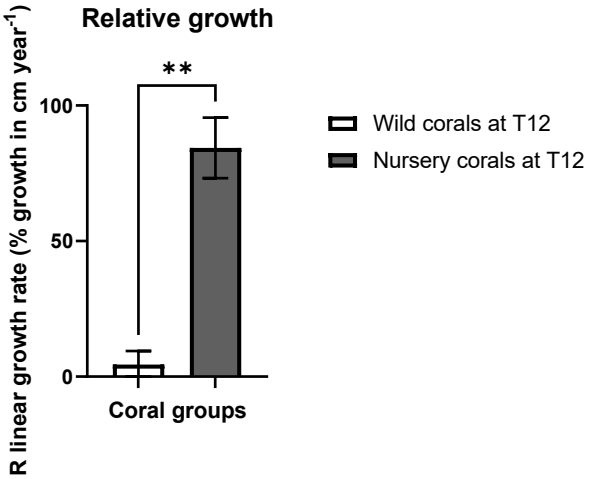

B)

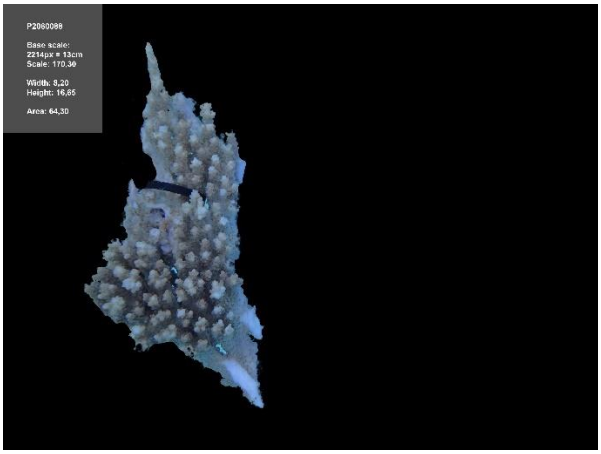

C)

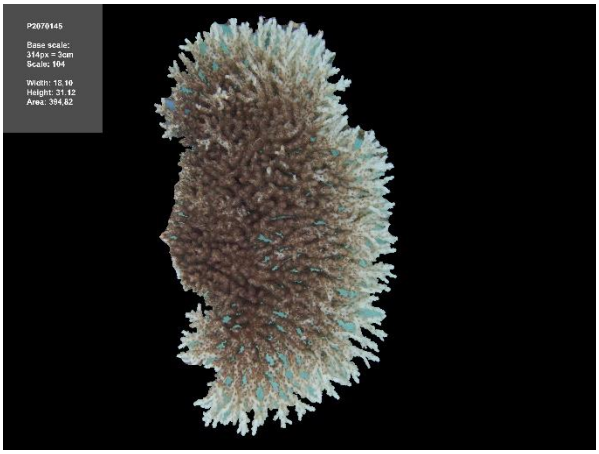

Figure S2.3 A) Mean (± SEM) relative linear growth rate (% growth in cm yr^{-1}) of wild and nursery corals from 12 months propagation. All data are fragments of *Acropora* cf. *hyacinthus* (n = 6 for both groups). Means were compared by paired Student's t-tests (see main text) where ** indicates a statistical significance of $p \leq 0.01$. B) Nursery-grown coral derived from colony #1 with an initial area of 64.3 cm^2 in February 2020 (B) and 12 months post-fragmentation the same nursery coral was six times higher (394.8 cm^2) compared to its initial size (C).

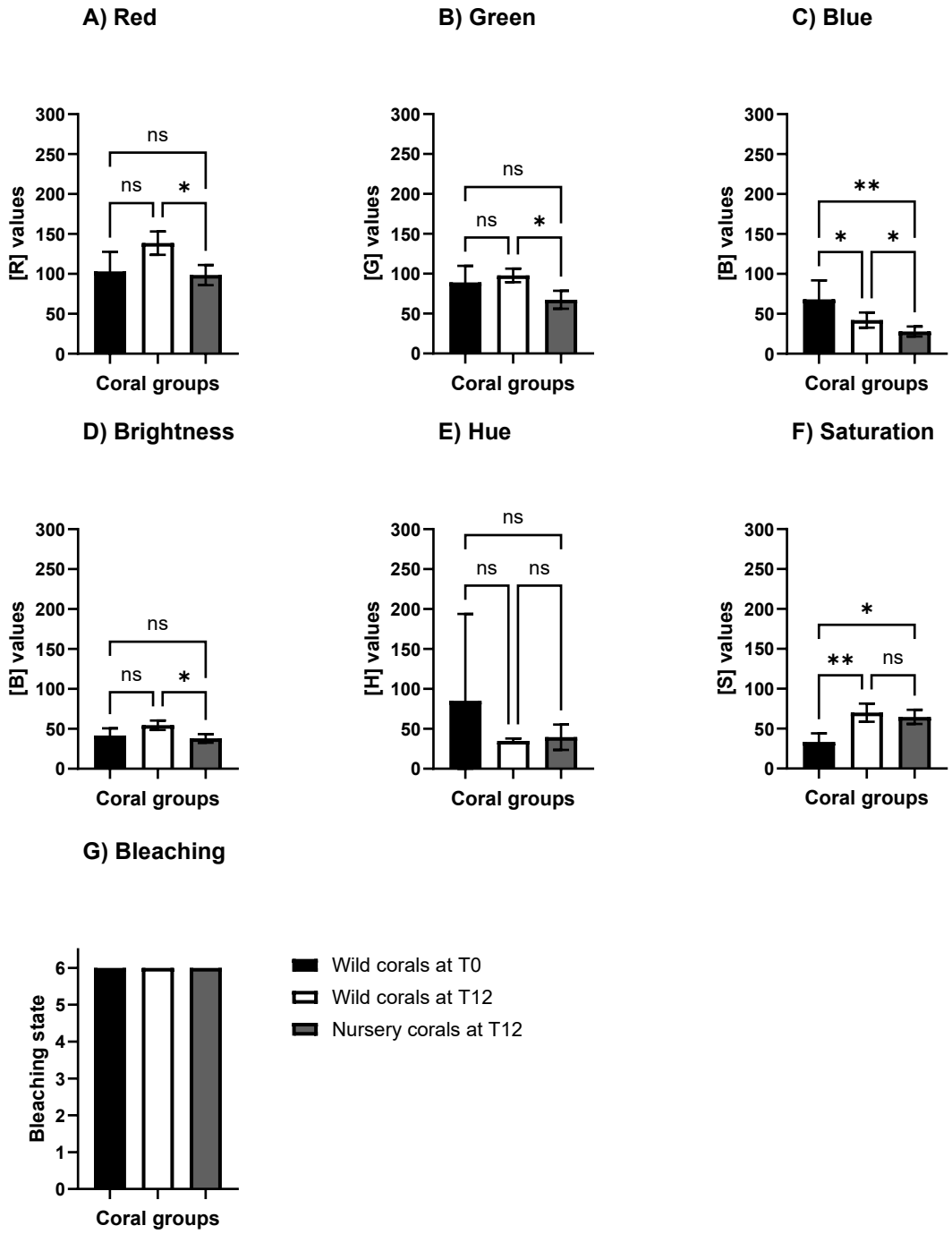
A) Red
B) Green
C) Blue
[R] values
[G] values
[B] values
Coral groups
ns
*
**
D) Brightness
E) Hue
F) Saturation
[H] values
[S] values
G) Bleaching
Bleaching state
Wild corals at T0
Wild corals at T12
Nursery corals at T12

Figure S2.4 Bio-physical colouration of wild and nursery corals. Traits encompass (a) red (R), b) green (G), (c) blue (B), (d) hue, (e) saturation, (f) brightness, and bleaching state. Significant differences in the RGB values among coral groups were revealed by a one-way RM ANOVA ($F_{(1.9,9.5)} = 7.5$, $p = 0.0114$ for R; $F_{(1.8,8.8)} = 7.6$, $p = 0.0137$ for G; and $F_{(1.3,6.7)} = 21.0$, $p = 0.0021$ for B). Tukey's test revealed significant differences between WT12 and NT12 ($p = 0.0247$, 0.0126, and 0.0215 for R, G, and B, respectively), suggesting a different colouration between these two coral groups. Additional differences in B values among WT0 vs WT12, and WT0 vs NT12 ($p = 0.0317$ and 0.0077, respectively) were also found. Hue values were approximately doubled for WT0 (85.2 ± 44.4, $n = 6$) compared to WT12 (34.8 ± 1.2, $n = 6$) and NT12 (39.5 ± 6.5, $n = 6$). However, no significant differences in hue levels were detected among coral groups (one-way RM ANOVA, $F_{(1.5,7.7)} = 0.2$, $p = 0.7972$). Regarding the saturation levels, they approximately halved in WT0 (33.3 ± 4.4, $n = 6$) compared to WT12 and NT12 (70.0 ± 4.6, and 64.7 ± 3.6, respectively; $n = 6$), and significant differences were found among coral groups (one-way RM ANOVA, $F_{(1.9,9.3)} = 19.0$, $p = 0.0006$). Tukey's test showed significant differences for WT0 vs WT12 ($p = 0.0029$) and WT0 vs NT12 ($p = 0.0113$). In general, brightness values were low among coral groups 41.7 ± 3.7, 54.5 ± 2.4, and 38.0 ± 2.2 for WT0, WT12, and NT12, respectively ($n = 6$ for each coral group). Significant differences in brightness levels were found (one-way RM ANOVA, $F_{(2.0,9.9)} = 8.0$, $p = 0.0087$), and Tukey's test revealed to be between WT12 vs NT12 ($p = 0.0257$). Statistical significance is shown as ns (no statistical significance), * and ** ($p \leq 0.05$ and 0.01, respectively).

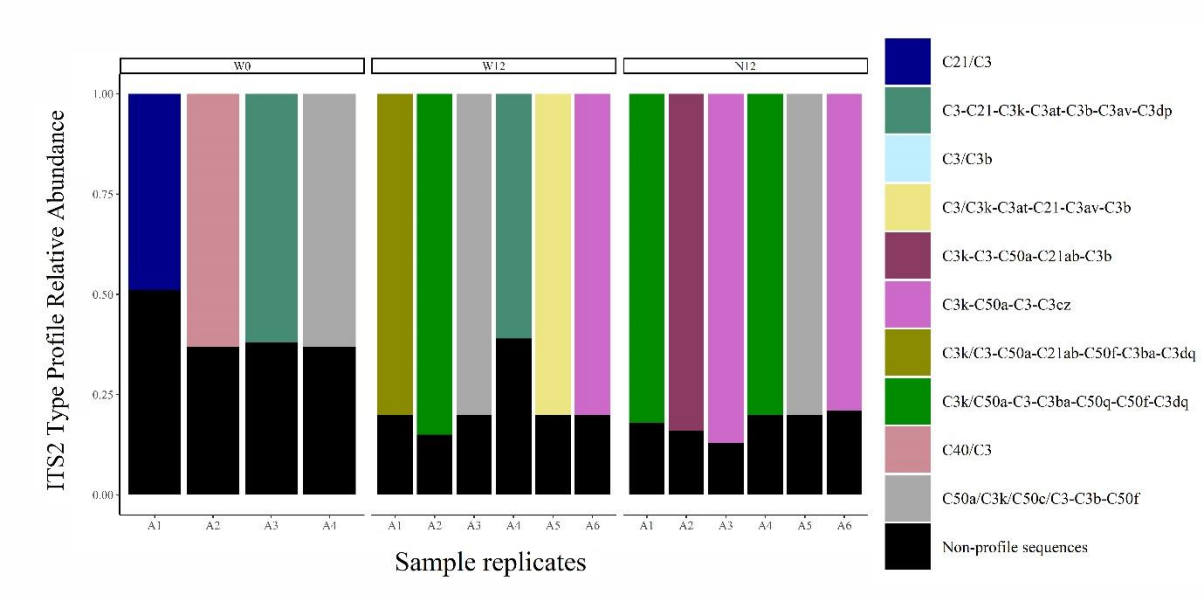

Figure S2.5 Predicted ITS2 type profiles for wild and nursery corals. Corresponding samples are visualised as a stacked bar chart with a single column representing a sample. The relative abundance of predicted ITS2 type profiles is plotted for each column in the stacked bar plots. All data are fragments of *Acropora* cf. *hyacinthus* (n = 4, 6, and 6 for W0, W12, and N12, respectively).

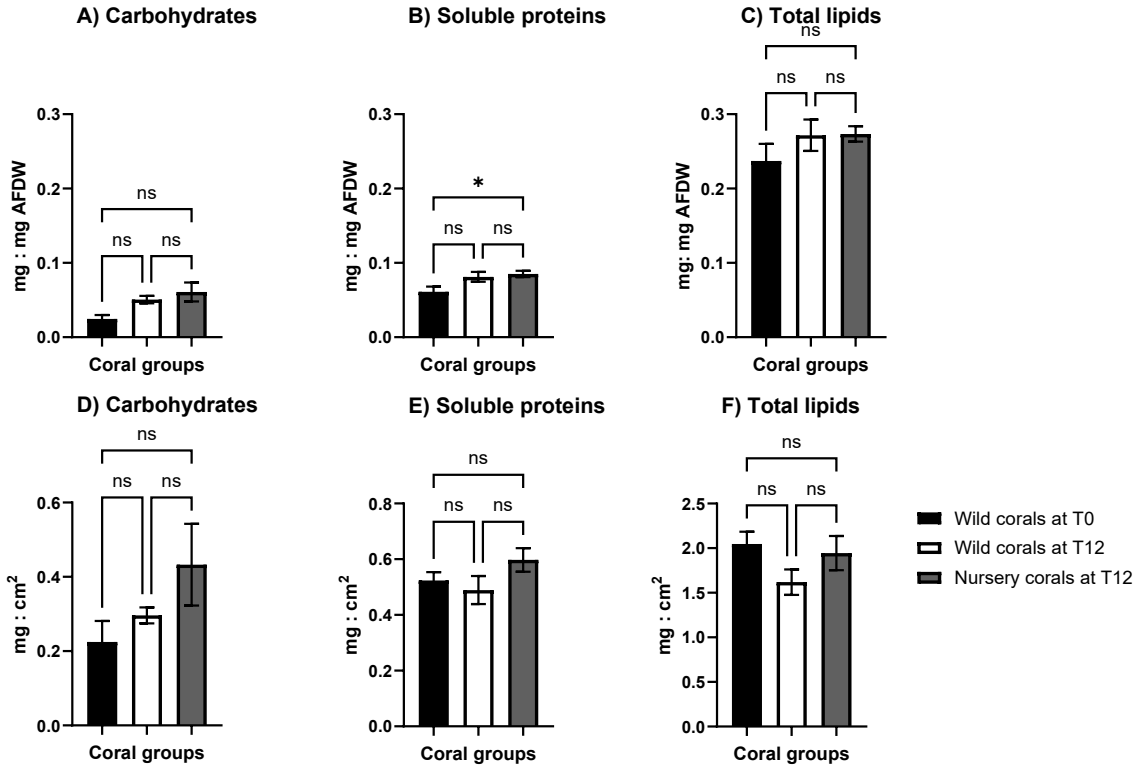

Figure S2.6 Mean (± SEM) (a) carbohydrates, (b) soluble proteins, and (c) total lipids (mg per ash-free dry mass), and same biomolecule content normalised to mg per surface area (d-f) of the initial wild colonies (WT0) and wild and nursery corals from 12 months propagation (WT12 and NT12). All data are fragments of *Acropora* cf. *hyacinthus* (n = 4, 6, and 6 for WT0, WT12, and NT12, respectively). Means were compared by analysis of variance (ANOVA) with post hoc Tukey tests (see main text) where ns indicates no statistical significance, and * and ** indicates $p \leq 0.05$ and 0.01, respectively.

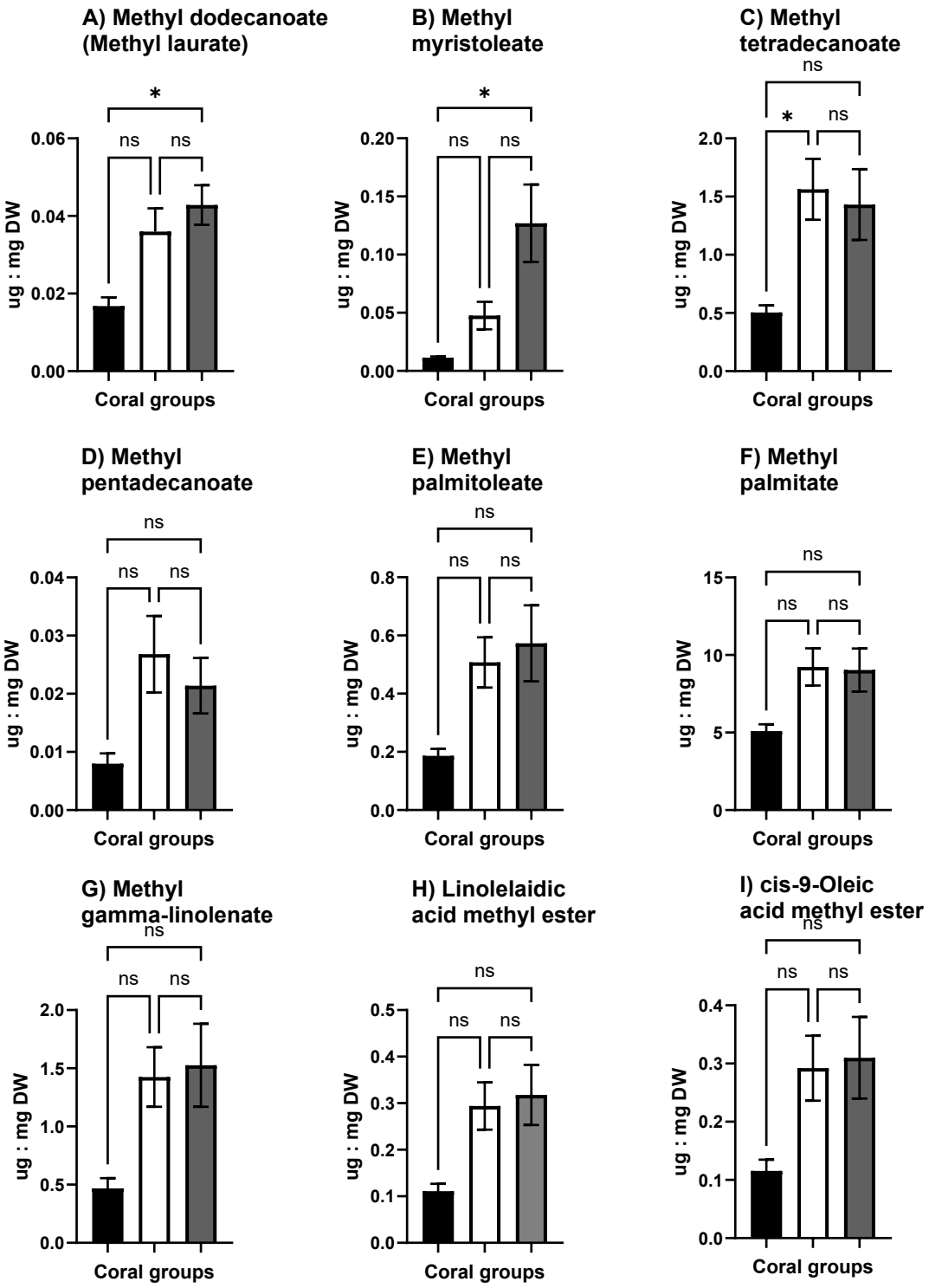
A) Methyl dodecanoate (Methyl laurate)
B) Methyl myristoleate
C) Methyl tetradecanoate
D) Methyl pentadecanoate
E) Methyl palmitoleate
F) Methyl palmitate
G) Methyl gamma-linolenate
H) Linolelaidic acid methyl ester
I) cis-9-Oleic acid methyl ester
ug : mg DW
Coral groups
ns
*

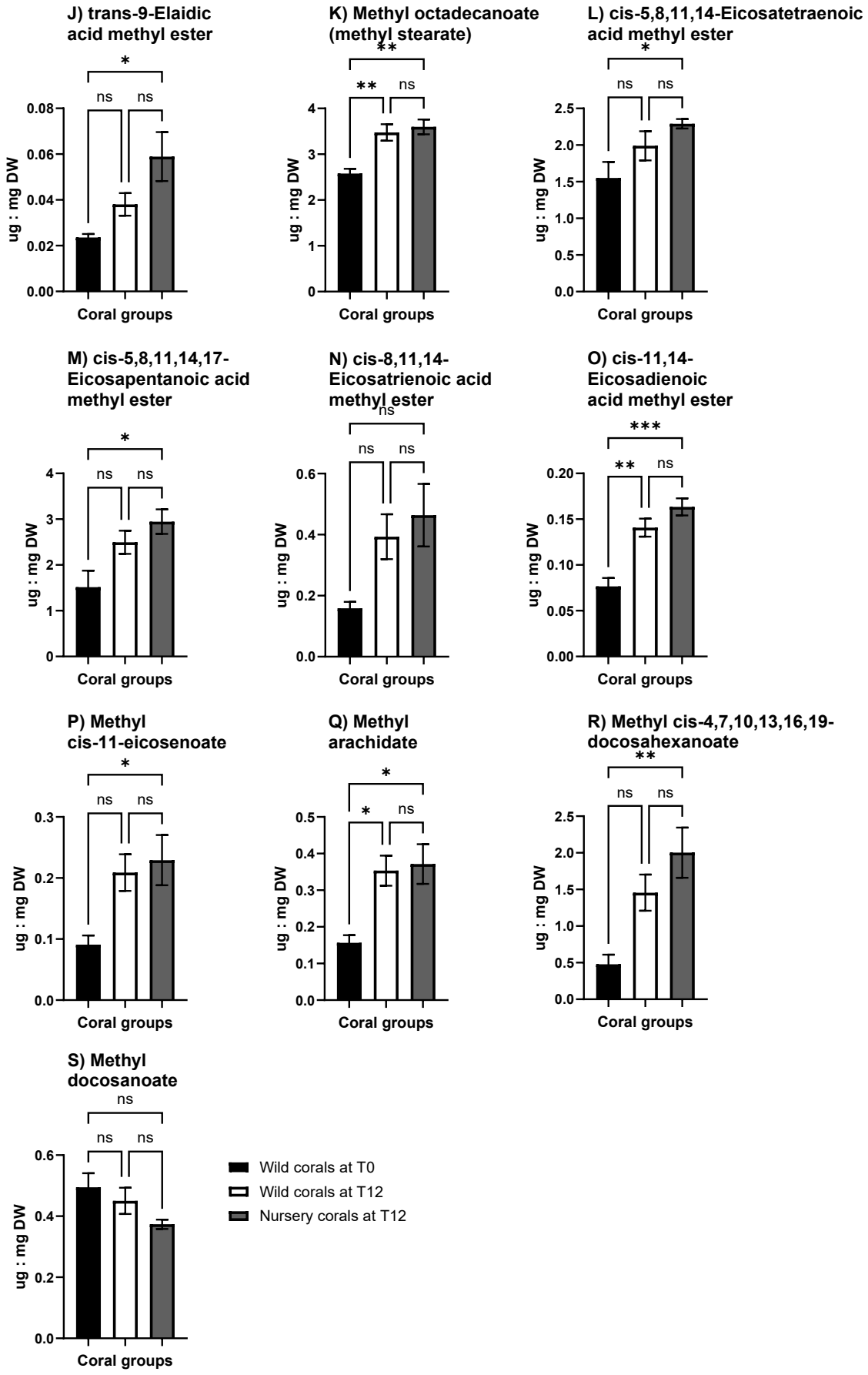
J) trans-9-Elaidic acid methyl ester
K) Methyl octadecanoate (methyl stearate)
L) cis-5,8,11,14-Eicosatetraenoic acid methyl ester
M) cis-5,8,11,14,17-Eicosapentanoic acid methyl ester
N) cis-8,11,14-Eicosatrienoic acid methyl ester
O) cis-11,14-Eicosadienoic acid methyl ester
P) Methyl cis-11-eicosenoate
Q) Methyl arachidate
R) Methyl cis-4,7,10,13,16,19-docosahexanoate
S) Methyl docosanoate
ug : mg DW
Coral groups
ns
Wild corals at T0
Wild corals at T12
Nursery corals at T12

Figure S2.7 Mean (± SEM) of 19 fatty acid methyl esters (mg per dry mass) (A-S) of the initial wild colonies (WT0) and wild and nursery corals from 12 months propagation (WT12 and NT12). All data are fragments of *Acropora* cf. *hyacinthus* (n = 4, 6, and 6 for WT0, WT12, and NT12, respectively). Means were compared by analysis of variance (ANOVA) with *post hoc* Tukey tests (see main text) where ns indicates no statistical significance, and *, ** and *** indicates $p \leq 0.05$, 0.01 and 0.001, respectively.

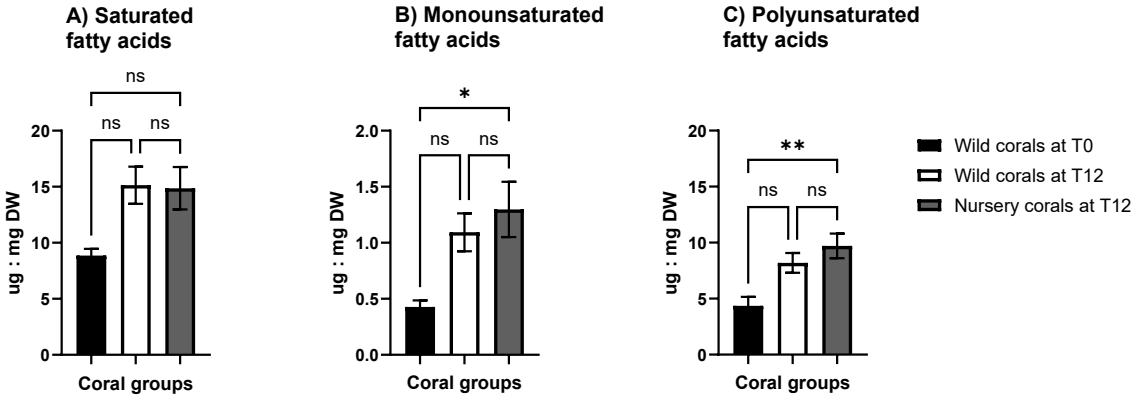

Figure S2.8 Mean (± SEM) of (a) saturated fatty acids (SFA), (b) mono- and (c) poly-unsaturated fatty acids (MUFA and PUFA, respectively) (µg per dry mass) of the initial wild colonies (WT0) and wild and nursery corals from 12 months propagation (WT12 and NT12). All data are fragments of *Acropora* cf. *hyacinthus* (n = 4, 6, and 6 for WT0, WT12, and NT12, respectively). No significant differences in SFA were found (one-way ANOVA, $F_{(2,13)} = 3.8$, $p = 0.0501$), however, differences in MUFA and PUFA were detected among coral groups ($p = 0.0324$ and 0.0099, respectively). Tukey's test revealed significant differences between WT0 and NT12 ($p = 0.0287$ and 0.0080, respectively). Statistical significance is shown as ns (no statistical significance), * and ** ($p \leq 0.05$ and 0.01, respectively).

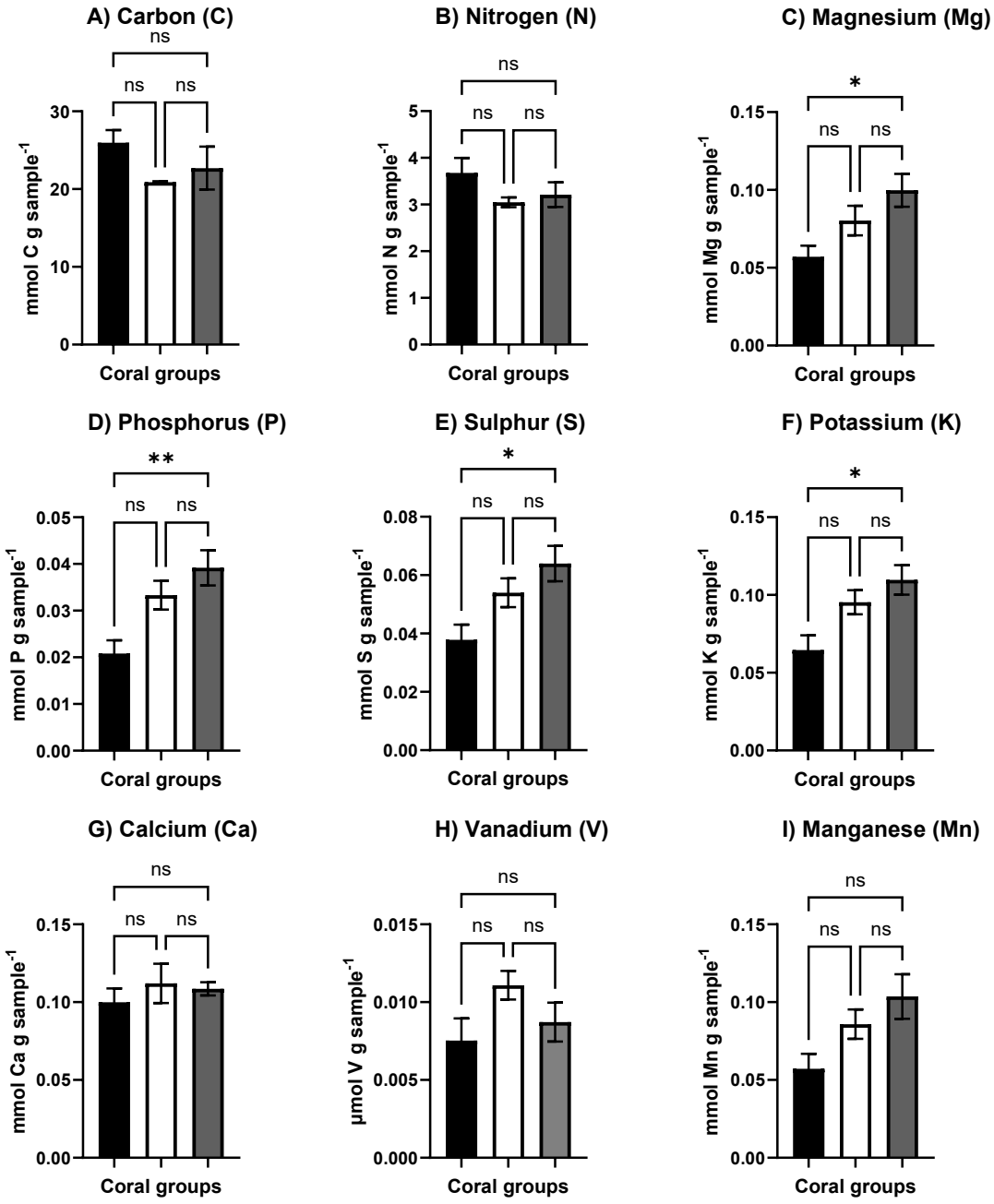
A) Carbon (C)
mmol C g sample-1
Coral groups
B) Nitrogen (N)
mmol N g sample-1
Coral groups
C) Magnesium (Mg)
mmol Mg g sample-1
Coral groups
D) Phosphorus (P)
mmol P g sample-1
Coral groups
E) Sulphur (S)
mmol S g sample-1
Coral groups
F) Potassium (K)
mmol K g sample-1
Coral groups
G) Calcium (Ca)
mmol Ca g sample-1
Coral groups
H) Vanadium (V)
µmol V g sample-1
Coral groups
I) Manganese (Mn)
mmol Mn g sample-1
Coral groups
ns
*
**

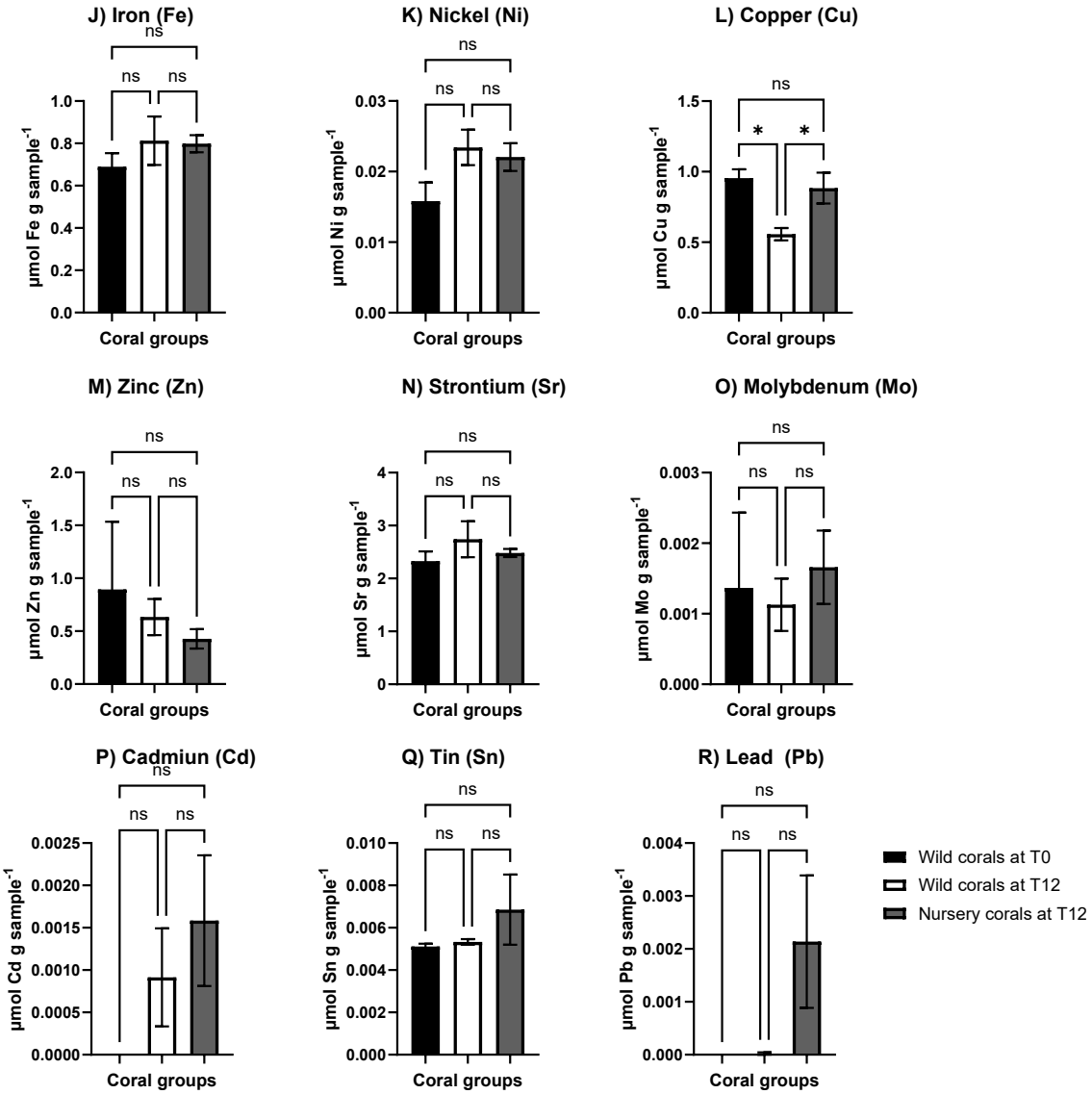

Figure S2.9 Mean (± SEM) of 18 elements, (A) Carbon [C], (B) Nitrogen [N], (C) Magnesium [Mg], (D) Phosphorus [P], (E) Sulphur [S], (F) Potassium [K], (G) Calcium [Ca], (H) Vanadium [V], (I) Manganese [Mn], (J) Iron [Fe], (K) Nickel [Ni], (L) Copper [Cu], (M) Zinc [Zn], (N) Strontium [Sr], (O) Molybdenum [Mo], (P) Cadmium [Cd], (Q) Tim [Sn], and (R) Lead [Pb] — macronutrients (A-G) and micronutrients (H-R) in mmol or µmol (element) per dry mass, respectively; absolute values — of the initial wild colonies (WT0) and wild and nursery corals from 12 months propagation (WT12 and NT12). All data are fragments of *Acropora* cf. *hyacinthus* (n = 4, 6, and 6 for WT0, WT12, and NT12, respectively). Means were compared by analysis of variance (ANOVA) with *post hoc* Tukey tests, except for Cd and Pb (Kruskal-Wallis's test followed by Dunn's test) where ns indicates no statistical significance, and * and ** indicates $p \leq 0.05$ and 0.01, respectively. Cobalt [Co] and Selenium [Se] values were negligible and hence not shown here.

A) Physical appearance

A.1) PCA biplot, including a cut-off for the cos2 = 0.5

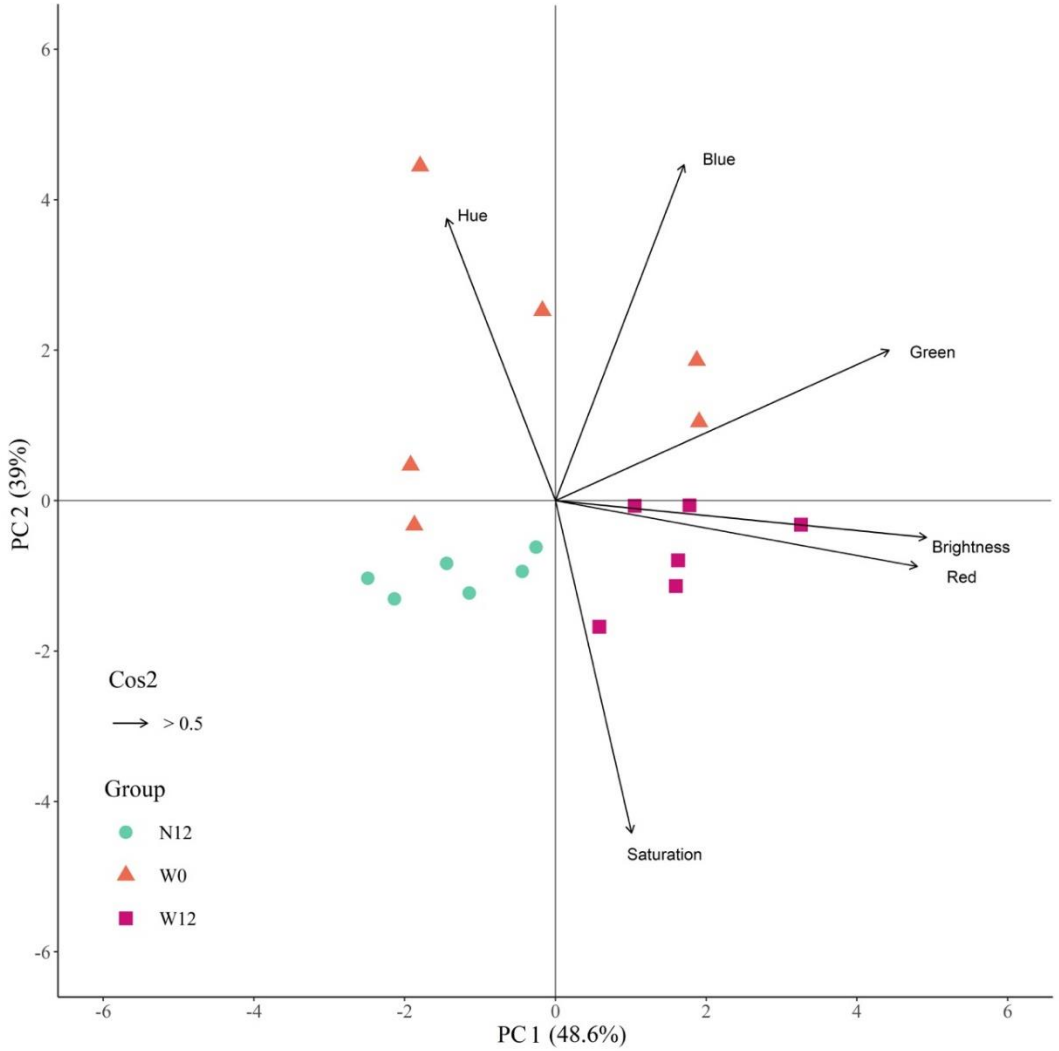

A.2) Contribution of variables to PC1 and PC2

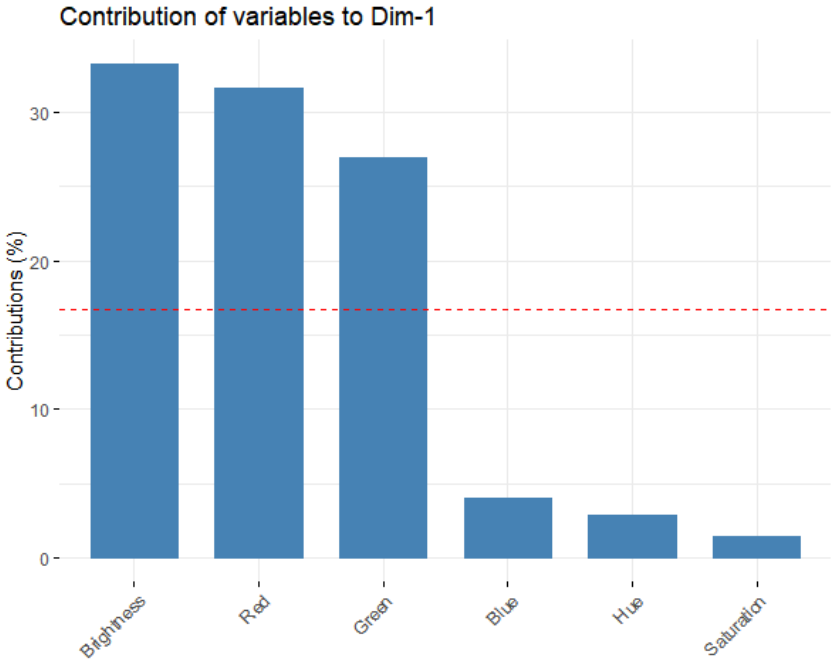

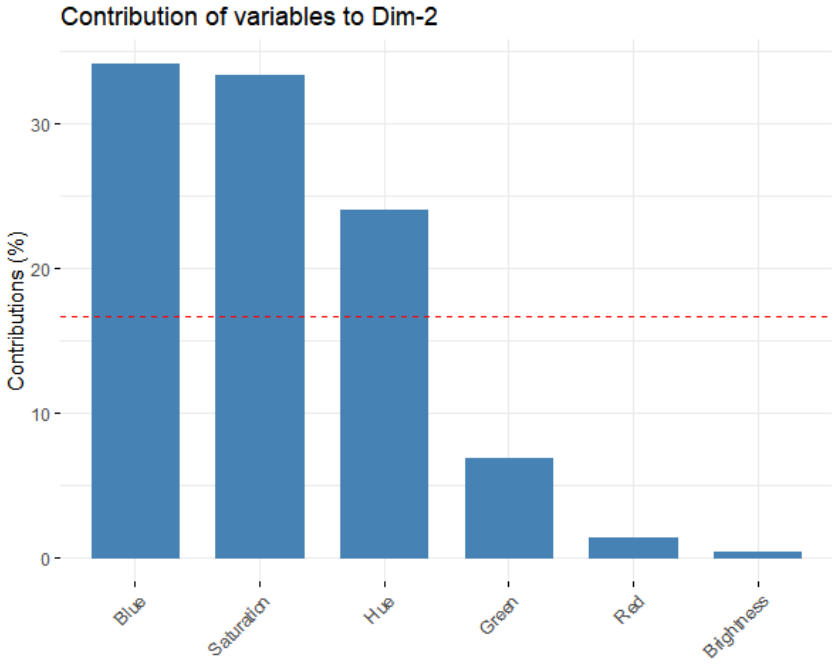

B) Photobiology

B.1) PCA biplot, including a cut-off for the cos2 = 0.5

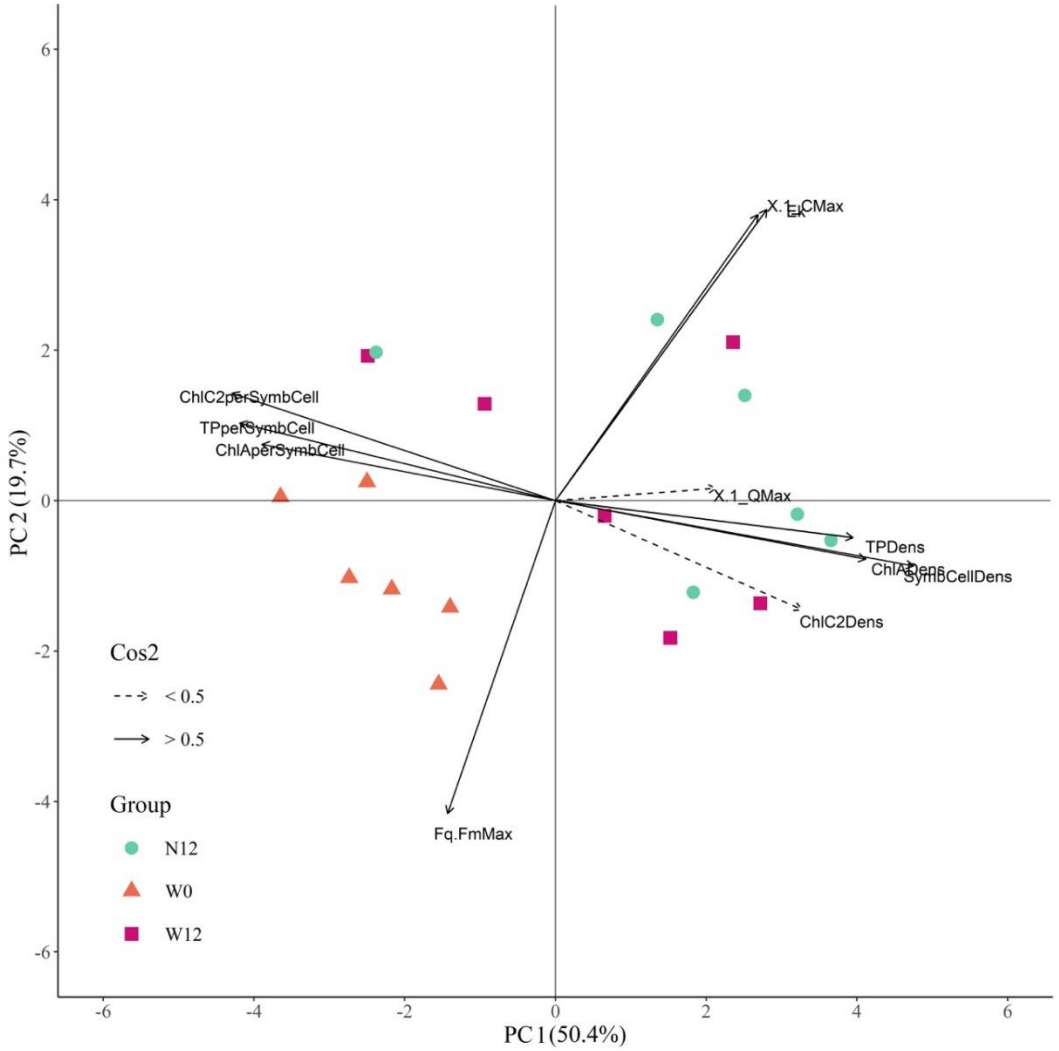

B.2) Contribution of variables to PC1 and PC2

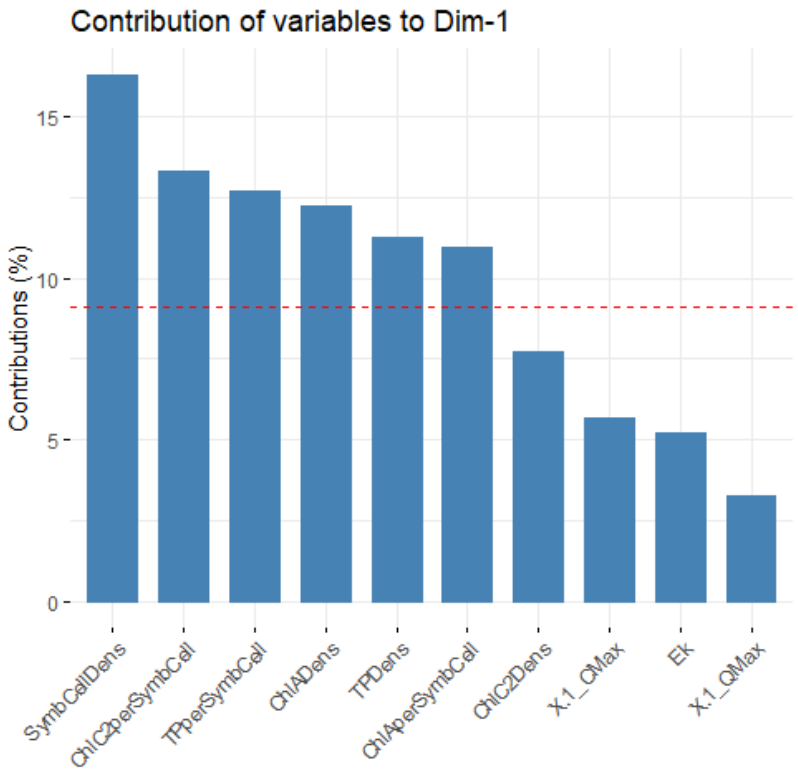

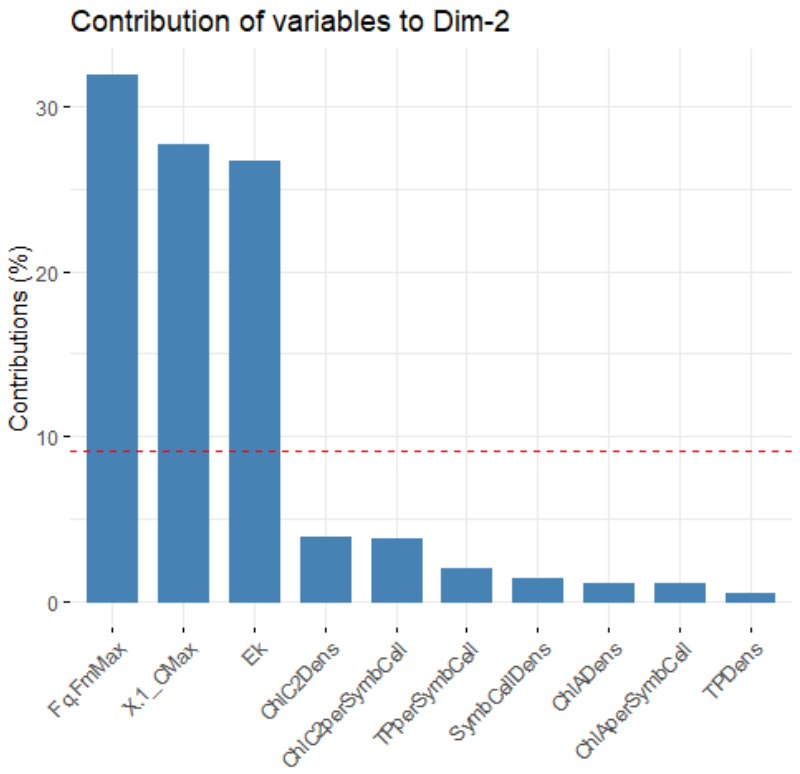

C) Metabolism

C.1) PCA biplot, including a cut-off for the cos2 = 0.5

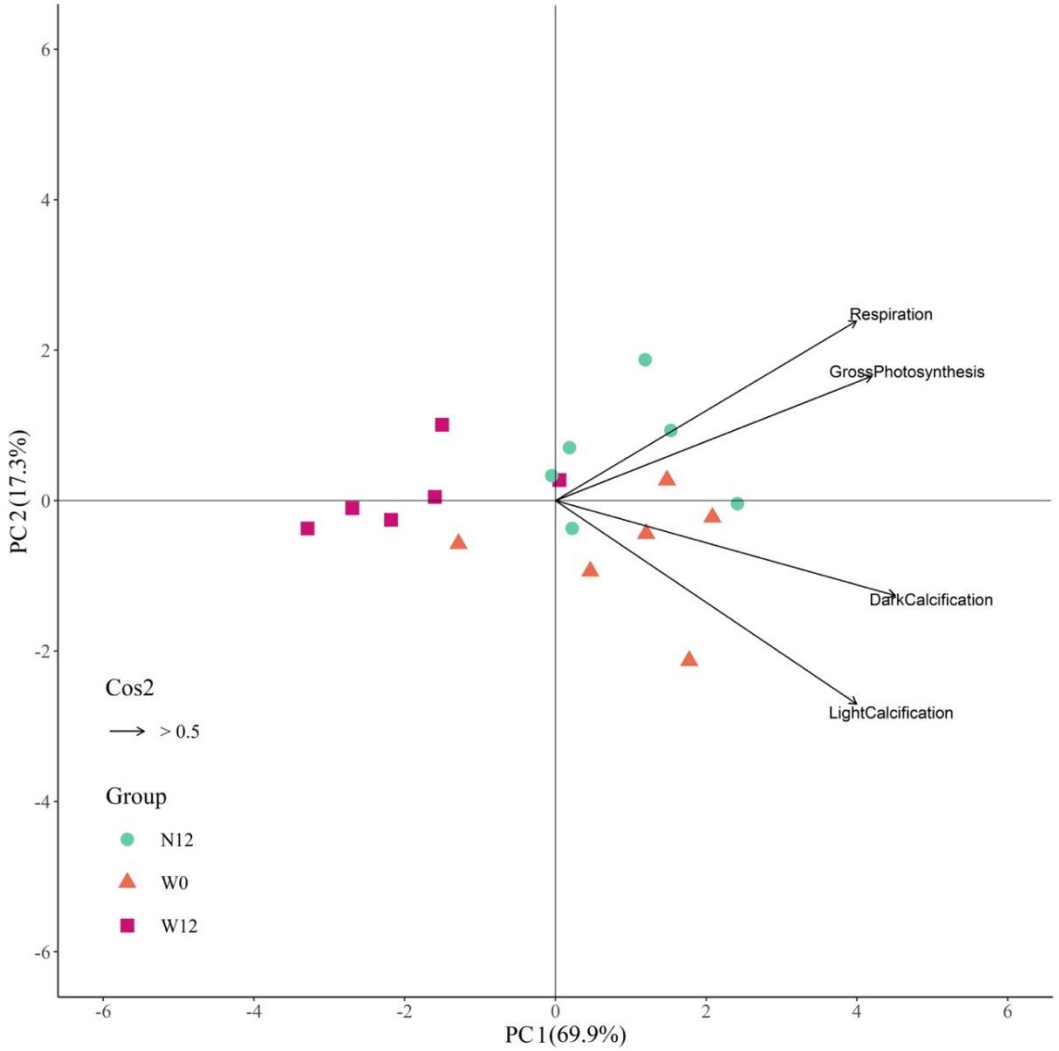

C.2) Contribution of variables to PC1 and PC2

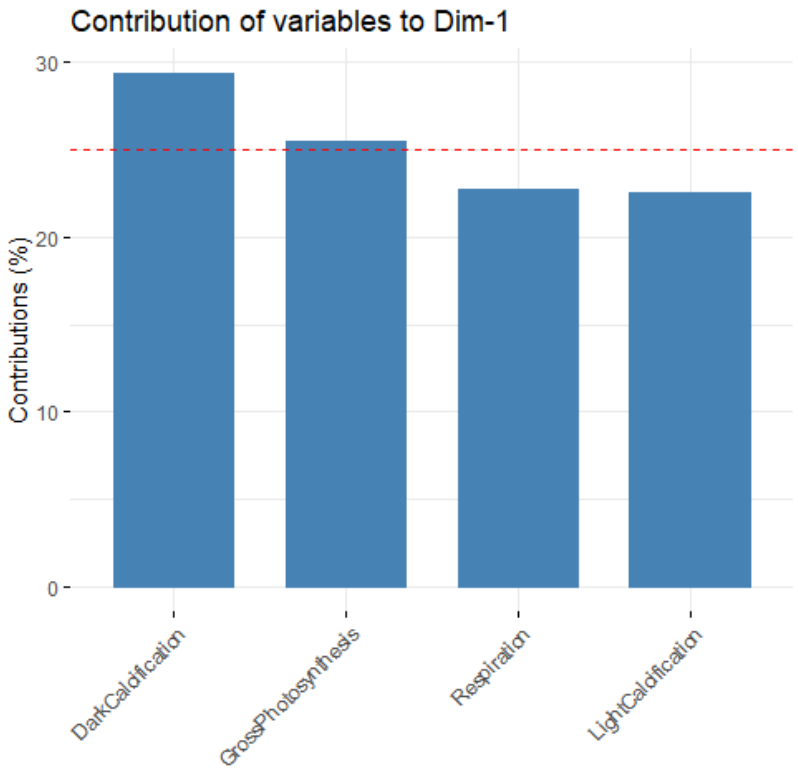

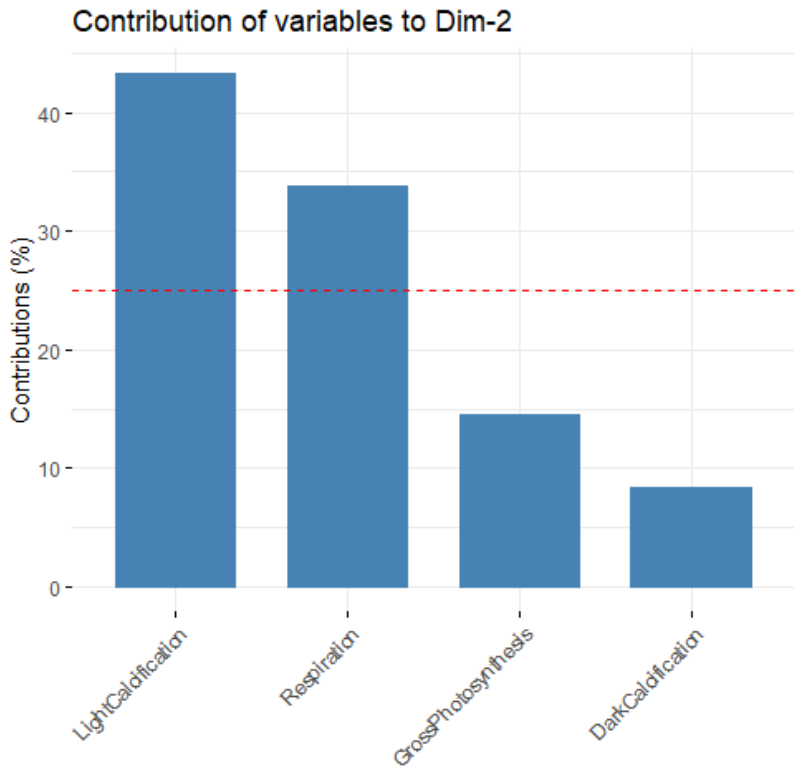

D) Energy reserves

D.1) PCA biplot, including a cut-off for the cos2 = 0.5

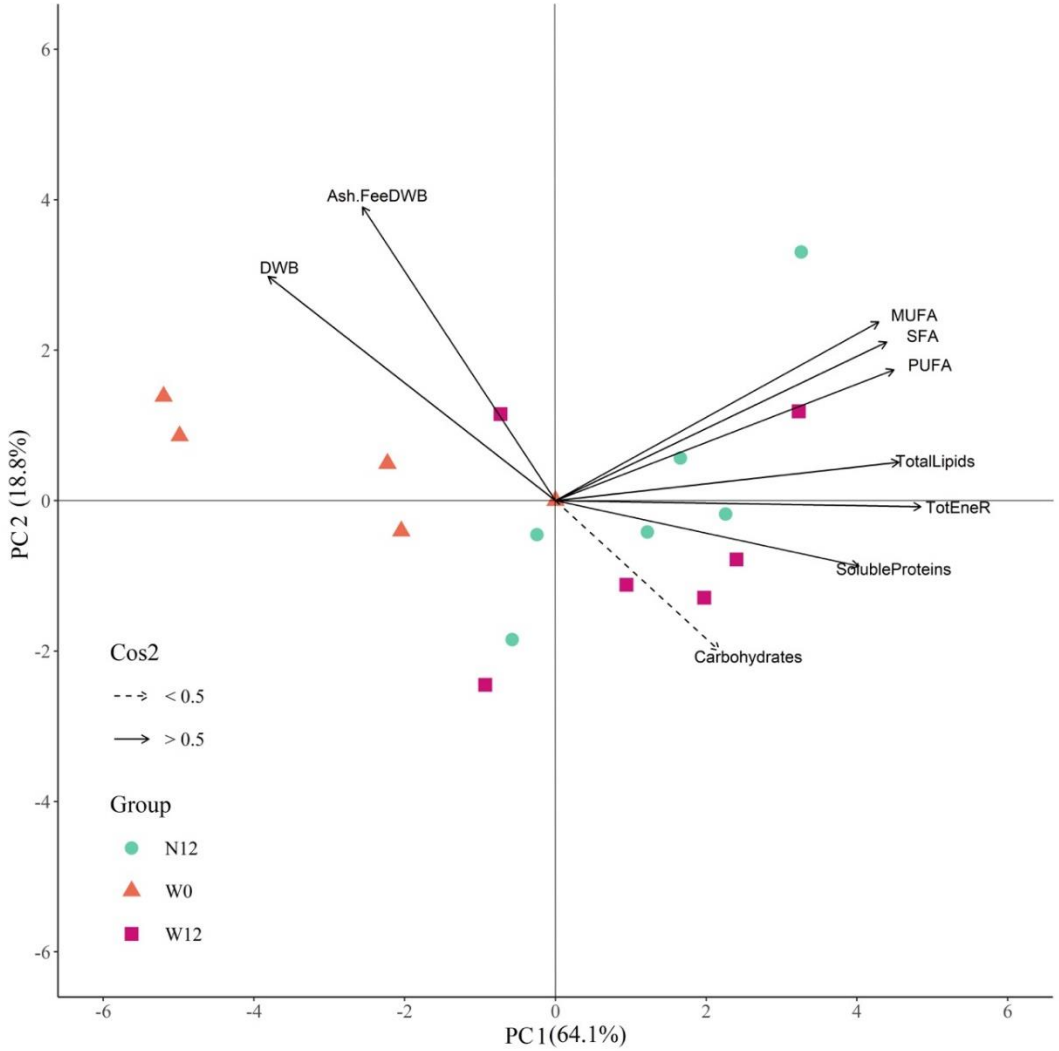

D.2) Contribution of variables to PC1 and PC2

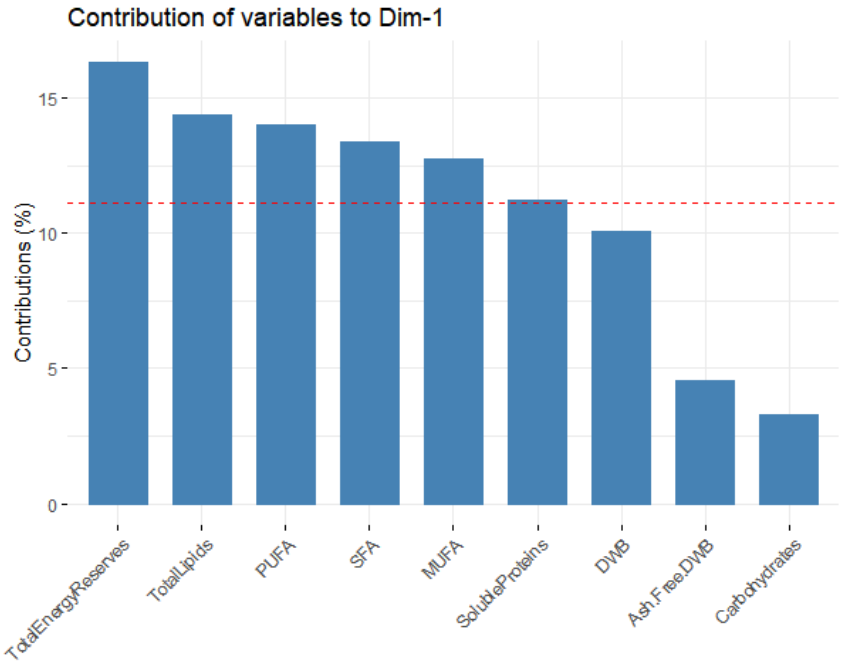

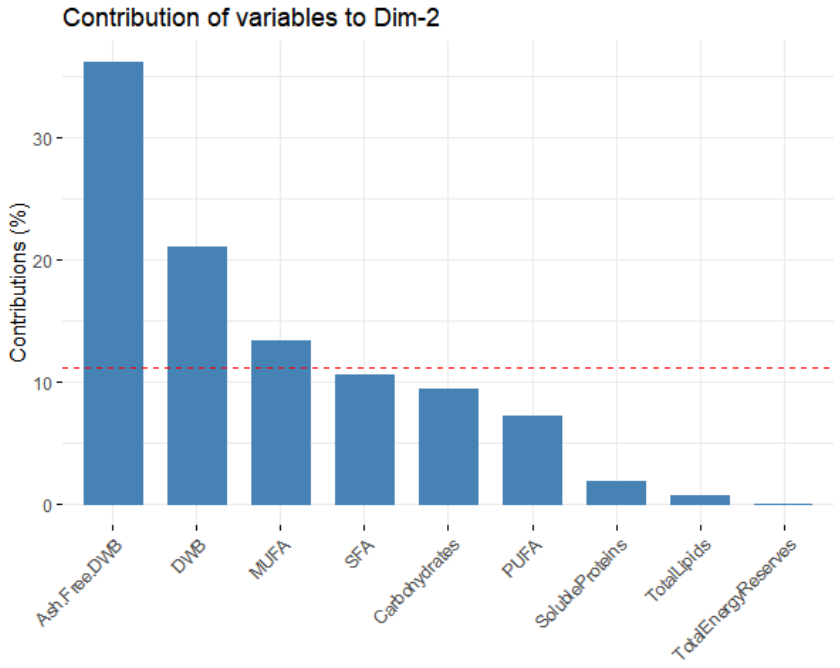

E) FAME

E.1) PCA biplot, including a cut-off for the cos2 = 0.5

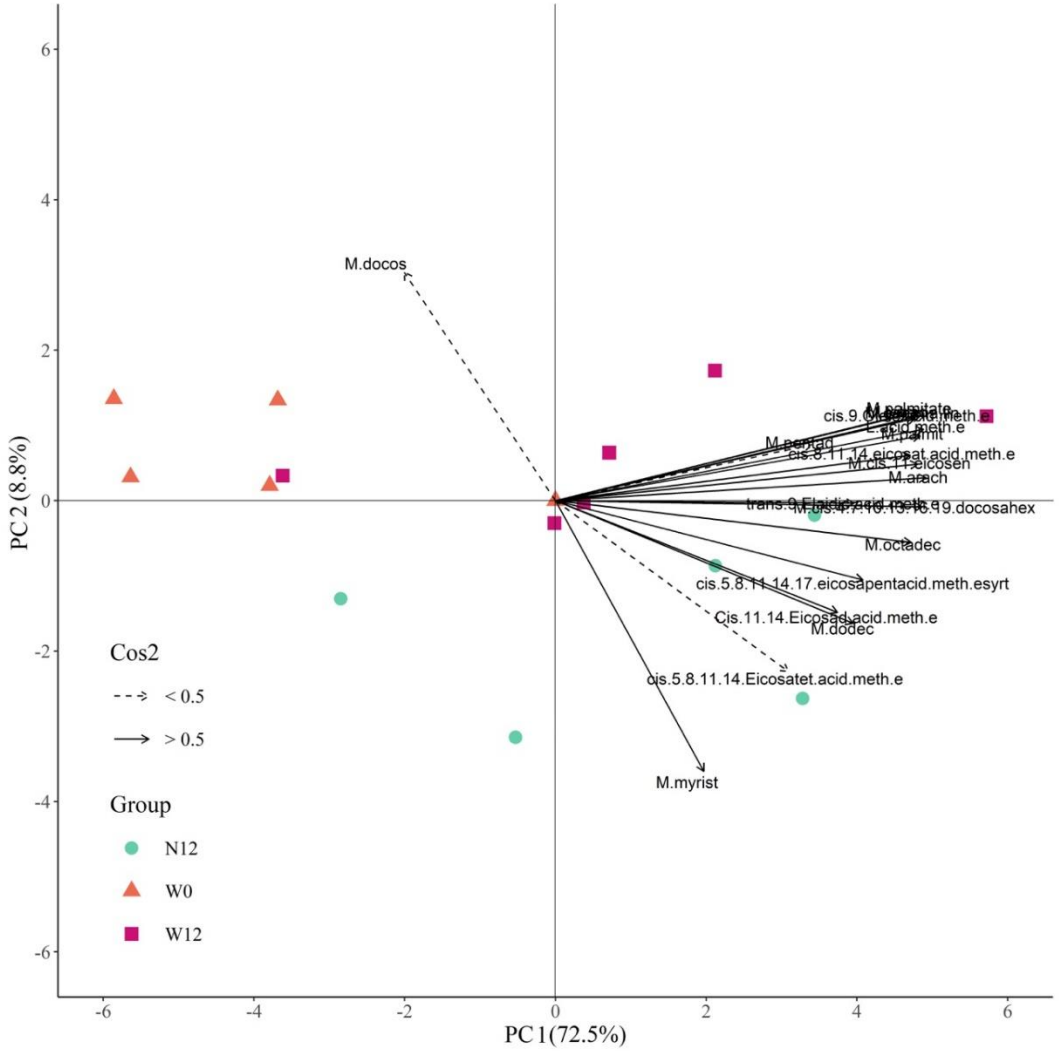

E.2) Contribution of variables to PC1 and PC2

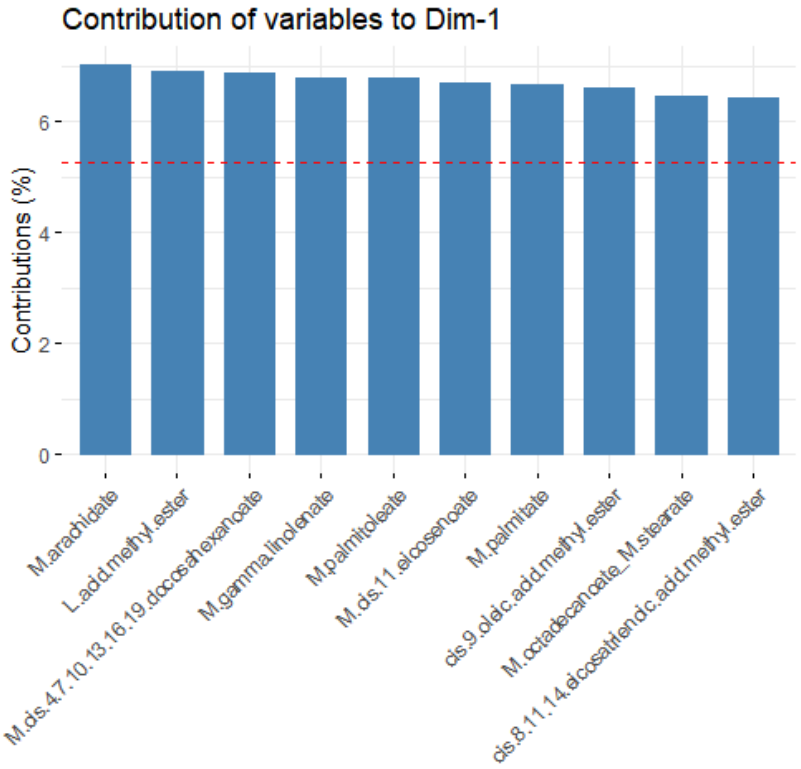

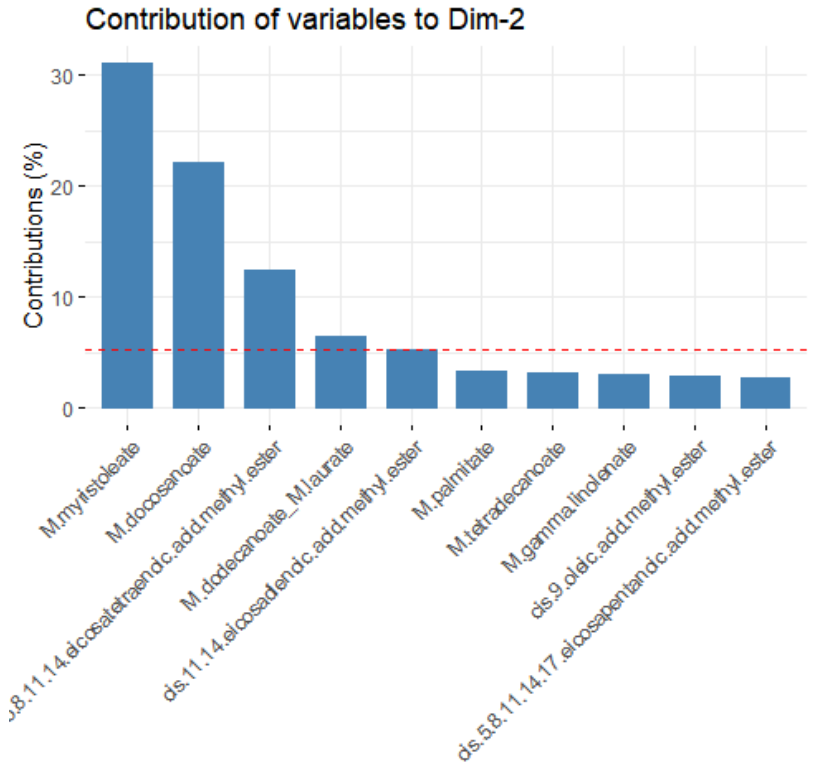

F) Elementome

F.1) PCA biplot, including a cut-off for the cos2 = 0.5

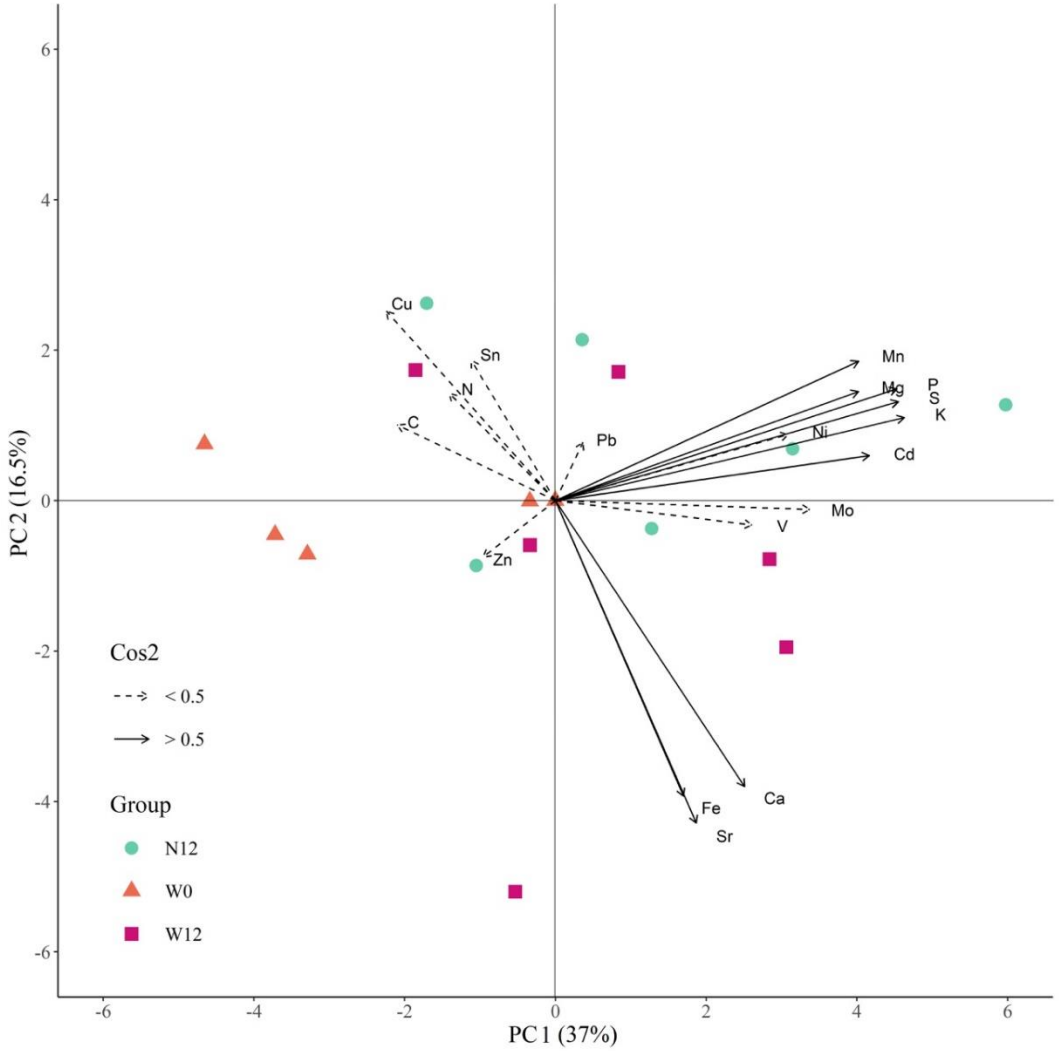

F.2) Contribution of variables to PC1 and PC2

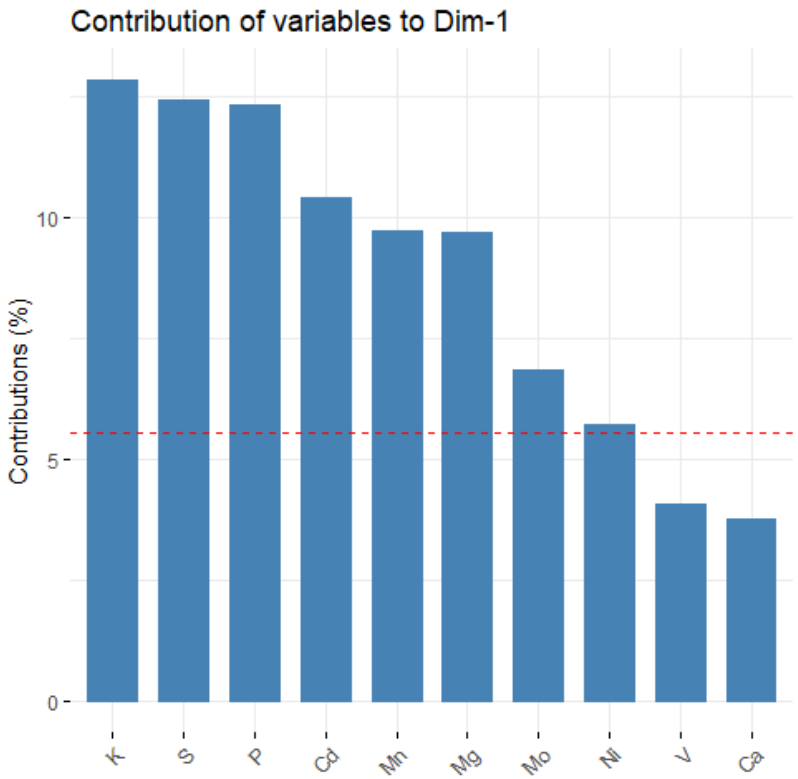

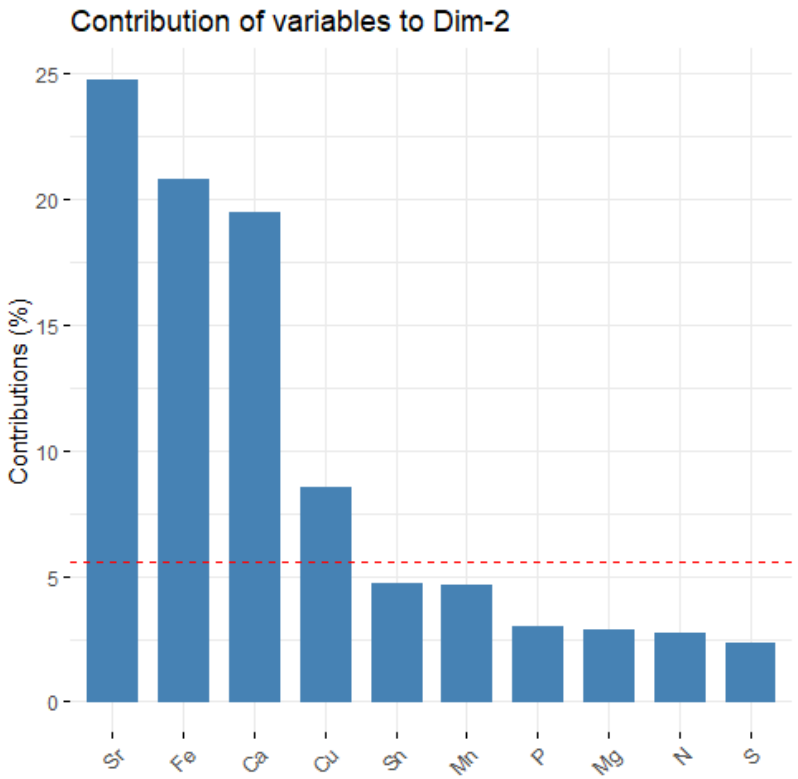

G) Skeletal properties

G.1) PCA biplot, including a cut-off for the cos2 = 0.5

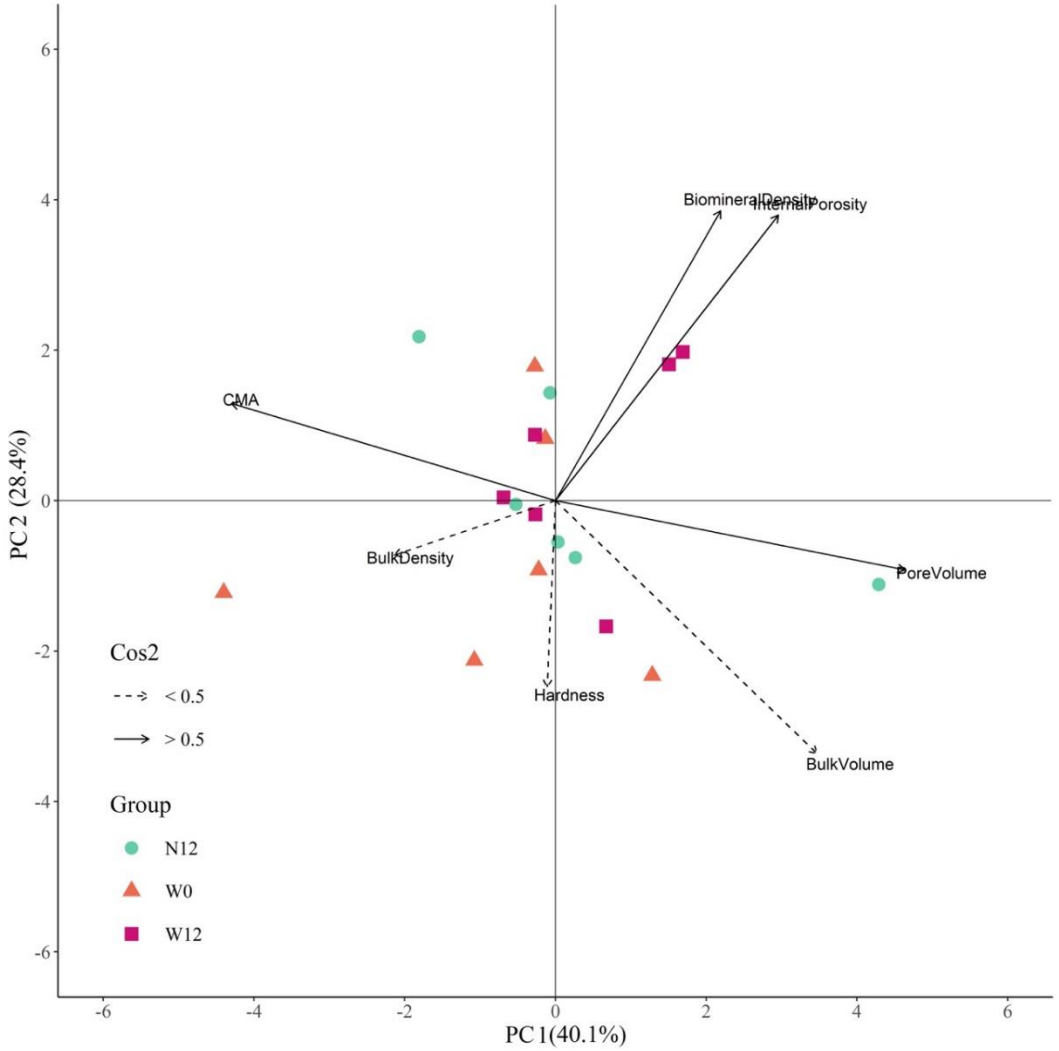

F.2) Contribution of variables to PC1 and PC2

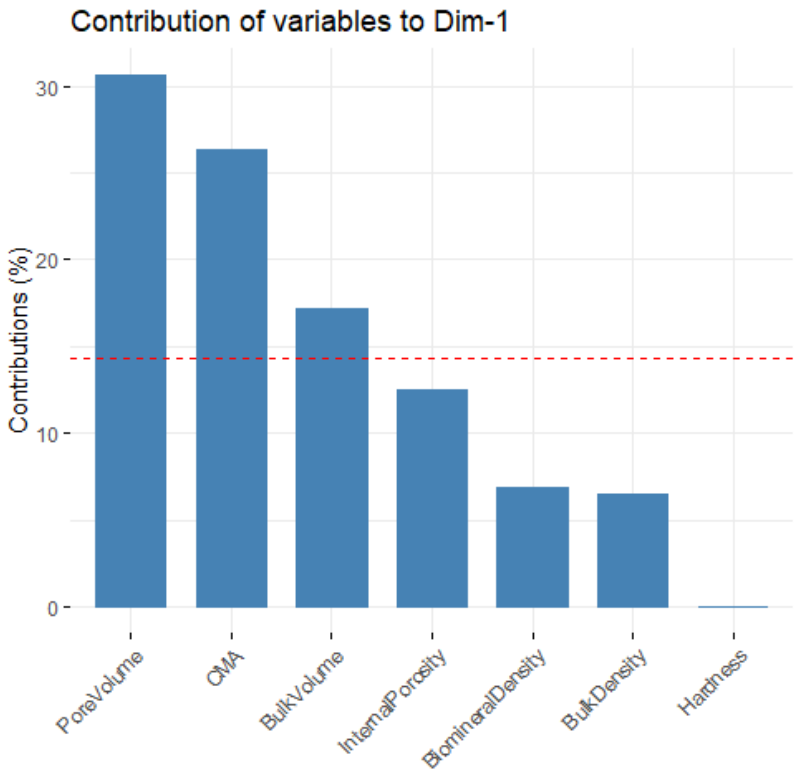

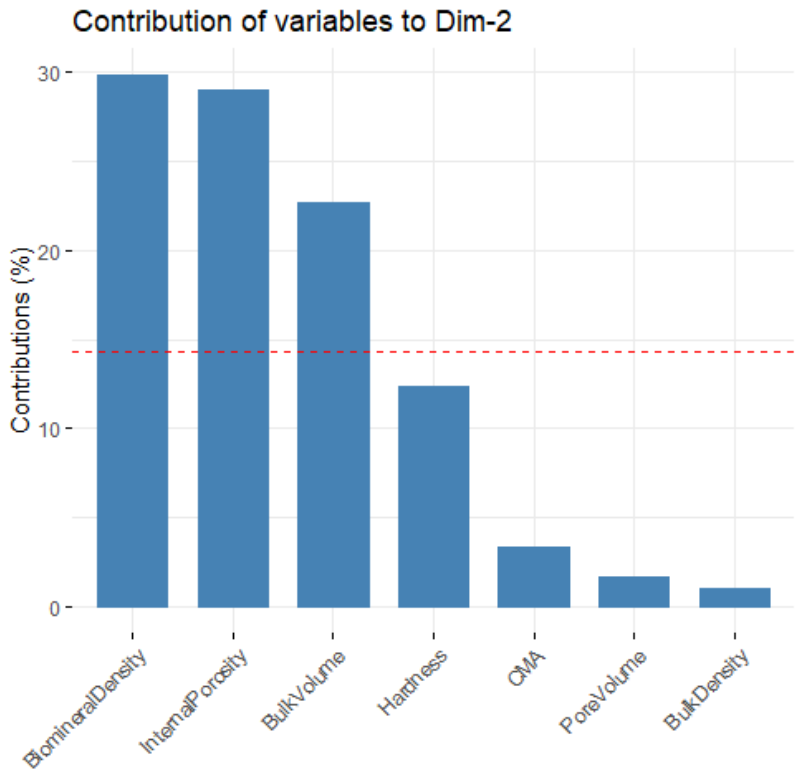

H) Multitraits

H.2) PCA biplot, including a cut-off for the cos2 = 0.5

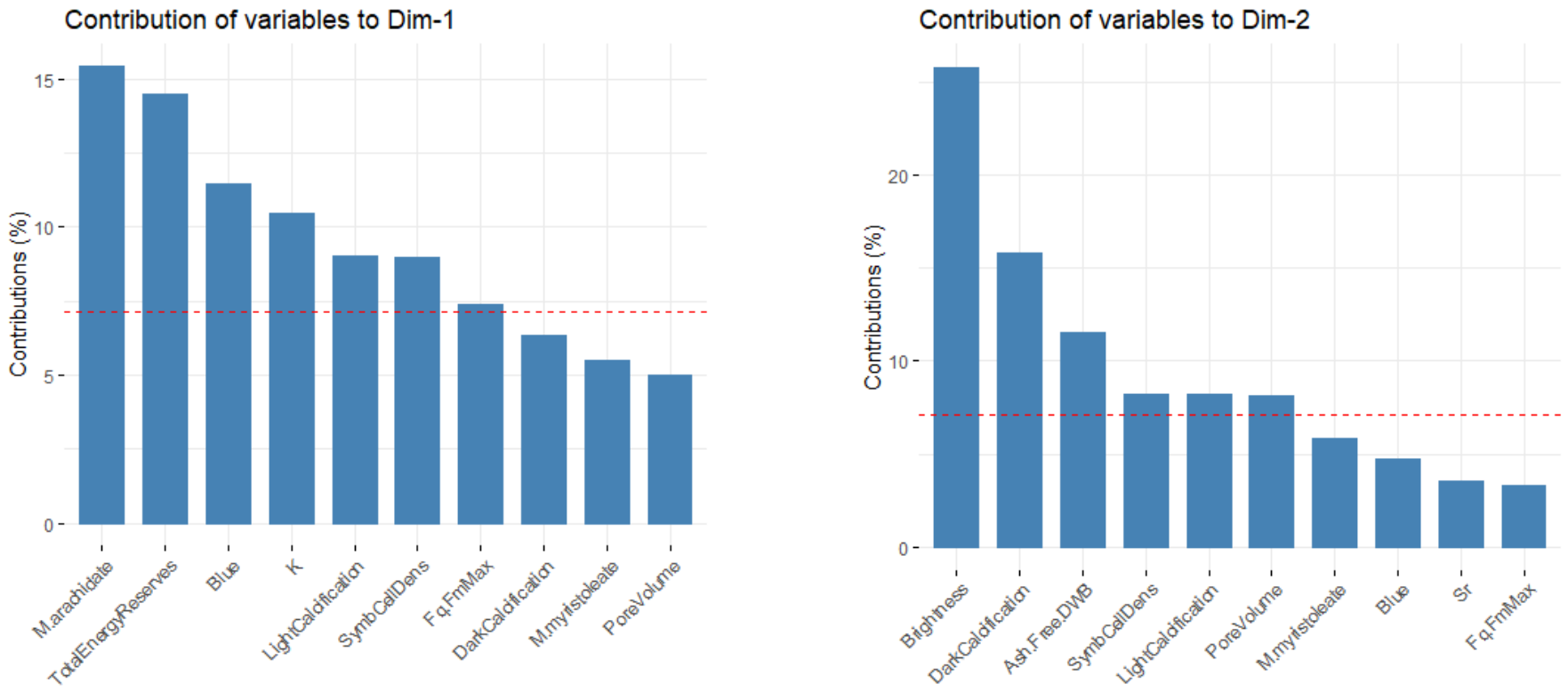

Figure S2.10 Examination of the traits per biological property. 1) Principal Component Analysis (PCA) biplot, including a cut-off for the cos2 = 0.5, and 2) the contribution of variables to dimensions (principal components, PC) 1 and 2, for the following seven biological properties: (A) physical appearance (tissue colouration), (B) photobiology, (C) metabolism, (D) energy reserves, (E) fatty acid methyl esters (FAME), (F) elementome, and (G) skeletal properties. Regarding the cut-off for the cos2 = 0.5, a good representation of the variable on the PC is indicated in a solid line (>0.5). As opposed, <0.5 (dashed line) indicates that the variable is not perfectly represented by the PCs. (H) Contribution plot for the 14 (out of 90) selected traits used in the final PCA (the so-called multitraits).

Table S2.1 A total of 90 traits were selected for this study. Survival and growth are considered emergent properties. Seven biological properties were investigated to unveil the biological machinery underpinning coral survival and growth: physical appearance (tissue colouration), photobiology, metabolism, energy reserves, fatty acid methyl esters (FAME), elementome, and skeletal properties.

	Variable	**Biological property**
1	Individual survival success	Survival (emergent property) (1 trait)
2	Relative linear growth rate	Growth (emergent property) (3 traits)
3	Relative areal growth rate	
4	Relative increase in areal tissue	
5	Red [R]	Physical appearance (7 traits)
6	Green [G]	
7	Blue [B]	
8	Hue [H]	
9	Saturation [S]	
10	Brightness [B]	
11	Bleaching state	
12	Light saturation coefficient [E_K]	Photobiology (13)
13	Derived maximum photochemical efficiency [$F_q'/F_{m'MAX}$]	
14	Photochemical quenching [1-C]$_{MAX}$	
15	Non-photochemical quenching [1-Q]$_{MAX}$	
16	Symbiont cell density	
17	Total pigment density	
18	Chl *a* density	
19	Chl *c2* density	
20	Total pigments per cell	
21	Chl *a* per cell	
22	Chl *c2* per cell	
23	*a*:*c2* ratio	
24	*Symbiodiniaceae* ITS2 identity	
25	Gross Photosynthesis rate [P_G]	Metabolism (7 traits)
26	Net Photosynthesis rate [P_N]	
27	Respiration rate [R]	
28	P_G:R ratio	
29	Light-dependent calcification [G_L]	
30	Dark-dependent calcification [G_D]	
31	G_L:G_D ratio	
32	Carbohydrates	Energy reserves (9 traits)
33	Soluble proteins	
34	Total lipids	
35	Total energy reserves	
36	Dry weight biomass [DW]	

37	Ash-free dry weight biomass [AFDW]	
38	Saturated fatty acids [SFA]	
39	Mono-unsaturated fatty acids [MUFA]	
40	Poly-unsaturated fatty acids [PUFA]	
41	Methyl dodecanoate (Methyl laurate)	Fatty acid methyl esters (19 traits)
42	Methyl myristoleate	
43	Methyl tetradecanoate	
44	Methyl pentadecanoate	
45	Methyl palmitoleate	
46	Methyl palmitate	
47	Methyl gamma-linolenate	
48	Linolelaidic acid methyl ester	
49	cis-9-Oleic acid methyl ester	
50	trans-9-Elaidic acid methyl ester	
51	Methyl octadecanoate (methyl stearate)	
52	cis-5,8,11,14-Eicosatetraenoic acid methyl ester	
53	cis-5,8,11,14,17-Eicosapentanoic acid methyl ester	
54	cis-8,11,14-Eicosatrienoic acid methyl ester	
55	cis-11,14-Eicosadienoic acid methyl ester	
56	Methyl cis-11-eicosenoate	
57	Methyl arachidate	
58	Methyl cis-4,7,10,13,16,19-docosahexanoate	
59	Methyl docosanoate	
60	Carbon [C]	Elementome (24 traits)
61	Nitrogen [N]	
62	Phosphorus [P]	
63	Magnesium [Mg]	
64	Sulphur [S]	
65	Potassium [K]	
66	Calcium [Ca]	
67	Vanadium [V]	
68	Manganese [Mn]	
69	Iron [Fe]	
70	Nickel [Ni]	
71	Copper [Cu]	
72	Zinc [Zn]	
73	Strontium [Sr]	
74	Molybdenum [Mo]	
75	Cadmium [Cd]	
76	Tin (Sn)	
77	Lead (Pb)	
78	Cobalt [Co]	
79	Selenium [Se]	
80	C:N ratio	
81	C:P ratio	
82	N:P ratio	

83	C:N:P ratio	
84	Bulk volume	Skeletal properties (7 traits)
85	Bulk density	
86	Biomineral density	
87	Pore volume	
88	Apparent (internal) porosity	
89	Hardness	
90	Colony mass per area [CMA]	

Table S2.2 (A) Contributions of traits to the first (PC1) and second (PC2) principal components (dimensions, Dim.), and (B) cumulative variance percent of PC1 and PC2 of the Principal Component Analysis (PCA) for all coral groups (WT0, WT12, and NT12) for the following seven biological properties: (1) physical appearance (tissue colouration), (2) photobiology, (3) metabolism, (4) energy reserves, (5) fatty acid methyl esters (FAME), (6) elementome, and (7) skeletal properties. Variables not considered in the PCA, followed by a brief rationale, are written in italic font.

(1) Physical appearance

A)

Variable	**Dim.1**	**Dim.2**	**Dim.3**	**Dim.4**	**Dim.5**
R	31.6206	1.3084	1.9096	13.0399	19.0309
G	26.9003	6.8402	0.0569	11.9012	46.7686
B	3.9886	34.0950	4.4406	24.2456	31.1878
H	2.8506	23.9952	70.5499	2.4823	0.0023
S	1.4011	33.3520	22.6193	39.1327	2.8521
B	33.2388	0.4092	0.4237	9.1983	0.1584
Bleaching state	*Not considered in the PCA – Same mean among coral groups*				
Max	**33.2388**	**34.0950**			

B)

	Eigenvalue	**Variance percent**	**Cumulative variance percent**
Dim.1	2.913796342	48.56327	48.56327
Dim.2	2.341441905	39.02403	87.5873
Dim.3	0.497617839	8.293631	95.88093
Dim.4	0.162169825	2.70283	98.58377
Dim.5	0.076554886	1.275915	99.85968
Dim.6	0.008419204	0.14032	100

(2) Photobiology

A)

Variable	**Dim.1**	**Dim.2**	**Dim.3**	**Dim.4**	**Dim.5**
E_K	5.1987	26.6999	1.4242	0.0001	5.2212
$F_q'/F_m'_{MAX}$	1.4808	31.9670	1.1472	0.4556	2.5874
$[1\text{-}C]_{MAX}$	5.6758	27.6816	1.1604	1.8134	0.0906
$[1\text{-}Q]_{MAX}$	3.2701	0.0498	11.4605	55.7836	26.3817
Symbiont cell density	16.2934	1.3953	0.9728	0.0348	8.1392
Total pigments per cell	12.6732	1.9627	15.8342	1.9703	0.4704
Chl *a* per cell	10.9460	1.0385	18.3146	6.8279	5.6070

Chl *c2* per cell	13.2879	3.7717	9.1909	0.8278	5.7688
Total pigment density	11.2486	0.4460	21.2471	0.0570	9.5985
Chl *a* density	12.2270	1.1168	18.1577	1.5564	2.7992
Chl *c2* density	7.6984	3.8706	1.0902	30.6730	33.3359
a:c2 ratio	*Not considered in the PCA – correlated variable*				
Symbiodiniaceae ITS2 identity	*Not considered in the PCA – separated analysis*				
Max	**16.2934**	**31.9670**			

B)

	Eigenvalue	**Variance percent**	**Cumulative variance percent**
Dim.1	5.5426	50.3868	50.3868
Dim.2	2.1633	19.6668	70.0536
Dim.3	1.4563	13.2390	83.2926
Dim.4	0.9174	8.3403	91.6329
Dim.5	0.5093	4.6298	96.2626
Dim.6	0.3281	2.9825	99.2452
Dim.7	0.0504	0.4585	99.7037
Dim.8	0.0216	0.1966	99.9003
Dim.9	0.0108	0.0978	99.9982
Dim.10	0.0002	0.0018	100
Dim.11	0.0000	0.0000	100

(3) Metabolism

A)

Variable	**Dim.1**	**Dim.2**	**Dim.3**	**Dim.4**
P_G	25.2170	15.7727	58.8025	0.2077
R	22.8459	32.9157	38.9191	5.3194
G_L	22.8623	42.1456	0.0145	34.9776
G_D	29.0748	9.1660	2.2639	59.4953
P_N	*Not considered in the PCA – correlated variable*			
P_G:R ratio	*Not considered in the PCA – correlated variable*			
G_L:G_D ratio	*Not considered in the PCA – correlated variable*			
Max	**29.0748**	**43.2690**		

B)

	Eigenvalue	**Variance percent**	**Cumulative variance percent**
Dim.1	2.7954	69.8843	69.8843
Dim.2	0.6937	17.3420	87.2263
Dim.3	0.3151	7.8769	95.1031
Dim.4	0.1959	4.8969	100

(4) Energy reserves

A)

Variable	Dim.1	Dim.2	Dim.3	Dim.4	Dim.5
Carbohydrates	3.2689	9.3847	80.7235	2.5182	1.3333
Soluble proteins	11.2480	1.7960	0.3635	56.1005	5.0368
Total lipids	14.4013	0.6165	2.2743	21.5480	17.3157
Total energy reserves	16.3038	0.0155	0.1611	7.2519	13.1736
DW	10.0800	21.0473	4.8151	0.0496	1.2671
AFDW	4.5481	36.1047	10.5442	0.6925	24.9418
SFA	13.3980	10.5302	0.6915	1.8248	13.8113
MUFA	12.7655	13.3530	0.4101	0.0141	22.8679
PUFA	13.9865	7.1521	0.0167	10.0004	0.2526
Max	**16.3038**	**36.1047**			

B)

	Eigenvalue	Variance percent	Cumulative variance percent
Dim.1	5.7656	64.0623	64.0623
Dim.2	1.6886	18.7617	82.8239
Dim.3	0.7897	8.7748	91.5988
Dim.4	0.5422	6.0249	97.6236
Dim.5	0.1299	1.4429	99.0665
Dim.6	0.0416	0.4624	99.5289
Dim.7	0.0329	0.3656	99.8945
Dim.8	0.0095	0.1055	100
Dim.9	0.0000	0.0000	100

(5) FAME

A)

Variable	Dim.1	Dim.2	Dim.3	Dim.4	Dim.5
Methyl dodecanoate (Methyl laurate)	4.5296	6.3910	8.2101	12.1580	5.7245
Methyl myristoleate	1.1248	31.0531	15.5815	0.2351	2.1852
Methyl tetradecanoate	6.2957	3.1204	1.1346	1.0295	0.1908
Methyl pentadecanoate	3.3638	1.3373	15.5860	0.7500	43.3103
Methyl palmitoleate	6.7975	1.7657	0.1563	0.2544	3.4341
Methyl palmitate	6.6846	3.3675	0.0522	1.1446	0.0015
Methyl gamma-linolenate	6.8010	3.0476	0.0342	0.1024	0.6519
Linolelaidic acid methyl ester	6.9194	2.1673	0.0130	0.5957	0.2817
cis-9-Oleic acid methyl ester	6.6072	2.8631	0.1934	1.2013	0.2376
trans-9-Elaidic acid methyl ester	4.5489	0.0025	6.3168	23.2085	9.8063
Methyl octadecanoate (methyl stearate)	6.4669	0.7402	0.8740	1.6713	1.2937
cis-5,8,11,14-Eicosatetraenoic acid methyl ester	2.7717	12.3910	19.9539	6.8242	1.3452

cis-5,8,11,14,17-Eicosapentanoic acid methyl ester	4.8286	2.6687	11.9613	14.1291	0.4607
cis-8,11,14-Eicosatrienoic acid methyl ester	6.4285	0.8736	1.6020	1.8776	3.9898
cis-11,14-Eicosadienoic acid methyl ester	4.0681	5.3021	5.4458	13.6460	8.8238
Methyl cis-11-eicosenoate	6.7016	0.5646	0.9777	0.3517	0.0324
Methyl arachidate	7.0173	0.2211	0.0674	0.0234	0.9073
Methyl cis-4,7,10,13,16,19-docosahexanoate	6.8776	0.0167	0.0003	0.8352	0.7760
Methyl docosanoate	1.1671	22.1064	11.8395	19.9621	16.5470
Max	**7.0173**	**31.0531**			

B)

	Eigenvalue	Variance percent	Cumulative variance percent
Dim.1	13.7769	72.5101	72.5101
Dim.2	1.6666	8.7714	81.2815
Dim.3	1.3988	7.3619	88.6434
Dim.4	0.7310	3.8476	92.4910
Dim.5	0.5610	2.9528	95.4437
Dim.6	0.3666	1.9294	97.3731
Dim.7	0.2672	1.4062	98.7793
Dim.8	0.1146	0.6033	99.3826
Dim.9	0.0481	0.2533	99.6359
Dim.10	0.0305	0.1605	99.7964
Dim.11	0.0187	0.0982	99.8946
Dim.12	0.0092	0.0486	99.9432
Dim.13	0.0068	0.0358	99.9790
Dim.14	0.0031	0.0165	99.9956
Dim.15	0.0008	0.0044	100
Dim.16	0.0000	0.0000	100
Dim.17	0.0000	0.0000	100

(6) Elementome

A)

Variable	Dim.1	Dim.2	Dim.3	Dim.4	Dim.5
C	2.6486	1.3640	26.0665	0.3851	1.0684
N	1.1952	2.7462	24.1221	1.2097	0.0000
Mg	9.7099	2.8341	0.0201	0.3247	13.3444
P	12.3261	2.9743	0.2688	0.1815	0.4344
S	12.4359	2.3319	0.2149	0.0710	4.0831
K	12.8652	1.6407	0.7068	0.4213	0.6535
Ca	3.7779	19.4596	3.5618	3.1166	0.5431
V	4.0875	0.1406	9.7251	6.0440	0.2984
Mn	9.7192	4.6204	0.8377	0.1391	0.1436

Fe	1.7347	20.7758	5.1418	4.0856	0.0744
Ni	5.7239	1.0432	2.8882	0.5712	1.8847
Cu	3.0263	8.5536	7.5049	6.0276	0.0028
Zn	0.5536	0.7571	0.5293	7.1245	62.4249
Sr	2.0974	24.7451	1.9668	3.5381	0.0553
Mo	6.8485	0.0187	3.1194	0.3931	12.1547
Cd	10.4207	0.4837	5.3482	0.5565	0.0173
Sn	0.7494	4.6955	0.2076	32.4132	2.6328
Pb	0.0800	0.8154	7.7699	33.3973	0.1843
Co	*Not considered in the PCA – negligible values*				
Se	*Not considered in the PCA – negligible values*				
C:N ratio	*Not considered in the PCA – correlated variable*				
C:P ratio	*Not considered in the PCA – correlated variable*				
N:P ratio	*Not considered in the PCA – correlated variable*				
C:N:P ratio	*Not considered in the PCA – correlated variable*				
Max	**12.8652**	**24.7451**			

B)

	eigenvalue	**Variance percent**	**Cumulative variance percent**
Dim.1	6.6577	36.9874	36.9874
Dim.2	2.9695	16.4970	53.4844
Dim.3	2.6163	14.5352	68.0196
Dim.4	1.4923	8.2908	76.3104
Dim.5	1.1061	6.1451	82.4555
Dim.6	1.0025	5.5695	88.0250
Dim.7	0.7559	4.1994	92.2244
Dim.8	0.5615	3.1197	95.3441
Dim.9	0.3185	1.7697	97.1137
Dim.10	0.2198	1.2210	98.3347
Dim.11	0.1602	0.8901	99.2248
Dim.12	0.0822	0.4569	99.6817
Dim.13	0.0337	0.1873	99.8690
Dim.14	0.0183	0.1019	99.9710
Dim.15	0.0052	0.0290	100
Dim.16	0.0000	0.0000	100
Dim.17	0.0000	0.0000	100

(7) Skeletal properties

A)

Variable	**Dim.1**	**Dim.2**	**Dim.3**	**Dim.4**	**Dim.5**
Bulk volume	17.1538	22.7144	0.9498	4.6148	10.9643
Biomineral density	6.8420	29.8519	12.7337	0.5533	4.4352

Bulk density	6.5315	1.0573	38.4064	42.3730	11.2445
Apparent internal porosity	12.4627	28.9573	2.7592	0.0639	8.4386
Pore volume	30.6449	1.7048	4.8685	1.3828	10.7470
Hardness	0.0173	12.3524	31.8928	50.6400	5.0352
CMA	26.3478	3.3620	8.3896	0.3721	49.1353
Max	**30.6449**	**29.8519**			

B)

	Eigenvalue	**Variance percent**	**Cumulative variance percent**
Dim.1	2.8077	40.1093	40.1093
Dim.2	1.9907	28.4380	68.5473
Dim.3	1.3188	18.8401	87.3874
Dim.4	0.6429	9.1849	96.5723
Dim.5	0.1471	2.1012	98.6735
Dim.6	0.0791	1.1294	99.8029
Dim.7	0.0138	0.1971	100

Table S2.3 (A) Contributions of traits in the first (PC1) and second (PC2) principal components, and (B) cumulative variance percent of PC1 and PC2 of the Principal Component Analysis (PCA) for all coral groups (WT0, WT12, and NT12) for the following 14 traits: brightness, blue, symbiont cell density, maximum photochemical efficiency of PSII [$F_q'/F_m'_{MAX}$], dark and light calcifications [G_D and G_L, respectively) , total energy reserves, ash-free dry weight biomass (AFDW), methyl arachidate, methyl myristoleate, potassium [K], strontium [Sr], pore volume, and biomineral density (the so-called multitraits).

Multitraits

A)

Variable	Dim.1	Dim.2	Dim.3	Dim.4	Dim.5
Brightness	0.2833	**25.7740**	0.2306	2.2163	2.2905
Blue	**11.4690**	4.7036	0.5115	2.2645	6.0934
Symbiont cell density	8.9553	**8.2251**	5.2107	6.1435	0.5043
$F_q'/F_m'_{MAX}$	7.4004	3.3073	2.2258	7.9685	21.9005
G_D	6.3396	**15.7967**	6.5647	0.0450	2.5363
G_L	9.0069	8.1766	4.6114	2.2954	3.1284
Total energy reserves	**14.4930**	0.5451	4.6535	0.6593	2.2232
AFDW	3.2435	**11.5057**	1.0206	4.3227	36.5346
Methyl arachidate	**15.4141**	1.3167	0.5815	5.8518	1.0506
Methyl myristoleate	5.4729	5.8476	7.8773	24.7291	0.1513
K	**10.4707**	2.2531	5.7307	5.5037	0.3124
Sr	2.0983	3.5268	11.9187	26.2633	9.1224
Pore volume	5.0154	8.1006	8.8985	5.8832	9.0851
Biomineral density	0.3376	0.9210	39.9643	5.8534	5.0671
Max	**15.4141**	**25.7740**			

B)

	Eigenvalue	Variance percent	Cumulative variance percent
Dim.1	4.8285	34.4891	34.4891
Dim.2	2.3888	17.0631	51.5522
Dim.3	1.9974	14.2674	65.8197
Dim.4	1.2469	8.9066	74.7262
Dim.5	0.9305	6.6465	81.3728
Dim.6	0.7767	5.5481	86.9208
Dim.7	0.6209	4.4348	91.3556
Dim.8	0.3677	2.6262	93.9817
Dim.9	0.3270	2.3355	96.3172
Dim.10	0.2993	2.1377	98.4549
Dim.11	0.1470	1.0499	99.5048

Dim.12	0.0455	0.3250	99.8298
Dim.13	0.0142	0.1011	99.9309
Dim.14	0.0097	0.0691	100.0000

Table S2.4 Analysis of variance (ANOVA) and post hoc Tukey HSD to compare the extracted ordination axes (A) PC1 and (B) PC2 of **Fig. 2.8** across coral groups, WT0, WT12, and NT12. Data were assessed for normality. Means were compared by one-way (repeated measures) analysis of variance (ANOVA) with *post hoc* Tukey tests, where ns indicates no statistical significance, and * indicates $p \leq 0.05$.

A) PC1

Repeated measures ANOVA summary						
Assume sphericity?	No					
F	**6.167**					
P value	**0.0337**					
P value summary	*					
Statistically significant (P < 0.05)?	**Yes**					
Geisser-Greenhouse's epsilon	0.719					
R squared	0.5523					
Was the matching effective?						
F	1.67					
P value	0.2291					
P value summary	ns					
Is there significant matching (P < 0.05)?	No					
R squared	0.2721					
ANOVA table	**SS**	**DF**	**MS**	**F (DFn**	**DFd)**	**P value**
Treatment (between columns)	**139290**	**2**	**69645**	**F (1.438**	**7.190) = 6.167**	**P=0.0337**
Individual (between rows)	**94268**	**5**	**18854**	**F (5**	**10) = 1.670**	**P=0.2291**
Residual (random)	**112928**	**10**	**11293**			
Total	**346487**	**17**				

Data summary						
Number of treatments (columns)	3					
Number of subjects (rows)	6					
Number of missing values	0					

Post-hoc comparisons (Tukey's test)								
Number of families	1							
Number of comparisons per family	3							
Alpha	0.05							
Tukey's multiple comparisons test	Mean Diff.	95.00% CI of diff.	Below threshold?	Summary	Adjusted P Value			
Wild corals at T0 vs. Wild corals at T12	**-166.3**	**-332.7 to 0.01167**	**No**	**ns**	**0.05**	**A-B**		
Wild corals at T0 vs. Nursery corals at T12	**-201.8**	**-366.5 to -37.10**	**Yes**	*****	**0.0237**	**A-C**		
Wild corals at T12 vs. Nursery corals at T12	**-35.45**	**-290.0 to 219.1**	**No**	**ns**	**0.8952**	**B-C**		
Test details	Mean 1	Mean 2	Mean Diff.	SE of diff.	n1	n2	q	DF
Wild corals at T0 vs. Wild corals at T12	126.4	292.8	-166.3	51.12	6	6	4.601	5
Wild corals at T0 vs. Nursery corals at T12	126.4	328.2	-201.8	50.61	6	6	5.638	5
Wild corals at T12 vs. Nursery corals at T12	292.8	328.2	-35.45	78.21	6	6	0.641	5

B) PC2

Repeated measures ANOVA summary						
Assume sphericity?	No					
F	**21.94**					
P value	**0.0025**					
P value summary	**					
Statistically significant (P < 0.05)?	**Yes**					
Geisser-Greenhouse's epsilon	0.6203					
R squared	0.8144					
Was the matching effective?						
F	4.454					
P value	0.0214					
P value summary	*					
Is there significant matching (P < 0.05)?	Yes					
R squared	0.2925					
ANOVA table	**SS**	**DF**	**MS**	**F (DFn**	**DFd)**	**P value**
Treatment (between columns)	**0.4375**	**2**	**0.2188**	**F (1.241**	**6.203) = 21.94**	**P=0.0025**
Individual (between rows)	**0.2221**	**5**	**0.04442**	**F (5**	**10) = 4.454**	**P=0.0214**
Residual (random)	**0.09973**	**10**	**0.009973**			
Total	**0.7594**	**17**				
Data summary						
Number of treatments (columns)	3					
Number of subjects (rows)	6					
Number of missing values	0					

Post-hoc comparisons (Tukey's test)								
Number of families	1							
Number of comparisons per family	3							
Alpha	0.05							
Tukey's multiple comparisons test	**Mean Diff.**	**95.00% CI of diff.**	**Below threshold?**	**Summary**	**Adjusted P Value**			
Wild corals at T0 vs. Wild corals at T12	**0.2665**	**0.04586 to 0.4872**	**Yes**	*	**0.025**	**A-B**		
Wild corals at T0 vs. Nursery corals at T12	**-0.1036**	**-0.1911 to -0.01609**	**Yes**	*	**0.027**	**A-C**		
Wild corals at T12 vs. Nursery corals at T12	**-0.3701**	**-0.5920 to -0.1482**	**Yes**	**	**0.0067**	**B-C**		
Test details	Mean 1	Mean 2	Mean Diff.	SE of diff.	n1	n2	q	DF
Wild corals at T0 vs. Wild corals at T12	0.6146	0.3481	0.2665	0.06782	6	6	5.558	5
Wild corals at T0 vs. Nursery corals at T12	0.6146	0.7182	-0.1036	0.0269	6	6	5.448	5
Wild corals at T12 vs. Nursery corals at T12	0.3481	0.7182	-0.3701	0.0682	6	6	7.676	5

Table S2.5 PERMANOVA using Bray-Curtis dissimilarity to compare differences between coral groups (WT0, WT12, and NT12) at “Mojo” site at Opal reef on the Great Barrier Reef.

Permutation test for adonis under reduced model					
Terms added sequentially (first to last)					
Permutation: free					
Number of permutations: 9999					
adonis2(formula = multi.dist ~ Group, data = multi, permutations = 9999, method = "bray")					
	Df	SumOfSqs	R2	F	Pr(>F)
Group	2	23344.1	0.89567	64.385	**0.3767**
Residual	15	2719.3	0.10433		
Total	17	26063.3	1.00000		

Chapter 3

Resolving differences in thermotolerance among corals propagated for restoration on the Great Barrier Reef

C. Isabel Nuñez Lendo[1]*, David J. Suggett[1,2], Samantha Goyen[1,3], John Edmondson[4], Emma F. Camp[1]

[1]Climate Change Cluster, University of Technology Sydney, Ultimo, NSW 2007, Australia2

[2]KAUST Reefscape Restoration Initiative (KRRI) and Red Sea Research Centre (RSRC), King Abdullah University of Science and Technology, Thuwal, 23955, Saudi Arabia

[3]Australian Institute of Marine Science, Townsville, QLD, Australia

[4]Wavelength Reef Cruises, Port Douglas, QLD, Australia

Author contributions: CINL, SG, EFC, and DJS, designed the experiment, and the field-based experimental set up, with logistic support from JE, were conducted by CINL and SG, in addition to sample collection. CINL analysed the bio-physical and photobiological samples. CINL conducted the statistical analysis and prepared the figures. CINL wrote the manuscript with editorial support from DJS and EFC, and with all authors contributing their relevant expertise in methods reporting and evaluation, and overall manuscript editing.

3. Abstract

Global warming is resulting in unprecedented levels of coral mortality due to mass bleaching events, challenging the resilience and persistence of coral reefs. To minimise accelerating climate-driven reef decline, coral restoration practices are increasingly being used globally as a management tool to boost coral biomass and support coral reef recovery. A key challenge for coral restoration is considering how to "future-proof" coral propagation stock to maximise the chance of survival to future environmental change and how the propagation process may impact the innate thermal tolerance of coral taxa. Here we use a standardised short-term acute heat stress assay (i.e., Coral Bleaching Automated Stress System, CBASS) to resolve differences in coral thermotolerance of wild and 12-month nursery-propagated *Acropora* cf. *hyacinthus* from Opal Reef, the northern Great Barrier Reef. Nursery corals have been documented to grow larger and faster within this restoration program, and thus, whether this comes at the cost of their ability to maintain stress tolerance remains unresolved. We have previously shown that these 12-month propagated corals exhibit higher growth rates compared to their wild source colonies, and thus, whether this comes with a trade-off to altered thermal tolerance is unexplored. Overall, nursery-propagated corals exhibited remarkably similar bio-physical (e.g., measures of tissue colour change) and photo-physiological (e.g., photosynthetic efficiency [F_v/F_m], and algal symbiont and pigment density) responses to wild corals facing acute thermal stress. Similar F_v/F_m effective dose values (i.e., ED50; proxy for thermal tolerance) for wild and nursery corals for the acute thermal assay (33.67 °C vs 33.88 °C) were observed, demonstrating that coral propagation retains innate heat tolerance despite higher growth rates before outplanting back to degraded areas. In the 34 °C temperature treatment, no differences in mean F_v/F_m values at the final time point (T_{end}) among wild and nursery corals were observed. However, the nursery corals had a greater range in F_v/F_m values due to three genotypes having ~2-3 higher F_v/F_m values at

T_{end} in the nursery compared to their respective wild donor colonies, which could reflect subtle thermotolerance enhancement for some genotypes in the nursery environment.

3.1 Introduction

Coral reefs are critically important marine systems yet one of the most susceptible to the impacts of climate change (Suggett and Smith, 2020). Of particular concern has been the rise of more frequent and intense "marine heatwaves" that result in mass coral bleaching events (Frölicher et al., 2018; Hughes et al., 2017b), whereby thermal stress drives the breakdown of symbiosis between corals and their photosynthetic symbiotic algae (*Symbiodiniaceae*) (Baker and Cunning, 2015; Suggett and Smith, 2020). While corals can recover from bleaching, the increase in frequency and intensity of thermal stress events, alongside other anthropogenic stressors, is leading to global declines in coral reef structure, functionality, and associated service value (Harborne et al., 2017; Hughes et al., 2017a; Williams and Graham, 2019); in turn, these various declines are eroding reef resilience to further stress (Ellis et al., 2019; Hughes et al., 2021). Local management efforts are increasingly turning to restoration practices to aid reef recovery in efforts to offset the continued declines in reef health (e.g., Kleypas et al., 2021). Current restoration practices are diverse (reviewed in Suggett and van Oppen, 2022), spanning direct interventions to speed repopulation of corals and hence rebuild coral biomass, targeting specific coral traits and processes (e.g., coral cover and growth, coral recruitment; Boström-Einarsson et al., 2020), whereas others focus on the reef environment (e.g., substrate stabilisation; Ceccarelli et al., 2020) to enable corals to recolonise. Such restoration activities do not negate prioritising immediate climate action to reduce climate change-driven impacts on reef health (Anthony et al., 2017, 2015; Kleypas et al., 2021; Suggett and Smith, 2020), but increasing evidence suggests local coral restoration can boost

coral cover and diversity at sites around the world (van Woesik et al., 2020; Williams et al., 2019), including the Great Barrier Reef (Howlett et al., 2023; Nuñez Lendo et al., 2024, **Chapter 4**; Roper et al., 2022). The rate and extent of emission reductions remain uncertain, and hence a fundamental prerequisite is the need for restored corals to be resistant to future thermal stress events.

To address the fundamental need to "future-proof" restoration activities, research has started to trial strategies that may increase the likelihood of long-term survivorship (Camp, 2022). Examples include (i) targeting restoration in natural refugia (Mertz and McDonald, 2021), (ii) employing assisted evolution methods to boost preferential traits (Buerger et al., 2020; Quigley et al., 2023) via the selective breeding of sexual recruits (Guest et al., 2014; Quigley et al., 2020) and/or assisted gene flow (i.e., corals or their sexual gametes from one population are imported to another population; Bay et al., 2017; Hagedorn et al., 2021; Van Oppen et al., 2015), and (iii) identifying and propagating naturally resilient corals (Lirman and Schopmeyer, 2016; Rinkevich, 2014). Potential for enhanced coral thermotolerance has been identified in recent years by sampling across diverse coral genotypes (Bay and Palumbi, 2014; Dixon et al., 2015; Lundgren et al., 2013; Morikawa et al., 2019; Muller et al., 2018; Osman et al., 2018; Parkinson et al., 2015), populations (e.g., Barshis et al., 2013; Kenkel et al., 2013; Palumbi et al., 2014), and reef regions (Fine et al., 2013; Guest et al., 2012; Hume et al., 2013); these include some examples for heritability and hence persistent thermotolerance (e.g., Dixon et al., 2015; Kenkel et al., 2015; Meyer et al., 2009).

Importantly, heat-tolerant corals could be used as broodstock and source material for restorative interventions and help boost the number of heat-tolerant individuals in restored

populations (Lohr and Patterson, 2017; Morikawa et al., 2019; van Oppen et al., 2017). However, a prerequisite for field implementation of this strategy is to first locate and identify heat-tolerant colonies in an efficient and consistent manner and move beyond the more traditional approaches for colony selection. Specifically, selecting "survivors" after a bleaching event (Cunning et al., 2016; Glynn et al., 2001; McClanahan, 2004), incorrectly assuming all survived by enhanced heat tolerance (e.g., Gardner et al., 2019), or relying on time-consuming and expensive experimental approaches (Edmunds, 1994; Muller et al., 2018). Nevertheless, for restoration purposes, it is important to ascertain whether the corals' ability to withstand thermal stress was either the result of the native environment (e.g., a coral population adapted to a mangrove lagoon) (Camp et al., 2019), local conditioning (e.g., aclimation when propagating corals on a nursery setting; i.e., the objective of this current study), or environmental memory or history (e.g., the memory of previous exposure to environmental stress; Hackerott et al., 2021). In the latter case, environmental memory of a thermal stress event can lead to "thermal stress hardening" (Martell, 2023), or alternatively, corals may possess an innate thermal tolerance or have survived stress via refugia (Camp et al., 2018); thus understanding the factors underlying coral thermal variation is important to estimate the likelihood of future survival to stress events and in turn, maximise return-on-effort of coral restoration activities.

Significant variability in coral heat tolerance has been observed across geographical and environmental gradients (Berkelmans, 2002; Coles et al., 1976; Dixon et al., 2015; Drury and Lirman, 2021; Kenkel et al., 2013; Osman et al., 2018; Ulstrup et al., 2006; Voolstra et al., 2021b), with higher thermotolerance in coral populations from warmer locations. Such thermal differences have also been recorded amongst populations distributed over small spatial scales (i.e., microhabitats) (Oliver and Palumbi, 2011; Schoepf et al., 2015; Voolstra

et al., 2020), highlighting strong natural selection across microenvironments (i.e., evolutionary adaptation) and/or acclimatisation mechanisms (Brown et al., 2002; Humanes et al., 2022; Palumbi et al., 2014). Thus, optimising restoration strategies requires investigating the potential for restoration practices themselves to impact thermotolerance; for example, propagation of corals in nurseries, which can have very different environments compared to wild source colonies on the reef, drive different biological responses (e.g., Nuñez Lendo et al., 2023, **Chapter 2**; Strudwick et al., 2022). In particular, vastly greater growth accompanied by an enhanced metabolism (i.e., photosynthesis, calcification, and/or respiration; Nuñez Lendo et al., 2023, **Chapter 2**) was observed in 12-month nursery-reared corals compared to their native donor coral colonies (hereafter referred to as "Wild"). Thus, it seems plausible to expect that nurseries could also change other important coral biological traits, including the potential to induce more thermally tolerant coral taxa (i.e., coral thermotolerance), specifically where higher respiration rates have been reported in corals that thrive in extreme environmental conditions, including hot waters (Camp et al., 2019). Alternatively, and still unresolved, high coral growth may come at an energetic cost to the ability to maintain stress tolerance and, thus, may reduce thermal tolerance.

Additionally, the higher gases exchange during photosynthesis-respiration is manifested in a more dynamic boundary layer around the coral tissue, which could alleviate thermal stress (Jimenez et al., 2011; Merk and Prins, 1954). Also, coral nursery propagation may select for very different microbiomes as a result of different environments (and hence nutritional strategy) (Nuñez Lendo et al., 2023, **Chapter 2**; Strudwick et al., 2022). Microbial associations do not always have the same thermotolerant effect on corals as conspecifics from the same habitat, despite hosting the same symbiont types, can show marked differences in bleaching susceptibility (Cunning et al., 2016; Ritson-Williams and Gates, 2020).

Consequently, thermal tolerance varies significantly at the individual level (Drury, 2020; Drury et al., 2017; Kavousi et al., 2020; Kirk et al., 2018; Morikawa et al., 2019; Wright et al., 2019), and the result of complex interactions of the coral (host) genotype and its symbiotic partners (Baums et al., 2014; Kenkel et al., 2013).

Resolving variation in coral thermal tolerance is commonly achieved using experiments and observations that track bleaching severity (e.g., Suggett & Smith 2020, Nielsen et al.,2022), and unsurprisingly restoration efforts are adopting these assays to screen populations for selecting more stress-tolerant individuals (e.g., Morikawa & Palumbi 2019, Cunning et al.,2021). Bleaching monitoring in coral nurseries has traditionally been based on observations of naturally occurring bleaching severity and mortality (e.g., dela Cruz et al., 2015; Lohr and Patterson, 2017; Merselis et al., 2018; O'Donnell et al., 2017; Shaish et al., 2010, 2008). However, exceptions include long-term laboratory heat stress exposure (200 days) of multiple species from nurseries (American Samoa; Morikawa et al., 2019), and both long-term (~2 months) (Muller et al., 2018) and a standardised 18-h short-term acute experiments (Cunning et al., 2021) of nursery reared *Acropora cervicornis*, the latter case using the Coral Bleaching Automated Stress System (CBASS, Voolstra et al., 2020). Mapping the natural occurrence of coral bleaching resistance on reefs (Cornwell et al., 2021) has also been used to guide initial nursery stock selection (Morikawa et al., 2019). Despite these few studies, we still have a limited understanding of how to identify (thermal) resilient individual coral colonies to propagate, as well as how nursery-propagation impacts coral bleaching thresholds of propagated corals that will be later used for outplanting activities.

Here, we assessed the thermal performance of nursery propagated colonies of the coral *Acropora* cf. *hyacinthus* versus their wild adult counterparts — source colonies retained on the reef — from the northern Great Barrier Reef (GBR, Australia) to resolve differences in coral thermally induced bleaching susceptibility using the CBASS assay. We first examined the thermotolerance of wild coral colonies and then whether identical genotypes in the nursery exhibited decreased, enhanced, or conserved thermotolerance. For this, we compared the corals' response to the CBASS standardised 18-h heat stress assay (3 h heat-ramp, 3 h heat-hold, 1 h ramp-down, 11 h hold) using 12-month-old nursery and adult fragments. We analysed a suite of bio-physical (tissue colouration) and photo-physiological metrics (maximum photochemical efficiency [F_v/F_m], symbiont density, and chlorophyll *a* and *c2* (Chl *a* and c2) concentrations at three temperature treatments (31 °C, 34 °C, and 37 °C). The effective dose of heat stress required to reduce F_v/F_m by 50% (ED50) was also determined. We discuss how restorative interventions such as nursery propagation may aid/complement increasing coral biomass without compromising the critical trait of thermal resistance and providing heat-resilient coral material for outplanting activities.

3.2 Materials and Methods

3.2.1 Study site and sample collection

Thermal tolerance of wild and nursery-propagated colonies of *Acropora* cf. *hyacinthus* (n = 6 each), a key coral species for the northern Great Barrier Reef (GBR), Australia (Ortiz et al., 2021), including for restoration activities (e.g., Howlett et al., 2022, 2021), was investigated in February 2021. Wild adult colonies (129.0 ± 18.3 cm in diameter, n = 6) for propagation were first selected at "Mojo" site at Opal Reef, 50–60 km from Port Douglas, Queensland (145° 53' 50.3''E, 16°12' 30.4''S) (**Fig. 3.1**) in February 2020. Colonies were located at

depths 5–6 m and spaced by a minimum of 10 m apart to minimise the potential of sampling clonal genotypes (Baums et al., 2006; Howlett et al., In Review). Wild colonies were tagged and photographed for subsequent relocation, and a partial fragment was carefully removed for nursery propagation. Each partial fragment was subsequently further fragmented into three (each triplicate with an average initial area of 127.1 ± 8.2 cm^2), tagged, and secured with cable ties in an adjacent coral nursery facility to grow out for 12 months (as per Nuñez Lendo et al., 2023, **Chapter 2**). The coral nursery was comprised of two aluminium diamond-mesh frames (2.0 x 1.2 m) placed 1–2 m above a sand patch by means of 2 × 9 kg Besser blocks and a 20-L float (Howlett et al., 2021; Suggett et al., 2019) so that corals were suspended at 4–5 m depth (Nuñez Lendo et al., 2023, **Chapter 2**).

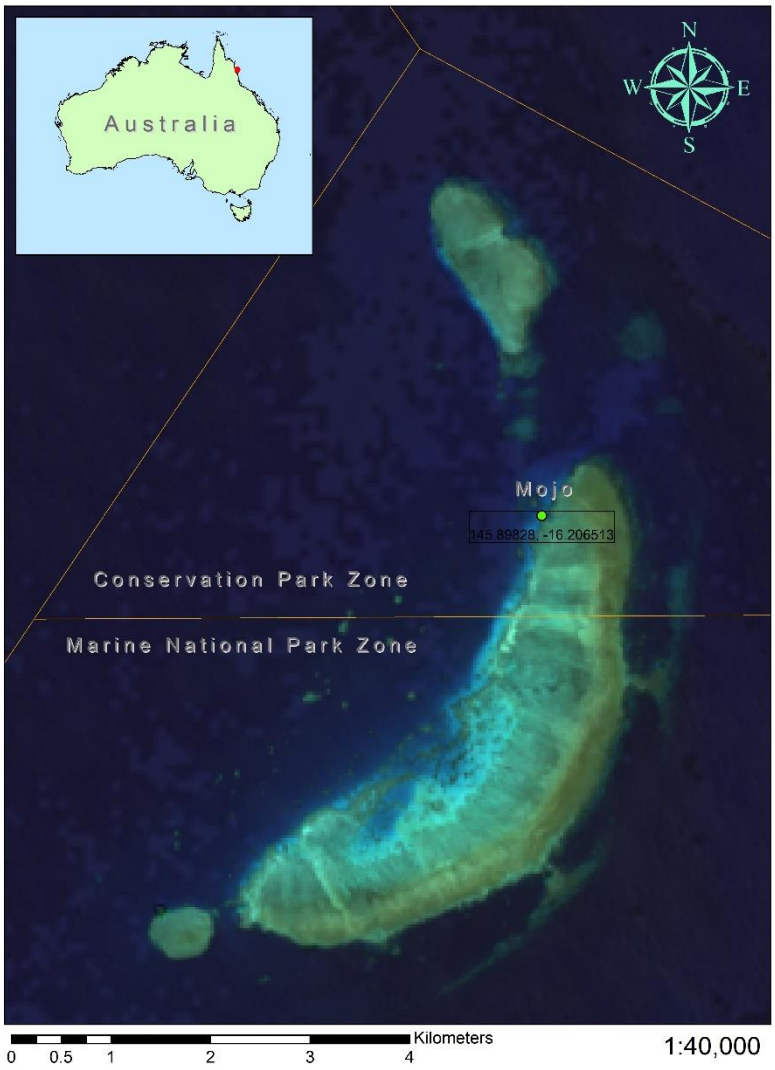

Figure 3.1 Map of study site on Mojo, Opal Reef, Great Barrier Reef, Australia. Corals were collected from the reef patch adjacent to the coral nursery at 5–6 m in depth. Coral fragments were held on the coral nursery, which is located on the sand patch, suspended at 4–5 m in depth. Delineation of the management zones for Opal Reef is shown. Satellite image: Landsat 8 OLI, bathymetric composite RBG bands 431, acquired September 5th, 2021. Source: NASA/USGS/Pearce, S. 2021.

Both the wild colonies and nursery retained fragments were then all sampled after 12 months (February 2021; termed wild and nursery, respectively) to resolve differences in coral thermally-induced bleaching susceptibility using the Coral Bleaching Automated Stress System (CBASS) method (Voolstra et al., 2020). Fragments (~60 cm^2) were taken from each wild colony and nursery-propagated fragments (n = 6 each; 12 fragments) using wire clippers

for CBASS experimentation, detailed below. Each sample was temporarily stored in Ziploc plastic bags upon underwater collection and transported to the operations vessel (*Wavelength 5*). All samples were held onboard in a flow-through tank supplied with native seawater for 1 h until experimentation (i.e., before temperature ramping began). All corals were collected under permits from the Australian Great Barrier Reef Marine Park Authority (Permit no. G21/45224.1).

Temperature was initially set up to record in 1-h intervals for the reef, and the nursery using *in situ* deployed Temperature HOBO^{TM} loggers over the 12 months of growth (i.e., from February 2020 to February 2021). However, the logger installed at the reef failed post-deployment, and the nursery one lasted nine months. Therefore, sea surface temperature (SST) was extracted from GIOVANNI online system for satellite-derived data maintained by NASA (https://giovanni.gsfc.nasa.gov/giovanni/) by using monthly area-averaging bounded to 145° 53' 50.3''E, 16°12' 30.4''S (Opal Reef) between the beginning of February 2020 and the end of February 2021. Additionally, HOBO SST data from the nursery at Mojo was overlaid with Giovanni SST data for Opal Reef (**Fig. S3.1A**). Maximum Monthly Mean (MMM) temperature for February 2021 was 28 °C and was calculated using the 5 km resolution SST dataset (Coral Reef Watch CoralTemp V3.1 1985–2012 climatology; https://coralreefwatch.noaa.gov/product/5km/index_5km_sst.php). Note that during the time the HOBO^{TM} logger was recording, the temperature at the nursery environment was ~1 °C above than the Maximum Monthly Mean for Opal Reef. During this period, the GBR experienced its third (and most widespread) mass bleaching event in five years (i.e., March 2020, 1 month after the onset of our study, **Fig. S3.1B**), and our studied *A.* cf. *hyacinthus* colonies and fragments at Opal Reef visibly paled (including on the nurseries, JE, Pers. Comm.); however, no mortality of our experimental coral material was observed. The extent

and intensity of the bleaching event are represented in the 5-km product from NOAA Coral Reef Watch (CRW) (https://coralreefwatch.noaa.gov/) and includes SST anomaly, Degree Heating Weeks (DHW) and bleaching alert (**Fig. S3.1C**).

3.2.2 Short-term acute heat stress assays (CBASS)

Six small fragments (~5 cm^2) were prepared from each sample (i.e., 6 replicates x 6 nursery and 6 wild; n = 36 for each coral group and n = 72 fragments in total). Fragments were individually tagged and distributed across the CBASS temperature treatment replicated tanks (n = 6); specifically, one fragment of nursery and wild coral was placed in each tank. The system consisted of two replicate tanks (21 L flow-through tanks) capable of running three independent temperature profiles with light settings adjusted *in situ* light conditions. Each fragment was secured with a wire cable coated in PVC to a plastic frame at the bottom of each tank, and all fragments per tank were photographed for consistent monitoring over the CBASS assay. Initially, we intended a target of four temperature treatments in line with previous CBASS assays: control/baseline corresponding to MMM for February 2021 – 28 °C (**Fig. S3.1A**), medium – 31 °C, high – 34 °C, extreme – 37 °C. However, the ambient temperature at the onset of the heat stress assay in February 2021 was 31 °C and cooling to 28 °C was not possible due to technical difficulties. Therefore, our heat stress assay ultimately consisted of two replicated flow-through tanks corresponding to three temperature profiles spaced by 3 °C such that fragments from each coral (i.e., 6 colonies x 2 coral groups) were in each treatment condition (new control/baseline – 31 °C, medium – 34 °C, high – 37 °C), to yield a total of 2 x 36 fragments (6 colonies x 2 coral groups = 12 fragments; 12 fragments per tank x 3 temperatures = 36 fragments x 2 replicated tanks = 72 fragments) that

were subjected to an 18 h standardised short-term acute heat stress assay (CBASS) (**Fig. 3.2A-B**).

A)

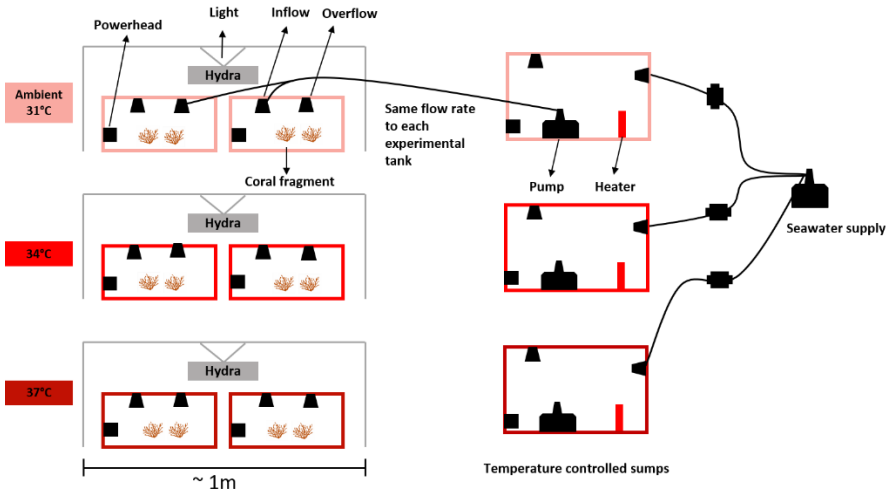

B)

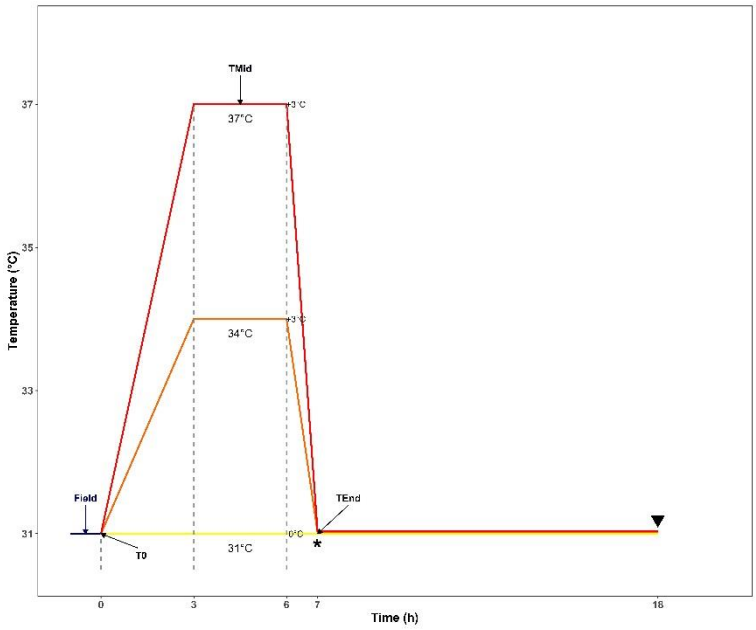

Figure 3.2 Schematic experimental setup for the Coral Bleaching Automated Stress System (CBASS). A) Fragments of six coral colonies from two coral groups (donor and their nursery-derived corals) were subjected to an 18 h short-term acute heat stress assay (CBASS), run at control (31 °C), medium (34 °C) and high (37 °C) temperatures. To note, fragments from each coral colony were exposed to each temperature treatment. B) Targeted temperature profiles for the acute heat stress assay (CBASS). The graph shows the ambient temperature (31 °C) in February 2021 before exposing the corals to target experimental temperatures of 34 °C and 37 °C. Asterisk indicates the time point (T_{end}) of dark-adapted photosynthetic efficiency measurements together with coral sampling. Additionally, photosynthetic efficiency measurements were taken before starting the experiment (T_0) and after 4.5 h as a check control to ensure the corals held in the CBASS were still alive. Dashed vertical lines designate the start and end of the heating hold.

Each temperature treatment was controlled by an independent sump that was continuously supplied with Opal Reef seawater (Eheim CompactON 5000L/h) and fitted with a 600L/h powerhead (Aqua One Moray 360) to circulate water. Titanium aquarium heaters (200W, Schego, Germany) connected to a thermostat and temperature probe were used to maintain the target temperature in each tank. Treatment tanks were supplied with native seawater (Eheim CompactON 2500 L/h) at a rate of approximately 0.6 L/min (turnover = approx. 1.7 h), receiving an equal flow rate in each replicate tank. Seawater was circulated within each tank using a submersible powerhead (Aqua One 320 lph), and temperature and light were recorded using inter-calibrated HOBO^{TM} Pendant Data Loggers (30-minute interval, Microdaq, USA) for the duration of the experiment. Light intensity for experimental tanks was set to 300 µmol photons m^{-2} s^{-1}, corresponding to the average light saturation coefficient (E_K, mmol photons m^{-2} s^{-1}) — a measure of the long-term light acclimation state (e.g., Suggett et al., 2022) — as determined via rapid light curves (RLCs) assessed by Pulse Amplitude-Modulated (PAM) fluorometer (Walz GmbH, Germany) as previously (e.g., Nitschke et al., 2018). For each RLC, an initial dark measurement and 8 actinic light steps were applied, whereby each light intensity was applied for 20 s. The actinic light levels (verified against a factory-calibrated LI-192 quantum sensor, Li-Cor) of the RLC were 0, 115, 195, 265, 350, 500, 710, 1020, 1400 µmol photons m^{-2} s^{-1}. Irradiance was supplied via white LED aquarium lights (Hydra 52, Aqua Illuminations, Illinois, USA) positioned directly above the experimental tanks and measured using a PAR meter equipped with a 4π sensor (Li-Cor LI-250A) to match reef *in situ* light fields (~300 µmol photons m^{-2} s^{-1}).

The CBASS assay was initiated at noon (12:00 h), and the three temperature treatments were as follows: the control/baseline replicated tanks were maintained at 31 °C for the entire duration of the experiment (18 h). A 3-h heat-ramp was applied to the two thermal stress

treatment replicated tanks to reach 34 °C and 37 °C. Once target temperatures were achieved, they were held for 3 h, followed by a 1 h ramp-down to return to the control/baseline temperature of 31 °C (19:00 h). Maximum photochemical efficiency of the photosystem II (PSII) (F_v/F_m, dimensionless) was measured on each coral fragment by means of the PAM as a proxy for heat stress response before the start of the experiment (field temperature, T_0), approximately halfway down of the assay (4.5 h; T_{mid}), and after 7 h for each target temperature (T_{end}) (**Fig. 3.2A-B**). Only the resulting data from T_{end} were used to build a dose-response curve for each coral (6 wild and 6 nursery corals) based on the effective dose of heat stress required to reduce F_v/F_m by 50% (ED50 value; Evensen et al., 2021), and used as a metric of coral thermal tolerance (**Fig. 3.3**, **Fig. S3.3**). All corals were kept at 31 °C overnight until sampling the following day (08:00 h), thereby completing the 18-h cycle of the CBASS. All tanks were continuously supplied with Opal Reef seawater (see above) and active photosynthetic radiation of 300 µmol photons m^{-2} s^{-1} on a 12:12 h day/night cycle. At the end of the CBASS experiment, all coral fragments were photographed (to describe the bio-physical colouration of the coral tissue) before being snap-frozen in liquid nitrogen and stored at -80 °C until further photo-physiological analysis at UTS.

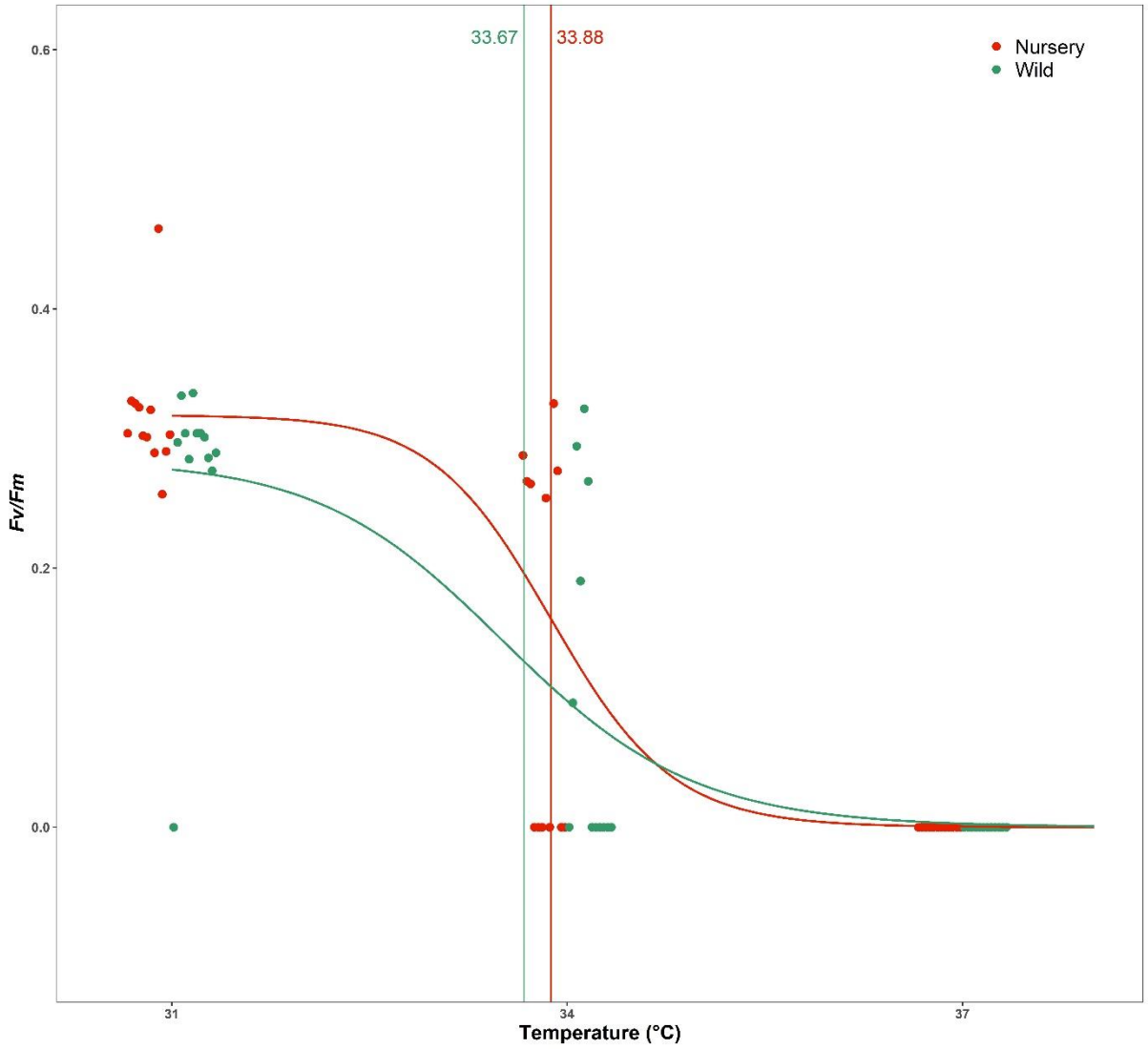

Figure 3.3 Thermal tolerances of donor (wild) and 12-months-propagated *Acropora* cf. *hyacinthus* (nursery) in Opal Reef (the northern Great Barrier Reef). Maximum quantum yield of photosystem II (F_v/F_m) at the final time point (T_{end}) fitted to log-logistic, dose response curves. Curve fits were used to determine the F_v/F_m ED50 for each coral group (vertical lines), which represent the x-value (in temperature) at the inflection point of the curve where F_v/F_m values in the model fit were 50% lower in comparison to the initial values of the model.

3.2.3 Photographic assessment of coral bleaching

Changes in coral tissue colouration can result from a loss of symbiont cells, a loss of chlorophyll pigment content within those cells (Chow et al., 2016), or the loss of coral tissue itself. On the other hand, photosynthetic efficiency is a direct measure of viability of the algal

symbiotic partners and only an indirect indicator of thermotolerance of the coral holobiont (Middlebrook et al., 2010; Suggett and Smith, 2011). For this reason, we examined whether tissue colour change also captured differences among coral groups during the acute thermal assay (Nielsen et al., 2022). Each tank (containing 12 coral fragments corresponding to 6 wild and 6 nursery corals) was photographed at both the start (T_0) and end (T_{end}) of the heat stress assay before being snap-frozen in liquid nitrogen and stored at -80 °C until further laboratory processing. Only values from T_{end} are reported for the purpose of comparison with thermotolerance obtained from F_v/F_m (T_{end}). Photographs were taken at exposure 0 and a fixed distance of 25 cm with an Olympus Stylus TOUGH TG-4 digital camera, together with two underwater colour references — a black and white reference (Chow et al., 2016) and the Coral Watch bleaching card (Siebeck et al., 2006). Manual settings were used to ensure the gain and white balance settings remained constant. Using the histogram function from Adobe Photoshop (version 20.013.20074), photographs were subsequently analysed to determine the hue (reflected colour, with values of 0-360°), saturation (proportion of grey in the hue), and brightness (relative lightness and darkness, both having values of 0-255, where 0 and 255 are absolute white and black, respectively) from ten selected sampling points on the coral fragment, which were then averaged (with the black and white colours as a reference) as per Nuñez Lendo et al., 2023, **Chapter 2**. In addition, red, green, and blue (RGB) values (values from 0 to 255 corresponding to standard white and black, respectively) were also extracted with Adobe Photoshop to infer loss of chlorophyll density (a measure that comprises symbiont cell density and chlorophyll content within each cell) as determined from an increase in R intensity (Nuñez Lendo et al., 2023, **Chapter 2**; Winters et al., 2009). Coral tissue colouration was further categorised according to the bleaching state by use of the Coral Watch bleaching card as per Siebeck et al., (2006), where a colour score difference > 2 is

considered indicative of a significant change in symbiont density and chlorophyll *a* concentration, and thus bleaching state.

3.2.4 *Symbiodiniaceae* cell density and pigment content

Previously snap-frozen fragments in liquid nitrogen were defrosted to analyse symbiont cell density and pigment content. Coral tissue was removed from the coral fragments with an air-gun (Deschaseaux et al., 2013) in a small Ziplock bag containing 4 mL of 0.2 µm filtered seawater (FSW) (Minisart NML 16534 syringe filters, Sartorius, Germany). A 1 mL aliquot of the resulting coral slurry was used to determine chlorophyll *a* and *c2* concentration. Host and symbiont fractions were separated via centrifugation (4 °C at 3500 RPM for 5 min), and the pellet was resuspended in 1 mL FSW. The 1 mL-algal suspension was washed twice, pelleted, and the cells lysed with 3 mL of 100% acetone in a scintillation vial placed on an ice bath and sonicated for 10 min. To minimise any chlorophyll degradation, samples were covered with aluminium foil throughout. After sonication, samples were stored at -4 °C to allow pigment extraction. After 24 h, samples were centrifuged to remove cellular debris and measured on a spectrophotometer (Cary 60 UV-Vis, Agilent Technologies, Santa Clara, CA, USA); λ = 630, 663 and 750 nm in a 4 mL-glass cuvette. Chlorophyll *a* and *c2* were derived from spectrophotometric equations (Jeffrey and Humphrey, 1975) by standardising values to fragment surface area through the wax dipping method (pg $cell^{-1}$ and pg cm^{-2}), in addition to calculating chlorophylls ratio (*a*:*c2*).

A second aliquot of the coral slurry (1 mL) was then used to determine symbiont cell concentrations. The symbiont fraction was again isolated from the host tissue via centrifugation (as described above), and the symbiont pellet was resuspended in 1 mL FSW.

The algal suspension was preserved with 20 µL of 2% glutaraldehyde, and cell counts were later performed using a hemacytometer under a Nikon Ti microscope at 10x magnification. Cell density was obtained by standardising the values to volume and fragment surface area.

3.2.5 Statistical analysis

Data analyses were performed using Rstudio (version 1.4.1717) and GraphPad Prism (version 9.1.2). Assumptions of normality were assessed visually via QQ plots and a Shapiro-Wilk's test, and equal variances were assessed using the Brown-Forsythe test (Shapiro and Wilk, 1965). Data were transformed to meet normality assumptions where required. In particular, log transformation [log (Y)] was carried out for symbiont cell density; arcsine (Y/100) for percentages (1-100%), such as saturation and brightness; and sin (Y) for degree data, such as hue. Significance was set at $p < 0.05$ (for all tests), and the mean ± the standard error of the mean (SEM) was reported unless expressly noted. A series of (repeated measures) two-way analysis of variance (ANOVA) with post hoc tests (Tukey) were undertaken to evaluate differences among coral groups (also referred to as environments, wild vs nursery) across temperature treatments at the end of the experiment (T_{end}) for the bio-physical and photo-physiological traits (RGB, HSB, bleaching state, symbiont cell density, pigment content, and F_v/F_m).

The effects of time point and temperature on F_v/F_m response variable for the start of the experiment (T_0), halfway down the assay (4.5 h, T_{mid}), and after 7 h (T_{end}) for each target temperature (31 °C, 34 °C, and 37 °C) were analysed (e.g., Evensen et al., 2021). Data were first standardised and analysed using a pairwise permutational multivariate analysis of variance (PERMANOVA; perm = 999) on Euclidian distances using the "*vegan*" R package

(time point and temperature as fixed variables). Post hoc pairwise comparisons were conducted using "*pairwiseAdonis*" R package with Bonferroni adjusted p-values.

A second PERMANOVA (coral group as a fixed variable) was performed within each time point (T_0, T_{mid}, and T_{end}) to detect differences in F_v/F_m among coral groups and temperature treatments (31 °C, 34 °C, and 37 °C) to (i) record initial photosynthetic efficiencies (T_0) (i.e., to detect any coral group effect on F_v/F_m within their native seawater of 31 °C before starting the CBASS experiment), (ii) monitor photosynthetic efficiencies halfway down the experiment (T_{mid}) (i.e., checkpoint control to ensure the continuation of the experiment), and (iii) record final F_v/F_m values (T_{end}) (i.e., to report values as per Voolstra et al., (2020) and to calculate the F_v/F_m ED50 metric as a proxy for the thermal tolerance of coral, Evensen et al., (2021). Data were first standardised, and PERMANOVA was conducted on Euclidian distances, with 999 permutations used to generate p values. Post hoc pairwise comparisons were conducted using "*pairwiseAdonis*" R package with Bonferroni adjusted p-values.

Individual response variables were also analysed using linear mixed-effects (LME) models, with coral group and temperature as fixed effects and genotype and tank replicate as random effects to account for any potential genotype or tank effects. Time points were again analysed separately. Models were conducted in the "*lmerTest*" R package (Evensen et al., 2021).

Finally, F_v/F_m values (T_{end}) were used to build a dose-response curve for each colony based on the effective dose of heat stress required to observe a 50% reduction in photosynthetic efficiency relative to the baseline temperature, used as a metric of colony thermal tolerance as per Evensen et al., 2021. Log-logistic dose-response curves of the wild and 12-month-

propagated *A.* cf. *hyacinthus* (nursery) were compared through the function "*EDcomp*" (Eldridge et al., 2022).

3.3 Results

3.3.1 Initial screening of photosynthetic efficiency

Maximum PSII photosynthetic efficiency (F_v/F_m) varied among time points (T_0, T_{mid}, and T_{end}) and temperature treatments (31 °C, 34 °C, and 37 °C) ($p < 0.001$ and < 0.001 for time point and temperature, respectively, **Fig. S3.2**, **Table S3.1**). Values of F_v/F_m were similar for T_{mid} vs T_{end} ($p = 0.7223$; **Table S3.1**), highlighting that after 4.5 h of heat stress treatment (T_{mid}), the decrease in photosynthetic efficiency was similar to that of 7 h of thermal stress (T_{end}).

No differences in F_v/F_m values were found for nursery vs wild corals (within their native seawater of 31 °C) (T_0, $p = 0.567$), and hence at the start of the experiment, but also for T_{mid} ($p = 0.852$) and T_{end} ($p = 0.852$) (**Table S3.2**). More specifically, wild corals exhibited F_v/F_m values of 0.2759 ± 0.0254 (31 °C), 0.0975 ± 0.0257 (34 °C), and 0.0000 ± 0.0000 (37 °C), with slightly higher values observed in nursery corals, 0.3175 ± 0.0140 (31 °C), 0.1396 ± 0.0627 (34 °C), and 0.0000 ± 0.0000 (37 °C). Colony-specific differences were observed for some temperatures. At the medium temperature (34 °C), 3 of the 6 nursery corals exhibited higher values of F_v/F_m — putatively indicative of enhanced thermotolerance (2.02-2.74 times higher) — than their wild corals (0.2605 ± 0.0065, 0.2700 ± 0.0050, and 0.3070 ± 0.0200 for nursery colonies #2, #3, and #5, respectively, compared to 0.0950 ± 0.0950, 0.1335 ± 0.1335, and 0.1470 ± 0.1470 for wild colonies #2, #3, and #5, respectively). However, a 100% decrease in photosynthetic efficiency was observed in nursery colony #4 compared to their

wild colony (0.0000 ± 0.0000 vs 0.1615 ± 0.1615). These findings suggest that more divergent phenotypes resulted in the nursery (e.g., greater variance in F_v/F_m at 34 °C; **Fig. 3.4A**) than on the reef. For the purpose of resolving thermotolerance of propagated corals vs wild corals, only F_v/F_m values from T_{end} were used (as per Evensen et al., 2021; Voolstra et al., 2020), where differences were only observed among temperature treatments ($p < 0.0001$) but not coral groups ($p = 0.852$) (PERMANOVA; **Table S3.2C**). Linear mixed-effects (LME) models discarded any genotype effect on the initial F_v/F_m values of propagated and wild corals (T_0, $p = 0.6515$; **Table S3.3A**) and similarly discarded any genotype or tank effect at T_{end} ($p = 0.2261$ and 0.2284, respectively; **Table S3.3C**).

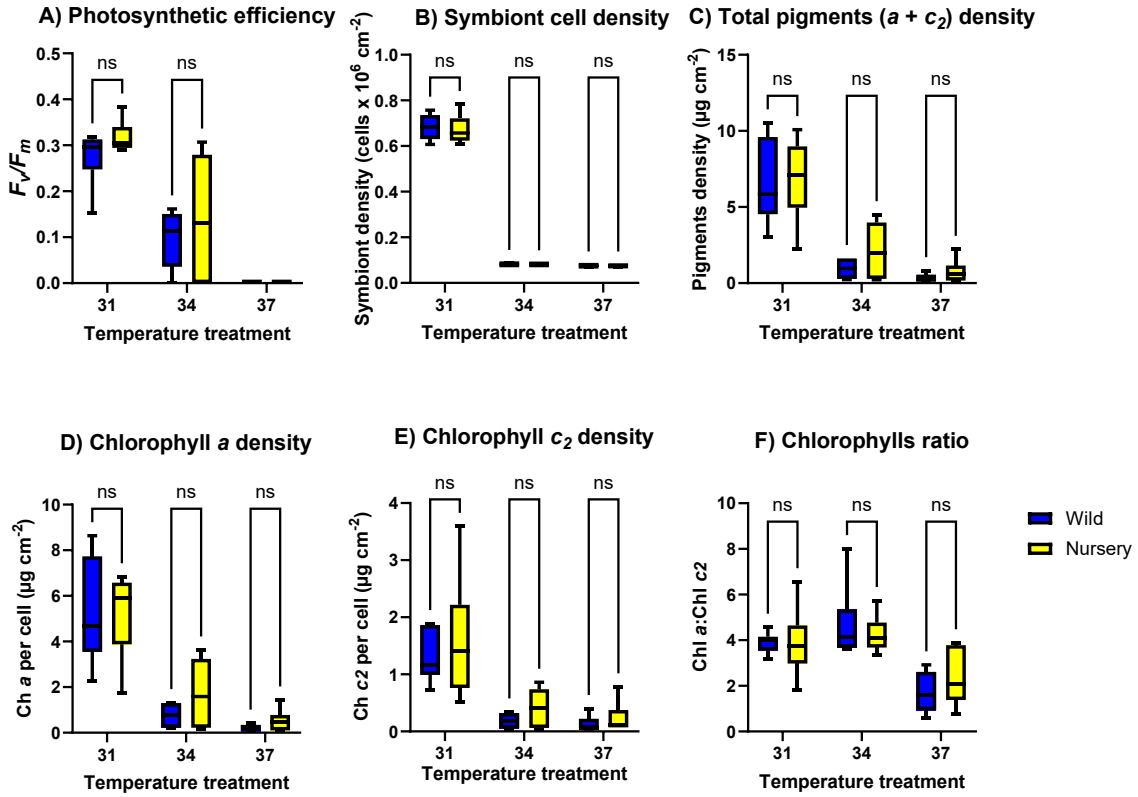

Figure 3.4 Photobiological performance under heat stress of donor (wild) and 12-months-propagated *Acropora* cf. *hyacinthus* (nursery). Mean (± SEM) (A) dark-adapted photosynthetic efficiency (F_v/F_m), (B) symbiont cell density (cells x 10^6 cm^{-2}), (C) total pigments, (D) chlorophyll *a* and (E) *c2* density (C-E, µg cm^{-2}), and chlorophylls ratio (F) of donor (wild, in blue) and 12-months propagated *Acropora* cf. *hyacinthus* (nursery, in yellow) at different heat stress temperatures. All data are fragments of *Acropora* cf. *hyacinthus* (n = 6 for each coral group and temperature treatment). Means were compared by RM-ANOVA (A-F), ANOVA with post hoc tests (see main text) where ns indicates no statistical significance.

3.3.2 ED50 thermal threshold to resolve coral thermotolerance differences during nursery propagation

A small increase in ED50 thermal thresholds was observed for 12-month nursery-propagated *A.* cf. *hyacinthus* compared to wild colonies (**Fig. 3.3**, **Fig. S3.3**); specifically, thresholds were 33.67 °C ± 1.49 (n = 6) for wild corals, and 33.88 °C ± 0.53 (n = 6) for the propagated corals. However, log-logistic dose-response curves of these thermal thresholds

analysed through the function "*EDcomp*" (Eldridge et al., 2022) yielded no significant difference (p = 0. 8979; **Table S3.5**).

3.3.3 Algal symbiont density and chlorophylls metrics in response to acute thermal stress

More traditional metrics of coral bleaching, i.e., symbiont densities and chlorophyll content (McLachlan et al., 2020), were also measured at the end of the 18 h assay (**Fig. 3.2A**). Symbiont cell densities (cells x 10^6 cm^{-2}) were higher in the control (31 °C) treatment — 0.6820 ± 0.0228 and 0.6725 ± 0.0253 for wild and nursery corals, respectively — compared to the 34 °C and 37 °C treatments (0.0817 ± 0.0009 and 0.0818 ± 0.0009, and 0.0760 ± 0.0012 and 0.0747 ± 0.0015, respectively; two-way RM ANOVA test of temperature, $F_{(2,10)}$ = 5207, p < 0.0001; **Fig. 3.4B**, **Table S3.4I**). Additionally, no differences in symbiont densities among nursery vs wild corals across temperatures were found (two-way RM ANOVA test of environment, $F_{(1.0,5.0)}$ = 0.4677, p = 0.5245).

Pigment content (chlorophyll *a* and *c2* concentration, µg cm^{-2}) of corals from the nursery and reef (wild corals) decreased with temperature, in line with tissue whitening (two-way RM ANOVA test of environment: $F_{(1.0,5.0)}$ = 3.149, p = 0.1361 for total pigments; $F_{(1.0,5.0)}$ = 1.574, p = 0.2650 for Chl *a*; and $F_{(1.0,5.0)}$ = 3.634, p = 0.1149 for Chl *c2*; **Table S3.4J-L**). Specifically, total pigment values were 6.6 ± 1.1, 0.9 ± 0.3, and 0.3 ± 0.1 (31 °C, 34 °C, and 37 °C, respectively) for wild corals and 6.8 ± 1.1, 2.1 ± 0.8, and 0.7 ± 0.3 for nursery corals; **Fig. 3.4C**. For Chl *a* (**Fig. 3.4D**), values were 5.3 ± 1.0, 0.8 ± 0.2, and 0.2 ± 0.1 for wild corals, and 5.2 ± 0.8, 1.7 ± 0.6, and 0.5 ± 0.2 for nursery corals. Finally, for Chl *c2* values

were 1.31 ± 0.19, 0.19 ± 0.06, and 0.13 ± 0.06 for wild corals, and 1.6 ± 0.4, 0.4 ± 0.2, and 0.2 ± 0.1 for nursery corals.

Total pigment, Chl *a* and Chl *c2* concentration all varied among temperatures treatments (31 °C, 34 °C, and 37 °C) but not coral groups (nursery vs wild corals) (two-way RM ANOVA test of temperature: $F_{(1.3,6.4)} = 23.52$, $p = 0.0018$; $F_{(1.4,6.8)} = 26.75$, $p = 0.0010$; and $F_{(1.1,5.6)} = 13.46$, $p = 0.0109$, respectively; two-way RM ANOVA test of environment: $F_{(1.0,5.0)} = 3.149$, $p = 0.1361$, $F_{(1.0,5.0)} = 1.574$, $p = 0.2650$, and $F_{(1.0,5.0)} = 3.634$, $p = 0.1149$, respectively); **Fig. 3.4C-E**, **Table S3.4J-L**. Interestingly, the chlorophyll ratio (*a*:*c2*) was higher in the control (31 °C) and medium (34 °C) treatments — 3.9 ± 0.2 and 3.9 ± 0.6 for wild and nursery corals, respectively — compared to the 37 °C treatments (1.7 ± 0.4 and 2.4 ± 0.5, respectively); two-way RM ANOVA test of temperature, $F_{(1.4,7.0)} = 10.32$, $p = 0.0112$ (**Fig. 3.4F**, **Table S3.4M**). Furthermore, no differences in the chlorophyll *a*-to-*c*2 ratio among nursery vs wild corals across temperatures were observed (two-way RM ANOVA test of environment, $F_{(1.0,5.0)} = 0.02802$, $p = 0.8736$; **Fig. 3.4F**, **Table S3.4M**).

In summary, after 12 months of growth, nursery and wild colonies contained similar symbiont cell (and pigment) concentrations that collectively decreased with increasing temperature treatment. However, loss of total pigmentation with temperature preceded a temperature-induced change in pigment ratio.

3.3.4 Increased whitening of corals from the wild and nursery environments under heat stress

We determined changes in traits related to bio-physical colouration (red [R], green [G], blue [B], hue, saturation, brightness, and bleaching state) of pictures taken from coral fragments to examine the effect of different temperature treatments on the relative Chl concentrations of corals from different environments (wild vs nursery; **Fig. S3.4**). Higher RGB and brightness values correspond to a paler colouration (i.e., closer to white). This approach is based on the negative relationship between the relative loss of Chl density and value intensity increase in the RGB channels in standardised digital photographs (Nishiguchi et al., 2018; Winters et al., 2009) and the positive relationship between relative loss of symbiont density and chlorophyll *a* concentration when colour score (1-6) decrease in the Coral Watch bleaching card (Siebeck et al., 2006).

RGB values for wild corals (**Fig. S3.4A-C)** at the end of the 18 h assay (**Fig. 3.2A**) were 127.2 ± 12.4 (31 °C), 210.2 ± 10.9 (34 °C), and 217.8 ± 6.6 (37 °C) for R; 96.7 ± 10.8 (31 °C), 181.8 ± 14.4 (34 °C), and 213.0 ± 5.9 (37 °C) for G; and lastly 77.3 ± 9.9 (31 °C), 152.3 ± 13.9 (34 °C), and 202.3 ± 5.4 (37 °C) for B. For nursery corals (**Fig. S3.4A-C**), final RGB values were 126.2 ± 12.5 (31 °C), 199.0 ± 14.0 (34 °C), and 202.8 ± 8.1 (37 °C) for R; 97.5 ± 12.0 (31 °C), 178.8 ± 17.5 (34 °C), and 198.8 ± 7.3 (37 °C) for G; and for B values as follows, 76.3 ± 11.3 (31 °C), 151.3 ± 17.4 (34 °C), and 185.0 ± 13.1 (37 °C). Nursery and wild corals displayed a similar increase in red channel pixel intensity (two-way RM ANOVA test of environment, $F_{(1.0,5.0)} = 1.280$, $p = 0.3093$) (alongside the green and blue channel pixel intensities; **Table S3.4A-C**) with increasing temperature treatments. This increase in red value corresponded with tissue whitening (i.e., increase in bleaching state; two-way RM

ANOVA test of environment, $F_{(1.0,5.0)}$ = 0.6897, p = 0.4441; **Fig. S3.4G**) (alongside brightness values, two-way RM ANOVA test of environment, $F_{(1.0,5.0)}$ = 1.486, p = 0.2773; **Fig. S3.4D**, **Table S3.4D**). The results indicated similar colouration between these two coral groups at each temperature treatment. We also observed similar saturation and hue levels among wild and nursery corals (see two-way RM ANOVA test of environment: $F_{(1.0,5.0)}$ = 0.0000, p = 0.9945, and $F_{(1.0,5.0)}$ = 0.03441, p = 0.8601, respectively; **Fig. S3.4E-F**, **Table S3.4E-F**). For more details on the two-way ANOVA test of temperature and interaction for all studied bio-physical traits, refer to **Table S3.4**. In summary, at 12 months post-fragmentation, corals propagated within the nursery had similar colouration compared to those retained in the reef (wild corals) at each temperature treatment.

3.4 Discussion

In situ nurseries have been shown to change the underlying growth and metabolism of propagated corals (Nuñez Lendo et al., 2023, **Chapter 2**), yet how these changes potentially, in turn, alter tolerance to stressors remains unexplored. This study investigates for the first time the thermotolerance response of nursery-propagated *Acropora* cf. *hyacinthus* vs their wild colonies from Opal Reef, a key coral species for the northern Great Barrier Reef (GBR), Australia (Ortiz et al., 2021), including for restoration activities (e.g., Howlett et al., 2021). Using F_v/F_m ED50 as a standardised metric (Evensen et al., 2021), we found a generally homogenised (i.e., conserved) variation in thermal tolerance among 12 colonies, ranging from 33.67 °C to 33.88 °C (**Fig. 3.3**, **Fig. S3.3**). While these temperatures are not representative of the temperatures of a natural mass bleaching event, they do serve as a reliable metric of relative coral thermal tolerance (Voolstra et al., 2020) that enables comparing thermal differences among multiple individuals (e.g., Cunning et al., 2021;

Nielsen et al., 2022). The 0.21 °C difference in ED50 between the wild and nursery propagated populations is small in relation to the broad thermal ranges of corals inhabiting larger distribution ranges (e.g., ~2.5-2.7 °C; Cunning et al., 2021; Evensen et al., 2022; Voolstra et al., 2021), however, this small but insignificant difference might be due to the low statistical power of our small sample size (n = 12; 6 nursery and 6 wild corals).

Our study revealed a range in thermal tolerance among coral groups of < 1 °C, which seems plausible for a highly interconnected coral population (i.e., our nursery and wild corals were separated approximately 10 m apart in Opal Reef and had a Maximum Monthly Mean (MMM) temperature for February 2021 of 28 °C), compared to other coral populations such as the Red Sea populations which span approximately 900 km and have a MMM temperature gradient of 3.7 °C (Evensen et al., 2022; Voolstra et al., 2021b), or the Florida population which covers 300 km and has 1 °C in MMM (Cunning et al., 2021). Despite likely different environmental conditions of the nursery vs the reef (Howlett et al., 2021; Nuñez Lendo et al., 2023, **Chapter 2**), such as improved light availability (lower sedimentation), increased water flow, enhanced planktonic supply, reduced intra- and interspecific competition, and controlled corallivory within the nurseries (Bongiorni et al., 2011; Levy et al., 2010; Rinkevich, 2005; Shafir and Rinkevich, 2010, 2008), we detected small but insignificant ED50 (0.21 °C) between the wild and nursery propagated. Such reduced transport of nutrients, sediment and flow — and hence transport of heat — is therefore expected on the reef compared to the nursery setting, which may reduce thermal tolerance (Pomeroy et al., 2023). As such, our observations would imply that our nursery platforms, which are located close to the native reef site, do not exhibit substantial environmentally-driven changes in coral thermotolerance but could be important for coral recovery after a heat stress event (Morikawa et al., 2019; Shaish et al., 2010), which is not examined by the CBASS approach.

Furthermore, it is plausible that the heat stress event that occurred in March 2020 might have dampened — or conditioned — the thermal response of all local coral populations.

In addition, resource allocation was prioritised towards growth in the nursery corals, as observed by their higher growth (Nuñez Lendo et al., 2023, **Chapter 2**), yet it did not impact their thermotolerance. Regardless of the different initial sizes of the nursery and wild corals, the thermal response of corals was similar.. The size and life stage (age) of corals used in restoration endeavours will inevitably impact the resource allocation towards the vital processes of survival (maintenance), growth (development), and reproduction. Consequently, freshly fragmented coral tends to display higher growth/regeneration (Bak, 1983; Chadwick and Loya, 1990; Loya, 1976; Meesters et al., 1994). This stands in contrast to well-established adult colonies, which, upon reaching a size threshold, allocate resources from growth to sexual reproduction (Babcock, 1991; Kojis and Quinn, 2001; Soong, 1993).

As expected from other CBASS studies (e.g., Cunning et al., 2021), the mean thermal tolerance (ED50) for each coral group (33.67 °C and 33.88 °C for wild and nursery corals, respectively) did not correlate with the MMM temperature of Opal Reef (28 °C), indicating no straightforward thermal acclimatisation response to this temperature. Mean thermal tolerance was slightly lower for wild corals (33.67 °C) than nursery corals (33.88 °C). This slight and non-significant thermal reduction was observed despite the different metabolic responses we have previously reported for these same groups of corals (i.e., higher calcification, photosynthesis, and respiration rates of nursery corals vs their wild colonies; Nuñez Lendo et al., 2023, **Chapter 2**). Specifically, we previously found that these nursery corals exhibited a higher growth rate and comparable survivorship than their wild colonies

via enhanced metabolic traits and particularly respiration (Nuñez Lendo et al., 2023, **Chapter 2**). However, a high variation in F_v/F_m values at T_{end} values was observed in nursery corals, explained by a ~2-3 increase fold of some genotypes (i.e, 3 out of 6). Such an outcome of subtle variation in thermotolerance may not, in fact, come as a surprise whereby our sampling approach was designed to capture different "wild" genotypes, specifically, where work at Opal Reef has recently shown that *A.* cf. *hyacinthus* genetic diversity is retained on the reef by as little as 2 m distance between colonies (Howlett et al., In Review). In this case, our findings are perhaps intriguingly consistent with reports of corals adapted to extreme environmental conditions, including hot waters (Camp et al., 2019, 2017), whereby corals consistently exhibit higher respiration rates than their conspecific populations on neighbouring reefs. Such higher respiration rates are, of course, species-specific in these extreme environments (Jacquemont et al., 2022), and thus more research is needed to understand the different thermal responses of different coral species when nursery propagating.

Differences in ED50 capture the average response of the tested population; higher thermotolerance variation (as greater variability in F_v/F_m values at T_{end}) within nursery-grown corals compared to the wild corals raises a critical operational point. Specifically, current restoration practices aiming to screen thermotolerant wild individuals to use for propagation may not well resolve thermotolerance variation that can ultimately be achieved through nursery propagation. Our study shows that nursery propagation can enhance the thermotolerance of a priori lower thermotolerant corals, as well as can also have negative impacts (e.g., a 100% decrease in thermotolerance for 1 out 6 of coral genotypes). However, detecting a potentially higher effect on thermotolerance was not possible to resolve with the small sample size of our study.

Both bio-physical colouration and photobiological traits were observed to be similar for nursery- compared to wild-grown corals across temperature treatments. Photographic-based traits revealed colonies became paler in both coral groups (**Fig. S3.4**), accompanied by less pigmentation per colony surface area (**Fig. 3.4C-E**). At face value, this paler colouration might appear indicative of lower symbiont cell densities and less photosynthetic efficiency (F_v/F_m), as decreases in coral pigmentation commonly occur via thermal stress (e.g., Evensen et al., 2022, 2021; Voolstra et al., 2020). Intriguingly, despite the reduction in symbiont cell density, the chlorophyll ratio (*a*:*c2*) was maintained similarly (~4) at 31 °C and 34 °C and halved at the highest temperature treatment (37 °C). These findings correspond with similar ratios in *Goniastrea aspera* during a bleaching event, where each individual symbiont cell maintains the chlorophylls ratio under limited thermal stress as a potential photoprotective function of the chlorophylls to maintain the coral/algal symbiosis (Baghdasarian et al., 2017). As such, nursery-propagated corals retained the same symbiosis photoprotection (i.e., as seen by similar chlorophyll ratios at high temperatures) as their wild counterparts.

3.5 Conclusion

In conclusion, despite no differences observed in mean thermotolerance (ED50) between nursery vs wild corals, we observed a high variation in F_v/F_m values for 3 out of 6 coral genotypes of ~2-3-fold higher in thermotolerance in a 12-month period. Such variability may reflect growth in environments that differ for nurseries compared to the reef (Nuñez Lendo et al., 2023, **Chapter 2**) that may result in divergence of thermotolerance for some individuals in the nurseries compared to reef. However, how such divergence further translates to bleaching recovery potential remains to be further investigated. Quantitative thermal tolerance rankings represent valuable information for restoration programmes designed to

build thermotolerant coral biomass to increase climate reef resilience (Baums et al., 2019). For example, more thermotolerant nursery corals can serve as stock — through both sexual and asexual propagation — to aid targeted restoration strategies (e.g., Shaver et al., 2022). Furthermore, selective breeding techniques could be applied to more thermotolerant nursery corals to boost the resilience of new sexual recruits used for restoration (van Oppen et al., 2015), and thermal priming can be applied to these already corals with existing enhanced thermotolerance to push their thresholds to higher temperatures (Hackerott et al., 2021; Martell, 2023). Our findings strongly support the notion of the need for coral restoration practices to move beyond a few "simple" metrics of growth and survivorship as measures of success and include critical metrics for a projected warming climate, such as thermotolerance thresholds, if restoration goals are to improve (or retain) the reef resilience. However, more sophisticated assays of thermotolerance may be required — that can not only capture rates of decline but also recovery — to resolve subtle differences amongst genetically diverse populations.

3.6 Acknowledgements

We wish to thank the past, present, and emerging Gadigal of the Eora Nation, Yidinji, Gunggandji, Yirrganydji, and Kuku Yalanji Traditional Owners of the land and sea country where our research took place. Also, to Amanda Grima, Paige Strudwick, Sage Fitzgerald; Wavelength crew including Jenny Edmondson, Lorna Howlett, Christine Roper, Tahn Miller, and Climate Change Cluster and Faculty technical staff, Erin Lockhart, Scott Allchin, Helen Price, Rachel Keeys, Susan Fenech, and Penny McCracken. This research was supported by an International Research Scholarship (IRS) and UTS President's Scholarship (UTSP) to CINL. Access to sites and coral material, as well as contributions of DJS, EFC and JE to

writing and manuscript preparation, was facilitated through funding to the Coral Nurture Program from the Australian & Queensland Governments “Solving the bottleneck of reef rehabilitation through boosting coral abundance: Miniaturising and mechanising coral out-planting” in 2020; and the partnership between the Australian Government’s Reef Trust and the Great Barrier Reef Foundation in 2021; also, the many in kind contributions from Wavelength Reef Cruises crew who have tirelessly supported the work at Opal Reef since 2018. Contribution of EFC was through the University of Technology Sydney Chancellor’s Postdoctoral Research Fellowship and ARC Discovery Early Career Research Award (DE190100142). Fieldwork was supported by a UNESCO-L’Oreal fellowship awarded to EFC. All material was collected under permit G20/43740.1 and G21/45224.1 (2020, and 2021, respectively) from the Great Barrier Reef Marine Park Authority.

3.7 Supplementary Material

A)

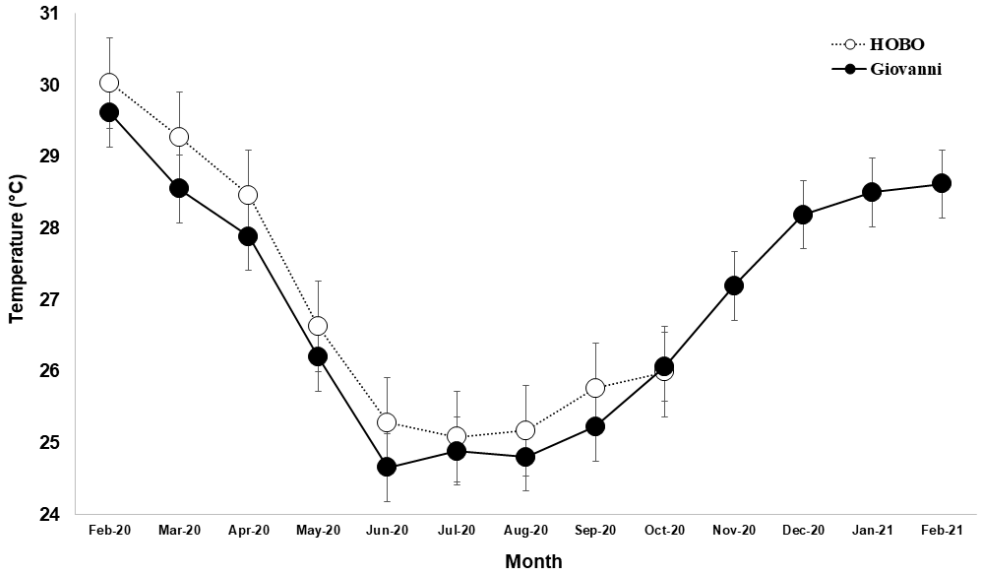

B)

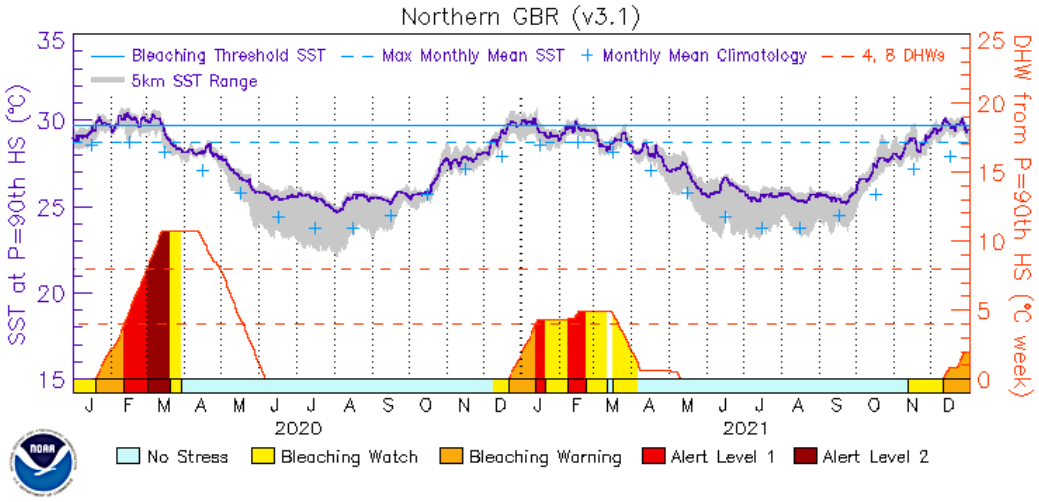

C)

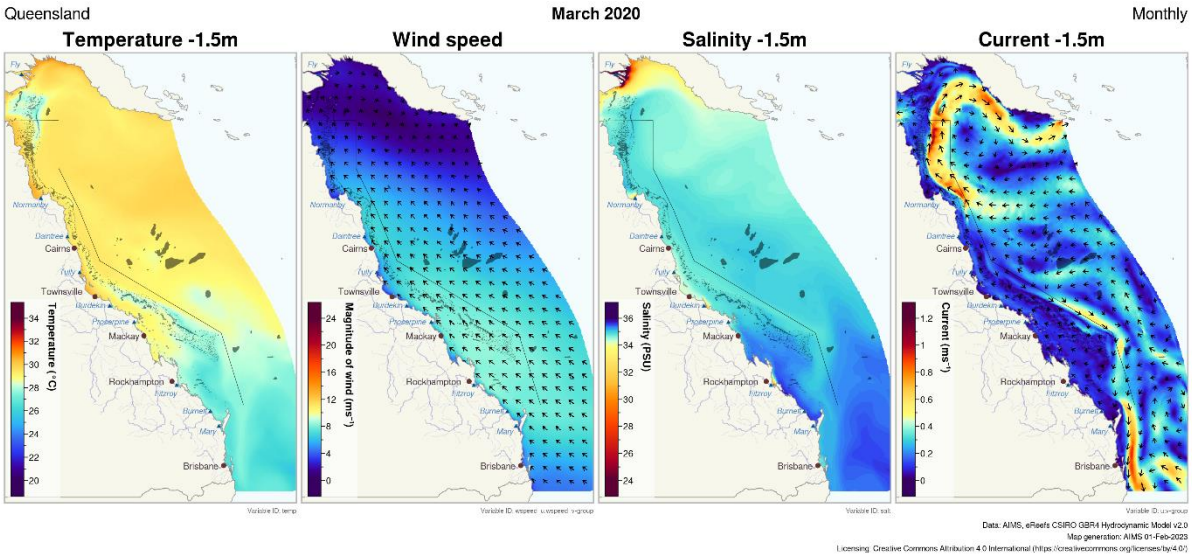

Figure S3.1 Sea Surface Temperatures (SST, °C) for A) Opal Reef and Mojo nursery (mean ± SEM, n = 13 and 9 months, respectively) and for B) the Northern Great Barrier Reef (GBR), and C) physical parameters during the 2020 bleaching event on the GBR. A) Satellite-derived data (MODIS-aqua) was extracted from the GIOVANNI online system maintained by NASA (https://giovanni.gsfc.nasa.gov/giovanni/). SST were obtained using monthly area-averaging bounded to 145° 53' 53.8''E, 16°12' 23.4''S between February 2020 and February 2021 (encompassing the entire Opal Reef of ca. 30 km^2 for a year); black line. Imposed onto the SST are the mean monthly SST recorded by the HOBO logger (every 1 h) from February to September 2021 at the Mojo nursery; dashed line. B) Temperature, wind, salinity and ocean currents on the GBR for the month of March 2020 when the mass bleaching event occurred (based on the 4 km eReefs Hydrodynamic model https://ereefs.aims.gov.au/. C) Two-year time series graphic of the 5 km product of SST, Degree Heating Week (DHW) and bleaching alert from NOAA Coral Reef Watch (CRW) (https://coralreefwatch.noaa.gov/).

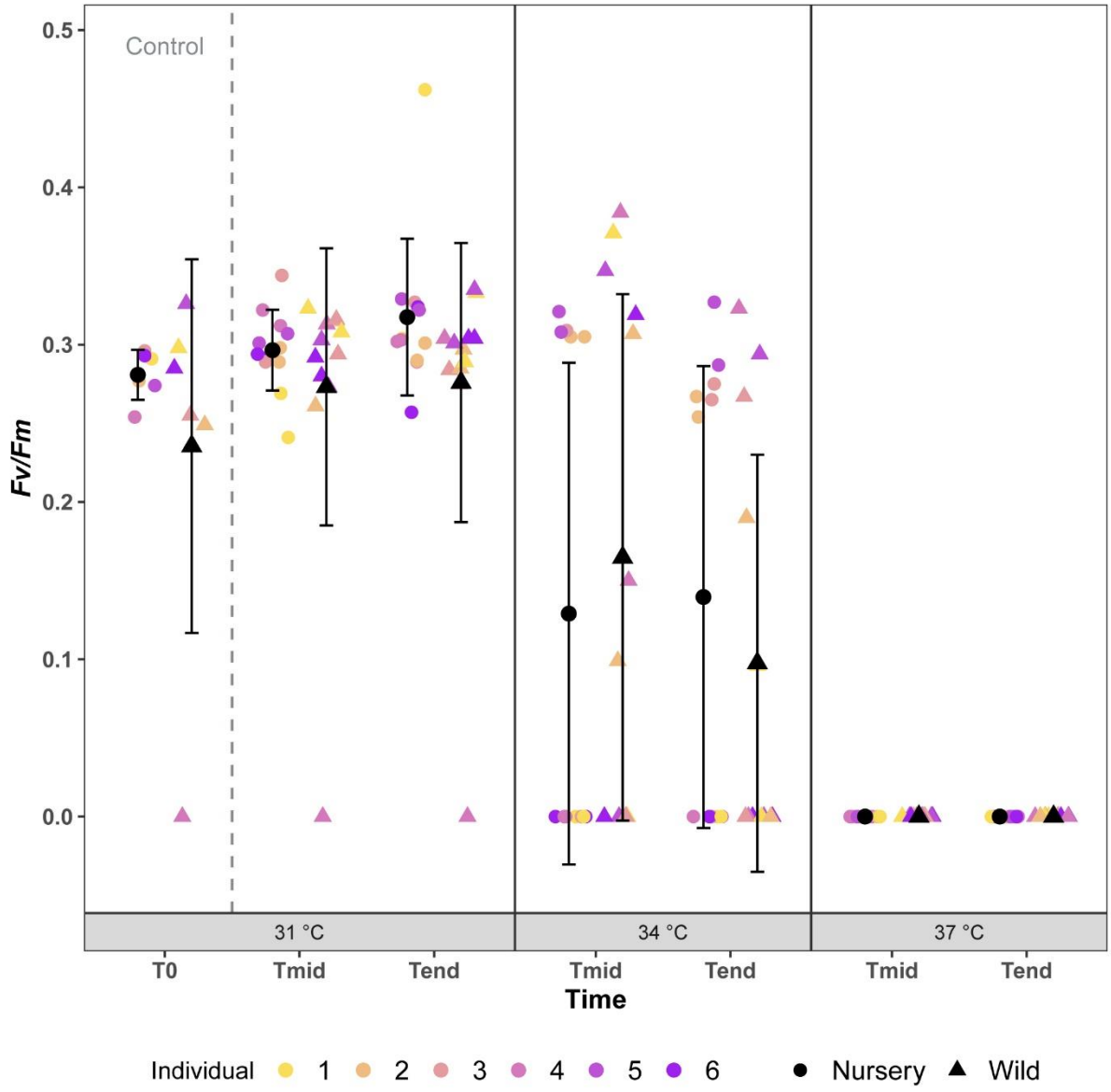

Figure S3.2 Maximum quantum yield of photosystem II (F_v/F_m) measurements in response to temperature treatment for each coral individual (1-6) across coral groups. Measurements were taken at at the initial, middle, and final time points (T_0, T_{mid}, and T_{end}, respectively). Circles refer to nursery corals and triangles to their wild donors. Individual measurements (corresponding to each coral individual) are plotted according to the colour legend. Donor and 12-months-propagated *A.* cf. *hyacinthus* are referred as wild and nursery, respectively, in the graph. The mean ± the standard error of the mean (SEM) of each coral individual is represented by a black circle (nursery) or triangle (wild) in each time point and temperature treatment.

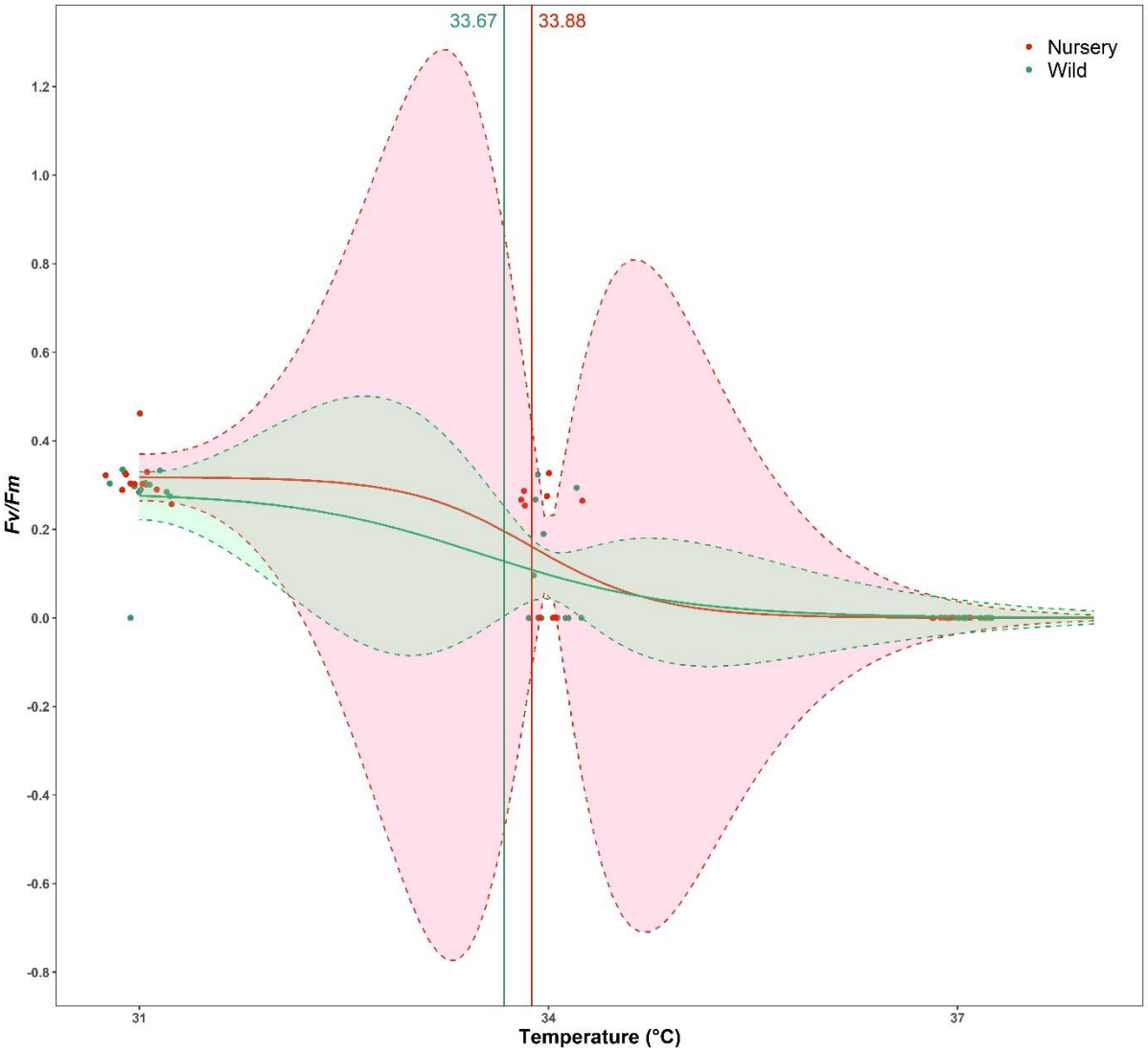

Figure S3.3 Thermal tolerances of donor and 12-months-propagated *Acropora* cf. *hyacinthus* in Opal Reef (the northern Great Barrier Reef). Maximum quantum yield of photosystem II (F_v/F_m) measurements at the final time point (T_{end}) fitted to log-logistic dose-response curves. Dotted lines represent 95% confidence intervals. Curve fits were used to determine the Fv/Fm ED50 for each coral group (vertical lines), which represent the x-value (in temperature) at the inflexion point of the curve where F_v/F_m values in the model fit were 50% lower in comparison to the initial values of the model. Donor and 12-months-propagated *A.* cf. *hyacinthus* are referred as wild and nursery, respectively, in the graph.

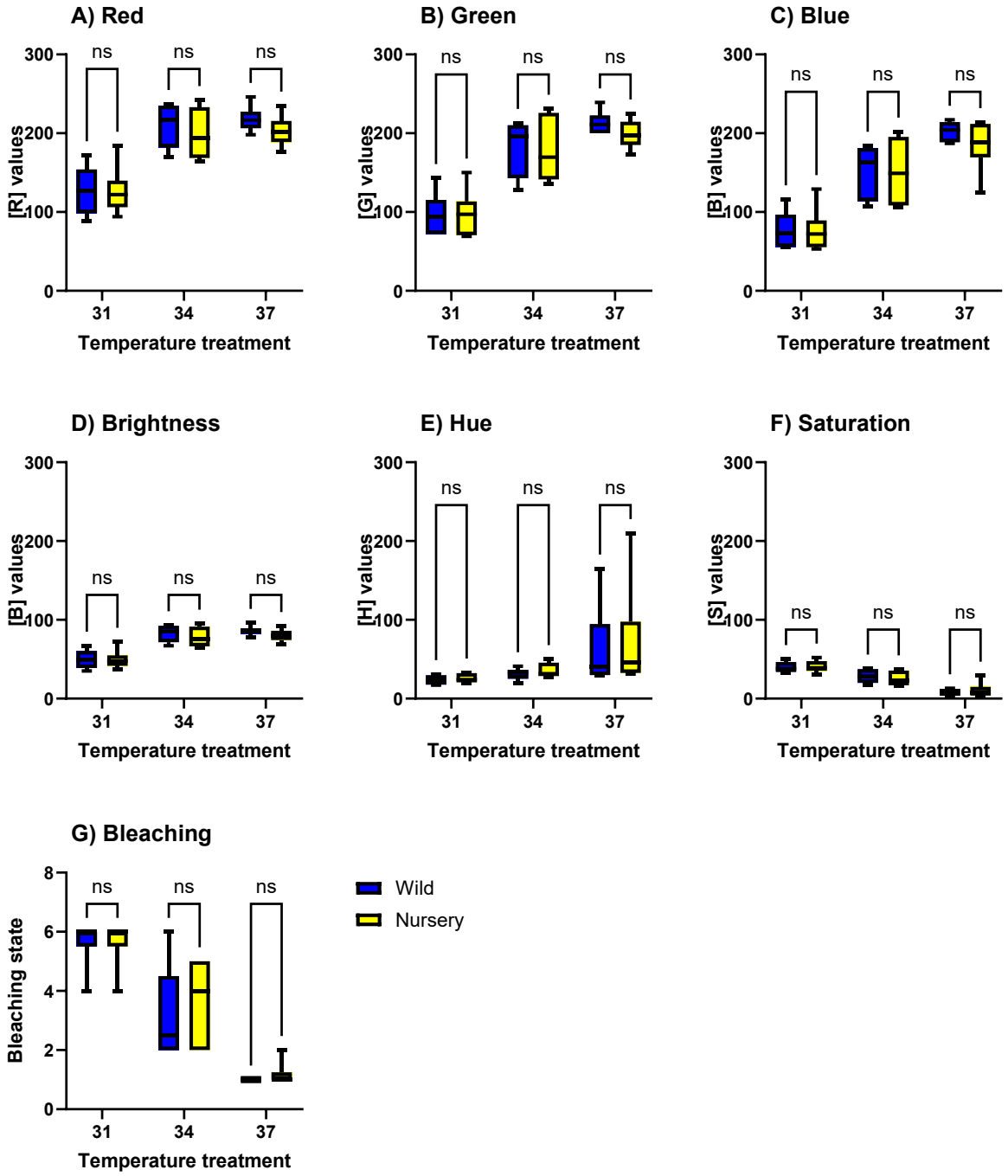

Figure S3.4 Bio-physical colouration of donor and 12-months-propagated *A.* cf. *hyacinthus* during the Coral bleaching automated stress systems (CBASS). Traits encompass (a) red (R), b) green (G), (c) blue (B), (d) brightness, (e) hue, (f) saturation, and (g) bleaching state. Donor and 12-months-propagated *A.* cf. *hyacinthus* are referred as wild (ib blue) and nursery (in yellow), respectively (n = 6 for each coral group). Graphs show only the two-way RM ANOVA test of environment (i.e., coral group). See **Table S3.4** for the results of the two-way RM ANOVA test of temperature and interaction. No significant differences in the RGB values among coral groups were revealed by a two-way RM ANOVA test of environment ($F_{(1.0,5.0)}$ = 1.280, p = 0.3093 for R; $F_{(1.0,5.0)}$ = 0.6242, p = 0.4653 for G; and $F_{(1.0,5.0)}$ = 0.6265, p = 0.4645 for B). Furthermore, no significant differences in brightness, hue, and saturarion levels, and bleaching state were detected among coral groups (two-way RM ANOVA test of environment ($F_{(1.0,5.0)}$ = 1.486, p = 0.2773 for brightness; $F_{(1.0,5.0)}$ = 0.03441, p = 0.8601 for hue; $F_{(1.0,5.0)}$ = 0.03441, p = 0.8601 for saturation; and ($F_{(1.0,5.0)}$ = 0.6897, p = 0.4441 for bleaching state). Statistical significance is shown as ns (no statistical significance).

Table S3.1 Pairwise permutational multivariate analysis of variance (PERMANOVA; perm = 999) on Euclidian distances using the "*vegan*" R package (time point and temperature as fixed variables) for maximum quantum yield of photosystem II (F_v/F_m) measurements. Post hoc pairwise comparisons were conducted using "*pairwiseAdonis*" R package with Bonferroni adjusted p-values. The effects of time point and temperature on F_v/F_m response variable for the start of the experiment (T_0), halfway down the assay (4.5 h, T_{mid}), and after 7 h (T_{end}) for each target temperature (31 °C, 34 °C, and 37 °C) were analysed (e.g., Evensen et al., 2021).

Results PERMANOVA fixed variables TimePoint and Temperature						
	Df	**SumOfSqs**	**R2**	**F**	**Pr(>F)**	
Timepoint	2	0,152733507	0,043242207	8,597253105	0,001	***
Temp	1	2,02914426	0,574495261	228,4379778	0,001	***
Residual	152	1,350169226	0,382262532			
Total	155	3,532046994	1			
POST-HOC COMPARISONS						
Results Pairwise PERMANOVA fixed variables TimePoint and Temperature						
T0_vs_Tmid						
	Df	**SumOfSqs**	**R2**	**F**	**Pr(>F)**	
Timepoint	1	0,1342927163	0,07152471867	14,13207814	1,00E-04	***
Temp	1	0,9735603333	0,5185212637	102,4510568	1,00E-04	***
Residual	81	0,7697176528	0,4099540176			
Total	83	1,877570702	1			
T0_vs_Tend						
	Df	**SumOfSqs**	**R2**	**F**	**Pr(>F)**	
Timepoint	1	0,1474977857	0,07923466732	18,16797976	1,00E-04	***
Temp	1	1,056430021	0,5675060194	130,1253381	1,00E-04	***
Residual	81	0,6576031458	0,3532593133			
Total	83	1,861530952	1			

Tmid_vs_Tend						
	Df	**SumOfSqs**	**R2**	**F**	**Pr(>F)**	
Timepoint	1	0,001083506944	0,0003280968888	0,1200895257	0,7223	
Temp	1	2,02914426	0,6144454561	224,8983942	1,00E-04	***
Residual	141	1,272171559	0,385226447			
Total	143	3,302399326	1			

Table S3.2 PERMANOVA for maximum quantum yield of photosystem II (F_v/F_m) measurements (perm = 999) on Euclidian distances using the "*vegan*" R package (coral group as fixed variable) was performed within each time point (T_0, T_{mid}, and T_{end}) to detect differences in F_v/F_m among coral groups and temperature treatments (31 °C, 34 °C, and 37 °C) to (a) record initial photosynthetic efficiencies (T_0) (i.e., to detect any coral group effect on F_v/F_m within their native seawater of 31 °C before starting the CBASS experiment), (b) monitor photosynthetic efficiencies halfway down the experiment (T_{mid}) (i.e., checkpoint control to ensure the continuation of the experiment), and (c) record final F_v/F_m values (T_{end}) (i.e., to report values as per Voolstra et al., (2020) and to calculate the F_v/F_m ED50 metric as a proxy for the thermal tolerance of coral, Evensen et al., (2021). Post hoc pairwise comparisons were conducted using "*pairwiseAdonis*" R package with Bonferroni adjusted p-values.

a)

Results PERMANOVA Data T0 fixed variables Coral Group					
	Df	**SumOfSqs**	**R2**	**F**	**Pr(>F)**
CoralGroup	1	0,006165333333	0,07904509964	0,8582950111	0,567
Residual	10	0,07183233333	0,9209549004		
Total	11	0,07799766667	1		

b)

Results PERMANOVA Data Tmid fixed variables Coral Group						
	Df	**SumOfSqs**	**R2**	**F**	**Pr(>F)**	
Temp	1	0,9735603333	0,5846224939	97,15726381	0,001	***
CoralGroup	1	0,0003083472222	0,0001851623529	0,03077176769	0,852	
Residual	69	0,6914116389	0,4151923438			
Total	71	1,665280319	1			

POST-HOC COMPARISONS						
Results Pairwise PERMANOVA Data Tmid fixed variables Coral Group						
31_vs_34						
	Df	**SumOfSqs**	**R2**	**F**	**Pr(>F)**	
Temp	1	0,2283900208	0,2483061671	14,87474933	4,00E-04	***
CoralGroup	1	0,0004625208333	0,0005028537363	0,03012338907	0,8631	
Residual	45	0,6909394375	0,7511909792	NA	NA	
Total	47	0,9197919792	1	NA	NA	
31_vs_37						
	Df	**SumOfSqs**	**R2**	**F**	**Pr(>F)**	
Temp	1	0,9735603333	0,9103427919	464,8298674	1,00E-04	***
CoralGroup	1	0,001633333333	0,001527273838	0,7798408488	0,3745	
Residual	45	0,09425	0,08812993422			
Total	47	1,069443667	1			
34_vs_37						
	Df	**SumOfSqs**	**R2**	**F**	**Pr(>F)**	
Temp	1	0,2588671875	0,3029862899	19,68789899	2,00E-04	***
CoralGroup	1	0,0038341875	0,004487653521	0,2916055021	0,6051	
Residual	45	0,5916844375	0,6925260565			
Total	47	0,8543858125	1			

c)

Results PERMANOVA Data Tend fixed variables Coral Group						
	Df	SumOfSqs	R2	F	Pr(>F)	
Temp	1	0,9735603333	0,5846224939	97,15726381	0,001	***
CoralGroup	1	0,0003083472222	0,0001851623529	0,03077176769	0,852	
Residual	69	0,6914116389	0,4151923438	NA	NA	
Total	71	1,665280319	1	NA	NA	

POST-HOC COMPARISONS						
Results Pairwise PERMANOVA Data Tend fixed variables Coral Group						
31_vs_34						
	Df	**SumOfSqs**	**R2**	**F**	**Pr(>F)**	
Temp	1	0,2283900208	0,2483061671	14,87474933	4,00E-04	***
CoralGroup	1	0,0004625208333	0,0005028537363	0,03012338907	0,8631	
Residual	45	0,6909394375	0,7511909792			
Total	47	0,9197919792	1			
31_vs_37						
	Df	**SumOfSqs**	**R2**	**F**	**Pr(>F)**	
Temp	1	0,9735603333	0,9103427919	464,8298674	1,00E-04	***
CoralGroup	1	0,001633333333	0,001527273838	0,7798408488	0,3745	
Residual	45	0,09425	0,08812993422			
Total	47	1,069443667	1			
34_vs_37						
	Df	**SumOfSqs**	**R2**	**F**	**Pr(>F)**	
Temp	1	0,2588671875	0,3029862899	19,68789899	2,00E-04	***
CoralGroup	1	0,0038341875	0,004487653521	0,2916055021	0,6051	
Residual	45	0,5916844375	0,6925260565			
Total	47	0,8543858125	1			

Table S3.3 Linear mixed-effects models (LME) were used to analyse individual response variables, with coral group and temperature as fixed effects, and genotype and tank replicate as random effects to account for any potential genotype or tank effects.

A) Field/T_0 - comparing Coral Group at the start of experiment values:

At the time T_0 only was used in 1 tank. No random effect from the tank could be evaluated. The random effect was evaluated just by Genotypes.

There is no random effect by genotypes. There are no differences between Coral Groups at T_0:

```
Backward reduced random-effect table:

             Eliminated npar logLik      AIC     LRT Df Pr(>Chisq)
<none>                    4 8.8009  -9.6018
(1 | Genotype)         0    3 8.6989 -11.3978 0.20407  1     0.6515

Backward reduced fixed-effect table:
Degrees of freedom method: Satterthwaite

          Eliminated    Sum Sq   Mean Sq NumDF DenDF F value Pr(>F)
CoralGroup          1 0.0061653 0.0061653     1     5  1.0728 0.3478

Model found:
AVE_PAM ~ (1 | Genotype)
```

ANOVA results from the model (The same as above, Not differences between Coral Groups – Nursery and Wild):

```
Type III Analysis of Variance Table with Satterthwaite's method
            Sum Sq   Mean Sq NumDF DenDF F value Pr(>F)
CoralGroup 0.0061653 0.0061653     1     5  1.0728 0.3478
```

B) T_{mid} - comparing temp and Coral Group at the middle of experiment values:

At T_{mid} random effect from the tank was found, and there are no by Genotypes. Differences were found between Temperatures.

```
Backward reduced random-effect table:

             Eliminated npar logLik     AIC    LRT Df Pr(>Chisq)
<none>                    9 53.279 -88.558
(1 | Genotype)         1    8 53.253 -90.507 0.0516  1   0.820326
(1 | NewTank)          0    7 49.858 -85.716 6.7902  1   0.009166 **
---
Signif. codes:  0 ‘***’ 0.001 ‘**’ 0.01 ‘*’ 0.05 ‘.’ 0.1 ‘ ’ 1

Backward reduced fixed-effect table:
Degrees of freedom method: Satterthwaite

              Eliminated   Sum Sq  Mean Sq NumDF DenDF F value  Pr(>F)
Temp:CoralGroup          1 0.010627 0.005313     2    63  0.6162 0.54321
CoralGroup               2 0.000308 0.000308     1    65  0.0362 0.84972
Temp                     0 0.178746 0.089373     2     3 10.6442 0.04341 *
---
Signif. codes:  0 ‘***’ 0.001 ‘**’ 0.01 ‘*’ 0.05 ‘.’ 0.1 ‘ ’ 1

Model found:
```

ANOVA results from the model (The same as above, with differences between temperatures):

```
Type III Analysis of Variance Table with Satterthwaite's method
     Sum Sq  Mean Sq NumDF DenDF F value  Pr(>F)
Temp 0.17619 0.088095     2     3  10.644 0.04341 *
---
Signif. codes:  0 ‘***’ 0.001 ‘**’ 0.01 ‘*’ 0.05 ‘.’ 0.1 ‘ ’ 1
```

Post-Hoc analysis emmeans (Estimated marginal means): Differences were found between temp31 – temp37

```
$`emmeans of Temp`
 Temp emmean     SE   df lower.CL upper.CL
 31    0.285 0.0439 3.06   0.0764    0.493
 34    0.147 0.0439 3.06  -0.0616    0.355
 37    0.000 0.0439 3.06  -0.2085    0.208

Degrees-of-freedom method: kenward-roger
Confidence level used: 0.95
Conf-level adjustment: sidak method for 3 estimates

$`pairwise differences of Temp`
 1              estimate     SE df t.ratio p.value
 Temp31 - Temp34    0.138 0.0617  3   2.234  0.2107
 Temp31 - Temp37    0.285 0.0617  3   4.613  0.0386
 Temp34 - Temp37    0.147 0.0617  3   2.379  0.1862

Degrees-of-freedom method: kenward-roger
P value adjustment: tukey method for comparing a family of 3 estimates
```

C) T_{end} - comparing temp and Coral Group at the end of experiment values:

At T_{end} Not random effect from the tank was found, and neither was by Genotypes. Differences were found between Temperatures.

```
Backward reduced random-effect table:

            Eliminated npar logLik      AIC    LRT Df Pr(>Chisq)
<none>                     9 58.679  -99.359
(1 | Genotype)          1    8 57.947  -99.893 1.4653  1     0.2261
(1 | NewTank)           2    7 57.221 -100.443 1.4508  1     0.2284

Backward reduced fixed-effect table:
             Eliminated Df Sum of Sq     RSS     AIC F value Pr(>F)
```

```
Temp:CoralGroup          1  2    0.0070 0.55138 -342.78  0.4244 0.6559
CoralGroup               2  1    0.0140 0.56538 -342.98  1.7266 0.1933
Temp                     0  2    1.0707 1.63604 -270.48 65.3315 <2e-16 ***
---
Signif. codes:  0 ‘***’ 0.001 ‘**’ 0.01 ‘*’ 0.05 ‘.’ 0.1 ‘ ’ 1

Model found:
AVE_PAM ~ Temp
```

ANOVA results from the model (The same as above, with differences between temperatures):

```
Type III Analysis of Variance Table with Satterthwaite's method
     Sum Sq Mean Sq NumDF  DenDF F value  Pr(>F)
Temp 0.40766 0.20383     2 3.0028  28.524 0.01113 *
---
Signif. codes:  0 ‘***’ 0.001 ‘**’ 0.01 ‘*’ 0.05 ‘.’ 0.1 ‘ ’ 1
```

Post-Hoc analysis emmeans (Estimated marginal means): Differences were found between temp31 – temp 34 and temp31 – temp37

```
$`emmeans of Temp`
 Temp  emmean     SE   df lower.CL upper.CL
 31   0.29671 0.0297 3.71  0.17413    0.419
 34   0.11854 0.0297 3.71 -0.00404    0.241
 37   0.00091 0.0297 3.72 -0.12165    0.123

Degrees-of-freedom method: kenward-roger
Confidence level used: 0.95
Conf-level adjustment: sidak method for 3 estimates

$`pairwise differences of Temp`
 1              estimate     SE df t.ratio p.value
 Temp31 - Temp34    0.178 0.0394  3   4.519  0.0408
 Temp31 - Temp37    0.296 0.0394  3   7.498  0.0100
 Temp34 - Temp37    0.118 0.0394  3   2.982  0.1143
```

Degrees-of-freedom method: kenward-roger
P value adjustment: tukey method for comparing a family of 3 estimates

Table S3.4 Statistical analysis for bio-physical colouration and photobiological performance of donor and 12-months-propagated *A.* cf. *hyacinthus* during the CBASS. Mean ± the standard error of the mean (SEM) and N (sample size) alongside a two-way RM ANOVA is reported for (a) red (R), (b) green (G), (c) blue (B), (d) brightness, (e) hue, (f) saturation, (g) bleaching state, (h) maximum photochemical efficiency [F_v/F_m], (i) symbiont density, (j) pigment density (k) chlorophyll *a* and *c2* density. Values were obtained at the end of the 18-h heat stress assay (a-g) and at T_{end} (7 h after the onset of the experiment).

At the end of the 18-h experiment

a)

CBASS_RED	**Wild**			**Nursery**		
Temperature	**Mean**	**SEM**	N	**Mean**	**SEM**	N
31	**127.2**	**12.4**	6	**126.2**	**12.5**	6
34	**210.2**	**10.9**	6	**199.0**	**14.0**	6
37	**217.8**	**6.6**	6	**202.8**	**8.1**	6

Table Analyzed	**CBASS_RED_Grouped: RM Two-way ANOVA**				
Two-way RM ANOVA	Matching: Both factors				
Assume sphericity?	No				
Alpha	0.05				
Source of Variation	% of total variation	P value	P value summary	Significant?	Geisser-Greenhouse's epsilon
Temperature	69.4	<0.0001	****	Yes	0.7615
Environment	0.9771	0.3093	ns	No	1
Temperature x Environment	0.4158	0.6599	ns	No	0.6531

Coral x Temperature	4.895				
Coral x Environment	3.818				
Coral	13.62				
ANOVA table	SS	DF	MS	F (DFn, DFd)	P value
Temperature	**52417**	**2**	**26208**	**F (1.523, 7.615) = 70.89**	**P<0.0001**
Environment	**738**	**1**	**738**	**F (1.000, 5.000) = 1.280**	**P=0.3093**
Temperature x Environment	**314.1**	**2**	**157**	**F (1.306, 6.531) = 0.3022**	**P=0.6599**
Coral x Temperature	3697	10	369.7		
Coral x Environment	2883	5	576.7		
Coral	10283	5	2057		
Residual	5196	10	519.6		

b)

CBASS_GREEN	**Wild**			**Nursery**		
Temperature	**Mean**	**SEM**	N	**Mean**	**SEM**	N
31	**96.7**	**10.8**	6	**97.5**	**12.0**	6
34	**181.8**	**14.4**	6	**178.8**	**17.5**	6
37	**213.0**	**5.9**	6	**198.8**	**7.3**	6

Table Analyzed	**CBASS_GREEN_Grouped: RM Two-way ANOVA**

Two-way RM ANOVA	Matching: Both factors				
Assume sphericity?	No				
Alpha	0.05				
Source of Variation	% of total variation	P value	P value summary	Significant?	Geisser-Greenhouse's epsilon
Temperature	74.57	<0.0001	****	Yes	0.6573
Environment	0.256	0.4653	ns	No	1
Temperature x Environment	0.3496	0.6581	ns	No	0.776
Coral x Temperature	5.087				
Coral x Environment	2.05				
Coral	12.83				
ANOVA table	SS	DF	MS	F (DFn, DFd)	P value
Temperature	**77719**	**2**	**38860**	**F (1.315, 6.573) = 73.29**	**P<0.0001**
Environment	**266.8**	**1**	**266.8**	**F (1.000, 5.000) = 0.6242**	**P=0.4653**
Temperature x Environment	**364.4**	**2**	**182.2**	**F (1.552, 7.760) = 0.3594**	**P=0.6581**
Coral x Temperature	5302	10	530.2		
Coral x Environment	2137	5	427.4		
Coral	13367	5	2673		
Residual	5069	10	506.9		

c)

CBASS_BLUE	**Wild**	**Nursery**

Temperature	**Mean**	**SEM**	N	**Mean**	**SEM**	N
31	**77.3**	**9.9**	6	**76.3**	**11.3**	6
34	**152.3**	**13.9**	6	**151.3**	**17.4**	6
37	**202.3**	**5.4**	6	**185.0**	**13.1**	6

Table Analyzed	**CBASS_BLUE_Grouped: RM Two-way ANOVA**				
Two-way RM ANOVA	Matching: Both factors				
Assume sphericity?	No				
Alpha	0.05				
Source of Variation	% of total variation	P value	P value summary	Significant?	Geisser-Greenhouse's epsilon
Temperature	74.65	<0.0001	****	Yes	0.6733
Environment	0.3318	0.4645	ns	No	1
Temperature x Environment	0.4736	0.6406	ns	No	0.9569
Coral x Temperature	5.15				
Coral x Environment	2.648				
Coral	11.52				
ANOVA table	SS	DF	MS	F (DFn, DFd)	P value
Temperature	**84100**	**2**	**42050**	**F (1.347, 6.733) = 72.48**	**P<0.0001**
Environment	**373.8**	**1**	**373.8**	**F (1.000, 5.000) = 0.6265**	**P=0.4645**

Temperature x Environment	**533.6**	**2**	**266.8**	**F (1.914, 9.569) = 0.4528**	**P=0.6406**
Coral x Temperature	5801	10	580.1		
Coral x Environment	2983	5	596.6		
Coral	12975	5	2595		
Residual	5891	10	589.1		

d)

CBASS_BRIGHTNESS	**Wild**			**Nursery**		
Temperature	**Mean**	**SEM**	N	**Mean**	**SEM**	N
31	**49.8**	**4.8**	6	**49.3**	**4.9**	6
34	**82.5**	**4.3**	6	**78.0**	**5.5**	6
37	**85.8**	**2.4**	6	**80.0**	**3.2**	6

Table Analyzed	**CBASS_BRIGHTNESS % - Transform - Arcsin (Y/100)**				
Two-way RM ANOVA	Matching: Both factors				
Assume sphericity?	No				
Alpha	0.05				
Source of Variation	% of total variation	P value	P value summary	Significant?	Geisser-Greenhouse's epsilon
Temperature	64.93	0.0002	***	Yes	0.6339

Environment	1.242	0.2773	ns	No	1
Temperature x Environment	0.6207	0.6258	ns	No	0.7764
Coral x Temperature	5.753				
Coral x Environment	4.18				
Coral	15.78				
ANOVA table	SS	DF	MS	F (DFn, DFd)	P value
Temperature	**1.633**	**2**	**0.8166**	**F (1.268, 6.339) = 56.43**	**P=0.0002**
Environment	**0.03124**	**1**	**0.03124**	**F (1.000, 5.000) = 1.486**	**P=0.2773**
Temperature x Environment	**0.01561**	**2**	**0.007807**	**F (1.553, 7.764) = 0.4144**	**P=0.6258**
Coral x Temperature	0.1447	10	0.01447		
Coral x Environment	0.1051	5	0.02103		
Coral	0.3969	5	0.07938		
Residual	0.1884	10	0.01884		

e)

CBASS_HUE	**Wild**			**Nursery**		
Temperature	**Mean**	**SEM**	N	**Mean**	**SEM**	N
31	**23.7**	**2.4**	6	**25.5**	**2.4**	6
34	**31.3**	**3.0**	6	**35.5**	**3.8**	6
37	**62.5**	**21.5**	6	**70.8**	**28.3**	6

Table Analyzed	**CBASS_HUE - Transform - Sin (Y) - change**				
Two-way RM ANOVA	Matching: Both factors				
Assume sphericity?	No				
Alpha	0.05				
Source of Variation	% of total variation	P value	P value summary	Significant?	Geisser-Greenhouse's epsilon
Temperature	0.5787	0.8271	ns	No	0.7203
Environment	0.2116	0.8601	ns	No	1
Temperature x Environment	5.209	0.4155	ns	No	0.8396
Coral x Temperature	24.57				
Coral x Environment	30.74				
Coral	10.64				
ANOVA table	SS	DF	MS	F (DFn, DFd)	P value
Temperature	**0.1005**	**2**	**0.05027**	**F (1.441, 7.203) = 0.1178**	**P=0.8271**
Environment	**0.03675**	**1**	**0.03675**	**F (1.000, 5.000) = 0.03441**	**P=0.8601**
Temperature x Environment	**0.9049**	**2**	**0.4524**	**F (1.679, 8.396) = 0.9284**	**P=0.4155**
Coral x Temperature	4.269	10	0.4269		
Coral x Environment	5.34	5	1.068		
Coral	1.848	5	0.3696		
Residual	4.873	10	0.4873		

f)

CBASS_SATURATION	Wild			Nursery		
Temperature	**Mean**	**SEM**	N	**Mean**	**SEM**	N
31	**39.7**	**2.7**	6	**40.5**	**3.1**	6
34	**28.2**	**3.6**	6	**25.2**	**3.7**	6
37	**8.0**	**1.9**	6	**10.2**	**4.0**	6

Table Analyzed	CBASS_SATURATION % - Transform - Arcsin (Y/100)				
Two-way RM ANOVA	Matching: Both factors				
Assume sphericity?	No				
Alpha	0.05				
Source of Variation	% of total variation	P value	P value summary	Significant?	Geisser-Greenhouse's epsilon
Temperature	74.75	0.0001	***	Yes	0.5851
Environment	3.7E-05	0.9945	ns	No	1
Temperature x Environment	0.5574	0.6896	ns	No	0.8125
Coral x Temperature	4.693				
Coral x Environment	3.509				
Coral	7.89				

ANOVA table	SS	DF	MS	F (DFn, DFd)	P value
Temperature	**0.626**	**2**	**0.313**	**F (1.170, 5.851) = 79.64**	**P=0.0001**
Environment	**3.1E-07**	**1**	**3.125E-07**	**F (1.000, 5.000) = 5.317e-005**	**P=0.9945**
Temperature x Environment	**0.00467**	**2**	**0.002334**	**F (1.625, 8.125) = 0.3240**	**P=0.6896**
Coral x Temperature	0.0393	10	0.00393		
Coral x Environment	0.02938	5	0.005877		
Coral	0.06608	5	0.01322		
Residual	0.07205	10	0.007205		

g)

CBASS_BLEACHING	**Wild**			**Nursery**		
Temperature	**Mean**	**SEM**	N	**Mean**	**SEM**	N
31	**5.7**	**0.3**	6	**5.7**	**0.3**	6
34	**3.2**	**0.7**	6	**3.7**	**0.6**	6
37	**1.0**	**0.0**	6	**1.2**	**0.2**	6
Table Analyzed	**CBASS_BLEACHING_Grouped: RM Two-way ANOVA**					
Two-way RM ANOVA	Matching: Both factors					
Assume sphericity?	No					
Alpha	0.05					

Source of Variation	% of total variation	P value	P value summary	Significant?	Geisser-Greenhouse's epsilon
Temperature	79.5	0.0002	***	Yes	0.6068
Environment	0.2803	0.4441	ns	No	1
Temperature x Environment	0.2453	0.6887	ns	No	0.8174
Coral x Temperature	7.323				
Coral x Environment	2.032				
Coral	6.868				

ANOVA table	SS	DF	MS	F (DFn, DFd)	P value
Temperature	**126.1**	**2**	**63.03**	**F (1.214, 6.068) = 54.28**	**P=0.0002**
Environment	**0.4444**	**1**	**0.4444**	**F (1.000, 5.000) = 0.6897**	**P=0.4441**
Temperature x Environment	**0.3889**	**2**	**0.1944**	**F (1.635, 8.174) = 0.3271**	**P=0.6887**
Coral x Temperature	11.61	10	1.161		
Coral x Environment	3.222	5	0.6444		
Coral	10.89	5	2.178		
Residual	5.944	10	0.5944		

At T_{end} (7 h)

h)

CBASS_Fv/Fm	**Wild**			**Nursery**		
Temperature	**Mean**	**SEM**	N	**Mean**	**SEM**	N
31	**0.2759**	**0.0254**	6	**0.3175**	**0.0140**	6
34	**0.0975**	**0.0257**	6	**0.1396**	**0.0627**	6

37	**0.0000**	**0.0000**	6	**0.0000**	**0.0000**	6

Table Analyzed	**CBASS_Fv/Fm_Grouped: RM Two-way ANOVA**				
Two-way RM ANOVA	Matching: Both factors				
Assume sphericity?	No				
Alpha	0.05				
Source of Variation	% of total variation	P value	P value summary	Significant?	Geisser-Greenhouse's epsilon
Temperature	75.5	0.0006	***	Yes	0.6158
Environment	0.9873	0.0783	ns	No	1
Temperature x Environment	0.4937	0.5761	ns	No	0.5241
Coral x Temperature	10.26				
Coral x Environment	1.012				
Coral	5.149				
ANOVA table	SS	DF	MS	F (DFn, DFd)	P value
Temperature	**0.5353**	**2**	**0.2677**	**F (1.232, 6.158) = 36.81**	**P=0.0006**
Environment	**0.007**	**1**	**0.007**	**F (1.000, 5.000) = 4.877**	**P=0.0783**
Temperature x Environment	**0.0035**	**2**	**0.00175**	**F (1.048, 5.241) = 0.3741**	**P=0.5761**
Coral x Temperature	0.07272	10	0.007272		
Coral x Environment	0.007177	5	0.001435		

Coral	0.0365	5	0.007301
Residual	0.04678	10	0.004678

i)

CBASS_Cell density (cells x 106 x cm-2)	**Wild**			**Nursery**		
Temperature	**Mean**	**SEM**	N	**Mean**	**SEM**	N
31	**0.6820**	**0.0228**	6	**0.6725**	**0.0253**	6
34	**0.0817**	**0.0009**	6	**0.0818**	**0.0009**	6
37	**0.0760**	**0.0012**	6	**0.0747**	**0.0015**	6

Table Analyzed	**CBASS_Cell density (cells x cm-2)_Grouped: RM Two-way ANOVA**				
Two-way RM ANOVA	Matching: Both factors				
Assume sphericity?	No				
Alpha	0.05				
Source of Variation	% of total variation	P value	P value summary	Significant?	Geisser-Greenhouse's epsilon
Temperature	98.78	<0.0001	****	Yes	0.5064
Environment	0.004091	0.7554	ns	No	1
Temperature x Environment	0.005336	0.8016	ns	No	0.5035
Coral x Temperature	0.4155				

Coral x Environment	0.1889				
Coral	0.2279				
ANOVA table	SS	DF	MS	F (DFn, DFd)	P value
Temperature	**2.8687E+12**	**2**	**1.43E+12**	**F (1.013, 5.064) = 1189**	**P<0.0001**
Environment	**118802733**	**1**	**1.19E+08**	**F (1.000, 5.000) = 0.1083**	**P=0.7554**
Temperature x Environment	**154966804**	**2**	**77483402**	**F (1.007, 5.035) = 0.07143**	**P=0.8016**
Coral x Temperature	1.2067E+10	10	1.21E+09		
Coral x Environment	5484551633	5	1.1E+09		
Coral	6617333054	5	1.32E+09		
Residual	1.0847E+10	10	1.08E+09		

j)

CBASS_Total pigments (a + c2) density	**Wild**			**Nursery**		
Temperature	**Mean**	**SEM**	N	**Mean**	**SEM**	N
31	**6.6**	**1.1**	6	**6.8**	**1.1**	6
34	**0.9**	**0.3**	6	**2.1**	**0.8**	6
37	**0.3**	**0.1**	6	**0.7**	**0.3**	6

Table Analyzed	**CBASS_Total pigments (a + c2) density_Grouped: RM Two-way ANOVA**
Two-way RM ANOVA	Matching: Both factors

Assume sphericity?	No				
Alpha	0.05				
Source of Variation	% of total variation	P value	P value summary	Significant?	Geisser-Greenhouse's epsilon
Temperature	71.52	0.0018	**	Yes	0.6391
Environment	0.9386	0.1361	ns	No	1
Temperature x Environment	0.4078	0.2423	ns	No	0.7738
Coral x Temperature	15.2				
Coral x Environment	1.49				
Coral	9.233				
ANOVA table	SS	DF	MS	F (DFn, DFd)	P value
Temperature	**263.6**	**2**	**131.8**	**F (1.278, 6.391) = 23.52**	**P=0.0018**
Environment	**3.46**	**1**	**3.46**	**F (1.000, 5.000) = 3.149**	**P=0.1361**
Temperature x Environment	**1.503**	**2**	**0.7515**	**F (1.548, 7.738) = 1.691**	**P=0.2423**
Coral x Temperature	56.04	10	5.604		
Coral x Environment	5.492	5	1.098		
Coral	34.03	5	6.807		
Residual	4.445	10	0.4445		

k)

CBASS_Chlorophyll a (ug/cm2)	**Wild**	**Nursery**

Temperature	**Mean**	**SEM**	N	**Mean**	**SEM**	N
31	**5.3**	**1.0**	6	**5.2**	**0.8**	6
34	**0.8**	**0.2**	6	**1.7**	**0.6**	6
37	**0.2**	**0.1**	6	**0.5**	**0.2**	6

Table Analyzed	**CBASS_Chlorophyll a (ug/cm2)_Col: _Grouped: RM Two-way ANOVA**				
Two-way RM ANOVA	Matching: Both factors				
Assume sphericity?	No				
Alpha	0.05				
Source of Variation	% of total variation	P value	P value summary	Significant?	Geisser-Greenhouse's epsilon
Temperature	72.18	0.001	***	Yes	0.6786
Environment	0.6887	0.265	ns	No	1
Temperature x Environment	0.6659	0.2087	ns	No	0.6244
Coral x Temperature	13.49				
Coral x Environment	2.187				
Coral	9.131				
ANOVA table	SS	DF	MS	F (DFn, DFd)	P value
Temperature	**164.2**	**2**	**82.09**	**F (1.357, 6.786) = 26.75**	**P=0.0010**
Environment	**1.567**	**1**	**1.567**	**F (1.000, 5.000) = 1.574**	**P=0.2650**

Temperature x Environment	**1.515**	**2**	**0.7574**	**F (1.249, 6.244) = 2.006**	**P=0.2087**
Coral x Temperature	30.69	10	3.069		
Coral x Environment	4.976	5	0.9951		
Coral	20.77	5	4.154		
Residual	3.776	10	0.3776		

l)

CBASS_Chlorophyll c2 (ug/cm2)	**Wild**			**Nursery**		
Temperature	**Mean**	**SEM**	N	**Mean**	**SEM**	N
31	**1.31**	**0.19**	6	**1.6**	**0.4**	6
34	**0.19**	**0.06**	6	**0.4**	**0.2**	6
37	**0.13**	**0.06**	6	**0.2**	**0.1**	6

Table Analyzed	CBASS_Chlorophyll c2 (ug/cm2)_Grouped: RM Two-way ANOVA				
Two-way RM ANOVA	Matching: Both factors				
Assume sphericity?	No				
Alpha	0.05				
Source of Variation	% of total variation	P value	P value summary	Significant?	Geisser-Greenhouse's epsilon
Temperature	57.85	0.0109	*	Yes	0.5597

Environment	1.806	0.1149	ns	No	1
Temperature x Environment	0.2382	0.7467	ns	No	0.6474
Coral x Temperature	21.5				
Coral x Environment	2.485				
Coral	9.516				
ANOVA table	SS	DF	MS	F (DFn, DFd)	P value
Temperature	**11.79**	**2**	**5.894**	**F (1.119, 5.597) = 13.46**	**P=0.0109**
Environment	**0.368**	**1**	**0.368**	**F (1.000, 5.000) = 3.634**	**P=0.1149**
Temperature x Environment	**0.04854**	**2**	**0.02427**	**F (1.295, 6.474) = 0.1803**	**P=0.7467**
Coral x Temperature	4.38	10	0.438		
Coral x Environment	0.5064	5	0.1013		
Coral	1.939	5	0.3878		
Residual	1.346	10	0.1346		

m)

CBASS_Ratio (a : c2)	**Wild**			**Nursery**		
Temperature	**Mean**	**SEM**	N	**Mean**	**SEM**	N
31	**3.9**	**0.2**	6	**3.9**	**0.6**	6
34	**4.7**	**0.7**	6	**4.2**	**0.3**	6
37	**1.7**	**0.4**	6	**2.4**	**0.5**	6

Table Analyzed	CBASS_Ratio (a : c2)_Grouped: RM Two-way ANOVA				
Two-way RM ANOVA	Matching: Both factors				
Assume sphericity?	No				
Alpha	0.05				
Source of Variation	% of total variation	P value	P value summary	Significant?	Geisser-Greenhouse's epsilon
Temperature	46.99	0.0112	*	Yes	0.6991
Environment	0.0461	0.8736	ns	No	1
Temperature x Environment	2.134	0.4432	ns	No	0.5254
Coral x Temperature	22.77				
Coral x Environment	8.227				
Coral	4.811				
ANOVA table	SS	DF	MS	F (DFn, DFd)	P value
Temperature	**38.75**	**2**	**19.38**	**F (1.398, 6.991) = 10.32**	**P=0.0112**
Environment	**0.03803**	**1**	**0.03803**	**F (1.000, 5.000) = 0.02802**	**P=0.8736**
Temperature x Environment	**1.761**	**2**	**0.8803**	**F (1.051, 5.254) = 0.7103**	**P=0.4432**
Coral x Temperature	18.78	10	1.878		
Coral x Environment	6.786	5	1.357		
Coral	3.968	5	0.7936		
Residual	12.39	10	1.239		

Table S3.5 Statistical comparison of relative potencies between the ED50 dose-response curves. Log-logistic dose-response curves of the donor (wild) and 12-month-propagated *A.* cf. *hyacinthus* (nursery) were compared through the R function "*EDcomp*".

Estimated ratios of effect doses				
	Estimate	**Std. Error**	**t-value**	**p-value**
W/N:50/50	0,993995	46,598	-0,128868	0,897854

Chapter 4

Carbonate budgets induced by coral restoration of a Great Barrier Reef site following cyclone damage

C. Isabel Nuñez Lendo[1]*, David J. Suggett[1], Chloë Boote[1], Alicia McArdle[2], Freda Nicholson[2], Eric E. Fisher[3], David Smith[2], Emma F. Camp[1]

[1]Climate Change Cluster, University of Technology Sydney, Ultimo, NSW 2007, Australia

[2]Mars Sustainable Solutions, Cairns, QLD 4870, Australia

[3]GBR Biology, Cairns, QLD 4870, Australia

Author contributions: CINL, DJS, and EFC designed the experiment, and field-based surveys and sample collection were conducted by CINL and CB. CINL analysed the bio-physical, photobiological, and skeletal samples. CINL conducted the statistical analysis and prepared the figures. CINL wrote the manuscript with editorial support from DJS and EFC, and with all authors contributing their relevant expertise in methods reporting and evaluation, and overall manuscript editing.

C. Isabel Nuñez Lendo	Production Note: Signature removed prior to publication.
David J. Suggett	Production Note: Signature removed prior to publication.
Chloë Boote	Production Note: Signature removed prior to publication.
Alicia McArdle	Production Note: Signature removed prior to publication.
Freda Nicholson	Production Note: Signature removed prior to publication.
Eric Fisher	Production Note: Signature removed prior to publication.
David Smith	Production Note: Signature removed prior to publication.
Emma F. Camp	Production Note: Signature removed prior to publication.

4. Abstract

Coral carbonate production is fundamental to reef accretion and, consequently, the preservation of essential reef ecosystem services, such as wave attenuation and sustained reef biodiversity. However, the unprecedented loss of coral reefs from anthropogenic impacts has put these valuable ecosystem services at risk. To counteract this loss, active rehabilitation of degraded reef sites has accelerated globally. A variety of restoration practices exist, tailored to local site needs and reef types. For sites where there is a significant unconsolidated substrate, Mars Assisted Reef Restoration System (MARRS, or "Reef Stars") has been utilised to contribute toward rubble stabilisation and reef accretion. However, the effect of the Reef Stars on the local carbonate budgets and structural complexity has not been assessed. For that purpose, we assess coral cover and reef complexity through a census-based approach to identify the contribution of carbonate producers and eroders alongside studying coral skeletal properties to estimate current carbonate budgets on a rehabilitated site compared to natural unrehabilitated reef and rubble patches on the mid-Great Barrier Reef. Our research identified positive ecological processes and ecological functions such as increased carbonate budget, coral cover and structural complexity at the restored site compared to the non-intervened reef and rubble patches. In general, no impacts on skeletal rigour relative to this active reef restoration were found for two key coral species and the *Acropora* rubble for most of the skeletal traits. However, *Pocillopora damicornis* hardness seemed to decrease on the restored site compared to the other sites, demonstrating different performances of coral species during restoration activities that should be considered to maximise return-on-effort of restoration activities. Overall, our data demonstrate that consideration of carbonate budgets is important for measuring success of coral restoration initiatives and that coral restoration can be a relevant tool to recover lost local carbonate budgets.

4.1 Introduction

Declines in live coral cover since the 1970s have dramatically slowed reef accretion on a global scale. Mean rates of contemporary reef carbonate production for the Caribbean are below mean historical and geological levels (Alvarez-Filip et al., 2009; Gardner et al., 2003; Perry et al., 2012). Similarly, Indo-Pacific reefs have been driven into net negative accretion states and reef structural collapse following coral mortality (Bak, 1990; Eakin, 1996), including recent bleaching-driven coral die-offs (Perry and Morgan, 2017). On the Great Barrier Reef (GBR), coral cover has been declining since the mid-1980s (De'Ath et al., 2012; Sweatman et al., 2011) from the combined effects of both local (e.g., coastal development; Halpern et al., 2008) and global (e.g., climate change; Hughes et al., 2018) stressors. Recent recurrent episodes of mass bleaching (i.e., four major events between 2016 and 2022), corresponding with extreme thermal anomalies in 2016, 2017, 2020, and notably the first documented mass bleaching event under La Niña cool conditions in 2022, have driven coral cover to all-time lows (e.g., Hughes et al., 2021, 2017). Despite catastrophic coral loss, only a few studies have investigated changes to reef carbonate budgets (i.e., balance between rates of carbonate production and erosion) for the GBR, often focussing on a particular organism, process, or environmental condition, such as the calcareous green alga *Halimeda* (Castro-Sanguino et al., 2020; Rees et al., 2007), bioerosion activity (Aline, 2008; Tribollet and Golubic, 2005), highly turbid reefs (Browne et al., 2013), and island geomorphological habitats (Brown et al., 2021). So far, few studies have focussed on carbonate budgets in the Southern and Middle GBR regions; therefore, knowledge of the entire GBR is wholly lacking.

Hard (scleractinian) corals are the main contributors to the structure and function of coral reef ecosystems, providing (1) reef accretion (Perry et al., 2013), (2) habitat structure (Alvarez-Filip et al., 2009; Graham et al., 2006), and (3) biogeochemical cycling (Cole et al., 2008; Goreau et al., 1979; Wild et al., 2004). Fundamental to the provision of these features is carbonate production. Scleractinian corals undergo skeletogenesis (Al-Horani, 2015) to rapidly precipitate calcium carbonate ($CaCO_3$) (reviewed in McCulloch et al., 2017) that — on a community level — results in the reef framework. $CaCO_3$ production is continuously exposed to both biological (associated with fish and invertebrate grazing and endolithic borers) and physical (e.g., storm disturbance) agents of reef bioerosion (Perry and Hepburn, 2008) that ultimately comprise the net three-dimensional structure and function of the reef (Leggat et al., 2019). Healthy-functioning reef systems in effect self-repair, balancing growth (carbonate production) with erosion processes (UNEP-WCMC, 2006); consequently, stressors that tip the balance in carbonate production versus loss will inevitably undermine the many ecosystem services that reef structure provides (Pratchett et al., 2021), both directly as wave attenuation and shoreline protection for coastal communities (Storlazzi et al., 2018; Yates et al., 2017) and indirectly via reef habitat structure (Perry et al., 2013; Perry and Morgan, 2017) as fisheries productivity (Bell et al., 2013; Rogers et al., 2014, 2018) and biodiversity (Stuart-Smith et al., 2018; Wilson et al., 2006).

To counteract rapidly declining coral cover, global management approaches are expanding beyond traditional protection (and stress mitigation) practices to include proactive interventions (e.g., Shaver et al., 2022; Suggett and Van Oppen, 2022) aimed at recovering reef ecosystem services (Hein et al., 2021). Measurements of restoration success have conventionally been evaluated via two coarse metrics of coral growth and survivorship (Boström-Einarsson et al., 2020; Hein et al., 2017; Nuñez Lendo et al., 2023, **Chapter 2**),

even though restoration goals are often centred on recovering broader ecosystem service value attributes (Hein et al., 2021, Shaver et al. 2022). As such, how restoration activities may impact healthy reef functioning — in terms of long-term consequences for different ecosystem service attributes — remains hard to ascertain. Maintaining desirable features such as high coral cover, structural complexity, and fish biomass are common conservation objectives. Even so, the processes underpinning these features (including calcium carbonate dynamics) are poorly defined and understood (Brandl et al., 2019). For example, trade-offs in resource acquisition and partitioning that potentially regulate growth versus survival may yield very different outcomes towards factors governing reef accretion and structural integrity (Nuñez Lendo et al., 2023, **Chapter 2**). For reef restoration programs focused on regaining reef structure and function, resolving goal-relevant metrics, such as carbonate production and coral skeletal traits, will therefore be critical to actually evaluate success.

Reef restoration methods span multiple disciplines ranging from coral biology and ecology to ecological modelling and geoengineering (Suggett and van Oppen, 2022). Where reef substrates have become unconsolidated — through blast fishing or framework collapse following mass bleaching or cyclone disturbance (Harmelin-Vivien, 1994; Leggat et al., 2019) — restoration often requires substrate enhancement to initiate regrowth (Ceccarelli et al., 2020). For example, practices that use mesh or netting over the rubble to boost natural binding and cementation processes (Raymundo et al., 2007), or rock piles placed on rubble fields to stabilise loose reef substrate (Fox et al., 2019). Such activities can significantly boost coral cover compared to neighbouring non-stabilised reefs (Fox et al., 2019). One example of substrate stabilisation that has recently gained popularity is the so-called MARRS (Mars Assisted Reef Restoration System, or “Reef Stars”), which are hexagonal-shaped structures made of reinforcing steel rods that each enclose an area of 0.337 m^2, and are interconnected

with cable ties in a web to cover large areas (**Fig. S4.1**; Williams et al., 2019). Reef Stars have been successfully used in Indonesia following physical damage caused by blast fishing and are in one of the world's largest restored reef efforts to date (Lamont et al., 2022; Williams et al., 2019). This successful example of a restored degraded area initially extended to 7,000 km^2 of stabilised coral rubble by using around 198,000 coral fragments on 11,000 Reef Stars (Williams et al., 2019).

Reef Stars were first installed on the GBR as part of a broader restoration plan for Moore Reef (central GBR) to stabilise an accumulated coral rubble field produced from the 2011 Cyclone Yasi. A set of 87 Reef Stars (named also "Block A2" to differentiate from other installations) holding corals of opportunity was installed in October 2020. By March 2023, a total of 439 Reef Stars have been completed, with 6,471 coral fragments of opportunity. Whilst ecological recovery from this and other Reef Stars installations is already evident (**Fig. 4.1**) — and is the focus of other ongoing research — the impact towards changes in reef accretion and structural rigour (i.e., coral density, porosity, and hardness) remains unknown. As such, we examined the Moore Reef installation as a novel means to identify how this reef stabilisation approach impacts the rate of reef-structure gain (or loss) compared to neighbouring non-restored reef controls via the balance of constructional (i.e., calcification) and de-constructional (i.e., erosion) processes (Hubbard et al., 1990; Perry et al., 2012; Scoffin et al., 1980; Stearn et al., 1977) and therefore resolve carbonate budgets (Lange et al., 2020). We specifically document spatial variability in carbonate budgets using a census-based approach (see a schematic view in **Fig. 4.2**; Perry et al. 2012) in which rates of carbonate production and erosion were estimated for three reef sites (i.e., at a 16 month restored reef site using the Reef Stars; a nearby representative natural reef; and a degraded area represented by coral rubble). We further studied the skeletal properties — bulk volume,

biomineral density, bulk density, pore volume, apparent (internal) porosity, and hardness — of the dominant calcifying biota (i.e., coral), focussing on the main coral species in Moore Reef (*Acropora intermedia* and *Pocillopora damicornis*) alongside branching *Acropora* rubble (which was dominantly present in the study area). For this approach, we identified how reef stabilisation can enhance accretion by 6-29% compared to unrestored sites, and we discuss how this approach potentially provides critical means for practitioners to evaluate wider ecosystem service values attained through restoration.

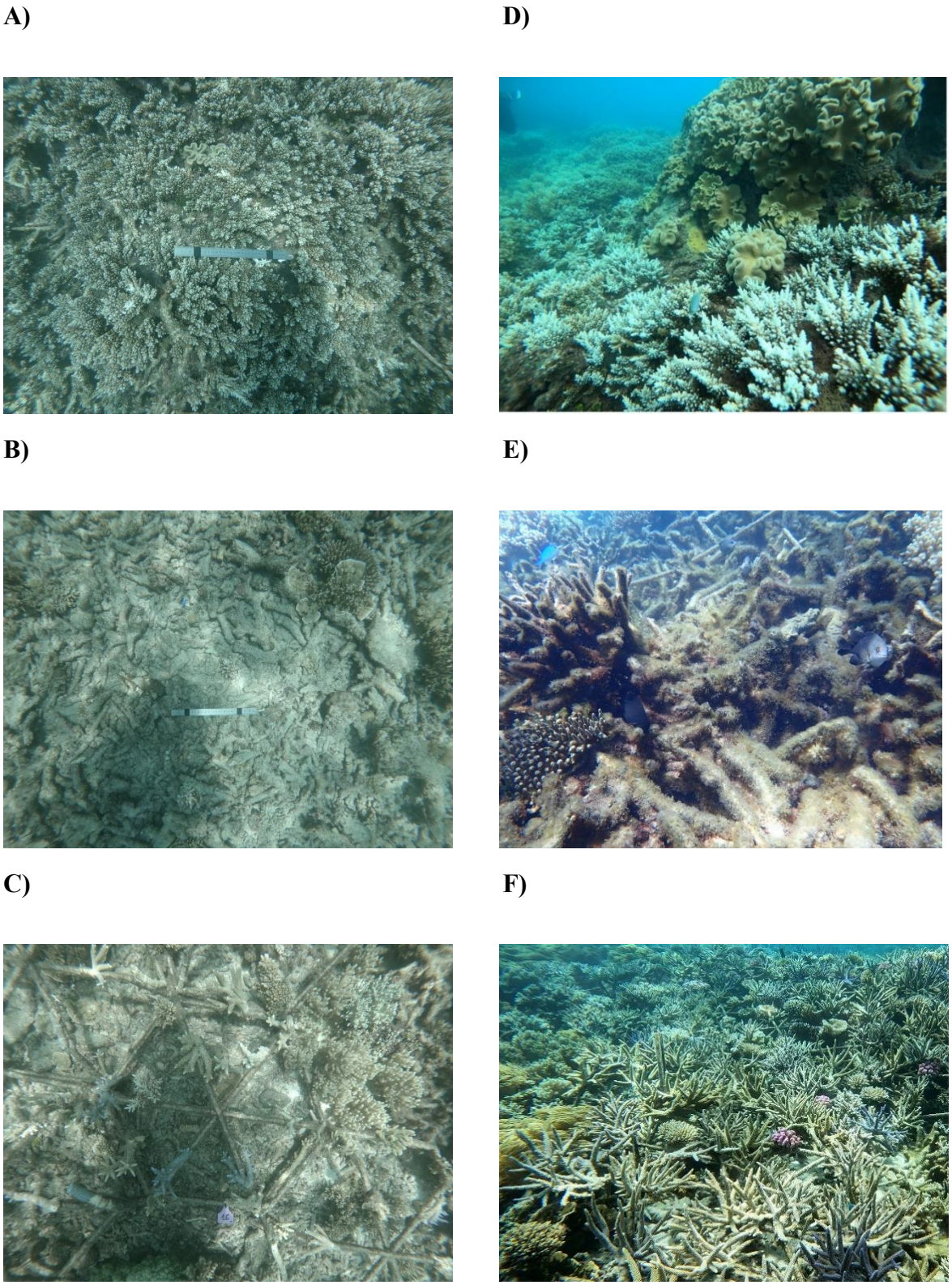

Figure 4.1 Moore Reef study sites. In February 2021, (A) Natural healthy-looking representative neighbouring reef with high coral cover (positive control, 'PC') (B) View of a 11-year-old rubble field, created by Cyclone Yasi without rehabilitation (negative control, 'NC') (C) Stabilisation reef plot, showing the Reef Stars structures holding corals of opportunity (4 months post-installation). Approximately 11 months later (December 2021), same reef sites 'PC', 'NC', and 'E' (D-F). Note the high coral cover observed on the Reef Stars in the intervened rubble site 'E'. Credits: Nuñez Lendo, C.I., and Mars Sustainable Solutions.

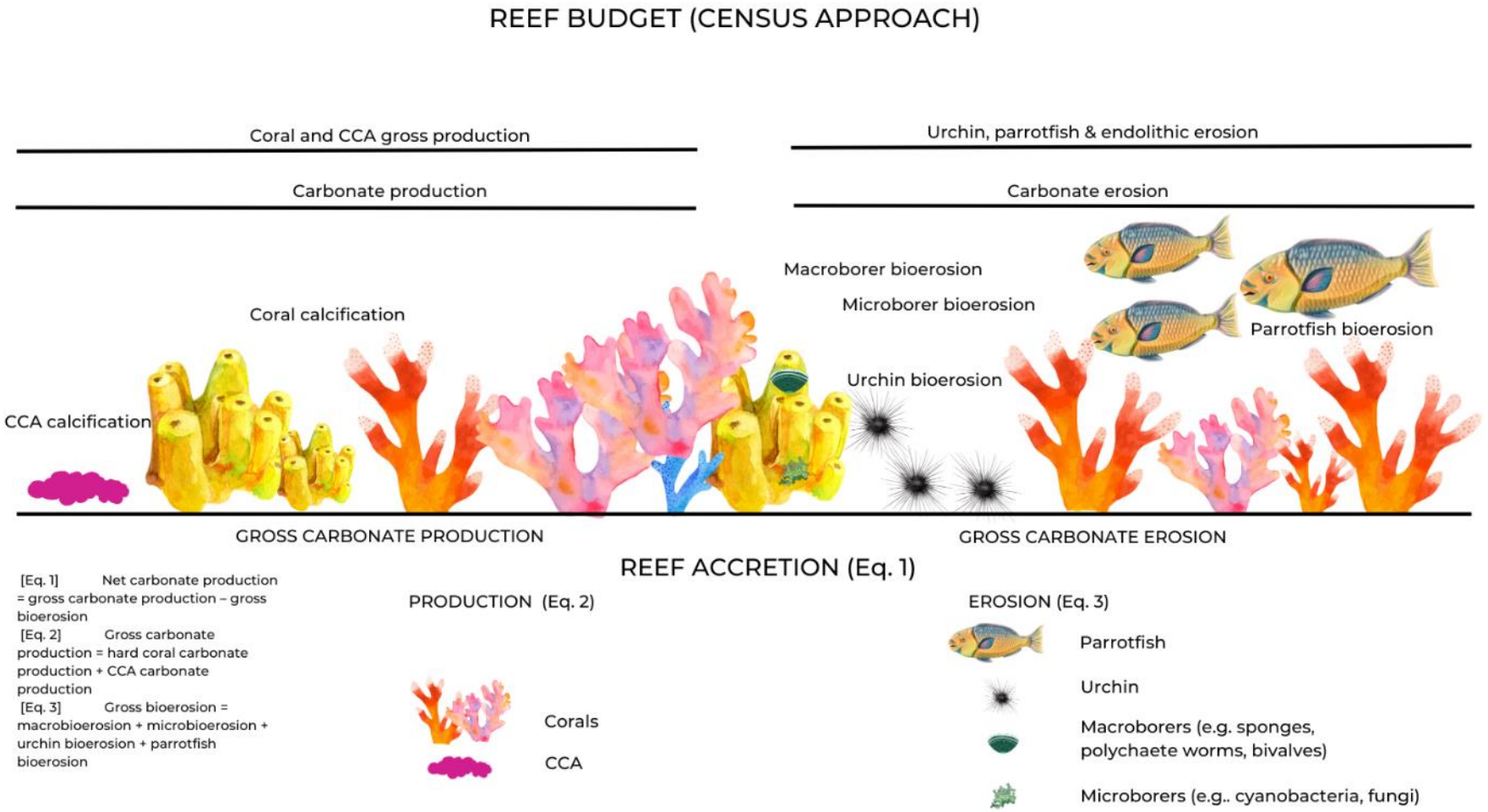

Figure 4.2 Schematic view of the methodology used to estimate coral reef carbonate budgets on the three studied Moore Reef sites. Our study was based on the Reef Budget methodology from Perry et al., (2012). Positive and negative contributions to reef accretion (production and erosion, respectively) are visualised. Specifically, net carbonate production [**Equation 1**], gross carbonate production [**Equation 2**], and gross bioerosion [**Equation 3**], and the main contributors to production and erosion processes. Credits: Nuñez Lendo, C.I.

4.2 Materials and Methods

4.2.1 Study location

MARRS Reef Stars were installed at Moore Reef (3–5 m depth), a mid-shelf patch reef located 50 km east of Cairns, in the central Great Barrier Reef (GBR), Australia (146° 14' 40.9''E, 16°51' 59.0''S). Our study location (~2,000 m^2) is an area divided into three sites (30 x 20 m), where each site is marked with star pickets at the corners corresponding to (i) a stabilised substrate section using the Reef Stars (Experimental, "E"), and two nearby sites of (ii) a rubble patch where no Reef Stars were deployed (negative control, "NC"), and (iii) a non-intervened healthy-looking representative neighbouring reef area with high coral cover and diversity (positive control, "PC") (**Fig. S4.2**). Herein we refer to Reef Stars, rubble, and reef site, as their abbreviations, E, NC and PC. Two months post-deployment hard coral cover on all sites was below 50% (25.8, 32.3 and 39.3% for the NC, PC, and E sites) (AM, FN, and EEF, Pers. Comm.).

On October 22, 2020, Mars Sustainable Solutions and partners deployed a set of 87 Reef Stars (the so-called Block A2 with ~29.32 m^2) with attached coral fragments (i.e., corals of opportunity, mainly *Acropora* and *Pocillopora* spp.). Whilst additional Reef Stars installations have been conducted, COVID-19 restrictions meant that our study site could only be first accessed in February 2021 (six months post-installation), and during this time, we took initial imagery data for coral growth. We revisited the study site after a 12-month period (February 2022) to examine the Reef Stars' effects on reef accretion (including hard coral cover, rugosity, carbonate budgets, skeletal properties of key coral taxa, and growth).

Temperature HOBO^{TM} loggers (1-h logging interval) were deployed in February 2021 to track key environmental variance over the 12 months of growth but unfortunately failed after 8 months. Therefore, additional environmental data for the entire 12-month study period were extracted from GIOVANNI online system for satellite-derived data maintained by NASA (https://giovanni.gsfc.nasa.gov/giovanni/). Sea surface temperature (SST) was obtained using monthly area-averaging bounded to 146° 14' 40.9''E, 16°51' 59.0''S (Moore Reef) between the beginning of the monitoring (February 2021) and the end of the experiment (February 2022). SST data from HOBO^{TM} loggers for the reef and MARRS/rubble sites was therefore overlayed onto that derived from Giovanni SST data for Moore Reef (**Fig. S4.3**).

4.2.2 Experimental design

In February 2022, a commonly applied census-based approach was undertaken to characterise benthos and determine the carbonate budget for the E, NC, and PC sites (i.e., restored, negative, and positive control sites; Perry et al., 2012). The Reef Budget methodology is detailed in the section below. In addition, coral fragments (< 5 cm; two coral species, n = 5 each) were collected from the inner side (avoiding cutting eroded fragments from the outer edge) of randomly selected colonies using steel pliers and stored in individual Ziploc bags. Once on board the research vessel, the collected fragments were firstly immersed in freshwater followed by sodium hypochlorite to remove coral tissue for subsequent analysis of skeletal properties of bulk volume, biomineral density, bulk density, pore volume, apparent (internal) porosity, and hardness (Fantazzini et al., 2015; Leggat et al., 2019; Madin et al., 2016b). Data on *Acropora* spp. coral growth was obtained by underwater photographs (Lirman et al., 2014; Siebeck et al., 2006) in February 2021 and 2022 (1-year growth period). The various methods for these attributes are detailed in the following sections.

4.2.3 Coral reef carbonate budgets and benthic characterisation

We developed carbonate budgets using an adapted version of the Reef Budget protocol (Perry et al., 2012), a census-based approach that quantifies cover/abundance of carbonate- ($CaCO_3$) producing (corals and crustose coralline algae (CCA)) and bioeroding taxa (urchins, parrotfish and micro- and macro-endolithic taxa), and combines these data with already published measures of species/genera $CaCO_3$ production and erosion rates to calculate net carbonate budget.

We estimated both gross carbonate production and bioerosion rates, and the resultant net carbonate production (G = kg $CaCO_3\ m^{-2}\ yr^{-1}$) on each site (E, NC, and PC) in February 2022 using 3 x 10 m transects, each separated by 5–10 m, with which to collect all relevant data (except parrotfish data). Along each transect, benthic classes (hard/soft corals, CCA, rubble, other calcareous encrusters, and eroders) were determined following the Reef Budget taxa-specific codes (Appendix A, Reef Budget, Perry et al., 2012). Categories were photographed with an Olympus Stylus TOUGH TG-4 digital camera, and codes were noted on an underwater notebook. Within each meter of the 10 m transect, the distance (cm) covered by each benthic component immediately beneath the transect was measured using a short (~1 m) flexible tape. Sea urchin bioerosion was determined from the abundance and size of bioeroding urchins of the family *Diadematidae* (*Diadema* spp., and *Echinothrix* spp.) and the genera *Echinometra*, *Echinostrephus*, and *Eucidaris*, which was tallied 2 m either side of each 10 m transect (and hence a 40 m^2 belt) (Bak, 1994, 1990). To complement bioerosion rates, we also collected data on fish abundance at each survey site by deploying additional belt transects (30 x 5 m, n = 3 separated by 5–10 m at each site) (Reef Budget, Perry et al., 2012). Initial and developmental phases of parrotfish species were tallied across

nine size classes as assigned based on fish fork length: 8–10 for the juvenile phase, 11– 20, 21–30, 31–40 for the initial phase, and 11–20, 21–30, 31–40, 41–50, and 51–60 for the terminal phase. At site E only, due to the reduced size being 30 m x 20 m, the fish transect was placed in an S-shaped to ensure the surveys were only conducted on that habitat.

Net (total) carbonate production (i.e., the carbonate budget) was estimated as the balance between gross carbonate production and gross bioerosion (see equations).

[Eq. 1] Net carbonate production = gross carbonate production – gross bioerosion

[Eq. 2] Gross carbonate production = hard coral carbonate production + CCA carbonate production

[Eq. 3] Gross bioerosion = macrobioerosion + microbioerosion + urchin bioerosion + parrotfish bioerosion

Within this methodology, carbonate production is driven by hard corals and CCA, whereas macro- and microbioerosion are related to the substrate (dead reef substrate, sponge and CCA cover for macrobioerosion, or rock, sand and seagrass cover for microbioerosion) available for internal bioeroders (e.g., reef-dwelling organisms such as worms, bivalves and sponges) (Rice et al., 2020; Tribollet et al., 2002). External bioeroders, such as parrotfish and urchins, are also major contributors to the bioerosion of the reefs and, together with macro- and microbioerosion, constitute the gross bioerosion.

In February 2022, benthic characterisation was also carried out as part of the Reef Budget protocol (Perry et al., 2012) for each site, and this included metrics such as the benthic cover of major functional categories (hard and soft coral, CCA, sediment producers, macro- and turf algae, rubble, rock, limestone pavement, sand, and others), alongside estimating the rugosity (R; **Equation 4**) which is an index of surface roughness that is a common measure for quantifying landscape structural complexity (i.e., topographic heterogeneity) (McCormick, 1994).

[Eq. 4] R = Contoured distance / Planar distance (OR Contoured area / Planar area)

4.2.4 Coral survival and growth

Since most of the corals seeded on the Reef Stars in October 2020 belong to the genus *Acropora* (> 95%; compared to < 5% for *Pocillopora* spp.; Mars Sustainable Solutions pers. comm.), coral survival and growth was followed on the same *Acropora* fragments (n = 15) for 12 months. Coral fragments were photographed *in situ* using a GoPro Hero 8 digital camera together with a scale reference by SCUBA in February 2021 (T0) and 2022 (T12) on site E. Survival rate as the proportion of all initial coral individuals remaining over time (%) and growth rates for each coral were determined as the change in size (areal and linear extension) over this 12-month period (ΔG; $cm^2\ y^{-1}$ and $cm\ y^{-1}$) and averaged.

4.2.5 Coral sampling and skeletal properties

Two key coral taxa (*Acropora intermedia* and *Pocillopora damicornis*) at Moore Reef (and used to originally seed the Reef Stars) were targeted to study their skeletal properties. Whilst

P. damicornis was present at all sites, *A. intermedia* was not present in the rubble patch (NC) where this site was predominantly covered by dead branching *Acropora* spp. or rubble. Therefore, we collected *Acropora* "rubble" instead (its homolog but in a non-living state). Fragments (< 5 cm in length) of *A. intermedia*, *P. damicornis* and *Acropora* rubble were thus collected (n = 5 each) as follows: *A. intermedia* at the E and PC sites, *P. damicornis* at the E, PC, NC sites, and *Acropora* rubble only from the rubble patch (NC site). See **Table S4.1** for details of the coral collection.

Hardness testing was conducted using a Shore D Hardness Tester (TE-271) calibrated using reference material in accordance with the manufacturer's recommendation (Vander Voort, 1999) as per Leggat et al., (2019) on a coral fragment (< 2 cm) which was previously cleaned and dried. Hardness was consistently determined on the base of the branch for all fragments, with 10 measurements performed for each. In addition, the buoyant method applied for corals (adapted from Bucher et al., 1998; Jokiel et al., 1978), combined with the Archimedes principles, were used to test bulk volume, biomineral density, bulk density, pore volume, and apparent (internal) porosity on a second coral sample (< 2 cm) (Fantazzini et al., 2015). Briefly, the fragment was previously weighed to obtain the dry weight (DW; g) before being inserted in a glass vessel in a 50 °C water bath for two h under vacuum. The glass vessel was filled with Mili-Q to obtain the saturated weight (SW; g) of the coral, followed by the measurement of the buoyant weight (BW; g). Skeletal properties were extracted using the previous measurements and the density of water (ρH_2O) at 20 °C (0.9982 g cm^{-3}) as per the following equations:

[Eq. 5] $V_A = (m_s - m)/\rho H_2O$; the pore volume connected to the external surface (V_A)

[Eq. 6] $V_B = (m_s - m_h)/ \rho H_2O$; the total volume occupied by the coral skeleton (called bulk volume)

[Eq. 7] $P_A = V_A/V_B = (m_s - m)/(m_s - m_h)$; the apparent porosity (or effective or connected porosity, P_A) (ratio of the pore volume connected to the external surface (V_A) to V_B)

[Eq. 8] $d_b = m/V_B$; the bulk density (ratio of the mass to V_B)

[Eq. 9] $d_r = m/(V_B - V_A)$; the biomineral density (ratio of the biomineral mass to biomineral volume, excluding pore volume connected to the external surface, also called real density or micro-density)

4.2.6 Statistical analysis

Data analyses were performed using Rstudio (version 1.4.1717) and GraphPad Prism (version 9.1.2). Assumptions of normality were assessed visually via QQ plots and a Shapiro-Wilk's test, and equal variances were assessed using Brown-Forsythe test (Shapiro and Wilk, 1965). Significance was set at $p < 0.05$ (for all tests), and the mean ± the standard error of the mean (SEM) was reported unless expressly noted. A series of analysis of variance (ANOVA) (or its non-parametric homolog, Kruskal-Wallis tests) with *post hoc* tests (Tukey or Dunn) were undertaken to compare each coral class (*A. intermedia*, *P. damicornis* and *Acropora* rubble) across sites (E, NC, and PC) for the skeletal traits, as well as comparing wild *A. intermedia* and *P. damicornis* fragments (from the PC site — the nearby healthy-looking-reef —) to observe potential natural interspecific differences.

4.3 Results

4.3.1 Benthic cover and rugosity

Three well-differentiated sites were studied on Moore Reef, (i) a stabilised substrate area using the MARRS Reef Stars (Experimental, "E"), and two nearby sites of (ii) a coral rubble substrate where no Reef Stars were installed (negative control, "NC"), and (iii) a non-intervened healthy-looking representative neighbouring reef zone with high coral cover and diversity (positive control, "PC"). All sites contained variations in substrate type including rubble cover, live and dead coral cover, primary or major secondary carbonate producers (i.e., corals, and CCA), and coral morphology. In February 2022, the benthic cover of major functional categories (e.g., hard and soft coral, crustose coralline algae (CCA), turf, rubble, limestone pavement; **Fig. S4.4**) was estimated (Reef Budget, Perry et al., 2012). Relatively high hard and soft coral cover (47.5 ± 3.8 and 22.5 ± 4.0 %, n = 3 each) alongside turf algae mats (25.1 ± 7.2 %, n = 3) were observed in the non-intervened reef site (PC). The non-restored impacted site (NC) was characterised by an open framework of rubble (84.7 ± 2.5 %, n = 3) and low hard coral cover (14.9 ± 2.4 %, n = 3). In contrast to both control sites, the MARRS restored site (E) had a high hard coral cover of 98.0 ± 2.0 % (n = 3), where the initial rubble patch became negligible (2.0 ± 2.0 %, n = 3) after 16 months of Reef Stars installation (**Fig. 4.3A**). High coral cover present in the site E consisted mainly of *Acropora* spp. (95.5 ± 3.9 %, n = 3) (in descending order, branching (47.7 ± 23.9 %, n = 3), corymbose/digitate (37.8 ± 30.5 %, n = 3), tabular (5.1 ± 3.2 %, n = 3), and hispidiose/arborescent (4.9 ± 3.2 %, n = 3) growth forms). Coral diversity was also dominated by *Acropora* spp. on the site PC (64.7 ± 11.9 %, n = 3), where 37.7 ± 0.8 % (n = 3) were corymbose/digitate, followed by 25.5 ± 12.8 % (n = 3) hispidiose/arborescent, tabular (1.2 ± 1.2 %, n = 3) and branching (0.3 ± 0.3 %, n = 3) morphologies. The low hard coral cover present at the site NC consisted of 11.8 ± 1.9 % *Acropora* spp., where 6.7 ± 0.4, 4.5 ±

2.3, and 0.6 ± 0.6 (n = 3 each) corresponded to hispidiose/arborescent, corymbose/digitate, and branching morphologies, respectively.

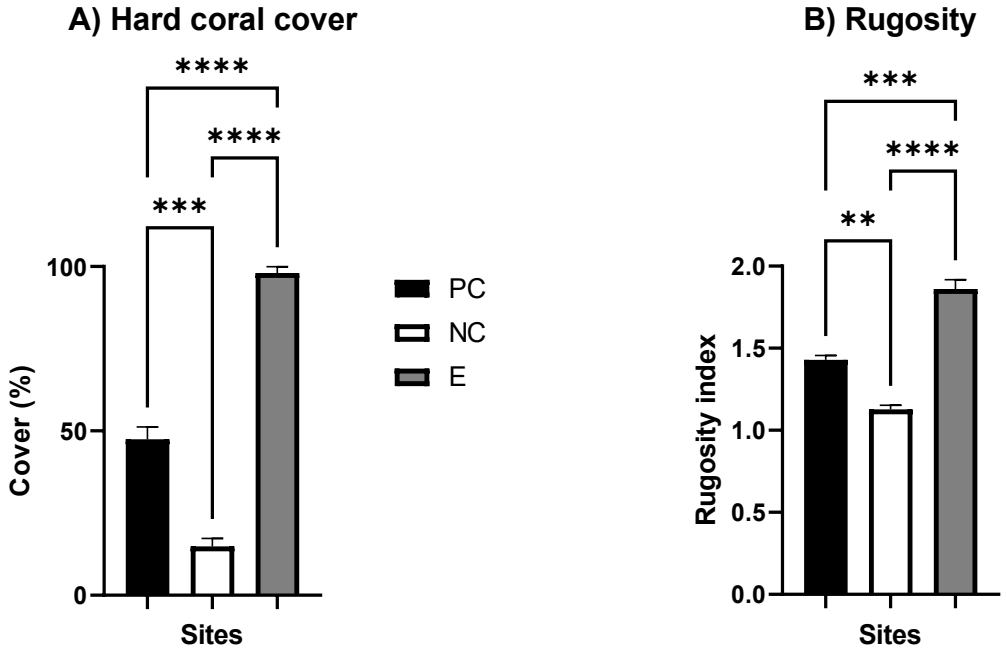

Figure 4.3 Average hard coral cover and rugosity. (A) Hard coral cover (%) and (B) rugosity index were estimated following the Reef Budget methodology (Perry et al., 2012) at the three studied sites, (i) Reef Stars (Experimental, 'E'), (ii) a rubble patch (negative control, 'NC'), and (iii) a non-intervened healthy-looking representative neighbouring reef zone (positive control, 'PC') in February 2022 (16 months post-deployment of the Reef Stars). Means (n = 3 per reef site) (± SEM; standard error of the mean) were compared by analysis of variance (ANOVA) with *post hoc* Tukey tests (see main text) where **, ***, and **** indicate $p \leq 0.01$, 0.001, and 0.0001, respectively.

Rugosity (dimensionless) was higher at the Reef Stars restored site (E) compared to the two control sites (PC and NC). In increasing order, the rugosity index was as follows: 1.13 ± 0.03, 1.43 ± 0.03, and 1.86 ± 0.06 for sites NC, PC, and E, respectively (**Fig. 4.3B**; one-way ANOVA, $F_{(2,6)} = 0.5$, $p < 0.0001$; Tukey's test PC-NC, PC-E, and NC-E, p = 0.0039, 0.0006, and < 0.0001, respectively).

4.3.2 Survivorship and growth

Acropora spp. survivorship after 12 months was 100% ± 0.0 at the Reef Stars (E; n = 15) alongside a moderate (close to 50%) relative areal growth rate (ΔG_A; % growth in cm^2 y^{-1}) over 12 months (43.9 ± 19.3) (**Fig. S4.5A**). This outcome was also observed in the relative increase in area covered by coral tissue (%), i.e., final areal size / initial starting size x 100 (143.9 ± 19.3). However, the observed relative linear growth rate (ΔG_L; % growth in cm y^{-1}) appeared to be < 50% (27.5 ± 11.0) for this 12-month period. Of the 15 fragments examined, the highest areal growth rates were consistently observed for fragment #9 (from 27.6 to 78.6 cm^2 in the same period; see example in **Fig. S4.5B-C**).

4.3.3 Net carbonate production

Calculating net (total) carbonate production (i.e., the carbonate budget, G; kg $CaCO_3$ m^{-2} yr^{-1}, **Fig. 4.4A)** using the Reef Budget census-based approach in February 2022, was estimated as the balance between gross carbonate production and gross bioerosion. Net carbonate production rates were significantly higher on reef site E compared to NC and PC sites. The unstabilised rubble patch (NC) was in a net negative carbonate budget state (-3.7 ± 1.8), and hence carbonate production processes for this area were highly susceptible to bioerosion processes. The same site, but that underwent a restoration intervention using the Reef Stars (E), exhibited much higher net carbonate production (25.3 ± 1.0), a rate that was also higher than the nearby natural coral reef, which had a net carbonate budget of 4.3 ± 3.4.

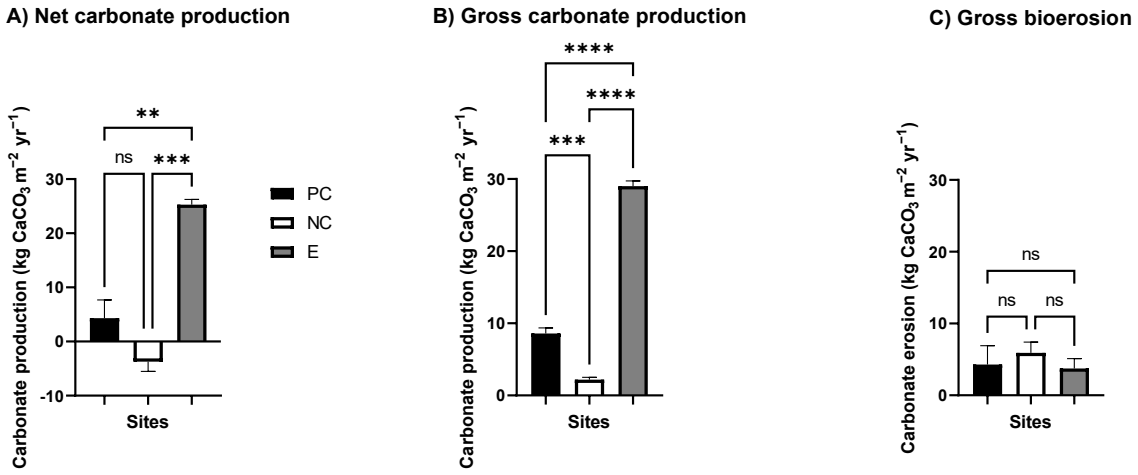

Figure 4.4 Average (A) net and (B) gross carbonate production, and (C) gross bioerosion expressed in kg $CaCO_3$ m^{-2} yr^{-1} (following the Reef Budget methodology, Perry et al., 2012) across Moore Reef studied sites, (i) Reef Stars (Experimental site, 'E'), (ii) the negative control 'NC' constituted of unconsolidated coral rubble substrate, and (iii) the positive control 'PC' represented by a natural healthy-looking neighbouring reef area, in February 2022 (16 months post-installation of the Reef Stars). Means (n = 3 per site) were compared by analysis of variance (ANOVA) with *post hoc* Tukey tests (see main text) where ns indicates no statistical significance, and **, ***, and **** indicate $p \leq 0.01$, 0.001, and 0.0001, respectively.

4.3.4 Gross carbonate production

Higher gross carbonate production (G; kg $CaCO_3$ m^{-2} yr^{-1}) was evident for the site E (29.0 ± 0.7), followed by the PC (8.6 ± 0.8) and NC (2.2 ± 0.3) sites. Carbonate production of the Reef Stars restored site (E) was 3.4 and 13.2 times higher than PC and NC sites, respectively, after 16 months post-deployment. This contrast was revealed as significant differences in gross carbonate production among sites (one-way ANOVA, $F_{(2,6)} = 488.4$, $p < 0.0001$; Tukey's test PC-NC, PC-E, and NC-E, $p = 0.0009$, < 0.0001, and < 0.0001, respectively; **Fig. 4.4B**). Thus, even in the absence of bio-erosion, carbonate production remained much lower for the two control sites than compared to the Reef Star site, presumably reflecting the different extent of coral cover/diversity amongst the sites.

4.3.5 Gross bioerosion

Bioerosion processes encompassed internal (micro- and macro-bioerosion) and external bioeroders (urchin and parrotfish bioerosion) (G; kg $CaCO_3$ m^{-2} yr^{-1}). In general, micro- and macro-borer erosion when combined was similar for all sites at ~0.5 (**Fig. S4.6A**) (one-way ANOVA, $F_{(2,6)}$ = 1.1, p = 0.4046). However, when considered individually, significant differences were evident for both erosion categories between sites (macrobioerosion, one-way ANOVA, $F_{(2,6)}$ = 46.1, p = 0.0002; Tukey's test PC-NC, PC-E, and NC-E, p = 0.0028, 0.0227, and 0.0002, respectively, and microbioerosion, one-way ANOVA, $F_{(2,6)}$ = 88.0, p < 0.0001; Tukey's test PC-NC, PC-E, and NC-E, p = 0.0039, 0.0006, and < 0.0001, respectively; **Fig. S4.6B-C**). The Reef Star site (E) showed the highest microbioeroding rates (0.4877 ± 0.0149), followed by PC and NC sites (0.3744 ± 0.0071 and 0.2952 ± 0.0068, respectively). In contrast, higher macrobioerosion rates were found at the rubble site NC (0.2001 ± 0.0086), followed by negligible levels on sites PC and E (0.0833 ± 0.0217 and 0.0082 ± 0.0081, respectively).

Urchins were not observed across sites during the daytime surveys (0.0 individual/m^2), and hence did not contribute to our gross bioerosion rates. The contribution of parrotfish to bioerosion was similar across sites and estimated, in ascending order, at 3.2 ± 1.3, 3.8 ± 2.6, and 5.4 ± 1.5 for the sites E, PC, and NC, respectively (one-way ANOVA, $F_{(2,6)}$ = 0.3, p = 0.7202; **Fig. S4.6D**). Lastly, an overall gross bioerosion rate (the sum of parrotfish, urchin, macro- and microbioerosion rates, G; kg $CaCO_3$ m^{-2} yr^{-}) was calculated to be 3.7 ± 1.4, 4.3 ± 2.6, and 5.9 ± 1.5 for E, PC, and NC, respectively. Despite the slightly higher gross bioerosion rates at NC, no significant differences were found among sites (one-way ANOVA, $F_{(2,6)}$ = 0.3, p = 0.7223; **Fig. 4.4C**).

4.3.6 Skeletal properties

Skeletal traits (bulk volume, bulk density, biomineral density, pore volume, and apparent (internal) porosity) for both *A. intermedia* (living and non-living forms) and *P. damicornis* were generally consistent across the three experimental sites (**Fig. 4.5A-E**). The exception was hardness (HD) (one-way ANOVA, $F_{(5,24)} = 14.8$, $p < 0.0001$). Fragments of *P. damicornis* had the lowest HD at the E site, where they were on the Reef Stars (36.3 ± 1.1) compared to those inhabiting the reef at the PC and NC sites (50.3 ± 1.4 and 44.1 ± 0.8; Tukey's test PC-NC, PC-E, and NC-E, p = 0.0297, < 0.0001, and 0.0041, respectively; **Fig. 4.5F**). Furthermore, the dead *Acropora* spp. rubble showed the lowest hardness (35.9 ± 2.4) compared to the alive *A. intermedia* fragments on the PC and E sites (42.0 ± 1.4 and 42.3 ± 0.7; Tukey's test PC-NC and NC-E, p = 0.0342, and 0.0223, respectively). Differences in pore volume (cm^3) and apparent (internal) porosity (%) among wild *A. intermedia* and *P. damicornis* from the natural-healthy looking reef (PC) were also observed (0.8 ± 0.1 vs 0.4 ± 0.0, and 80.2 ± 7.3 vs 31.9 ± 1.8, for *A. intermedia* vs *P. damicornis*, respectively; Tukey's test, p = 0.0016 and 0.0099) alongside differences in HD (42.0 ± 1.4 vs 50.3 ± 1.4, respectively; Tukey's test, p = 0.0021). Thus, overall, the Reef Stars did not appear to have an impact on coral skeletal properties examined, except for *P. damicornis* where HD was lowered.

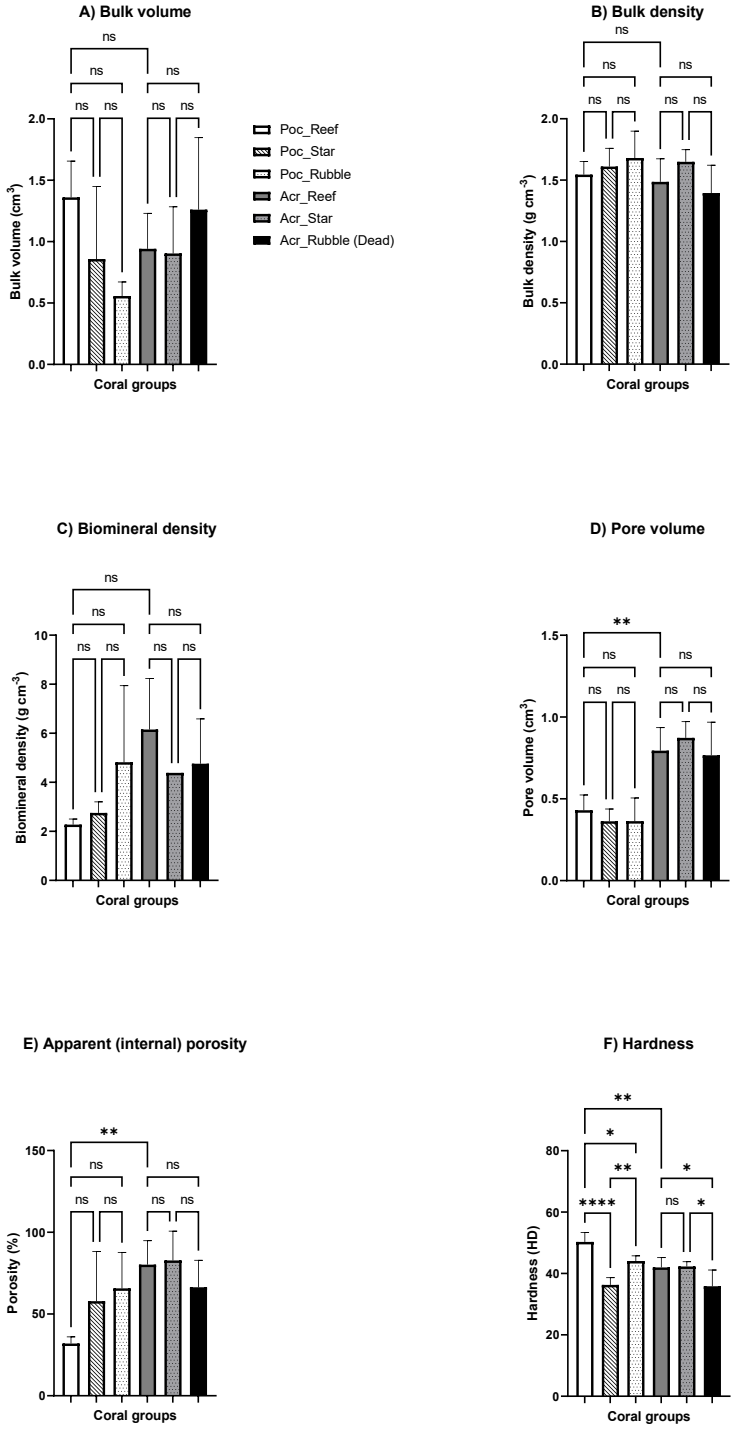

Figure 4.5 Mean (± SEM) skeletal (A) bulk volume (cm^3), (B) bulk density (g cm^{-3}), (C) biomineral density (g cm^{-3}), (D) pore volume (cm^3), (E) apparent (internal) porosity (%), and (F) hardness (HD) of three dominant coral classes (*Acropora intermedia*, *Acropora* rubble, and *Pocillopora damicornis*) across sites: E, NC, and PC). All data are fragments (n = 5 for each group). Means (n = 3 per reef site) were compared by one-way analysis of variance (ANOVA) with *post hoc* Tukey tests (see main text) where ns indicates no statistical significance, and *, **, and **** indicate $p \leq 0.05$, $p \leq 0.01$, and $p \leq 0.0001$.

4.4 Discussion

Reef stabilisation approaches are becoming increasingly popular as means to aid reef recovery where reef structure has become unconsolidated (e.g., Ceccarelli et al., 2020); however, how these approaches potentially enhance carbonate budgets and the means for reefs to enhance accretion rates remains untested. Our results using Reef Stars provide new evidence that such practices can increase carbonate budgets, from our example of a degraded mid-shelf patch reef on the central Great Barrier Reef (GBR), in turn, highlighting the importance of carbonate budgets as a metric to evaluate coral restoration success. In doing so, we also present new estimates for carbonate budgets for representative Australian reef environments.

Carbonate budgets (G = kg $CaCO_3$ m^{-2} yr^{-1}) we observed for the representative "healthy" control reef site (PC; 4.3 ± 3.4) were similar to values reported across the Indian Ocean (3.7; Perry et al., 2018) but surprisingly lower than turbid reefs on the central GBR (6.9-12.3 for Middle Reef and Paluma Shoals, respectively, Browne et al., 2013) and higher than for Western Australia (2.5 for Ningaloo Reef; Perry et al., 2018). All of these Australian reefs (including our studied reef) are characterised by similar gross carbonate production and hard coral cover but different coral community structure at the time of the study (Browne et al., 2013; Perry et al., 2018). However, gross bioerosion rates (mainly driven by parrotfish eroding activity), were doubled in Moore Reef compared to the two turbid reef zones (4.3 vs 1.51-1.62), which seems to explain the lower carbonate budget observed in our studied reef site. Whilst values for the carbonate production in Ningaloo Reef are considered amongst the highest contemporary budgets for the Indian Ocean (alongside those from Mozambique, Perry et al., 2018), they are lower than our study sites (and accompanied by ~3 times lower

bioerosion rates). However, this lower bioerosion for Ningaloo may reflect that the sites examined were deeper (8 m) compared to ours (3-5 m) and the associated coral community composition and associated fauna.

At the restored site (E), the highly concentrated (e.g., 15 coral fragments per Reef Star, and so ~750 corals in 600 m^2) deployment of typically fast-growing (e.g., branching *Acropora* spp.) corals resulted in a very high net carbonate budget (25.3 ± 1.0), and ~6 times higher than the carbonate budget of our representative "healthy" control site (PC; 4.3 ± 3.4). By including the NC rubble site within our experimental design, we demonstrated that without intervention, the rubble site — which is still evident post Cyclone Yasi 2011 — is in a state of net erosion (a net negative carbonate budget; -3.7 ± 1.8). Furthermore, rugosity, which is an important metric to describe reef habitat complexity (i.e., the structural changes that reefs undergo from coral renewal and mortality and balance between rates of carbonate bioerosion and production; Alvarez-Filip et al., 2009), was half that of the restored site (E). While our study only assesses the first 16 months of deployment, our data demonstrate that restoration structures, such as the MARRS Reef Stars, can positively enhance not only carbonate budgets and structural complexity (and the services they support, such as wave energy dissipation and habitat provision; Alvarez-Filip et al., 2011; Ferrario et al., 2014) on local reef sites but boost coral reef recovery that is often very low on rubble areas (Fox et al., 2019; Johns et al., 2018; Kenyon et al., 2020; Viehman et al., 2018). In the case of the NC site in our study, 11 years after Cyclone Yasi hit Moore Reef, the recovery trajectory of this unconsolidated reef patch (as seen by the number of small colonies and recruits on the rubble, and derived low carbonate production, 2.2 ± 0.3) cannot cope with the gross bioerosion processes (e.g., parrotfish erosion activity is intensified on the remaining/new small colonies; Huertas et al., 2021) or natural mortality of the corals when rubble moves (Kenyon et al., 2023). This

situation highlights that the balance in carbonate production versus loss will inevitably undermine the ecosystem services the reef structure provides (Pratchett et al., 2021) on Moore Reef unless a restoration intervention such as MARRS Reef Stars is taken place. To note that our study focused on a degraded reef originated by a cyclone, but there are more risks to coral calcification, and thus reef accretion, in the Anthropocene, including ocean acidification (Hoegh-Guldberg et al., 2017) and increased potential substrate loss post coral bleaching (Leggat et al., 2019). Thus, efforts to restore reefs and sustain $CaCO_3$ production are important to be considered in restoration programs (Hughes et al., 2023).

An important consideration for restoration activities is the selection of coral species. As observed for natural reef recovery (Lange and Perry, 2019), the community composition used in restoration will clearly influence the carbonate budget, rugosity and, ultimately, ecosystem service provision. Currently, the restored Moore Reef site use disproportionate fast-growing *Acropora* species that provide a high carbonate production and rugosity, but the lack of other coral growth forms could potentially come with other functional costs (e.g., Madin et al., 2023). For example, acroporids have been observed to be generally less heat-tolerant than both massive and encrusting growth forms (e.g., *Porites* spp., the non-scleractinian *Heliopora* spp., *Leptastrea* spp.) during past bleaching events (Carroll et al., 2016; Loya et al., 2001; Marshall and Baird, 2000; McClanahan et al., 2002; Pratchett et al., 2013). However, restoring with slower growing (and architecturally less complex) taxa is likely less beneficial for sites in need of fast recovery in terms of carbonate budgets (e.g., Tortolero-Langarica et al., 2019) and sustaining biodiversity (Lirman et al., 2010; Nithyanandan et al., 2018; Tiddy et al., 2021; Xin et al., 2016), but also where *Acropora* spp. were preferentially lost during recent bleaching of the GBR (Hoogenboom et al., 2017). Including heat-resistant variants of coral species may still come at a cost to growth (Cornwell et al., 2021) within the restoration

strategy but could potentially confer reef resilience and maintain reef framework while allowing the more susceptible coral species to recover as well as still providing (modified but not lost) services such as coastal protection and fish productivity (e.g., Tortolero-Langarica et al., 2019). Moreover, rugosity as a proxy for reef habitat complexity can increase fish diversity (Santoso et al., 2022) but not necessarily cryptofauna. Several studies have highlighted enhanced invertebrate density and diversity in coral rubble compared to sites with high live coral cover (Enochs et al., 2011; Fraser et al., 2021; Nelson et al., 2016; Stella et al., 2022; Wolfe et al., 2023). Therefore, restorative interventions through structures that support ecological communities (e.g., Reef Stars) should match the niche of target species, and this also includes the micro-habitat for reef-associated organisms (besides macro-habitat for coral species), thus, promoting habitat heterogeneity to enhance reef biodiversity and ecological functions (Bishop et al., 2022).

Another factor that may ultimately drive the enhanced carbonate budgets observed for the Reef Stars is presumably the size of material used for restoration. When a sexually mature coral colony is fragmented below a certain size, resources are directed towards regrowth instead of reproduction (Lirman, 2000; Zakai et al., 2000). As such, the size and life stage (age) of corals used for restoration will inevitably impact the carbonate budgets retrieved as freshly fragmented coral show higher growth/regeneration (i.e., following trauma, corals undergo rapid tissue and skeletal repair; Bak, 1983; Chadwick and Loya, 1990; Loya, 1976; Meesters et al., 1994) than well-established adult coral colonies, which above a size threshold, shift resources from growth to sexual reproduction (Babcock, 1991; Kojis and Quinn, 2001; Soong, 1993). Larger coral size classes will further exercise more inter- and intraspecific competition for resources (e.g., space, food, light), thus limiting potential coral growth and survival (Box and Mumby, 2007; Evensen et al., 2015).

Most structural property traits examined in our study were not compromised within the experimental restored setting (E) for either *A. intermedia* or *P. damicornis*, yet a reduction in hardness for *P. damicornis* was detected when they were on the Reef Stars (E). Whilst the cause of the reduced hardness cannot be ascertained from our current data set, it potentially indicates a trade-off in resource acquisition and partitioning towards mineral deposition from an altered resource landscape on the Reef Stars (E). For example, calcium carbonate dissolution (not measured with the used Reef Budget methodology) reduces coral skeletal hardness and density after a marine heatwave event (Leggat et al., 2019) and varies according to reef environmental conditions (inshore vs offshore reefs, Aline, 2008). Coral restoration efforts in the Caribbean have also shown reduced coral skeletal density (while calcification rate was conserved and growth was enhanced) attributed to the grow-out method used (thus nursery environment) (Kuffner et al., 2017). Taken together, this evidence would suggest that species-specific trade-offs in physiological properties require measurements of success to include structural properties to robustly resolve whether ecosystem service value (e.g., reef accretionary potential) will be retained. Importantly, hardness was lower in *Acropora* spp. rubble compared to its living form (*A. intermedia*). New coral rubble (dead coral) is known to be very breakable (Davies and Hutchings, 1983; Greenstein and Pandolfi, 2003; Scoffin, 1992), and hardness increases when crustose coralline algae (CCA) colonises the surface of the dead coral fragment. As such, 11 years post-cyclone, CCA colonisation on the coral rubble may still be in progress, again highlighting the importance of restoration interventions on reef sites with poor recovery trajectory.

Macroerosion was expected to be low in the restored site (E) because of the lack of substrate susceptible to being eroded compared to the rubble patch (NC). Our study showed that macrobioerosion was lower at the restored site (E; contrary to microbioerosion, which was

higher) (0.0082 ± 0.0081 and 0.4877 ± 0.0149, respectively), but combined rates and parrotfish erosion rates (and hence gross bioerosion rates) were similar across reef sites suggesting that bioeroders did not drive differences amongst net carbonate budgets we observed. However, our results should be taken with caution as eroding activity has been observed to be intensified on the scarce new small coral colonies due to a lack of larger coral size classes (Huertas et al., 2021). Despite parrotfish bioerosion being similar across sites, the unique coral composition of each reef site is intimately related to unique fish assemblages (Chong-Seng et al., 2012), which will have different effects on the reef community. Also note that the lack of urchins during our daytime census might not fully resolve erosion rates since urchins are more active at night (Young and Bellwood, 2011).

The census-based approach of the Reef Budget methodology (i.e., calculated from biota cover/abundance and taxa- or species-specific rates of growth/erosion) employed in our study is a frequent and globally used method to determine coral reefs carbonate budgets, and hence a useful means to inter-compare observations. Yet the methodology has assumptions that are acknowledged (e.g., potential error from using abundance snapshots, unconsidered lithification or dissolution processes, and limited spatial scale and depth; Lange et al., 2020). In the case of census-based net carbonate budgets (i.e., gross carbonate production – gross bioerosion) and chemistry-based net calcifications (i.e., balance between calcification and calcium carbonate dissolution), they quantify different processes at different spatial and temporal scales. Several studies have highlighted the significance of calcium carbonate dissolution within the reef framework and sediments in driving shifts in reef communities (Andersson et al., 2009; Cyronak et al., 2013; Tribble et al., 1990). Hence, coupling biogeochemical monitoring of coral reef state variables such as analysing the unique stoichiometry of elements (the so-called “elementome”; Grima et al., 2022; Peñuelas et al.,

2019) or through chemistry-based net calcification (Broecker and Takahashi, 1966; Chisholm and Gattuso, 1991; Smith and Key, 1975) is highly recommended to improve census based assumptions (Courtney et al., 2022).

Despite not having a tailor-made Reef Budget methodology for the GBR, the approach can (i) determine the relative contribution of different carbonate producers/eroders, (ii) allow spatial comparisons of different reef environments, and (iii) support other indices of reef functionality (e.g., rugosity) as has been successfully demonstrated at sites around the world (Courtney et al., 2022; Perry et al., 2018), and here for the first time in a restoration setting on the GBR. As such, within the context of reef restoration, and despite the need to tailor the methodology, there is clearly a benefit in expanding "best practice" to optimise return-on-effort by integrating this method into restoration guides so practitioners can consider carbonate assessments from the onset of their restorative interventions.

In 2019, the United Nations Environment Assembly adopted Resolution 4/13 on sustainable coral reefs management, requesting the United Nations Environment Programme (UNEP) and the International Coral Reef Initiative (ICRI) to better define best practices for coral restoration for the maintenance of ecosystem goods and services. However, reporting of success has primarily focused on a few metrics (e.g., coral growth and survival — see Suggett et al., 2019) rather than metrics related to ecosystem function and health (Boström-Einarsson et al., 2020; Hein et al., 2017; Nuñez Lendo et al., 2023, **Chapter 2**), making it difficult to assess the success of restorative interventions in maintaining or restoring desirable ecosystem service value. Therefore, understanding the carbonate budget of both natural and restored reefs will become increasingly important as they continue to experience

environmental stress (e.g., tropical cyclones/hurricanes and changes in sea-surface temperature; Done, 1992; Glynn, 1984) in order to evaluate their capacity to provide essential ecosystem goods and services (e.g., coastal protection and fish nursery areas).

4.5 Conclusion

In conclusion, our finding highlights the relevance of using more goal-oriented metrics (e.g., carbonate budgets, rugosity, and skeletal properties) to evaluate restoration success depending on the desired returned ecosystem service (e.g., coastal protection and habitat provision). In doing this, we can assess if a restoration intervention is maintaining or restoring reef functioning and associated ecosystem services, which is the ultimate goal of restoration, and optimised return-on-effort.

4.6 Acknowledgements

We wish to thank the past, present, and emerging Gadigal of the Eora Nation, Yidinji, Gunggandji, Yirrganydji, and Kuku Yalanji Traditional Owners of the land and sea country where our research took place. Also, to the partners Mars Sustainable Solutions, James Cook University, Yirrganydji Land and Sea Country Rangers, Biopixel, and Citizens of the GBR, who participated alongside the main project managers Reef Magic and GBR Biology to install the initial set of Reef Stars on Moore Reef. A special thanks to the dive masters Penny McCracken (faculty technical staff) who supervised my diving work and safety, Daniela Berenice Martínez Leon from Wavelength Reef Cruises who accompanied me during the February 2021 fieldwork; and representing Reef Magic and GBR Biology, Tessa Concannon and Justin Bovery-Spencer who ensured my diving safety during February 2022; and Caitlin Younis who helped me to contextualise my results with Moore Reef trajectory and characteristics. This research was supported by an International Research Scholarship (IRS) and UTS President's Scholarship (UTSP) to CINL. The contribution of EFC was supported by an Australian Research Council Discovery Early Career Research Award (DE190100142). Access to sites and coral material, as well as contributions of DJS, EFC, CB, AM, FN and EEF to writing and manuscript preparation, was facilitated through funding to the Coral Nurture Program from the Australian & Queensland Governments “Solving the bottleneck of reef rehabilitation through boosting coral abundance: Miniaturising and mechanising coral out-planting” in 2020; and the partnership between the Australian Government’s Reef Trust and the Great Barrier Reef Foundation in 2021; also, the many in-kind contributions from Reef Magic and GBR Biology crew who have tirelessly supported the work at Moore Reef since 2020. The Moore Reef MARSS installation and all coral material were collected under permits G20/42902.1 (2020) and G21/45224.1 (2021), respectively, from the Great Barrier Reef Marine Park Authority.

4.7 Supplementary Material

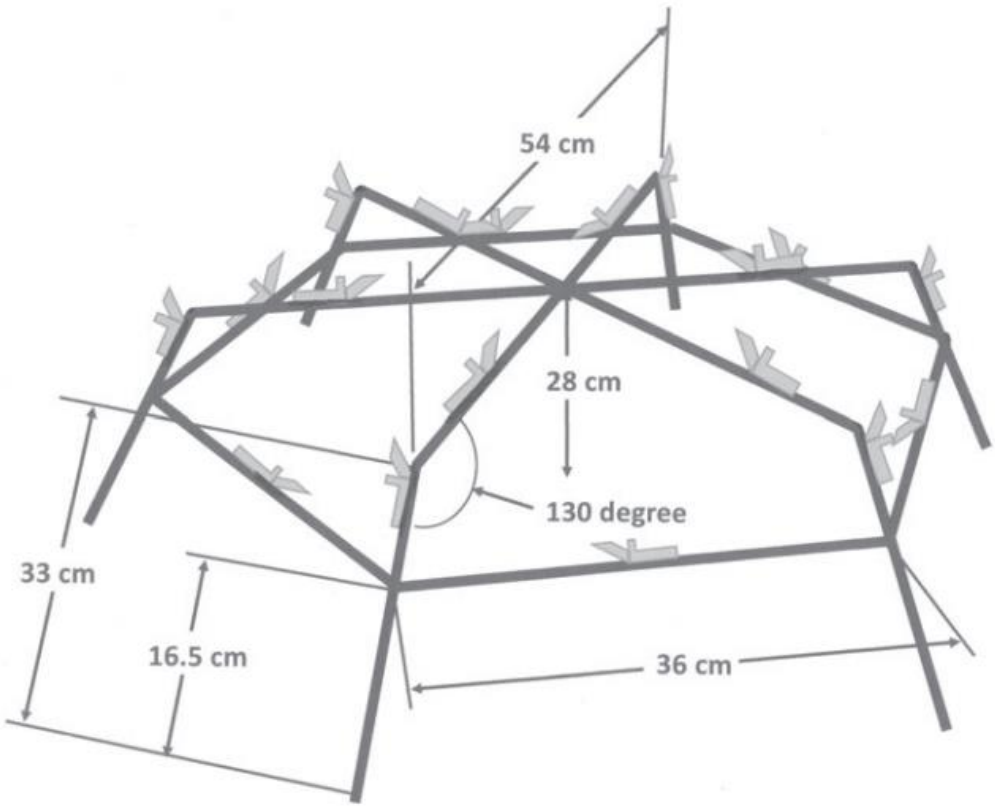

Figure S4.1 Diagram of a Mars Assisted Reef Restoration System (MARRS) Reef Star. The Reef Stars are hexagonal-shaped structures made of reinforcing steel rod and rust-protected with a double coating (first fibreglass resin and then coarse beach sand or limestone). The perimeter of the Reef Star's hexagon is 216 cm, covering an area of 0.337 m^2. The Reef Star is elevated by six 'legs' (each 15.6 cm), and the highest point above the reef substrate is 28 cm (in the middle of the Reef Star). Extracted from Williams et al., (2019).

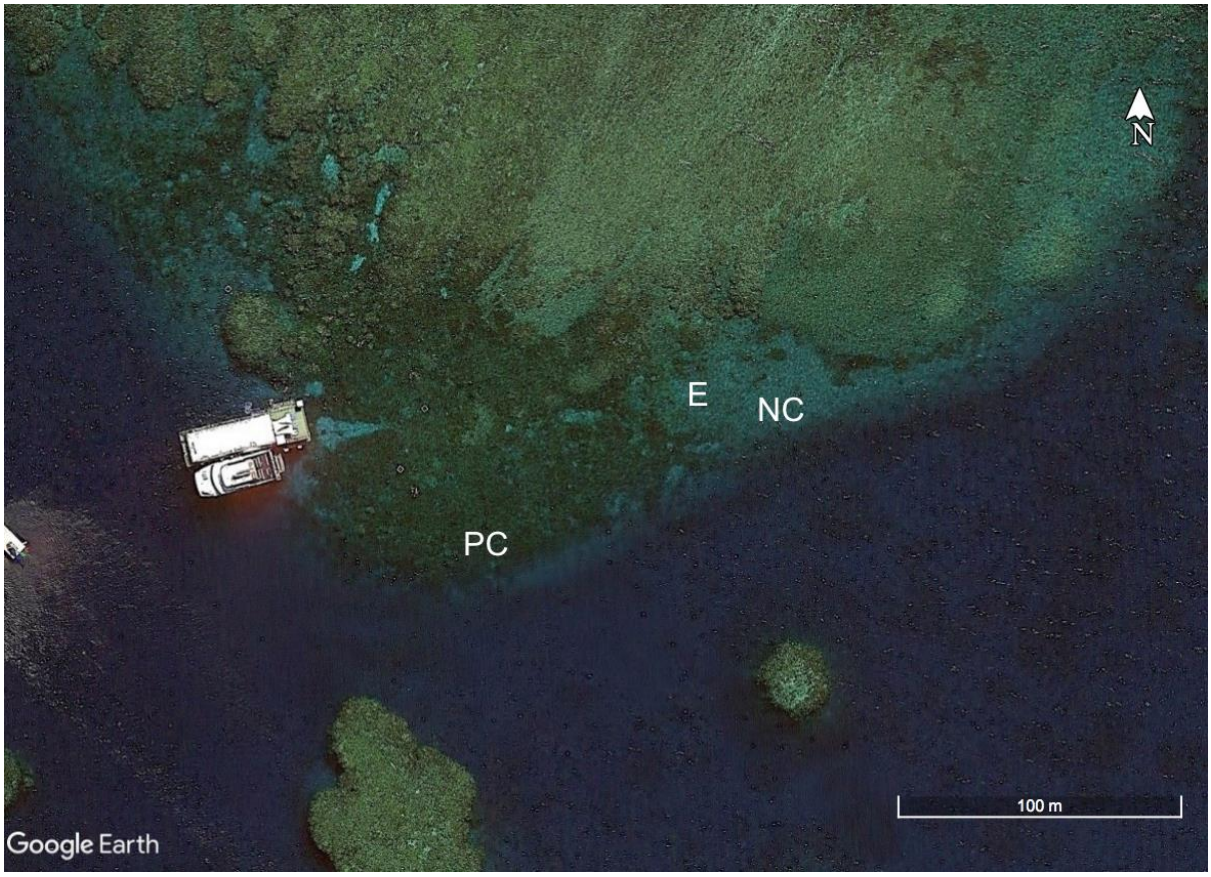

Figure S4.2 Map of MARRS study site on Moore Reef, Great Barrier Reef, Australia. The location (~ 2,000 m^2) targeted for restoration is an area divided into three zones (30 x 20 m), and each site is marked with star pickets at the corners, which correspond to a stabilised substrate section using the MARRS Reef Stars (Experimental, E). Two nearby sites, a rubble patch where no Reef Stars were deployed and that act as a negative control (NC), and a non-intervened healthy-looking neighbouring reef area that has not been influenced by cyclones and possesses high coral cover and diversity (positive control, PC). Extracted from the Operational Procedure for Reef Star installation, maintenance and monitoring (GBR Biology, 2021).

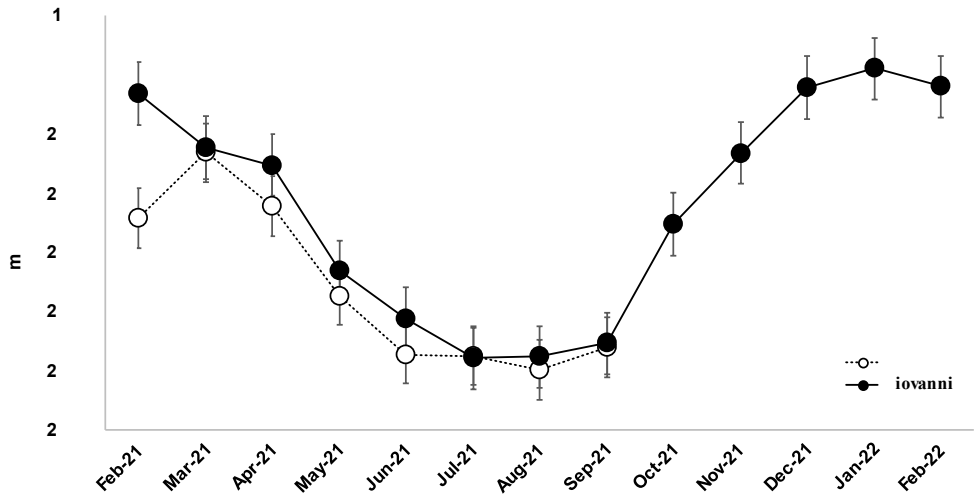

Figure S4.3 Sea Surface Temperatures (SST, °C) for Moore Reef (mean ± SEM; standard error of the mean, n = 13 and 8 months, respectively). Satellite-derived data (MODIS-aqua) was extracted from the GIOVANNI online system maintained by NASA (https://giovanni.gsfc.nasa.gov/giovanni/). SST were obtained using monthly area-averaging bounded to 146° 14' 40.9''E, 16°51' 59.0''S between February 2021 (Reef Stars' first monitoring) and February 2022 (16 months post-deployment of the Reef Stars), encompassing the entire Moore Reef of ca. 30 km^2 for a year; black line. Imposed onto the SST are the mean monthly SST recorded by the HOBO logger (every 1 h) from February 2021 to February 2022 at the Moore Reef; dashed line.

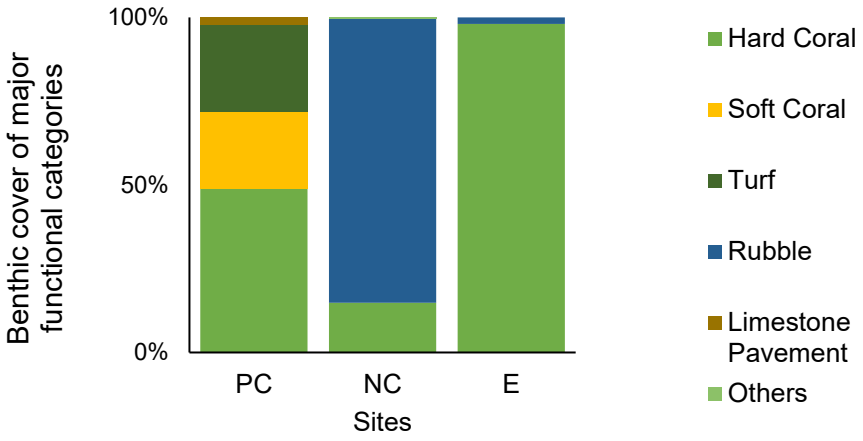

Figure S4.4 Average benthic cover (%). Benthic cover of major functional categories, including hard coral, crustose coralline algae (CCA), sediment producers, soft corals, macroalgae, turf, rubble, rock, limestone pavement, sand, and others, was estimated following the Reef Budget (Perry et al., 2012) at the three studied sites, (i) Reef Stars (Experimental, 'E'), (ii) a rubble patch (negative control, 'NC'), and (iii) a non-intervened healthy-looking representative neighbouring reef zone (positive control, 'PC') in February 2022 (16 months post-deployment of the Reef Stars).

A)

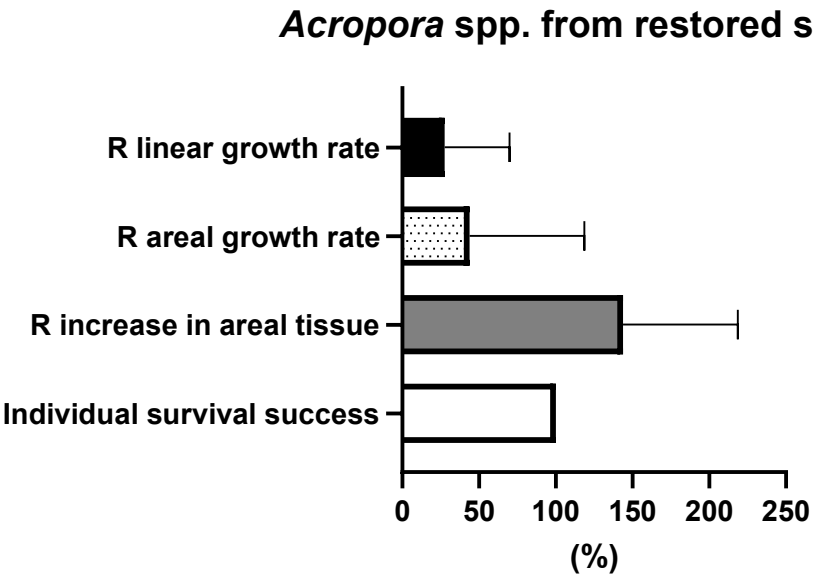

B) **C)**

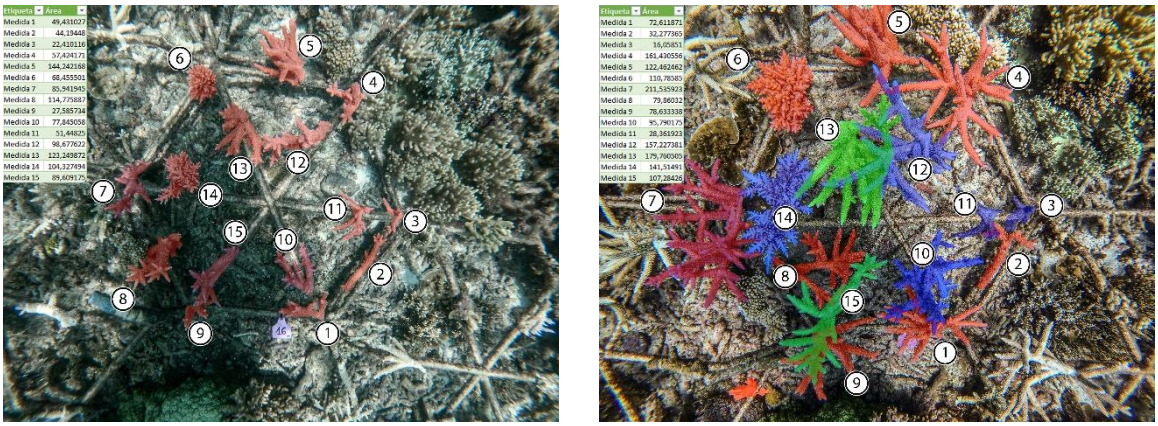

Figure S4.5 Mean (± SEM) (A) survivorship (%), relative linear and areal growth rate (% growth in cm and cm^2 yr^{-1}, respectively), and relative increase in area covered by coral tissue (%) of coral fragments held on the Reef Stars (experimental site, E) for a 12-month period. All data are fragments of *Acropora* spp. (n = 15). Reef Stars' corals derived from star #15 with an initial averaged area of 77.3 cm^2 in February 2021 (B) and 12 months after on the same Reef Star, corals were on average 1.4 times higher (106.4 cm^2) compared to its initial size (C). Note that fragment #9 was three times higher (from 27.6 to 78.6 cm^2) in the same period.

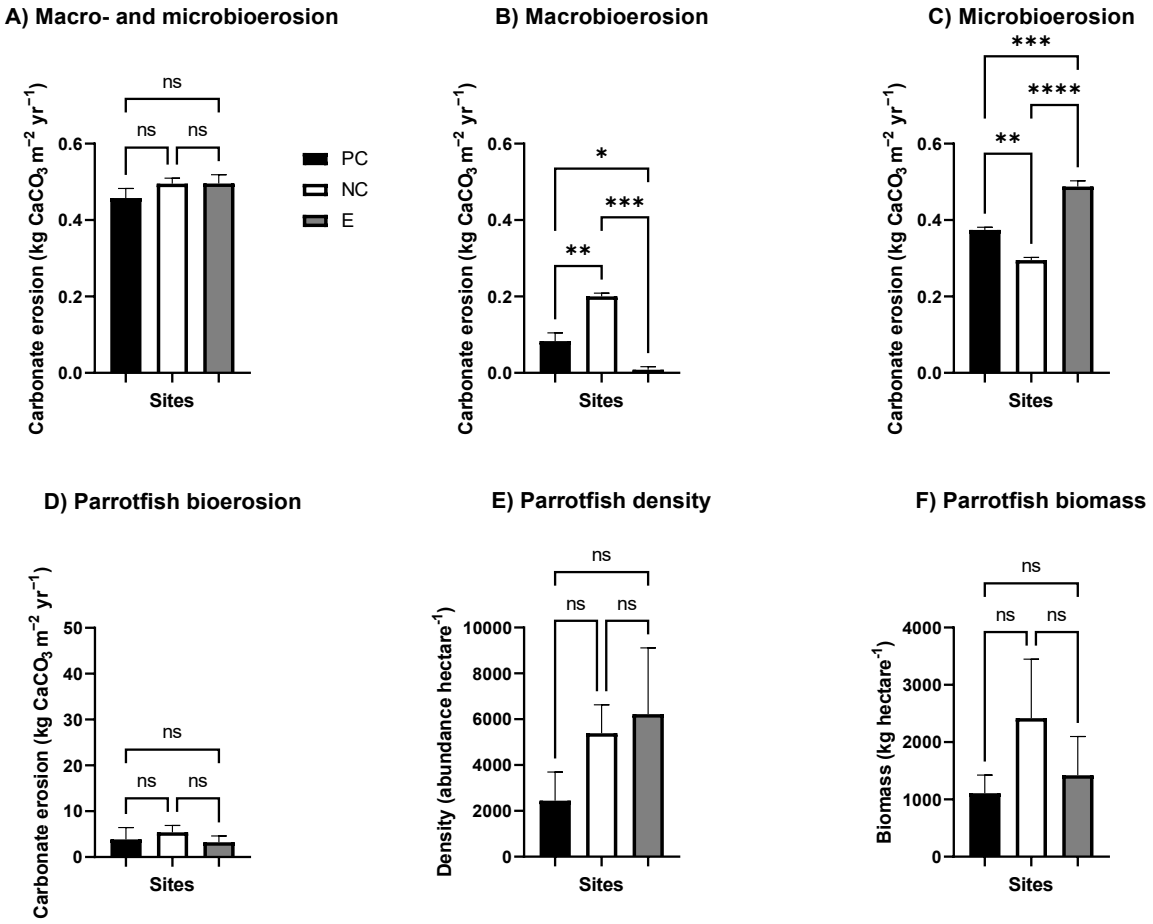

Figure S4.6 Mean (± SEM) (A) macro- and microbierosion, (B) macrobioerosion, (C) microbioerosion, parrotfish (D) bioerosion, (E) density and (F) biomass across Moore Reef studied sites. The three studied sites were (i) the restored site using Reef Stars (Experimental, 'E'), (ii) a rubble field (negative control, 'NC'), and (iii) a non-intervened healthy-looking representative neighbouring reef site (positive control, 'PC') in February 2022 (16 months post-installation of the Reef Stars). Bioerosion rates are expressed in kg $CaCO_3$ m^{-2} yr^{-1}, and density and biomass as abundance or kg $hectacte^{-1}$, respectively. Urchins were not present across sites (0.0 individual/m^2); hence, their bioerosion contribution is not plotted. Means (n = 3 per reef site) were compared by analysis of variance (ANOVA) with *post hoc* Tukey tests (see main text) where ns indicates no statistical significance, and *, **, ***, and **** indicate $p \leq 0.05$, 0.01, 0.001, and 0.0001, respectively.

Table S4.1 Coral individuals collected in February 2022 to study their skeletal properties. *Acropora intermedia*, *Acropora* spp. rubble, and *Pocillopora damicornis* are represented in light blue, mid-blue, and orange, respectively. The reef site where the corals were collected from is also provided in the table. Moore Reef studied sites consisted of (i) Reef Stars (Experimental site, 'E'), (ii) the negative control 'NC' constituted of unconsolidated coral rubble mat, and (iii) the positive control 'PC' represented by a natural healthy-looking neighbouring reef area. In detail, fragments (< 5 cm in length) of *A. intermedia*, *P. damicornis* and rubble were collected at each site (n = 5 each) as follows: *A. intermedia* at the E and PC sites, *P. damicornis* at the E, PC, NC sites, and *Acropora* rubble only from the rubble patch (NC site), in February 2022 (16 months post-deployment of the Reef Stars).

Coral spp.	**Reef site origin**	**No of individuals**	**Analysis**
A. intermedia	E	5	Coral skeletal properties: bulk volume, biomineral density, bulk density, pore volume, apparent (internal) porosity, and hardness
A. intermedia	PC	5	
Acropora spp. *rubble*	NC	5	
P. damicornis	E	5	
P. damicornis	PC	5	
P.damicornis	NC	5	

Chapter 5 General Discussion

Synthesis of results, future directions, and conclusions

5.1 Summary

Coral and/or reef restoration has increased in both need and popularity in response to the recent drastic decline in global coral populations (Hein et al., 2021; Kleypas et al., 2021), and since 2017 on the Great Barrier Reef (GBR, Australia) (McLeod et al., 2022). Recent coral restoration methods on the GBR have particularly adopted coral propagation and out-planting methods alongside substrate stabilisation (McLeod et al., 2022). Whilst these various methods diverge in terms of approach, they share the primary goal to increase coral cover at individual degraded reef sites (Bowden-Kerby, 2001; Rinkevich, 2015; Rinkevich, 1995; Young et al., 2012), and hence are considered "targeted" restoration. Success of such restoration efforts has traditionally been evaluated using common metrics of coral growth and survivorship (Boström-Einarsson et al., 2020; Hein et al., 2017; Lirman and Schopmeyer, 2016; Suggett et al., 2019), including recent restoration activities conducted on the GBR (e.g., Howlett et al., 2023, 2022; Roper et al., 2022), and only in some exceptional examples has success rested on ecological metrics (e.g., Calle-Triviño et al., 2021; Harrison et al., 2021; Hein et al., 2020). The ultimate restoration goals are often centred on maintaining or recovering a functionally healthy, and self-sustaining, reef ecosystem and associated service values. Consequently, there remains a vast mismatch between restoration current success metrics and goals, as well as uncertainty surrounding how restoration activities may impact coral reef performance, functionality and associated services, and resilience (Boström-Einarsson et al., 2020; Hein et al., 2021, 2017).

My PhD aimed to overcome this fundamental gap in knowledge associated with the growing interest in coral restoration; specifically, I evaluated the biological and ecological "success" of novel coral restoration efforts on the GBR by developing a holistic multi-trait measurement approach based on a broader range of coral traits beyond survival and growth. This multi-trait approach has facilitated the identification of key traits that better describe "success" during coral reef restoration techniques that more meaningfully contribute to desired ecosystem service outcomes. In particular, my research findings have provided new insights into the impacts of recent coral restoration practices on the GBR at the level of coral and/or reef performance, functioning, associated services, and resilience (**Fig. 5.1**). I evaluated the success of novel active reef management approaches that focus on coral propagation and outplanting, and rubble stabilisation to enhance reef accretion at a local scale. Specifically, building on actual GBR restoration activities that are showing immense promise to aid ongoing management (McLeod et al., 2022) of the (i) "Coral Nurture Program" (CNP) — a world-first partnership between tourism operators and scientists to up-scale coral restoration practices and identify high-value reef sites that can be managed by local stewardship (Howlett et al., 2022) — and (ii) Mars Incorporated "Mars Assisted Reef Restoration System (MARRS)", a global enterprise that specialises in stabilising large areas of unconsolidated rubble to boost coral recruitment (Williams et al., 2019).

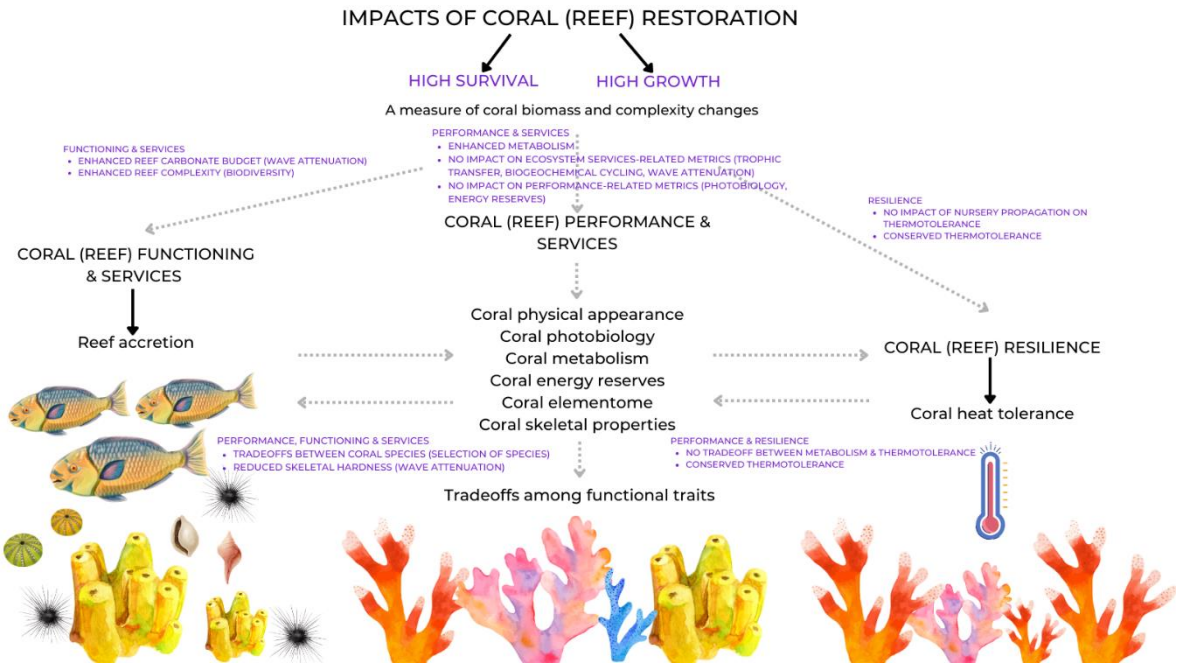

Figure 5.1 Schematic representation of some knowledge gaps regarding the impacts of coral reef restoration practices. Continuous arrows indicate traits or metrics that are acknowledged to inform coral reef restoration practices. Dotted arrows accompanied by violet text in capitals show aspects of coral restoration found in minimal studies (or even not considered yet) that have been addressed in the three Chapters of this PhD thesis.

5.2 Impacts of coral reef restoration practices to inform success

Throughout my thesis, I have identified how coral nursery propagation and substrate stabilisation impact coral biology and reef ecology, including those features (or traits) that are the foundation of reef services; as such, these provide, in effect, new goal-oriented metrics to evaluate the success of coral restoration interventions (**Fig. 5.1**). I conducted the first multi-trait assessment of coral nursery propagation success. Here, evaluation of 90 functional traits was pivotal in demonstrating how coral nurseries can effectively increase coral biomass without potentially impacting traits indicative of essential ecosystem services such as biogeochemical cycling and wave attenuation (Nuñez Lendo et al., 2023, **Chapter 2**; **Fig. 5.1**). These findings were achieved by integrating traits related to elemental composition (C:N:P:X; i.e., carbon [C] with nitrogen [N], phosphorus [P] and other elements [X]), and

skeletal properties that have previously only been used in coral biology studies (e.g., Fantazzini et al., 2015; Grima et al., 2022) but not applied to coral restoration practices. My approach also highlighted that photobiological and energetic traits — critical for coral reef functioning and resilience (Chapron et al., 2022; Nitschke et al., 2018; Rodrigues and Grottoli, 2007; Warner and Suggett, 2016) — were well-sustained by nursery propagation (Nuñez Lendo et al., 2023, **Chapter 2**; **Fig. 5.1**). In fact, faster coral growth within nurseries was accompanied by higher photosynthesis, respiration, and calcification rates (i.e., enhanced metabolism) (Nuñez Lendo et al., 2023, **Chapter 2**; **Fig. 5.1**). Collectively, my novel multi-trait-based approach was critical in revealing the biological machinery (and thus functional traits) supporting fast-tracked coral growth through nursery propagation, and hence useful to consider for propagation success (Nuñez Lendo et al., 2023, **Chapter 2**).

A broader picture of the impact of nursery propagation on coral fitness was achieved through subsequent consideration of metrics related to thermal resilience (i.e., bleaching susceptibility) (**Chapter 3**). Heat-stress response of high growth- and metabolic-enhanced nursery corals vs their wild donors was evaluated for the first time through the Coral Bleaching Automated Stress System (CBASS, Voolstra et al., 2020) (**Chapter 3**). Exposure to controlled acute thermal stress demonstrated that nursery corals displayed similar thermal tolerance to their donor colonies; as such, bleaching susceptibility was not impacted during nursery propagation (**Chapter 3**) despite enhanced metabolism and growth — processes that have previously been suggested to come at a cost to thermal tolerance for the species I investigated (*Acropora hyacinthus*; Cornwell et al., 2021). Bio-physical and photo-physiological metrics — common traits used to assess the effect of thermal stress on coral performance, functioning, and resilience (Nitschke et al., 2018) — all responded in a similar manner between nursery and donor material (**Chapter 3**). However, somewhat surprisingly,

despite small but insignificant differences in thermal tolerance among nursery and their wild donor corals, half of the nursery corals displayed a larger range in photosynthetic efficiency values (i.e., ~2-3 higher thermotolerance) compared to the respective donor colonies at the end of high-temperature treatment (i.e., 34 °C), suggesting some genotypic-variance in response that was masked by the relatively low sample size (**Chapter 3**).

My focus subsequently shifted from nursery propagation to the use of the MARRS structures to both stabilise substrate and propagate coral in parallel (Nuñez Lendo et al., 2024, **Chapter 4**). I demonstrated that MARRS resulted in remarkably enhanced reef accretion (i.e., high net carbonate budget) over a short period of time (16 months) compared to a nearby control reef site (Nuñez Lendo et al., 2024, **Chapter 4**). My research findings highlight the capacity of restoration interventions such as MARRS to regain coral cover, positive net reef accretion, and complexity of reef sites with poor recovery trajectory (Nuñez Lendo et al., 2024, **Chapter 4**). Through this work, I laid down the basis for improvement of traits indicative of an essential ecosystem service — wave attenuation (i.e., coastal protection Toth et al., 2023; Webb et al., 2023) — through the recovery of the three-dimensional structure of the reef. By integrating other metrics related to skeletal properties, I confirmed that species-specific trade-offs in functional traits (e.g., decreased skeletal hardness) could occur when selecting different coral species in restoration activities (Nuñez Lendo et al., 2024, **Chapter 4**). Thus, measurements of success should also include structural properties to robustly resolve whether ecosystem service values, such as reef accretionary potential, are retained during restoration efforts (Nuñez Lendo et al., 2024, **Chapter 4**). Furthermore, appropriate selection of coral species will be critical where different coral communities will retrieve species-specific carbonate budgets and potential trade-offs in functional traits (Nuñez Lendo et al., 2024, 2023, **Chapter 2** and **Chapter 4**).

In this final Chapter, I synthesise these results from **Chapters 2-4** to propose a new framework for how to evaluate future coral restoration efforts aimed at establishing self-sustaining coral populations to advance reef recovery (Hein et al., 2021; Kleypas et al., 2021; Vardi et al., 2021). In turn, I highlight the implications of my findings to better design, implement, monitor, and achieve desired goals needed for restoration programs to be effective. I discuss how these findings are embedded in current natural ecosystem restoration and management practices, as well as the implications for considering critical — as yet under-recognised — aspects of coral biology (e.g., reproduction) in restoration metrics. I recommend future directions for priority research to optimise coral reef restoration practices by considering goal-oriented metrics. Collectively, these steps highlight the need to better tailor restoration practices with appropriate metrics aligned to their specific goals, spanning maintenance or reestablishment of coral and/or reef performance, functioning, service value, and resilience.

5.3 Benefits of a multi-trait-based approach for coral reef restoration

Effectively up-scaling coral reef restoration, in terms of spatial footprint and cost-efficiency, is a global priority (Boström-Einarsson et al., 2020; Suggett and van Oppen, 2022). In order to improve coral reef management, it is necessary to optimise current methodologies and monitoring protocols by incorporating meaningful goal-oriented metrics that can quantify the impacts of restoration practices on coral reef performance, functionality and associated service value (Boström-Einarsson et al., 2020; Hein et al., 2021, 2017; Nuñez Lendo et al., 2024, 2023, **Chapter 2** and **Chapter 4**; **Chapter 3**). One solution — as evidenced in my thesis — is through trait-based approaches (Madin et al., 2023) that have traditionally been used in evolutionary and ecological studies (e.g., Madin et al., 2016a) since traits

systematically link organismal responses to the environment. Trait-based approaches enable assessment of a broader array of functional traits and identification of the main properties driving organismal (coral) to ecosystem (coral reef) processes in past (e.g., Brown et al., 2004; Finegan et al., 2015; Kunstler et al., 2016) and present (Nuñez Lendo et al., 2024, 2023, **Chapter 2** and **Chapter 4**; **Chapter 3**) environmental regimes.

Major advances in comparative plant functional ecology over the last two decades have been enabled by fast development of a trait-based approach for plant function in agricultural systems (Garnier and Navas, 2012), and notably evaluating the impacts of management practices of grasslands and crop weeds. For instance, agronomic value of grassland has been improved due to better prediction of grassland biomass production, the date of peak production and the digestibility of herbage from using traits such as leaf traits and/or plant height (Ansquer et al., 2009; Khaled et al., 2006; Pontes et al., 2007) instead of using only survival and growth metrics. This example directly translates to coral restoration by, for example, adopting metrics such as carbonate budgets and rugosity (Nuñez Lendo et al., 2024, **Chapter 4**), as these are better predictors of reef accretion and biodiversity potential. In this sense, restoration at scale — as a more industrialised process to propagate coral (or silviculture, *sensu* Rinkevich, 2019, 2006) — aligns closely with approaches that are already tried-and-tested in terrestrial-based agriculture. Another example is improvement in understanding functional composition and community structure of crop weeds and how they could impact crop functioning. Use of traits may be an opportunity to detect groups of "weedy" species which similarly respond to a set of management practices (e.g., use or non-use of pesticides) or affect crop yield (Garnier and Navas, 2012). Thus, whilst in **Chapter 2** (Nuñez Lendo et al., 2023), I focused on one coral species and screened 90 traits to identify how enhanced coral growth is modulated — and hence biological properties that could be

more appropriate— it is plausible that reef restoration practices also monitor traits of coral competitors in propagation habitats. Other applications of the use of traits are directed to detect plant responses to climate change (Lamarque et al., 2014; Madani et al., 2018; Schleuning et al., 2020). Thus, using trait-based approaches in coral reef restoration, but in a manner that capture complex ecological interactions, could also prove critical for modelling the future success of restoration activities that are inherently under environmental change pressures (Nuñez Lendo et al., 2024, 2023, **Chapter 2** and **Chapter 4**; **Chapter 3**).

5.4 Metrics used in ecosystem restoration and management

Evaluating the success of ecosystem restoration and management is often challenging (Hein et al., 2021). Preferential use of one metric over another can result in profoundly different outcomes and, hence, important consequences for the management decisions and activities taken by stakeholders involved in restoration programs (Basconi et al., 2018). Therefore, choosing appropriate metrics to evaluate restoration efforts is extremely important (Nuñez Lendo et al., 2024, 2023, **Chapter 2** and **Chapter 4**; **Chapter 3**). Generally, the most common metric when evaluating the success of restoration efforts in all marine habitats is the survival rate (Ruiz-Jaen and Aide, 2005), which for coral reefs is often combined with growth rate (Boström-Einarsson et al., 2020; Suggett et al., 2019). Along similar lines, oyster reef restoration programs carry three main success metrics: presence of (i) vertical structure above the seafloor, (ii) live oysters, and (iii) recruitment (La Peyre et al., 2014; Powers et al., 2009). In contrast, very different parameters are currently favoured when evaluating terrestrial habitats, such as biodiversity, vegetation structure and ecological functions (Löf et al., 2019; Ruiz-Jaen and Aide, 2005). In forest restoration, despite the high number of studies that still focus on survival (88% of seedling studies) and growth as height/length (60%), inclusion of

other metrics related to functioning (e.g., metrics related to seedling performance, seed performance, and plant community composition) is expanding (Dimson and Gillespie, 2020). So a lack of wider trait-based approaches for reef restoration success evaluations is currently at odds with more established disciplines.

Terrestrial ecosystems have been restored and managed long before coastal marine ecosystems, which in the latter case are still comparatively young disciplines (Bayraktarov et al., 2016; Suding, 2011). In addition to this difference in age in terms of restoration science, many monitoring programs evaluate the success of their interventions in the short term, as is also the case for coral restoration programs (Boström-Einarsson et al., 2020), despite the strong scientific evidence that longer time scales provide more accurate estimates of restoration success since recovery of ecosystem services can be highly prolonged (Bayraktarov et al., 2016; Bell et al., 2008; Hein et al., 2021). Importantly, ecosystem service-based metrics could also introduce economic and social service value while enhancing biodiversity (Benayas et al. 2009; Adame et al. 2015). In fact, current movements to biodiversity credits (Alvarado-Quesada et al., 2014; Baruch Rinkevich, 2015) may place more need to prioritise biodiversity-driven metrics in reef restoration outcome metrics, which could require many years to rigorously evaluate and detect. Such challenges are amplified in marine systems where measurements are simply harder and more time-consuming to make than in terrestrial systems, and hence the need to innovate more automated and/or cost-effective means to capture trait-based properties for reef restoration (e.g., Suggett et al., 2022).

Evaluating restoration success using traits that relate to ecosystem services is an emerging field in marine ecology, except for coastal wetlands (Zhao et al., 2016); in the latter case, this discipline arguably stems directly from terrestrial-based restoration practices. Such trait-based metrics, in fact, already exist for this habitat, such as the rapid assessment method (the so-called Galv-RAM), which combines biotic and abiotic parameters to obtain an ecosystem index score (Staszak and Armitage, 2013). New metrics are now under research for other habitats, such as the use of food web structure to assess restored macroalgae beds (Kang et al., 2008), fish assemblages to evaluate seagrass restoration efforts (Scapin et al., 2016), or fish tracking and habitat use to monitor the recovery of an estuary (Freedman et al., 2016). In addition, the next-generation restoration metric uses environmental DNA data to measure trajectories towards rehabilitation targets in soils (Liddicoat et al., 2022) and coastal estuaries (DiBattista et al., 2022). The findings of my thesis contribute to building this knowledge by identifying and testing new potential metrics that set the appropriate goals for coral reef restoration (i.e., maintenance or recovery of coral and/or reef performance, functioning, associated services, and resilience) to outweigh coral reef loss after a perturbation (Nuñez Lendo et al., 2024, 2023, **Chapter 2** and **Chapter 4**; **Chapter 3**).

To the best of my knowledge, no multi-trait-based approach has been applied to coral restoration except for the work of my thesis (Nuñez Lendo et al., 2024, 2023, **Chapter 2** and **Chapter 4**; **Chapter 3**); that said, it is plausible that restoration programs posess a wealth of data — and hence trait metrics — but have not considered them beyond growth and survival since the latter are most commonly used to benchmark across activity. Arguably, many ecosystem service values do not have indicative metrics still commonly addressed in coral restoration, such as fisheries productivity, trophic transfer, water quality, and aesthetic value (see **Fig. 5.2**). Therefore, more targetted metrics are required that will inevitably alter the

scope of data collection and ultimately how programs — and their inherent monitoring commitments — are conducted. Some metrics serve for more than one ecosystem service and resilience indicator, such as thermal tolerance and successful reproduction, as they apply to all ecosystem services the reef provides (**Fig. 5.2**), and hence may be logical starting points. In contrast, other metrics are more specific, such as carbonate budgets as an indicative measurement of wave attenuation (Nuñez Lendo et al., 2024, **Chapter 4**). In **Fig. 5.2**, I expanded the list of metrics studied in my thesis by bringing metrics commonly used in biology and ecology but not yet commonly used in restoration. The point here is that restoration needs to apply a better framework to evaluate success, thus focusing on more meaningful traits (related to functioning, resilience, and services) that are better aligned with their specific restoration goals.

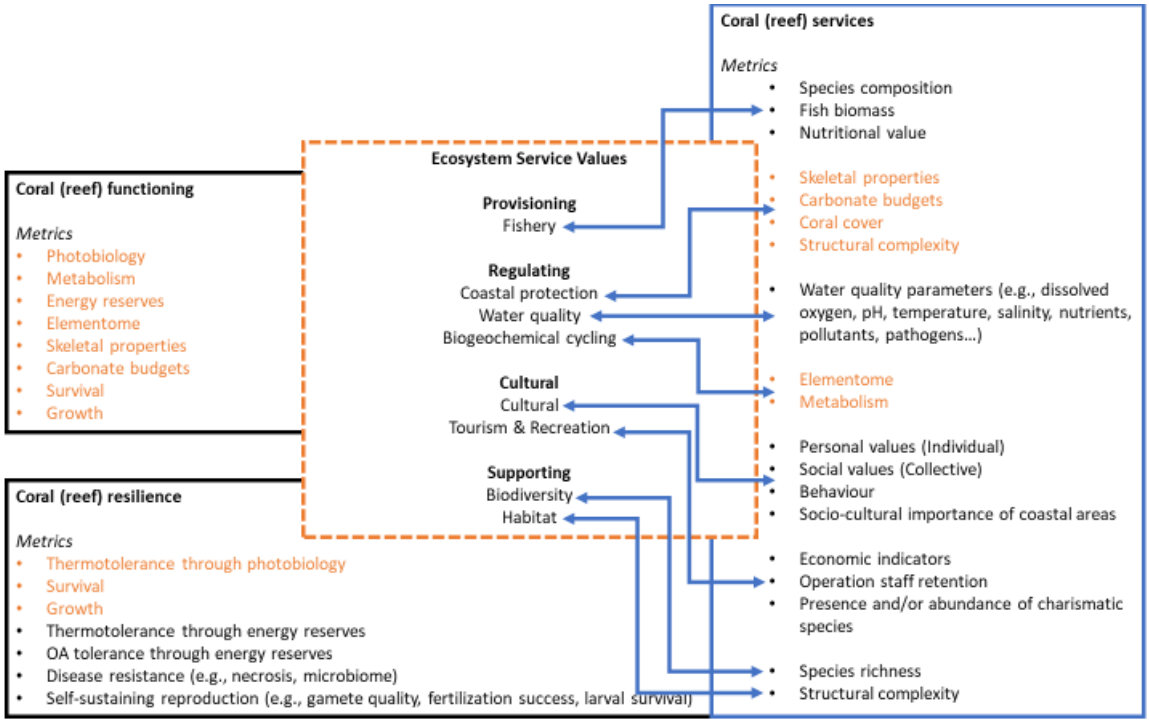

Figure 5.2 Framework to link coral (reef) traits to ecosystem service value. Ecosystem service values are diverse, but they all depend on the healthy functioning and resilience of the coral (reef), which are, in turn, informed through metrics related to coral (reef) functioning and resilience (left side), but also through already identified metrics that relate to ecosystem services (right side). In orange are the metrics studied in this thesis that inform coral (reef) functioning, resilience, and services. Ecosystem service values were initially defined by Woodhead et al., 2019, and expanded through the learnings of this thesis. OA = Ocean Acidification.

5.5 Resolving coral fitness during coral restoration

Survival and growth of corals are closely tied to the processes of coral reproduction, which is critical for the maintenance and persistence of coral reef ecosystems. Collectively, the survival (or "maintenance"), growth and reproduction capture fitness (e.g., Madin et al., 2016a). Despite my research not being able to include reproductive traits due to the compounded timeframe of my thesis due to COVID-19 pandemic challenges, I propose that it is critical to include coral reproductive metrics in coral restoration activities, specifically where restoration efforts aim to establish self-sustaining, sexually reproducing coral populations that have a sufficient genetic and phenotypic variation to adapt to changing

environments (Guest et al., 2012; Humanes et al., 2022, 2021; Lachs et al., 2023). Maintaining local genetic variation with populations capable of sexual recruitment and genetic exchange while environmental conditions become stabilised may enable corals to adapt to climate change for the next 100 years or longer (Matz et al., 2018). Therefore, promoting continuous genetic adaptation is, in fact, arguably more crucial for the recovery of endangered species than focusing on other ecological goals, such as coral cover and habitat provision (Baums et al., 2019) or classical restoration metrics (e.g., survival and growth) since ecological success may only be temporary in the absence of self-sustaining coral populations. Even if survival and growth are suboptimal in a nursery setting for certain coral genotypes, their performance, once out-planted, can be considered optimal (O'Donnell et al., 2018), including high reproductive output.

Restoration focus is often recommended to maintain the genetic diversity and phenotypic resilience required for corals to survive and produce genetically diverse and viable offspring that could serve as raw material for natural selection (e.g., Baums, 2008; Baums et al., 2019, 2022; Van Oppen et al., 2015; van Oppen et al., 2017; Voolstra et al., 2017). In order to protect coral populations and support their survival and growth (Nuñez Lendo et al., 2023, **Chapter 2**), it is important to understand and manage the factors that impact coral reproduction. However, sexual reproductive traits (such as fecundity, gamete quality, fertilisation success; **Fig. 5.3**) are hard to evaluate, not least because the majority of coral restoration projects are short-term (in general, less than two years of monitoring of the restored sites; Boström-Einarsson et al., 2020), but also where reproduction timings are often uncertain and activity — at least in the case of spawning — can be limited to only once per year.

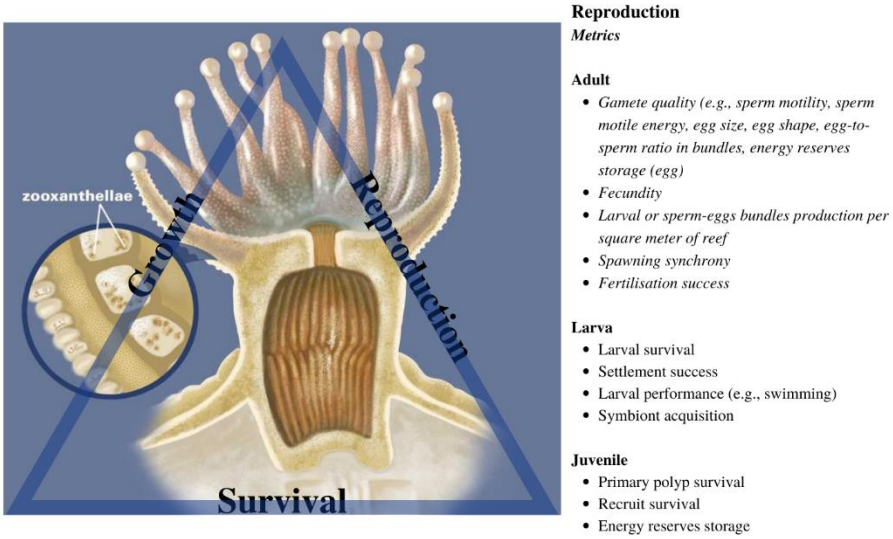

Figure 5.3 Emergent properties that define the coral "fitness triangle". Survival ("maintenance"), growth, and reproduction are emergent properties that are underpinned by complex biological machinery formed by functional traits. On the right side, various reproductive metrics for different coral life stages (adult, larva, and juvenile) are shown to be considered for initial screening to reduce the trait space and identify key reproductive metrics for restoration goals.

Timing and frequency of coral reproduction are dependent on environmental factors such as water temperature, light, and nutrient availability (Bouwmeester et al., 2023; Richmond, 1997; Shlesinger and Loya, 2019). In general, corals that are under stress, such as those exposed to increased temperatures or high levels of pollution, may be less likely to reproduce successfully (Richmond et al., 2018; Shlesinger and Loya, 2019). Thus, when propagating corals on a non-native structure and outside of their native reef location, impacts on spawning performance (e.g., gamete quality, spawning synchrony, energy reserves content; **Fig. 5.3**), compared to their wild conspecifics, could potentially appear as environmental conditions offered by the nursey are different from the native conditions (e.g., light and flow regimes), as seen in coral growth and metabolism in Nuñez Lendo et al., (2023), **Chapter 2**. In this regard, collecting data on metrics such as spawning cycles and synchrony (see **Fig. 5.3**) for different species, locations (including restored sites), and age and size classes would enable

restoration practitioners to have an efficient and reliable production of coral larvae for restoration (Randall et al., 2020).

Recognition of key reproductive traits enables assessment of trade-offs amongst the coral fitness space, and thus can be used to assess how "successful" restoration is. For example, when a sexually mature coral colony is fragmented below a certain size, resources are directed towards regrowth instead of reproduction (Lirman, 2000; Zakai et al., 2000). In captivity, the regular fragmentation of many coral species is likely to be a factor in the relatively low spawning frequency of coral colonies that have been maintained for many years in aquaria. Corals undergoing fragmentation (into small sizes) typically lose reproductive viability for 4–6 months, even if fragments were initially of a reproductively viable age and size (Wallace, 1985; Szmant-Froelich, 1985; Smith and Hughes,1999). As such, the size and life stage (age) of corals used for restoration will inevitably impact the resource allocation towards reproduction as freshly fragmented coral show higher growth/regeneration (i.e., following trauma, corals undergo rapid tissue and skeletal repair; Bak, 1983; Chadwick and Loya, 1990; Loya, 1976; Meesters et al., 1994) than well-established adult coral colonies, which above a size threshold shift resources from growth to sexual reproduction (Babcock, 1991; Kojis and Quinn, 2001; Soong, 1993). Similarly, stress "maintenance" can come at a cost to reproduction via the parallel need to make choices in allocation of energy. For example, the 1998 global bleaching event led to extensive coral bleaching at Heron Island, Great Barrier Reef (GBR), Australia. Nine months post-bleaching, the previously bleached and apparently recovered coral colonies had fewer reproductive polyps with fewer eggs (and these eggs were smaller than the eggs of unbleached colonies; Ward et al., 2002).

Despite not having data on reproductive traits of nursery corals and their donor colonies for my thesis, I would postulate that the enhanced metabolism of nursery corals that drives a higher growth in terms of coral biomass (Nuñez Lendo et al., 2023, **Chapter 2**) might be favourable for reproduction processes, as potentially enhanced feeding on the nursery might favour build-up of energy reserves in the coral available for stress tolerance (e.g., Grottoli et al., 2006). Furthermore, corals rely mainly on autotrophy to allocate carbon to gametes (Rodrigues and Padilla-Gamiño, 2022); thus it could be expected that corals with enhanced photosynthesis could have a greater reproductive output. In summary, coral reproduction is critical for the survival and growth of coral populations. Asexual reproduction is quick and efficient but potentially provides limited genetic diversity (e.g., Baums et al., 2019, 2022; Hagedorn et al., 2021). In contrast, sexual reproduction provides the genetic diversity essential for long-term coral survival, and new colonies established through genetic recombination are more likely to be robust and resistant to changing reef conditions, including environmental stress (Caruso et al., 2021; Morikawa et al., 2019; Rivera et al., 2022; Thomas et al., 2018). By understanding and managing the factors that impact coral reproduction, we can optimise current restoration projects to help to protect and conserve these vital ecosystems. Including traits that relate to reproduction traits (e.g., gamete quality, fecundity, fertilisation success), apart from those related to survival and growth, can build a robust approach to provide a complete picture of coral fitness during restoration activities (see **Fig. 5.2**).

5.6 Future directions

Not all traits are equally relevant to restoration success, and some traits are challenging to measure (i.e., time-consuming, not cost-effective, and not informative enough). Therefore,

collecting the most appropriate data will be necessary to optimally manage and restore coral reefs. Potentially valuable phenotypic traits (supertraits; Madin et al., 2016b) for future climate scenarios could be, apart from high survival and high growth rate, high wound healing rate, bleaching resilience (**Chapter 3**; **Table 5.1**), infectious disease resilience, and high sexual reproductive output (Baums et al., 2019; see **Table 5.1**). Other traits that can influence the capacity of the coral to withstand stress are the adjustment of the photosynthesis-to-respiration ratio and calcification rate (Nuñez Lendo et al., 2023, **Chapter 2**). Modulation of these physiological traits results from both the intraspecific trait variation and the individual phenotypic responses to the environment (e.g., nursery vs reef in Nuñez Lendo et al., 2023, **Chapter 2**). Furthermore, such traits are essential for corals to maintain their vital ecological functions (Nuñez Lendo et al., 2023, **Chapter 2**), and regulation of such traits is key in enabling corals to thrive in more extreme environments that are expected under climate change (Camp et al., 2017). Due to the novelty of my findings and the urgent need to actively propagate coral biomass at larger scales, it would be logical to recommend a future focus on developing new techniques that target metabolism-related traits (e.g., calcification, photosynthesis, and respiration) to increase growth yield (Nuñez Lendo et al., 2023, **Chapter 2**; **Table 5.1**). Similar to interest in engineering thermal-tolerant corals (Humanes et al., 2021; Quigley et al., 2021; van Oppen et al., 2017, 2015; Voolstra et al., 2021a), producing enhanced-metabolic corals could be an avenue to explore through the supplement of novel diets, different flow regimes and temperature pulses (e.g., Suggett and van Oppen, 2022; **Table 5.1**), or even assisted evolution to identify coral broodstock with enhanced metabolism for selective breeding and gene flow (Hagedorn et al., 2021; van Oppen et al., 2015) if these traits are heritable. Applying assisted evolution techniques (e.g., selective breeding or gene flow) and thermal priming (Brown et al., 2015; Hackerott et al., 2021; Martell, 2023) on nursery corals that have shown enhanced thermotolerance (**Chapter**

3, see also Cunning et al., 2021) provides a convenient operational approach to enable practitioners to enhance resilience of out-planted material.

Future direction	**Key next steps to meet this goal**
Use of multi-trait-based approaches in coral and/or reef restoration programs.	Collaboration between researchers and practitioners to apply multi-trait-based approaches to understand the impacts of coral and/or reef restoration practices (and also implement workflows to distill diverse trait matrices to key traits).
Modelling restoration success.	Identified key traits and range of values for commonly used coral species in restoration programs for models to predict restoration success outcomes of different combinations of techniques, species, reef environments, and climate scenarios.
Coral performance and reef functioning traits underpin services and resilience. Identify and establish a direct interaction link and integrate these key traits in coral restoration evaluation protocols.	Bring metrics (traits) from studies in coral biology and reef ecology to evaluate the success of coral restoration practices to fully understand factors that underpin survival and growth inherent to different ecosystem service values

Metabolism enhancement of corals.	Research towards engineering enhanced-metabolic corals by supplementing novel diets, different flow regimes and temperature pulses.
Carbonate budget is a key metric that informs about coral reef functioning (reef accretion) but also services (wave attenuation). Integrate into coral restoration evaluation protocols.	Provide training to researchers and practitioners for assessment of carbonate budgets. Advance accuracy, precision and suitability (e.g., across different reef regions) of carbonate budget techniques.
Thermal tolerance is a key metric for understanding if restored coral reefs survive a warming climate. Integrate into coral restoration evaluation protocols.	Provide training to researchers and practitioners for assessment of thermal tolerance. Advance accuracy, precision and suitability (e.g., across different reef regions) of stress assay techniques.
Include reproductive traits into trait-based approaches and coral restoration evaluation protocols.	Bring metrics (traits) from studies in coral biology and reef ecology specific to reproduction to evaluate the success of coral restoration practices to yield a complete picture of coral fitness, and fitness trade-offs.

Table 5.1 Future research priorities and key steps to advance coral reef (science) restoration.

In addition, coral morphology, also referred to as growth morph or growth form, is considered a key trait because it supports structural complexity and biodiversity in the reef

(Darling et al., 2012; Madin et al., 2016a, 2016b). It is also considered a good predictor of recovery after disturbances (Darling et al., 2012), including bleaching events (Graham et al., 2015). Structural complexity (measured through the metric "rugosity"; Nuñez Lendo et al., 2024, **Chapter 4**) is key in supporting services such as wave energy dissipation and habitat provision (Alvarez-Filip et al., 2011; Ferrario et al., 2014). Another very useful predictor of the balance between carbonate production and erosion processes, widely used in coral reef ecology, is the metric of "carbonate budgets". Its applicability for evaluating success in restoration efforts is key for restoration programs aiming to recover the lost three-dimensional reef structure in reef sites with unstabilised rubble substrate. It would be logical to use "carbonate budgets" as a key metric to evaluate reef accretion on degraded reefs for restoration (Nuñez Lendo et al., 2024, **Chapter 4**; **Table 5.1**) as this trait is directly related to the ecosystem service of wave attenuation and coastal protection (Nuñez Lendo et al., 2024, 2023, **Chapter 2** and **Chapter 4**; **Chapter 3**). In summary moving to key traits that capture coral performance and reef functioning that underpin reef services and resilience is a critical next step to advance reef restoration. By doing this, restoration programs will better tie their outcomes to specific reef ecosystem services that often frame their activity goals.

Supertraits are considered particularly informative for ecological and evolutionary drivers of organism success (e.g., Madin et al., 2016b). In the case of corals, it would be logical regulation to extend the previously proposed supertrait of growth (Madin et al., 2016b) to more broadly consider resource allocation and growth over their lifespan, and hence colony mass per unit tissue surface area, i.e., the relationship between coral weight and volume; CMA; Madin et al., 2016b; Nuñez Lendo et al., 2023, **Chapter 2**). However, integrating reproductive traits that inform preferential resource allocation towards reproduction instead of survival (or "maintenance") and growth into the evaluation of coral restoration practices is

paramount to fully understanding the impacts of restoration on coral fitness and reef functioning (**Table 5.1**).

5.7 Conclusion

I have demonstrated the value of employing a multi-trait-based approach to understand the effectiveness of coral and/or reef restoration practices on coral performance, reef functioning, and the supported services inherent to restoration success. Despite the considerable effort in time and resources needed to apply such an approach, my thesis has shown that the outcomes surpass the costs in knowledge and advancement in coral reef restoration science. Application of trait-based approaches might not be suitable for all cases. However, their integration into the structure of future restoration programs is key to fully understanding success and, ultimately, efficacy of restoration efforts. Whilst work presented throughout my PhD thesis focussed on real GBR restoration contexts, my findings carry widespread applicability to restoration programs aspiring to implement more diverse measures that are ultimately more meaningful descriptors of restoration outcomes. Whilst I have presented key examples of diverse trait landscapes to tackle specific ecosystem service attributes, it is clear that more research is warranted to examine the broader portfolio of ecosystem services sustained by the world's coral reefs as restoration activities continue to accelerate as aids to managing for healthy reefs.

References

AIMS, 2022. Annual Summary Report of Coral Reef Condition 2021/22 [WWW Document]. URL https://www.aims.gov.au/monitoring-great-barrier-reef/gbr-condition-summary-2021-22 (accessed 2.25.24).

AIMS, 2021. Annual Summary Report of Coral Reef Condition 2020/21 [WWW Document]. URL https://www.aims.gov.au/reef-monitoring/gbr-condition-summary-2020-2021 (accessed 2.25.24).

Al-Horani, F.A., 2015. Physiology of Skeletogenesis in Scleractinian Coral, in: Woodley, C.M., Downs, C.A., Bruckner, A.W., Porter, J.W., Galloway, S.B. (Eds.), Diseases of Coral. pp. 192–205. https://doi.org/10.1002/9781118828502.ch12

Aline, T., 2008. Dissolution of dead corals by euendolithic microorganisms across the northern Great Barrier Reef (Australia). Microb. Ecol. 55, 569–580. https://doi.org/10.1007/s00248-007-9302-6

Alvarado-Quesada, I., Hein, L., Weikard, H.P., 2014. Market-based mechanisms for biodiversity conservation: A review of existing schemes and an outline for a global mechanism. Biodivers. Conserv. 23, 1–21. https://doi.org/10.1007/s10531-013-0598-x

Alvarez-Filip, L., Dulvy, N.K., Gill, J.A., Côté, I.M., Watkinson, A.R., 2009. Flattening of Caribbean coral reefs: region-wide declines in architectural complexity. Proc. R. Soc. B 276, 3019–3025. https://doi.org/10.1098/rspb.2009.0339

Alvarez-Filip, L., Gill, J.A., Dulvy, N.K., 2011. Complex reef architecture supports more small-bodied fishes and longer food chains on Caribbean reefs. Ecosphere 2, 118. https://doi.org/10.1890/ES11-00185.1

Andersson, A.J., Kuffner, I.B., MacKenzie, F.T., Jokiel, P.L., Rodgers, K.S., Tan, A., 2009. Net Loss of CaCO3 from a subtropical calcifying community due to seawater acidification: Mesocosm-scale experimental evidence. Biogeosciences 6, 1811–1823. https://doi.org/10.5194/bg-6-1811-2009

Ansquer, P., Duru, M., Theau, J.P., Cruz, P., 2009. Functional traits as indicators of fodder provision over a short time scale in species-rich grasslands. Ann. Bot. 103, 117–126. https://doi.org/10.1093/aob/mcn215

Anthony, K., Bay, L.K., Costanza, R., Firn, J., Gunn, J., Harrison, P., Heyward, A., Lundgren, P., Mead, D., Moore, T., Mumby, P.J., Van Oppen, M.J.H., Robertson, J., Runge, M.C., Suggett, D.J., Schaffelke, B., Wachenfeld, D., Walshe, T., 2017. New interventions are needed to save coral reefs. Nat. Ecol. Evol. 1, 1420–1422. https://doi.org/10.1038/s41559-017-0313-5

Anthony, K., Bowen, J., Mead, D., Hardisty, P., 2019. Reef Restoration and Adaptation Program: Intervention Analysis and Recommendations.

Anthony, K.R.N., Helmstedt, K.J., Bay, L., Fidelman, P., Hussey, K.E., Lundgren, P., Mead, D., McLeod, I.M., Mumby, P.J., Newlands, M., Schaffelke, B., Wilson, K.A., Hardisty, P.E., 2020. Interventions to help coral reefs under global change—A complex decision challenge. PLoS One 15, e0236399. https://doi.org/10.1371/journal.pone.0236399

Anthony, K.R.N., Marshall, P.A., Abdulla, A., Beeden, R., Bergh, C., Black, R., Eakin, C.M., Game, E.T., Gooch, M., Graham, N.A.J., Green, A., Heron, S.F., van Hooidonk, R., Knowland, C., Mangubhai, S., Marshall, N., Maynard, J.A., Mcginnity, P., Mcleod, E., Mumby, P.J., Nyström, M., Obura, D., Oliver, J., Possingham, H.P., Pressey, R.L., Rowlands, G.P., Tamelander, J., Wachenfeld, D., Wear, S., 2015. Operationalizing resilience for adaptive coral reef management under global environmental change. Glob.

Chang. Biol. 21, 48–61. https://doi.org/10.1111/gcb.12700

Arif, C., Daniels, C., Bayer, T., Banguera-Hinestroza, E., Barbrook, A., Howe, C.J., LaJeunesse, T.C., Voolstra, C.R., 2014. Assessing Symbiodinium diversity in scleractinian corals via next-generation sequencing-based genotyping of the ITS2 rDNA region. Mol. Ecol. 23, 4418–4433. https://doi.org/10.1111/mec.12869

Arneth, A., Shin, Y.J., Leadley, P., Rondinini, C., Bukvareva, E., Kolb, M., Midgley, G.F., Oberdorff, T., Palomo, I., Saito, O., 2020. Post-2020 biodiversity targets need to embrace climate change. Proc. Natl. Acad. Sci. 117, 30882–30891. https://doi.org/10.1073/pnas.2009584117

Aronson, J., Clewell, A.F., Blignaut, J.N., Milton, S.J., 2006. Ecological restoration: A new frontier for nature conservation and economics. J. Nat. Conserv. 14, 135–139. https://doi.org/10.1016/j.jnc.2006.05.005

Aronson, R.B., Precht, W.F., 2001. White-band disease and the changing face of Caribbean coral reefs, in: Porter, J.W. (Ed.), The Ecology and Etiology of Newly Emerging Marine Diseases. Developments in Hydrobiology, Vol 159. Springer, Dordrecht, pp. 25–38. https://doi.org/10.1007/978-94-017-3284-0_2

Babcock, R.C., 1991. Comparative demography of three species of scleractinian corals using age- and size-dependent classifications. Ecol. Monogr. 61, 225–244. https://doi.org/10.2307/2937107

Baghdasarian, G., Osberg, A., Mihora, D., Putnam, H., Gates, R.D., Edmunds, P.J., 2017. Effects of temperature and pCO2 on population regulation of Symbiodinium spp. in a tropical reef coral. Biol. Bull. 232, 123–139. https://doi.org/10.1086/692718

Bahr, K.D., Rodgers, K.S., Jokiel, P.L., 2017. Impact of three bleaching events on the reef

resiliency of Kāne'ohe Bay, Hawai'i. Front. Mar. Sci. 4, 398. https://doi.org/10.3389/fmars.2017.00398

Bak, R.P.M., 1994. Sea urchin bioerosion on coral reefs: place in the carbonate budget and relevant variables. Coral Reefs 13, 99–103. https://doi.org/10.1007/BF00300768

Bak, R.P.M., 1990. Patterns of echinoid bioerosion in two Pacific coral reef lagoons. Mar. Ecol. Prog. Ser. 66, 267–272. https://doi.org/10.3354/meps066267

Bak, R.P.M., 1983. Neoplasia, regeneration and growth in the reef-building coral Acropora palmata. Mar. Biol. 77, 221–227. https://doi.org/10.1007/BF00395810

Baker, A.C., Cunning, R., 2015. Coral "Bleaching" as a Generalized Stress Response to Environmental Disturbance, in: Woodley, C.M., Downs, C.A., Bruckner, A.W., Porter, J.W., Galloway, S.B. (Eds.), Diseases of Coral. pp. 396–409. https://doi.org/10.1002/9781118828502.ch30

Barshis, D.J., Ladner, J.T., Oliver, T.A., Seneca, F.O., Traylor-Knowles, N., Palumbi, S.R., 2013. Genomic basis for coral resilience to climate change. Proc. Natl. Acad. Sci. 110, 1387–1392. https://doi.org/10.1073/pnas.1210224110

Basconi, L., Cadier, C., Guerrero-Limón, G., 2018. Challenges in Marine Restoration Ecology: How Techniques, Assessment Metrics, and Ecosystem Valuation Can Lead to Improved Restoration Success, in: Jungblut, S., Liebich, V., Bode-Dalby, M. (Eds.), The 2018 Conference for YOUng MArine RESearcher. Oldenburg, Germany, pp. 83–99. https://doi.org/10.1007/978-3-030-20389-4_5

Bates, A.E., Cooke, R.S.C., Duncan, M.I., Edgar, G.J., Bruno, J.F., Benedetti-Cecchi, L., Côté, I.M., Lefcheck, J.S., Costello, M.J., Barrett, N., Bird, T.J., Fenberg, P.B., Stuart-Smith, R.D., 2019. Climate resilience in marine protected areas and the 'Protection

Paradox.' Biol. Conserv. 236, 305–314. https://doi.org/10.1016/j.biocon.2019.05.005

Baumann, J., Grottoli, A.G., Hughes, A.D., Matsui, Y., 2014. Photoautotrophic and heterotrophic carbon in bleached and non-bleached coral lipid acquisition and storage. J. Exp. Mar. Bio. Ecol. 461, 469–478. https://doi.org/10.1016/j.jembe.2014.09.017

Baums, I.B., 2008. A restoration genetics guide for coral reef conservation. Mol. Ecol. 17, 2796–2811. https://doi.org/10.1111/j.1365-294X.2008.03787.x

Baums, I.B., Baker, A.C., Davies, S.W., Grottoli, A.G., Kenkel, C.D., Kitchen, S.A., Kuffner, I.B., LaJeunesse, T.C., Matz, M. V., Miller, M.W., Parkinson, J.E., Shantz, A.A., 2019. Considerations for maximizing the adaptive potential of restored coral populations in the western Atlantic. Ecol. Appl. 29, e01978. https://doi.org/10.1002/eap.1978

Baums, I.B., Chamberland, V.F., Locatelli, N.S., Conn, T., 2022. Maximizing genetic diversity in coral restoration projects, in: van Oppen, M.J.H., Aranda Lastra, M. (Eds.), Coral Reef Conservation and Restoration in the Omics Agee. Coral Reefs of the World, Vol 15. Springer, Cham, pp. 35–53. https://doi.org/10.1007/978-3-031-07055-6_3

Baums, I.B., Devlin-Durante, M.K., Lajeunesse, T.C., 2014. New insights into the dynamics between reef corals and their associated dinoflagellate endosymbionts from population genetic studies. Mol. Ecol. 23, 4203–4215. https://doi.org/10.1111/mec.12788

Baums, I.B., Miller, M.W., Hellberg, M.E., 2006. Geographic variation in clonal structure in a reef-building Caribbean coral, Acropora palmata. Ecol. Monogr. 76, 503–519. https://doi.org/10.1890/0012-9615(2006)076[0503:GVICSI]2.0.CO;2

Bay, L., Mead, D., Boström-Einarsson, L., 2019. Reef Restoration and Adaptation Program: Intervention Summary.

Bay, R.A., Palumbi, S.R., 2014. Multilocus adaptation associated with heat resistance in reef-

building corals. Curr. Biol. 24, 2952–2956. https://doi.org/10.1016/j.cub.2014.10.044

Bay, R.A., Rose, N.H., Logan, C.A., Palumbi, S.R., 2017. Genomic models predict successful coral adaptation if future ocean warming rates are reduced. Sci. Adv. 3, e1701413. https://doi.org/10.1126/sciadv.1701413

Bayraktarov, E., Saunders, M.I., Abdullah, S., Mills, M., Beher, J., Possingham, H.P., Mumby, P.J., Lovelock, C.E., 2016. The cost and feasibility of marine coastal restoration. Ecol. Appl. 26, 1055–1074. https://doi.org/10.1890/15-1077

Bayraktarov, E., Saunders, M.I., Mumby, P.J., Possingham, H.P., Abdullah, S., Lovelock, C.E., 2017. Response to "rebutting the inclined analyses on the cost-effectiveness and feasibility of coral reef restoration." Ecol. Appl. 27, 1974–1980. https://doi.org/10.1002/eap.1583

Bayraktarov, E., Stewart-Sinclair, P.J., Brisbane, S., Boström-Einarsson, L., Saunders, M.I., Lovelock, C.E., Possingham, H.P., Mumby, P.J., Wilson, K.A., 2019. Motivations, success, and cost of coral reef restoration. Restor. Ecol. 27, 981–991. https://doi.org/10.1111/rec.12977

Bednarz, V.N., Cardini, U., Van Hoytema, N., Al-Rshaidat, M.M.D., Wild, C., 2015. Seasonal variation in dinitrogen fixation and oxygen fluxes associated with two dominant zooxanthellate soft corals from the northern Red Sea. Mar. Ecol. Prog. Ser. 519, 141–152. https://doi.org/10.3354/meps11091

Bednarz, V.N., Naumann, M.S., Cardini, U., Van Hoytema, N., Rix, L., Al-Rshaidat, M.M.D., Wild, C., 2018. Contrasting seasonal responses in dinitrogen fixation between shallow and deep-water colonies of the model coral Stylophora pistillata in the northern Red Sea. PLoS One 13, e0199022. https://doi.org/10.1371/journal.pone.0199022

Beher, J., Possingham, H.P., Hoobin, S., Dougall, C., Klein, C., 2016. Prioritising catchment management projects to improve marine water quality. Environ. Sci. Policy 59, 35–43. https://doi.org/10.1016/j.envsci.2016.02.005

Bell, JD, Ganachaud, A., Gehrke, P., Hobday, A., Hoegh-Guldberg, O., Johnson, JE, Le Borgne, R., Lehodey, P., Lough, J., Pickering, T., Pratchett, M., Sikivou, M., Waycott, M., 2013. Vulnerability of fisheries and aquaculture to climate change in Pacific Island countries and territories, in: Johnson, J., Bell, J., De Young, C. (Eds.), Priority Adaptations to Climate Change for Pacific Fisheries and Aquaculture: Reducing Risks an Capitalizing on Opportunities. Rome: FAO, pp. 25–100.

Bell, S.S., Tewfik, A., Hall, M.O., Fonseca, M.S., 2008. Evaluation of seagrass planting and monitoring techniques: Implications for assessing restoration success and habitat equivalency. Restor. Ecol. 16, 407–416. https://doi.org/10.1111/j.1526-100X.2007.00308.x

Bellard, C., Bertelsmeier, C., Leadley, P., Thuiller, W., Courchamp, F., 2012. Impacts of climate change on the future of biodiversity. Ecol. Lett. 15, 365–377. https://doi.org/10.1111/j.1461-0248.2011.01736.x

Bellwood, D.R., Streit, R.P., Brandl, S.J., Tebbett, S.B., 2019. The meaning of the term 'function' in ecology: A coral reef perspective. Funct. Ecol. 33, 948–961. https://doi.org/10.1111/1365-2435.13265

Berkelmans, R., 2002. Time-integrated thermal bleaching thresholds of reefs and their variation on the Great Barrier Reef. Mar. Ecol. Prog. Ser. 229, 73–82. https://doi.org/10.3354/meps229073

Birkeland, C., Lucas, J.S., 1990. Acanthaster planci: major management problem of coral reefs. CRC Press, Boca Raton, FL, USA.

Bishop, M.J., Vozzo, M.L., Mayer-Pinto, M., Dafforn, K.A., 2022. Complexity–biodiversity relationships on marine urban structures: reintroducing habitat heterogeneity through eco-engineering. Philos. Trans. R. Soc. B 377, 20210393. https://doi.org/10.1098/rstb.2021.0393

Blanckaert, A.C.A., Reef, R., Pandolfi, J.M., Lovelock, C.E., 2020. Variation in the elemental stoichiometry of the coral–zooxanthellae symbiosis. Coral Reefs 39, 1071–1079. https://doi.org/10.1007/s00338-020-01932-8

Bongiorni, L., Giovanelli, D., Rinkevich, B., Pusceddu, A., Chou, L.M., Danovaro, R., 2011. First step in the restoration of a highly degraded coral reef (Singapore) by in situ coral intensive farming. Aquaculture 322, 191–200. https://doi.org/10.1016/j.aquaculture.2011.09.024

Borell, E.M., Yuliantri, A.R., Bischof, K., Richter, C., 2008. The effect of heterotrophy on photosynthesis and tissue composition of two scleractinian corals under elevated temperature. J. Exp. Mar. Bio. Ecol. 364, 116–123. https://doi.org/10.1016/j.jembe.2008.07.033

Boström-Einarsson, L., Babcock, R.C., Bayraktarov, E., Ceccarelli, D., Cook, N., Ferse, S.C.A., Hancock, B., Harrison, P., Hein, M., Shaver, E., Smith, A., Suggett, D., Stewart-Sinclair, P.J., Vardi, T., McLeod, I.M., 2020. Coral restoration–A systematic review of current methods, successes, failures and future directions. PLoS One 15, e0226631. https://doi.org/10.1371/journal.pone.0226631

Boström-Einarsson, L., Ceccarelli, D., Babcock, R.C., Bayraktarov, E., Cook, N., Harrison, P., Hein, M., Shaver, E., Smith, A., Stewart-Sinclair, P.J., Vardi, T., McLeod, I.M., 2018. Coral restoration in a changing world: A global synthesis of methods and techniques.

Bouwmeester, J., Daly, J., Zuchowicz, N., Lager, C., Henley, E.M., Quinn, M., Hagedorn, M., 2023. Solar radiation, temperature and the reproductive biology of the coral Lobactis scutaria in a changing climate. Sci. Rep. 13, 246. https://doi.org/10.1038/s41598-022-27207-6

Bowden-Kerby, A., 2001. Low-tech coral reef restoration methods modeled after natural fragmentation processes. Bull. Mar. Sci. 69, 915–931.

Box, S.J., Mumby, P.J., 2007. Effect of macroalgal competition on growth and survival of juenile Caribbean corals. Mar. Ecol. Prog. Ser. 342, 139–149. https://doi.org/10.3354/meps342139

Brandl, S.J., Rasher, D.B., Côté, I.M., Casey, J.M., Darling, E.S., Lefcheck, J.S., Duffy, J.E., 2019. Coral reef ecosystem functioning: eight core processes and the role of biodiversity. Front. Ecol. Environ. 17, 445–454. https://doi.org/10.1002/fee.2088

Broecker, W.S., Takahashi, T., 1966. Calcium carbonate precipitation on the Bahama Banks. J. Geophys. Res. 71, 1575–1602. https://doi.org/10.1029/JZ071i006p01575

Brown, B.E., Dunne, R.P., Ambarsari, I., Le Tissier, M.D.A., Satapoomin, U., 1999. Seasonal fluctuations in environmental factors and variations in symbiotic algae and chlorophyll pigments in four Indo-Pacific coral species. Mar. Ecol. Prog. Ser. 191, 53–69. https://doi.org/10.3354/meps191053

Brown, B.E., Dunne, R.P., Edwards, A.J., Sweet, M.J., Phongsuwan, N., 2015. Decadal environmental ‘memory’ in a reef coral? Mar. Biol. 162, 479–483. https://doi.org/10.1007/s00227-014-2596-2

Brown, B.E., Dunne, R.P., Goodson, M.S., Douglas, A.E., 2002. Experience shapes the susceptibility of a reef coral to bleaching. Coral Reefs 21, 119–126.

https://doi.org/10.1007/s00338-002-0215-z

Brown, J., Gillooly, J., Allen, A., Savage, V., West, G., 2004. Toward a metabolic theory of ecology. Ecology 85, 1771–1789. https://doi.org/10.1890/03-9000

Brown, K.T., Bender-Champ, D., Achlatis, M., van der Zande, R.M., Kubicek, A., Martin, S.B., Castro-Sanguino, C., Dove, S.G., Hoegh-Guldberg, O., 2021. Habitat-specific biogenic production and erosion influences net framework and sediment coral reef carbonate budgets. Limnol. Oceanogr. 66, 349–365. https://doi.org/10.1002/lno.11609

Browne, N.K., Smithers, S.G., Perry, C.T., 2013. Carbonate and terrigenous sediment budgets for two inshore turbid reefs on the central Great Barrier Reef. Mar. Geol. 346, 101–123. https://doi.org/10.1016/j.margeo.2013.08.011

Bruckner, A.W., 2002. Potential Application of the U.S. Endangered Species Act as a Conservation Strategy, in: The Caribbean Acropora Workshop, Vol 184. NOAA Technical Memorandum NMFSOPR-24, Silver Spring, Miami, Florida, p. 199.

Bruno, J.F., Edmunds, P.J., 1998. Metabolic consequences of phenotypic plasticity in the coral Madracis mirabilis (Duchassaing and Michelotti): the effect of morphology and water flow on aggregate respiration. J. Exp. Mar. Bio. Ecol. 229, 187–195. https://doi.org/10.1016/S0022-0981(98)00050-1

Bruno, J.F., Valdivia, A., 2016. Coral reef degradation is not correlated with local human population density. Sci. Rep. 6, 29778. https://doi.org/10.1038/srep29778

Bucher, D.J., Harriott, V.J., Roberts, L.G., 1998. Skeletal micro-density, porosity and bulk density of acroporid corals. J. Exp. Mar. Bio. Ecol. 228, 117–136. https://doi.org/10.1016/S0022-0981(98)00020-3

Buerger, P., Alvarez-Roa, C., Coppin, C.W., Pearce, S.L., Chakravarti, L.J., Oakeshott, J.G.,

Edwards, O.R., van Oppen, M.J.H., 2020. Heat-evolved microalgal symbionts increase coral bleaching tolerance. Sci. Adv. 6, eaba2498. https://doi.org/10.1126/sciadv.aba2498

Butler, J.R.A., Wong, G.Y., Metcalfe, D.J., Honzák, M., Pert, P.L., Rao, N., van Grieken, M.E., Lawson, T., Bruce, C., Kroon, F.J., Brodie, J.E., 2013. An analysis of trade-offs between multiple ecosystem services and stakeholders linked to land use and water quality management in the Great Barrier Reef, Australia. Agric. Ecosyst. Environ. 180, 176–191. https://doi.org/10.1016/j.agee.2011.08.017

Calle-Triviño, J., Muñiz-Castillo, A.I., Cortés-Useche, C., Morikawa, M., Sellares-Blasco, R., Arias-González, J.E., 2021. Approach to the Functional Importance of Acropora cervicornis in Outplanting Sites in the Dominican Republic. Front. Mar. Sci. 8, 668325. https://doi.org/10.3389/fmars.2021.668325

Calle-Triviño, J., Rivera-Madrid, R., León-Pech, M.G., Cortés-Useche, C., Sellares-Blasco, R.I., Aguilar-Espinosa, M., Arias-González, J.E., 2020. Assessing and genotyping threatened staghorn coral Acropora cervicornis nurseries during restoration in southeast Dominican Republic. PeerJ 8, e8863. https://doi.org/10.7717/peerj.8863

Camp, E.F., 2022. Contingency planning for coral reefs in the Anthropocene; The potential of reef safe havens. Emerg. Top. Life Sci. 6, 107–124. https://doi.org/10.1042/ETLS20210232

Camp, E.F., Edmondson, J., Doheny, A., Rumney, J., Grima, A.J., Huete, A., Suggett, D.J., 2019. Mangrove lagoons of the Great Barrier Reef support coral populations persisting under extreme environmental conditions. Mar. Ecol. Prog. Ser. 625, 1–14. https://doi.org/10.3354/meps13073

Camp, E.F., Kahlke, T., Nitschke, M.R., Varkey, D., Fisher, N.L., Fujise, L., Goyen, S., Hughes, D.J., Lawson, C.A., Ros, M., Woodcock, S., Xiao, K., Leggat, W., Suggett,

D.J., 2020a. Revealing changes in the microbiome of Symbiodiniaceae under thermal stress. Environ. Microbiol. 22, 1294–1309. https://doi.org/10.1111/1462-2920.14935

Camp, E.F., Krause, S.L., Santos, L.M.F., Naumann, M.S., Kikuchi, R.K.P., Smith, D.J., Wild, C., Suggett, D.J., 2015. The "Flexi-Chamber": A Novel Cost-Effective In Situ Respirometry Chamber for Coral Physiological Measurements. PLoS One 10, e0138800. https://doi.org/10.1371/journal.pone.0138800

Camp, E.F., Nitschke, M.R., Clases, D., Gonzalez de Vega, R., Reich, H.G., Goyen, S., Suggett, D.J., 2022. Micronutrient content drives elementome variability amongst the Symbiodiniaceae. BMC Plant Biol. 22, 184. https://doi.org/10.1186/s12870-022-03512-0

Camp, E.F., Nitschke, M.R., Rodolfo-Metalpa, R., Houlbreque, F., Gardner, S.G., Smith, D.J., Zampighi, M., Suggett, D.J., 2017. Reef-building corals thrive within hot-acidified and deoxygenated waters. Sci. Rep. 7, 2434. https://doi.org/10.1038/s41598-017-02383-y

Camp, E.F., Schoepf, V., Mumby, P.J., Hardtke, L.A., Rodolfo-Metalpa, R., Smith, D.J., Suggett, D.J., 2018. The future of coral reefs subject to rapid climate change: Lessons from natural extreme environments. Front. Mar. Sci. 5, 4. https://doi.org/10.3389/fmars.2018.00004

Camp, E.F., Smith, D.J., Evenhuis, C., Enochs, I., Manzello, D., Woodcock, S., Suggett, D.J., 2016a. Acclimatization to high-variance habitats does not enhance physiological tolerance of two key Caribbean corals to future temperature and pH. Proc. R. Soc. B 283, 20160442. https://doi.org/10.1098/rspb.2016.0442

Camp, E.F., Spencer-Smith, T., Chapple, R., Eccles, S., Spindler, R., Varcoe, T., 2020b. Healthy People in a Healthy Environment: Key Directions Statement. Australian

Committee for IUCN, Sydney.

Camp, E.F., Suggett, D.J., Gendron, G., Jompa, J., Manfrino, C., Smith, D.J., 2016b. Mangrove and seagrass beds provide different biogeochemical services for corals threatened by climate change. Front. Mar. Sci. 3, 52. https://doi.org/10.3389/fmars.2016.00052

Camp, E.F., Suggett, D.J., Pogoreutz, C., Nitschke, M.R., Houlbreque, F., Hume, B.C.C., Gardner, S.G., Zampighi, M., Rodolfo-Metalpa, R., Voolstra, C.R., 2020c. Corals exhibit distinct patterns of microbial reorganisation to thrive in an extreme inshore environment. Coral Reefs 39, 701–716. https://doi.org/10.1007/s00338-019-01889-3

Carroll, A.G., Harrison, P.L., Adjeroud, M., 2016. Susceptibility of coral assemblages to successive bleaching events at Moorea, French Polynesia. Mar. Freshw. Res. 68, 760–771. https://doi.org/10.1071/MF15134

Caruso, C., Hughes, K., Drury, C., 2021. Selecting Heat-Tolerant Corals for Proactive Reef Restoration. Front. Mar. Sci. 8, 632027. https://doi.org/10.3389/fmars.2021.632027

Castro-Sanguino, C., Bozec, Y.M., Mumby, P.J., 2020. Dynamics of carbonate sediment production by Halimeda: implications for reef carbonate budgets. Mar. Ecol. Prog. Ser. 639, 91–106. https://doi.org/10.3354/meps13265

Ceccarelli, D.M., McLeod, I.M., Boström-Einarsson, L., Bryan, S.E., Chartrand, K.M., Emslie, M.J., Gibbs, M.T., Gonzalez Rivero, M., Hein, M.Y., Heyward, A., Kenyon, T.M., Lewis, B.M., Mattocks, N., Newlands, M., Schläppy, M.L., Suggett, D.J., Bay, L.K., 2020. Substrate stabilisation and small structures in coral restoration: State of knowledge, and considerations for management and implementation. PLoS One 15, e0240846. https://doi.org/10.1371/journal.pone.0240846

Chadwick, N.E., Loya, Y., 1990. Regeneration after experimental breakage in the solitary reef coral Fungia granulosa Klunzinger, 1879. J. Exp. Mar. Bio. Ecol. 142, 221–234. https://doi.org/10.1016/0022-0981(90)90093-R

Chamberland, V.F., Petersen, D., Vermeij, M.J.A., 2013. Restoration of critically endangered elkhorn coral (Acropora palmata) using sexually produced recruits, in: Joint International Scientific Diving Symposium. Curaçao, October 24-27 2020, pp. 43–48.

Chamberland, V.F., Vermeij, M.J.A., Brittsan, M., Carl, M., Schick, M., Snowden, S., Schrier, A., Petersen, D., 2015. Restoration of critically endangered elkhorn coral (Acropora palmata) populations using larvae reared from wild-caught gametes. Glob. Ecol. Conserv. 4, 526–537. https://doi.org/10.1016/j.gecco.2015.10.005

Chapron, L., Schoepf, V., Levas, S.J., Aschaffenburg, M.D., Warner, M.E., Grottoli, A.G., 2022. Natural Variability in Caribbean Coral Physiology and Implications for Coral Bleaching Resilience. Front. Mar. Sci. 8, 811055. https://doi.org/10.3389/fmars.2021.811055

Cheal, A.J., MacNeil, M.A., Emslie, M.J., Sweatman, H., 2017. The threat to coral reefs from more intense cyclones under climate change. Glob. Chang. Biol. 23, 1511–1524. https://doi.org/10.1111/gcb.13593

Chisholm, J.R.M., Gattuso, J.P., 1991. Validation of the alkalinity anomaly technique for investigating calcification of photosynthesis in coral reef communities. Limnol. Oceanogr. 36, 1232–1239. https://doi.org/10.4319/lo.1991.36.6.1232

Chong-Seng, K.M., Mannering, T.D., Pratchett, M.S., Bellwood, D.R., Graham, N.A.J., 2012. The Influence of Coral Reef Benthic Condition on Associated Fish Assemblages. PLoS One 7, e42167. https://doi.org/10.1371/journal.pone.0042167

Chow, M.H., Tsang, R.H.L., Lam, E.K.Y., Ang, P., 2016. Quantifying the degree of coral bleaching using digital photographic technique. J. Exp. Mar. Bio. Ecol. 479, 60–68. https://doi.org/10.1016/j.jembe.2016.03.003

Christie, W.W., Han, X., 2010. Isolation, Separation, Identification and Lipidomic Analysis, in: Christie, W.W. (Ed.), Lipid Analysis. Oily Press, Bridgewater, UK.

Ciais, P., Sabine, C., Bala, G., Bopp, L., Brovkin, V., Canadell, J., Chhabra, A., DeFries, R., Galloway, J., Heimann, M., Jones, C., Le Quéré, C., Myneni, R.B., Piao, S., Thornton, P., 2013. Carbon and other biogeochemical cycles, in: Stocker, T.F., Qin, D., Plattner, G.-K., Tignor, M., Allen, S.K., Boschung, J., Nauels, A., Xia, Y., Bex, V., Midgle, P.M. (Eds.), Climate Change 2013: The Physical Science Basis. Contribution of Working Group I to the Fifth Assessment Report of the Intergovernmental Panel on Climate Change. Cambridge University Press, Cambridge, United Kingdom and New York, NY, USA, pp. 465–570.

Cinner, J.E., Aswani, S., 2007. Integrating customary management into marine conservation. Biol. Conserv. 140, 201–216. https://doi.org/10.1016/j.biocon.2007.08.008

Clark, S., Edwards, A.J., 1995. Coral transplantation as an aid to reef rehabilitation: evaluation of a case study in the Maldive Islands. Coral Reefs 14, 201–213. https://doi.org/10.1007/BF00334342

Cole, A.J., Pratchett, M.S., Jones, G.P., 2008. Diversity and functional importance of coral-feeding fishes on tropical coral reefs. Fish Fish. 9, 286–307. https://doi.org/10.1111/j.1467-2979.2008.00290.x

Coles, S.L., Okiel, P.L.J., Lewis, C.R., 1976. Thermal Tolerance in Tropical versus Subtropical Pacific Reef Corals. Pacific Sci. 30, 159–166.

Conlan, J.A., Rocker, M.M., Francis, D.S., 2017. A comparison of two common sample preparation techniques for lipid and fatty acid analysis in three different coral morphotypes reveals quantitative and qualitative differences. PeerJ 5, e3645. https://doi.org/10.7717/peerj.3645

Cook, N., Smith, A., Songcuan, A., Cassidy, D., Sartori, G., McLeod, I., 2022. Lessons learned from small-scale coral outplanting intervention at a restoration site on the Great Barrier Reef. Ecol. Manag. Restor. 23, 89–93. https://doi.org/10.1111/emr.12547

Cooper, R.J., Hiscock, K.M., Lovett, A.A., 2019. Mitigation Measures for Water Pollution and Flooding, in: von Haaren, C., Lovett, A., Albert, C. (Eds.), Landscape Planning with Ecosystem Services. Landscape Series, Vol 24. Springer Nature B.V., Dordrecht, The Netherlands, pp. 359–379. https://doi.org/10.1007/978-94-024-1681-7_23

Cornwell, B., Armstrong, K., Walker, N., Lippert, M., Nestor, V., Golbuu, Y., Palumbi, S.R., 2021. Widespread variation in heat tolerance and symbiont load are associated with growth tradeoffs in the coral Acropora hyacinthus in palau. Elife 10, e64790. https://doi.org/10.7554/eLife.64790

Coronado, I., Fine, M., Bosellini, F.R., Stolarski, J., 2019. Impact of ocean acidification on crystallographic vital effect of the coral skeleton. Nat. Commun. 10, 2896. https://doi.org/10.1038/s41467-019-10833-6

Courtney, T.A., Barkley, H.C., Chan, S., Couch, C.S., Kindinger, T.L., Oliver, T.A., Kriegman, D.J., Andersson, A.J., Mayagüez, R., Rico, P., 2022. Rapid assessments of Pacific Ocean net coral reef carbonate budgets and net calcification following the 2014-2017 global coral bleaching event. Limnol. Ocean. 67, 1687–1700. https://doi.org/10.1002/lno.12159

Crabbe, J., Rodríguez-Martínez, R., Villamizar, E., Goergen, L., Croquer, A., Banaszak, A.,

2022. Acropora cervicornis [WWW Document]. IUCN Red List Threat. Species. URL https://www.iucnredlist.org/es/species/133381/165860142 (accessed 2.10.24).

Cramer, K.L., Jackson, J.B.C., Donovan, M.K., Greenstein, B.J., Korpanty, C.A., Cook, G.M., Pandolfi, J.M., 2020. Widespread loss of Caribbean acroporid corals was underway before coral bleaching and disease outbreaks. Sci. Adv. 6, eaax9395. https://doi.org/10.1126/sciadv.aax9395

Crook, E.D., Cohen, A.L., Rebolledo-Vieyra, M., Hernandez, L., Paytan, A., 2013. Reduced calcification and lack of acclimatization by coral colonies growing in areas of persistent natural acidification. Proc. Natl. Acad. Sci. 110, 11044–11049. https://doi.org/10.1073/pnas.1301589110

Cunning, R., Parker, K.E., Johnson-Sapp, K., Karp, R.F., Wen, A.D., Williamson, O.M., Bartels, E., D'Alessandro, M., Gilliam, D.S., Hanson, G., Levy, J., Lirman, D., Maxwell, K., Million, W.C., Moulding, A.L., Moura, A., Muller, E.M., Nedimyer, K., Reckenbeil, B., Van Hooidonk, R., Dahlgren, C., Kenkel, C., Parkinson, J.E., Baker, A.C., 2021. Census of heat tolerance among Florida's threatened staghorn corals finds resilient individuals throughout existing nursery populations. Proc. R. Soc. B 288, 20211613. https://doi.org/10.1098/rspb.2021.1613

Cunning, R., Ritson-Williams, R., Gates, R.D., 2016. Patterns of bleaching and recovery of Montipora capitata in Kāneʻohe Bay, Hawaiʻi, USA. Mar. Ecol. Prog. Ser. 551, 131–139. https://doi.org/10.3354/meps11733

Cyronak, T., Andersson, A.J., Langdon, C., Albright, R., Bates, N.R., Caldeira, K., Carlton, R., Corredor, J.E., Dunbar, R.B., Enochs, I., Erez, J., Eyre, B.D., Gattuso, J.-P., Gledhill, D., Kayanne, H., Kline, D.I., Koweek, D.A., Lantz, C., Lazar, B., Manzello, D., McMahon, A., Meléndez, M., Page, H.N., Santos, I.R., Schulz, K.G., Shaw, E.,

Silverman, J., Suzuki, A., Teneva, L., Watanabe, A., Yamamoto, S., 2018. Taking the metabolic pulse of the world's coral reefs. PLoS One 13, e0190872. https://doi.org/10.1371/journal.pone.0190872

Cyronak, T., Santos, I.R., Eyre, B.D., 2013. Permeable coral reef sediment dissolution driven by elevated pCO2 and pore water advection. Geophys. Res. Lett. 40, 4876–4881. https://doi.org/10.1002/grl.50948

Darling, E.S., Alvarez-Filip, L., Oliver, T.A., Mcclanahan, T.R., Côté, I.M., 2012. Evaluating life-history strategies of reef corals from species traits. Ecol. Lett. 15, 1378–1386. https://doi.org/10.1111/j.1461-0248.2012.01861.x

Das, S., Islam, A.R.M.T., Kamruzzaman, M., 2022. Assessment of climate change impact on temperature extremes in a tropical region with the climate projections from CMIP6 model. Clim. Dyn. 60, 603–622. https://doi.org/10.1007/s00382-022-06416-9

Davies, P.J., Hutchings, P.A., 1983. Initial colonization, erosion and accretion of coral substrate. Coral Reefs 2, 27–35. https://doi.org/10.1007/BF00304729

De'Ath, G., Fabricius, K.E., Sweatman, H., Puotinen, M., 2012. The 27-year decline of coral cover on the Great Barrier Reef and its causes. Proc. Natl. Acad. Sci. 109, 17995–17999. https://doi.org/10.1073/pnas.1208909109

dela Cruz, D.W., 2019. Coral reef restoration using mass coral larval enhancement. Doctoral Dissertation. Southern Cross University.

dela Cruz, D.W., Rinkevich, B., Gomez, E.D., Yap, H.T., 2015. Assessing an abridged nursery phase for slow growing corals used in coral restoration. Ecol. Eng. 84, 408–415. https://doi.org/10.1016/j.ecoleng.2015.09.042

Deschaseaux, E.S.M., Deseo, M.A., Shepherd, K.M., Jones, G.B., Harrison, P.L., 2013. Air

blasting as the optimal approach for the extraction of antioxidants in coral tissue. J. Exp. Mar. Bio. Ecol. 448, 146–148. https://doi.org/10.1016/j.jembe.2013.07.002

Deschaseaux, E.S.M., Jones, G.B., Deseo, M.A., Shepherd, K.M., Kiene, R.P., Swan, H.B., Harrison, P.L., Eyre, B.D., 2014. Effects of environmental factors on dimethylated sulfur compounds and their potential role in the antioxidant system of the coral holobiont. Limnol. Oceanogr. 59, 758–768. https://doi.org/10.4319/lo.2014.59.3.0758

DiBattista, J.D., Fowler, A.M., Riley, I.J., Reader, S., Hay, A., Parkinson, K., Hobbs, J.P.A., 2022. The use of environmental DNA to monitor impacted coastal estuaries. Mar. Pollut. Bull. 181, 113860. https://doi.org/10.1016/j.marpolbul.2022.113860

Dietzel, A., Bode, M., Connolly, S.R., Hughes, T.P., 2020. Long-term shifts in the colony size structure of coral populations along the Great Barrier Reef. Proc. R. Soc. B 287, 20201432. https://doi.org/10.1098/rspb.2020.1432

Dimson, M., Gillespie, T.W., 2020. Trends in active restoration of tropical dry forest: Methods, metrics, and outcomes. For. Ecol. Manage. 467, 118150. https://doi.org/10.1016/j.foreco.2020.118150

Dixon, G., Matz, M., 2021. Benchmarking DNA methylation assays in a reef-building coral. Mol. Ecol. Resour. 21, 464–477. https://doi.org/10.1111/1755-0998.13282

Dixon, G.B., Davies, S.W., Aglyamova, G.A., Meyer, E., Bay, L.K., Matz, M. V., 2015. Genomic determinants of coral heat tolerance across latitudes. Science. 348, 1460–1462. https://doi.org/10.1126/science.1261224

Done, T.J., 1992. Effects of tropical cyclone waves on ecological and geomorphological structures on the Great Barrier Reef. Cont. Shelf Res. 12, 859–872. https://doi.org/10.1016/0278-4343(92)90048-O

Drury, C., 2020. Resilience in reef-building corals: The ecological and evolutionary importance of the host response to thermal stress. Mol. Ecol. 29, 448–465. https://doi.org/10.1111/mec.15337

Drury, C., Lirman, D., 2021. Genotype by environment interactions in coral bleaching. Proc. R. Soc. B 288, 20210177. https://doi.org/10.1098/rspb.2021.0177

Drury, C., Manzello, D., Lirman, D., 2017. Genotype and local environment dynamically influence growth, disturbance response and survivorship in the threatened coral, Acropora cervicornis. PLoS One 12, e0174000. https://doi.org/10.1371/journal.pone.0174000

Duarte, C.M., Agusti, S., Barbier, E., Britten, G.L., Castilla, J.C., Gattuso, J.-P.P., Fulweiler, R.W., Hughes, T.P., Knowlton, N., Lovelock, C.E., Lotze, H.K., Predragovic, M., Poloczanska, E., Roberts, C., Worm, B., 2020. Rebuilding marine life. Nature 580, 39–51. https://doi.org/10.1038/s41586-020-2146-7

Dubinsky, Z., Jokiel, P.L., 1994. Ratio of energy and nutrient fluxes regulates symbiosis between zooxanthellae and corals. Pacific Sci. 48, 313–324.

Dubinsky, Z., Stambler, N., Ben-Zion, M., McCloskey, L.R., Muscatine, L., Falkowski, P.G., 1990. The effect of external nutrient resources on the optical properties and photosynthetic efficiency of Stylophora pistillata. Proc. R. Soc. B 239, 231–246. https://doi.org/10.1098/rspb.1990.0015

DuBois, M., Gilles, K.A., Hamilton, J.K., Rebers, P.A., Smith, F., 1956. Colorimetric Method for Determination of Sugars and Related Substances. Anal. Chem. 28, 350–356. https://doi.org/10.1021/ac60111a017

Eakin, C.M., 1996. Where have all the carbonates gone? A model comparison of calcium

carbonate budgets before and after the 1982-1983 El Niño at Uva Island in the eastern Pacific. Coral Reefs 15, 109–119. https://doi.org/10.1007/BF01771900

Eakin, C.M., Sweatman, H.P.A., Brainard, R.E., 2019. The 2014–2017 global-scale coral bleaching event: insights and impacts. Coral Reefs 38, 539–545. https://doi.org/10.1007/s00338-019-01844-2

Edmunds, P.J., 1994. Evidence that reef-wide patterns of coral bleaching may be the result of the distribution of bleaching-susceptible clones. Mar. Biol. 121, 137–142. https://doi.org/10.1007/BF00349482

Edmunds, P.J., Elahi, R., 2007. The demographics of a 15-year decline in cover of the Caribbean reef coral Montastraea annularis. Ecol. Monogr. 77, 3–18. https://doi.org/10.1890/05-1081

Edwards, A., Guest, J., Shafir, S., Fisk, D., Gomez, E., Rinkevich, B., Heyward, A., Makoto, O., Iwao, K., Dizon, R., Morse, A., Boch, C., Job, S., Bongiorni, L., Levy, G., Shaish, L., Wells, S., 2010. Reef Rehabilitation Manual, The Coral Reef Targeted Research & Capacity. St. Lucia, Australia.

Ellis, J.I., Jamil, T., Anlauf, H., Coker, D.J., Curdia, J., Hewitt, J., Jones, B.H., Krokos, G., Kürten, B., Hariprasad, D., Roth, F., Carvalho, S., Hoteit, I., 2019. Multiple stressor effects on coral reef ecosystems. Glob. Chang. Biol. 25, 4131–4146. https://doi.org/10.1111/gcb.14819

Enochs, I.C., Toth, L.T., Brandtneris, V.W., Afflerbach, J.C., Manzello, D.P., 2011. Environmental determinants of motile cryptofauna on an eastern Pacific coral reef. Mar. Ecol. Prog. Ser. 438, 105–118. https://doi.org/10.3354/meps09259

Epstein, N., Bak, R.P.M., Rinkevich, B., 2003. Applying forest restoration principles to coral

reef rehabilitation. Aquat. Conserv. Mar. Freshw. Ecosyst. 13, 387–395. https://doi.org/10.1002/aqc.558

Epstein, N., Bak, R.P.M., Rinkevich, B., 2001. Strategies for gardening denuded coral reef areas: The applicability of using different types of coral material for reef restoration. Restor. Ecol. 9, 432–442. https://doi.org/10.1046/j.1526-100X.2001.94012.x

Evensen, N.R., Edmunds, P.J., Sakai, K., 2015. Effects of pCO2 on spatial competition between the corals Montipora aequituberculata and Porites lutea. Mar. Ecol. Prog. Ser. 541, 123–134. https://doi.org/10.3354/meps11512

Evensen, N.R., Fine, M., Perna, G., Voolstra, C.R., Barshis, D.J., 2021. Remarkably high and consistent tolerance of a Red Sea coral to acute and chronic thermal stress exposures. Limnol. Oceanogr. 66, 1718–1729. https://doi.org/10.1002/lno.11715

Evensen, N.R., Voolstra, C.R., Fine, M., Perna, G., Buitrago-López, C., Cárdenas, A., Banc-Prandi, G., Rowe, K., Barshis, D.J., 2022. Empirically derived thermal thresholds of four coral species along the Red Sea using a portable and standardized experimental approach. Coral Reefs 41, 239–252. https://doi.org/10.1007/s00338-022-02233-y

Fadli, N., Campbell, S.J., Ferguson, K., Keyse, J., Rudi, E., Riedel, A., Baird, A.H., 2012. The role of habitat creation in coral reef conservation: A case study from Aceh, Indonesia. Oryx 46, 501–507. https://doi.org/10.1017/S0030605312000142

Fagoonee, I., Wilson, H.B., Hassell, M.P., Turner, J.R., 1999. The dynamics of zooxanthellae populations: A long-term study in the field. Science. 283, 843–845. https://doi.org/10.1126/science.283.5403.843

Falkowski, P.G., Dubinsky, Z., 1981. Light-shade adaptation of Stylophora pistillata, a hermatypic coral from the Gulf of Eilat. Nature 289, 172–174.

https://doi.org/10.1038/289172a0

Fantazzini, P., Mengoli, S., Pasquini, L., Bortolotti, V., Brizi, L., Mariani, M., Di Giosia, M., Fermani, S., Capaccioni, B., Caroselli, E., Prada, F., Zaccanti, F., Levy, O., Dubinsky, Z., Kaandorp, J.A., Konglerd, P., Hammel, J.U., Dauphin, Y., Cuif, J.P., Weaver, J.C., Fabricius, K.E., Wagermaier, W., Fratzl, P., Falini, G., Goffredo, S., 2015. Gains and losses of coral skeletal porosity changes with ocean acidification acclimation. Nat. Commun. 6, 7785. https://doi.org/10.1038/ncomms8785

Ferrario, F., Beck, M.W., Storlazzi, C.D., Micheli, F., Shepard, C.C., Airoldi, L., 2014. The effectiveness of coral reefs for coastal hazard risk reduction and adaptation. Nat. Commun. 5, 3794. https://doi.org/10.1038/ncomms4794

Ferrier-Pagès, C., Schoelzke, V., Jaubert, J., Muscatine, L., Hoegh-Guldberg, O., 2001. Response of a scleractinian coral, Stylophora pistillata, to iron and nitrate enrichment. J. Exp. Mar. Bio. Ecol. 259, 249–261. https://doi.org/10.1016/S0022-0981(01)00241-6

Ferse, S.C.A., 2008. Multivariate responses of the coral reef fish community to artificial structures and coral transplants, in: The 11th International Coral Reef Symposium. 7-11 July 2008, Session number 24, Ft. Lauderdale, Florida, pp. 1225–1229.

Fine, M., Gildor, H., Genin, A., 2013. A coral reef refuge in the Red Sea. Glob. Chang. Biol. 19, 3640–3647. https://doi.org/10.1111/gcb.12356

Finegan, B., Peña-Claros, M., de Oliveira, A., Ascarrunz, N., Bret-Harte, M.S., Carreño-Rocabado, G., Casanoves, F., Díaz, S., Eguiguren Velepucha, P., Fernandez, F., Licona, J.C., Lorenzo, L., Salgado Negret, B., Vaz, M., Poorter, L., 2015. Does functional trait diversity predict above-ground biomass and productivity of tropical forests? Testing three alternative hypotheses. J. Ecol. 103, 191–201. https://doi.org/10.1111/1365-2745.12346

Fitt, W.K., 2000. Cellular growth of host and symbiont in a cnidarian-zooxanthellar symbiosis. Biol. Bull. 198, 110–120. https://doi.org/10.2307/1542809

Foden, W., Midgley, G.F., Hughes, G., Bond, W.J., Thuiller, W., Hoffman, M.T., Kaleme, P., Underhill, L.G., Rebelo, A., Hannah, L., 2007. A changing climate is eroding the geographical range of the Namib Desert tree Aloe through population declines and dispersal lags. Divers. Distrib. 13, 645–653. https://doi.org/10.1111/j.1472-4642.2007.00391.x

Fox, H.E., Harris, J.L., Darling, E.S., Ahmadia, G.N., Estradivari, Razak, T.B., 2019. Rebuilding coral reefs: success (and failure) 16 years after low-cost, low-tech restoration. Restor. Ecol. 27, 862–869. https://doi.org/10.1111/rec.12935

Fox, H.E., Pet, J.S., Dahuri, R., Caldwell, R.L., 2003. Recovery in rubble fields: Long-term impacts of blast fishing. Mar. Pollut. Bull. 46, 1024–1031. https://doi.org/10.1016/S0025-326X(03)00246-7

Frame, D.J., Rosier, S.M., Noy, I., Harrington, L.J., Carey-Smith, T., Sparrow, S.N., Stone, D.A., Dean, S.M., 2020. Climate change attribution and the economic costs of extreme weather events: a study on damages from extreme rainfall and drought. Clim. Change 162, 781–797. https://doi.org/10.1007/s10584-020-02729-y

Fraser, K.M., Stuart-Smith, R.D., Ling, S.D., Edgar, G.J., 2021. High biomass and productivity of epifaunal invertebrates living amongst dead coral. Mar. Biol. 168, 102. https://doi.org/10.1007/s00227-021-03911-1

Freedman, R.M., Espasandin, C., Holcombe, E.F., Whitcraft, C.R., Allen, B.J., Witting, D., Lowe, C.G., 2016. Using Movements and Habitat Utilization as a Functional Metric of Restoration for Estuarine Juvenile Fish Habitat. Mar. Coast. Fish. 8, 361–373. https://doi.org/10.1080/19425120.2016.1161681

Frieler, K., Meinshausen, M., Golly, A., Mengel, M., Lebek, K., Donner, S.D., Hoegh-Guldberg, O., 2013. Limiting global warming to 2 °C is unlikely to save most coral reefs. Nat. Clim. Chang. 3, 165–170. https://doi.org/10.1038/nclimate1674

Frölicher, T.L., Fischer, E.M., Gruber, N., 2018. Marine heatwaves under global warming. Nature 560, 360–364. https://doi.org/10.1038/s41586-018-0383-9

Gallagher, R. V., Falster, D.S., Maitner, B.S., Salguero-Gómez, R., Vandvik, V., Pearse, W.D., Schneider, F.D., Kattge, J., Poelen, J.H., Madin, J.S., Ankenbrand, M.J., Penone, C., Feng, X., Adams, V.M., Alroy, J., Andrew, S.C., Balk, M.A., Bland, L.M., Boyle, B.L., Bravo-Avila, C.H., Brennan, I., Carthey, A.J.R., Catullo, R., Cavazos, B.R., Conde, D.A., Chown, S.L., Fadrique, B., Gibb, H., Halbritter, A.H., Hammock, J., Hogan, J.A., Holewa, H., Hope, M., Iversen, C.M., Jochum, M., Kearney, M., Keller, A., Mabee, P., Manning, P., McCormack, L., Michaletz, S.T., Park, D.S., Perez, T.M., Pineda-Munoz, S., Ray, C.A., Rossetto, M., Sauquet, H., Sparrow, B., Spasojevic, M.J., Telford, R.J., Tobias, J.A., Violle, C., Walls, R., Weiss, K.C.B., Westoby, M., Wright, I.J., Enquist, B.J., 2020. Open Science principles for accelerating trait-based science across the Tree of Life. Nat. Ecol. Evol. 4, 294–303. https://doi.org/10.1038/s41559-020-1109-6

Gann, G., McDonald, T., Walder, B., Aronson, J., Nelson, C., Jonson, J., Hallett, J., Eisenberg, C., Guariguata, M., Liu, J., Hua, F., Echeverria, C., Gonzales, E., Shaw, N., Decleer, K., Dixon, K., 2019. International principles and standards for the practice of ecological restoration. Restor. Ecol. 27, S1–S46. https://doi.org/10.1111/rec.13035

Garcia, N.S., Sexton, J., Riggins, T., Brown, J., Lomas, M.W., Martiny, A.C., 2018. High variability in cellular stoichiometry of carbon, nitrogen, and phosphorus within classes of marine eukaryotic phytoplankton under sufficient nutrient conditions. Front.

Microbiol. 9, 543. https://doi.org/10.3389/fmicb.2018.00543

Gardner, S.G., Camp, E.F., Smith, D.J., Kahlke, T., Osman, E.O., Gendron, G., Hume, B.C.C., Pogoreutz, C., Voolstra, C.R., Suggett, D.J., 2019. Coral microbiome diversity reflects mass coral bleaching susceptibility during the 2016 El Niño heat wave. Ecol. Evol. 9, 938–956. https://doi.org/10.1002/ece3.4662

Gardner, S.G., Raina, J.B., Nitschke, M.R., Nielsen, D.A., Stat, M., Motti, C.A., Ralph, P.J., Petrou, K., 2017. A multi-trait systems approach reveals a response cascade to bleaching in corals. BMC Biol. 15, 117. https://doi.org/10.1186/s12915-017-0459-2

Gardner, T.A., Côté, I.M., Gill, J.A., Grant, A., Watkinson, A.R., 2003. Long-Term Region-Wide Declines in Caribbean Corals. Science. 301, 958–960. https://doi.org/10.1126/science.1086050

Garnier, E., Navas, M.L., 2012. A trait-based approach to comparative functional plant ecology: Concepts, methods and applications for agroecology. A review. Agron. Sustain. Dev. 32, 365–399. https://doi.org/10.1007/s13593-011-0036-y

GBR Biology, 2021. Operational Procedure for Reef Star installation, maintenance and monitoring.

Gillett, N.P., Kirchmeier-Young, M., Ribes, A., Shiogama, H., Hegerl, G.C., Knutti, R., Gastineau, G., John, J.G., Li, L., Nazarenko, L., Rosenbloom, N., Seland, Ø., Wu, T., Yukimoto, S., Ziehn, T., 2021. Constraining human contributions to observed warming since the pre-industrial period. Nat. Clim. Chang. 11, 207–212. https://doi.org/10.1038/s41558-020-00965-9

Glynn, P.W., 1984. Widespread Coral Mortality and the 1982–83 El Niño Warming Event. Environ. Conserv. 11, 133–146. https://doi.org/10.1017/S0376892900013825

Glynn, P.W., Maté, J.L., Baker, A.C., Calderón, M.O., 2001. Coral bleaching and mortality in Panama and Ecuador during the 1997-1998 El Niño-Southern Oscillation event: Spatial/temporal patterns and comparisons with the 1982-1983 event. Bull. Mar. Sci. 69, 79–109.

Gnaiger, E., Bitterlich, G., 1984. Proximate biochemical composition and caloric content calculated from elemental CHN analysis: a stoichiometric concept. Oecologia 62, 289–298. https://doi.org/10.1007/BF00384259

Good, A.M., Bahr, K.D., 2021. The coral conservation crisis: interacting local and global stressors reduce reef resiliency and create challenges for conservation solutions. SN Appl. Sci. 3, 312. https://doi.org/10.1007/s42452-021-04319-8

Goreau, T.F., Goreau, N.I., Goreau, T.J., 1979. Corals and coral reefs. Sci. Am. Mag. 241, 124. https://doi.org/10.1038/scientificamerican0879-124

Goreau, Thomas J., Hilbertz, W., 2012. Reef restoration using seawater electrolysis in Jamaica, in: Goreau, T. J., Trench, R.K. (Eds.), Innovative Methods of Marine Ecosystem Restoration. CRC Press, Boca Raton, FL, USA, pp. 35–45. https://doi.org/10.1201/b14314

Graham, N.A.J., Jennings, S., MacNeil, M.A., Mouillot, D., Wilson, S.K., 2015. Predicting climate-driven regime shifts versus rebound potential in coral reefs. Nature 518, 94–97. https://doi.org/10.1038/nature14140

Graham, N.A.J.J., Wilson, S.K., Jennings, S., Polunin, N.V.C.C., Bijoux, J.P., Robinson, J., 2006. Dynamic fragility of oceanic coral reef ecosystems. Proc. Natl. Acad. Sci. 103, 8425–8429. https://doi.org/10.1073/pnas.0600693103

Great Barrier Reef Marine Park Authority, 2021. Science and Knowledge Needs for

Management. Townsville.

Great Barrier Reef Marine Park Authority, 2020. Reef Health Update [WWW Document]. URL https://www2.gbrmpa.gov.au/learn/reef-health/past-reef-health-updates (accessed 3.25.22).

Great Barrier Reef Marine Park Authority, 2019. Great Barrier Reef Outlook Report 2019. Townsville.

Great Barrier Reef Marine Park Authority, 2017. Great Barrier Reef blueprint for resilience. Townsville.

Greenstein, B.J., Pandolfi, J.M., 2003. Taphonomic alteration of reef corals: Effects of reef environment and coral growth form II: The Florida Keys. Palaios 18, 495–509. https://doi.org/10.1669/0883-1351(2003)018<0495:TAORCE>2.0.CO;2

Greer, L., Clark, T., Waggoner, T., Busch, J., Guilderson, T.P., Wirth, K., Zhao, J., Curran, H.A., 2020. Coral Gardens Reef, Belize: A refugium in the face of Caribbean-wide Acropora spp. coral decline. PLoS One 15, e0239267. https://doi.org/10.1371/journal.pone.0239267

Grima, A.J., Clases, · David, Gonzalez De Vega, R., Nitschke, M.R., Goyen, S., David, ·, Suggett, J., Camp, E.F., 2022. Species-specific elementomes for scleractinian coral hosts and their associated Symbiodiniaceae. Coral Reefs 41, 1115–1130. https://doi.org/10.1007/s00338-022-02259-2

Grottoli, A.G., Rodrigues, L.J., Juarez, C., 2004. Lipids and stable carbon isotopes in two species of Hawaiian corals, Porites compressa and Montipora verrucosa, following a bleaching event. Mar. Biol. 145, 621–631. https://doi.org/10.1007/s00227-004-1337-3

Grottoli, A.G., Rodrigues, L.J., Palardy, J.E., 2006. Heterotrophic plasticity and resilience in

bleached corals. Nature 440, 1186–1189. https://doi.org/10.1038/nature04565

Grottoli, A.G., Tchernov, D., Winters, G., 2017. Physiological and biogeochemical responses of super-corals to thermal stress from the northern gulf of Aqaba, Red Sea. Front. Mar. Sci. 4, 215. https://doi.org/10.3389/fmars.2017.00215

Grottoli, A.G., Wilkins, M.J., Johnston, M.D., Levas, S., Schoepf, V., Dalcin, M.P., Wilkins, M.J., Warner, M.E., Cai, W.-J., Hoadley, K.D., Pettay, D.T., Melman, T.F., 2018. Coral physiology and microbiome dynamics under combined warming and ocean acidification. PLoS One 13, e0191156. https://doi.org/10.1371/journal.pone.0191156

Guest, J.R., Baird, A.H., Maynard, J.A., Muttaqin, E., Edwards, A.J., Campbell, S.J., Yewdall, K., Affendi, Y.A., Chou, L.M., 2012. Contrasting Patterns of Coral Bleaching Susceptibility in 2010 Suggest an Adaptive Response to Thermal Stress. PLoS One 7, e33353. https://doi.org/10.1371/journal.pone.0033353

Guest, J.R., Baria, M. V., Gomez, E.D., Heyward, A.J., Edwards, A.J., 2014. Closing the circle: Is it feasible to rehabilitate reefs with sexually propagated corals? Coral Reefs 33, 45–55. https://doi.org/10.1007/s00338-013-1114-1

Gutierrez-Heredia, L., Benzoni, F., Murphy, E., Reynaud, E.G., 2016. End to End Digitisation and Analysis of Three-Dimensional Coral Models, from Communities to Corallites. PLoS One 11, e0149641. https://doi.org/10.1371/journal.pone.0149641

Gutiérrez-Heredia, L., D'Helft, C., Reynaud, E.G., 2015. Simple methods for interactive 3D modeling, measurements, and digital databases of coral skeletons. Limnol. Oceanogr. Methods 13, e10017. https://doi.org/10.1002/lom3.10017

Habibullah, M.S., Din, B.H., Tan, S.H., Zahid, H., 2022. Impact of climate change on biodiversity loss: global evidence. Environ. Sci. Pollut. Res. 29, 1073–1086.

https://doi.org/10.1007/s11356-021-15702-8

Hackerott, S., Martell, H.A., Eirin-Lopez, J.M., 2021. Coral environmental memory: causes, mechanisms, and consequences for future reefs. Trends Ecol. Evol. 36, 1011–1023. https://doi.org/10.1016/j.tree.2021.06.014

Hagedorn, M., Page, C.A., O'Neil, K.L., Flores, D.M., Tichy, L., Conn, T., Chamberland, V.F., Lager, C., Zuchowicz, N., Lohr, K., Blackburn, H., Vardi, T., Moore, J., Moore, T., Baums, I.B., Vermeij, M.J.A., Marhaver, K.L., 2021. Assisted gene flow using cryopreserved sperm in critically endangered coral. Proc. Natl. Acad. Sci. 118, e2110559118. https://doi.org/10.1073/pnas.2110559118

Halpern, B.S., Walbridge, S., Selkoe, K.A., Kappel, C. V., Micheli, F., D'Agrosa, C., Bruno, J.F., Casey, K.S., Ebert, C., Fox, H.E., Fujita, R., Heinemann, D., Lenihan, H.S., Madin, E.M.P., Perry, M.T., Selig, E.R., Spalding, M., Steneck, R., Watson, R., 2008. A global map of human impact on marine ecosystems. Science. 319, 948–952. https://doi.org/10.1126/science.1149345

Harborne, A.R., Rogers, A., Bozec, Y.M., Mumby, P.J., 2017. Multiple Stressors and the Functioning of Coral Reefs. Ann. Rev. Mar. Sci. 9, 445–468. https://doi.org/10.1146/annurev-marine-010816-060551

Harmelin-Vivien, M., 1994. The Effects of Storms and Cyclones on Coral Reefs: A Review. J. Coast. Res. 12, 211–231.

Harrison, P.L., dela Cruz, D.W., Cameron, K.A., Cabaitan, P.C., 2021. Increased Coral Larval Supply Enhances Recruitment for Coral and Fish Habitat Restoration. Front. Mar. Sci. 8, 750210. https://doi.org/10.3389/fmars.2021.750210

Hastings, R.A., Rutterford, L.A., Freer, J.J., Collins, R.A., Simpson, S.D., Genner, M.J.,

2020. Climate Change Drives Poleward Increases and Equatorward Declines in Marine Species. Curr. Biol. 30, 1572–1577. https://doi.org/10.1016/j.cub.2020.02.043

Hein, M., Beeden, R., Birtles, A., Gardiner, N., Le Berre, T., Levy, J., Marshall, N., Scott, C., Terry, L., Willis, B., 2020a. Coral restoration effectiveness: Multiregional snapshots of the long-term responses of coral assemblages to restoration. Diversity 12, 153. https://doi.org/10.3390/d12040153

Hein, M., Beeden, R., Birtles, R.A., Chase, T.J., Couture, F., Haskin, E., Marshall, N., Ripple, K., Terry, L., Willis, B.L., Willis, R., Gardiner, N.M., 2020b. Effects of coral restoration on fish communities: snapshots of long-term, multi-regional responses and implications for practice. Restor. Ecol. 28, 1158–1171. https://doi.org/10.1111/rec.13177

Hein, M., McLeod, I.M., Shaver, E., Vardi, T., Pioch, S., Boström-Einarsson, L., Ahmed, M., Grimsditch, G., 2020c. Coral reef restoration as a strategy to improve ecosystem services – A guide to coral restoration methods, Ecological Engineering. Nairobi, Kenya.

Hein, M., Vardi, T., Shaver, E.C., Pioch, S., Boström-Einarsson, L., Ahmed, M., Grimsditch, G., McLeod, I.M., 2021. Perspectives on the Use of Coral Reef Restoration as a Strategy to Support and Improve Reef Ecosystem Services. Front. Mar. Sci. 8, 618303. https://doi.org/10.3389/fmars.2021.618303

Hein, M., Willis, B.L., Beeden, R., Birtles, A., 2017. The need for broader ecological and socioeconomic tools to evaluate the effectiveness of coral restoration programs. Restor. Ecol. 25, 873–883. https://doi.org/10.1111/rec.12580

Hennige, S.J., Suggett, D.J., Warner, M.E., McDougall, K.E., Smith, D.J., 2009. Photobiology of Symbiodinium revisited: Bio-physical and bio-optical signatures. Coral

Reefs 28, 179–195. https://doi.org/10.1007/s00338-008-0444-x

Heron, S.F., Maynard, J.A., van Hooidonk, R., Eakin, C.M., 2016. Warming trends and bleaching stress of the world's coral reefs 1985–2012. Sci. Rep. 6. https://doi.org/10.1038/srep38402

Hicks, C.C., McClanahan, T.R., Cinner, J.E., Hills, J.M., 2009. Trade-offs in values assigned to ecological goods and services associated with different coral reef management strategies. Ecol. Soc. 14, 10. https://doi.org/10.5751/ES-02712-140110

Hoadley, K.D., Pettay, D.T., Lewis, A., Wham, D., Grasso, C., Smith, R., Kemp, D.W., LaJeunesse, T., Warner, M.E., 2021. Different functional traits among closely related algal symbionts dictate stress endurance for vital Indo-Pacific reef-building corals. Glob. Chang. Biol. 27, 5295–5309. https://doi.org/10.1111/gcb.15799

Hock, K., Wolff, N.H., Ortiz, J.C., Condie, S.A., Anthony, K.R.N., Blackwell, P.G., Mumby, P.J., 2017. Connectivity and systemic resilience of the Great Barrier Reef. PLoS Biol. 15, e2003355. https://doi.org/10.1371/journal.pbio.2003355

Hoegh-Guldberg, O., Jacob, D., Taylor, M., Guillén Bolaños, T., Bindi, M., Brown, S., Camilloni, I.A., Diedhiou, A., Djalante, R., Ebi, K., Engelbrecht, F., Guiot, J., Hijioka, Y., Mehrotra, S., Hope, C.W., Payne, A.J., Pörtner, H.O., Seneviratne, S.I., Thomas, A., Warren, R., Zhou, G., 2019. The human imperative of stabilizing global climate change at 1.5°C. Science. 365, eaaw6974. https://doi.org/10.1126/science.aaw6974

Hoegh-Guldberg, O., Poloczanska, E.S., Skirving, W., Dove, S., 2017. Coral reef ecosystems under climate change and ocean acidification. Front. Mar. Sci. 4, 158. https://doi.org/10.3389/fmars.2017.00158

Holcomb, M., Cohen, A.L., McCorkle, D.C., 2013. An evaluation of staining techniques for

marking daily growth in scleractinian corals. J. Exp. Mar. Bio. Ecol. 440, 126–131. https://doi.org/10.1016/j.jembe.2012.12.003

Hoogenboom, M., Beraud, E., Ferrier-Pagès, C., 2010. Relationship between symbiont density and photosynthetic carbon acquisition in the temperate coral Cladocora caespitosa. Coral Reefs 29, 21–29. https://doi.org/10.1007/s00338-009-0558-9

Hoogenboom, M.O., Frank, G.E., Chase, T.J., Jurriaans, S., Álvarez-Noriega, M., Peterson, K., Critchell, K., Berry, K.L.E., Nicolet, K.J., Ramsby, B., Paley, A.S., 2017. Environmental drivers of variation in bleaching severity of Acropora species during an extreme thermal anomaly. Front. Mar. Sci. 4, 376. https://doi.org/10.3389/fmars.2017.00376

Howe-Kerr, L.I., Bachelot, B., Wright, R.M., Kenkel, C.D., Bay, L.K., Correa, A.M.S., 2020. Symbiont community diversity is more variable in corals that respond poorly to stress. Glob. Chang. Biol. 26, 2220–2234. https://doi.org/10.1111/gcb.14999

Howells, E.J., Abrego, D., Meyer, E., Kirk, N.L., McParland, D., Vaughan, G.O., Burt, J.A., 2021. Enhancing the heat tolerance of reef-building corals to future warming. Sci. Adv. 7, eabg6070. https://doi.org/10.1126/sciadv.abg6070

Howlett, L., Camp, E.F., Edmondson, J., Henderson, N., Suggett, D.J., 2021. Coral growth, survivorship and return-on-effort within nurseries at high-value sites on the Great Barrier Reef. PLoS One 16, e0244961. https://doi.org/10.1371/journal.pone.0244961

Howlett, L., Camp, E.F., Edmondson, J., Hosp, R., Taylor, B., Coulthard, P., Suggett, D.J., 2023. Active coral propagation outcomes on coral communities at high-value Great Barrier Reef tourism sites. Biol. Conserv. 279, 109930. https://doi.org/10.1016/J.BIOCON.2023.109930

Howlett, L., Camp, E.F., Edmondson, John, Edmondson, Jenny, Agius, T., Hosp, R., Coulthard, P., Edmondson, S., Suggett, D.J., 2022. Adoption of coral propagation and out-planting via the tourism industry to advance site stewardship on the northern Great Barrier Reef. Ocean Coast. Manag. 225, 106199. https://doi.org/10.1016/j.ocecoaman.2022.106199

Hubbard, D., Miller, A., Scaturo, D., 1990. Production and cycling of calcium carbonate in a shelf-edge reef system (St. Croix, U.S. Virgin Islands); applications to the nature of reef systems in the fossil record. J. Sediment. Res. 60, 335–360. https://doi.org/10.1306/212F9197-2B24-11D7-8648000102C1865D

Huertas, V., Morais, R.A., Bonaldo, R.M., Bellwood, D.R., 2021. Parrotfish corallivory on stress-tolerant corals in the Anthropocene. PLoS One 16, e0250725. https://doi.org/10.1371/journal.pone.0250725

Hughes, A.D., Grottoli, A.G., Pease, T.K., Matsui, Y., 2010. Acquisition and assimilation of carbon in non-bleached and bleached corals. Mar. Ecol. Prog. Ser. 420, 91–101. https://doi.org/10.3354/meps08866

Hughes, D.J., Alderdice, R., Cooney, C., Kühl, M., Pernice, M., Voolstra, C.R., Suggett, D.J., 2020. Coral reef survival under accelerating ocean deoxygenation. Nat. Clim. Chang. 10, 296–307. https://doi.org/10.1038/s41558-020-0737-9

Hughes, T.P., 1987. Skeletal density and growth form of corals. Mar. Ecol. Prog. Ser. 35, 259–266. https://doi.org/10.3354/meps035259

Hughes, T.P., Baird, A.H., Bellwood, D.R., Card, M., Connolly, S.R., Folke, C., Grosberg, R., Hoegh-Guldberg, O., Jackson, J.B.C., Kleypas, J., Lough, J.M., Marshall, P., Nyström, M., Palumbi, S.R., Pandolfi, J.M., Rosen, B., Roughgarden, J., 2003. Climate change, human impacts, and the resilience of coral reefs. Science. 301, 929–933.

https://doi.org/10.1126/science.1085046

Hughes, T.P., Baird, A.H., Morrison, T.H., Torda, G., 2023. Principles for coral reef restoration in the anthropocene. One Earth 6, 656–665. https://doi.org/10.1016/j.oneear.2023.04.008

Hughes, T.P., Barnes, M.L., Bellwood, D.R., Cinner, J.E., Cumming, G.S., Jackson, J.B.C., Kleypas, J., van de Leemput, I.A., Lough, J.M., Morrison, T.H., Palumbi, S.R., van Nes, E.H., Scheffer, M., 2017a. Coral reefs in the Anthropocene. Nature 546, 82–90. https://doi.org/10.1038/nature22901

Hughes, T.P., Kerry, J.T., Álvarez-Noriega, M., Álvarez-Romero, J.G., Anderson, K.D., Baird, A.H., Babcock, R.C., Beger, M., Bellwood, D.R., Berkelmans, R., Bridge, T.C., Butler, I.R., Byrne, M., Cantin, N.E., Comeau, S., Connolly, S.R., Cumming, G.S., Dalton, S.J., Diaz-Pulido, G., Eakin, C.M., Figueira, W.F., Gilmour, J.P., Harrison, H.B., Heron, S.F., Hoey, A.S., Hobbs, J.P.A., Hoogenboom, M.O., Kennedy, E. V, Kuo, C., Lough, J.M., Lowe, R.J., Liu, G., McCulloch, M.T., Malcolm, H.A., McWilliam, M.J., Pandolfi, J.M., Pears, R.J., Pratchett, M.S., Schoepf, V., Simpson, T., Skirving, W.J., Sommer, B., Torda, G., Wachenfeld, D.R., Willis, B.L., Wilson, S.K., 2017b. Global warming and recurrent mass bleaching of corals. Nature 543, 373–377. https://doi.org/10.1038/nature21707

Hughes, T.P., Kerry, J.T., Baird, A.H., Connolly, S.R., Chase, T.J., Dietzel, A., Hill, T., Hoey, A.S., Hoogenboom, M.O., Jacobson, M., Kerswell, A., Madin, J.S., Mieog, A., Paley, A.S., Pratchett, M.S., Torda, G., Woods, R.M., 2019. Global warming impairs stock-recruitment dynamics of corals. Nature 568, 387–390. https://doi.org/10.1038/s41586-019-1081-y

Hughes, T.P., Kerry, J.T., Baird, A.H., Connolly, S.R., Dietzel, A., Eakin, C.M., Heron, S.F.,

Hoey, A.S., Hoogenboom, M.O., Liu, G., McWilliam, M.J., Pears, R.J., Pratchett, M.S., Skirving, W.J., Stella, J.S., Torda, G., 2018. Global warming transforms coral reef assemblages. Nature 556, 492–496. https://doi.org/10.1038/s41586-018-0041-2

Hughes, T.P., Kerry, J.T., Connolly, S.R., Álvarez-Romero, J.G., Eakin, C.M., Heron, S.F., Gonzalez, M.A., Moneghetti, J., 2021. Emergent properties in the responses of tropical corals to recurrent climate extremes. Curr. Biol. 31, 5393–5399. https://doi.org/10.1016/j.cub.2021.10.046

Humanes, A., Beauchamp, E.A., Bythell, J.C., Carl, M.K., Craggs, J.R., Edwards, A.J., Golbuu, Y., Lachs, L., Martinez, H.M., Palmowski, P., Paysinger, F., Randle, J.L., van der Steeg, E., Sweet, M., Treumann, A., Guest, J.R., 2021. An Experimental Framework for Selectively Breeding Corals for Assisted Evolution. Front. Mar. Sci. 8, 669995. https://doi.org/10.3389/fmars.2021.669995

Humanes, A., Lachs, L., Beauchamp, E.A., Bythell, J.C., Edwards, A.J., Golbuu, Y., Martinez, H.M., Palmowski, P., Treumann, A., Van Der Steeg, E., Van Hooidonk, R., Guest, J.R., 2022. Within-population variability in coral heat tolerance indicates climate adaptation potential. Proc. R. Soc. B 289, 20220872. https://doi.org/10.1098/rspb.2022.0872

Hume, B., D'Angelo, C., Burt, J., Baker, A.C., Riegl, B., Wiedenmann, J., 2013. Corals from the Persian/Arabian Gulf as models for thermotolerant reef-builders: Prevalence of clade C3 Symbiodinium, host fluorescence and ex situ temperature tolerance. Mar. Pollut. Bull. 72, 313–322. https://doi.org/10.1016/j.marpolbul.2012.11.032

Hume, B.C.C., Smith, E.G., Ziegler, M., Warrington, H.J.M., Burt, J.A., LaJeunesse, T.C., Wiedenmann, J., Voolstra, C.R., 2019. SymPortal: A novel analytical framework and platform for coral algal symbiont next-generation sequencing ITS2 profiling. Mol. Ecol.

Resour. 19, 1063–1080. https://doi.org/10.1111/1755-0998.13004

Iglesias-Prieto, R., Trench, R.K., 1994. Acclimation and adaptation to irradiance in symbiotic dinoflagellates. I. Responses of the photosynthetic unit to changes in photon flux density. Mar. Ecol. Prog. Ser. 113, 163–175. https://doi.org/10.3354/meps113163

IPBES, 2019. Global Assessment Report on Biodiversity and Ecosystem Services of the Intergovernmental Science-Policy Platform on Biodiversity and Ecosystem Services. Bonn, Germany. https://doi.org/10.5281/zenodo.3831673

IPCC, 2019a. Technical Summary, in: Pörtner, H.-O., Roberts, D.C., Masson-Delmotte, V., Zhai, P., Poloczanska, E., Mintenbeck, K., Tignor, M., Alegría, A., Nicolai, M., Okem, A., Petzold, J., Rama, B., Weyer, N.M. (Eds.), Special Report on the Ocean and Cryosphere in a Changing Climate. Cambridge University Press, Cambridge, UK and New York, NY, USA, pp. 39–69. https://doi.org/10.1017/9781009157964.002

IPCC, 2019b. Summary for Policymakers, in: Shukla, P.R., Skea, J., Calvo Buendia, E., Masson-Delmotte, V., Pörtner, H.-O., Roberts, D.C., Zhai, P., Slade, R., Connors, S., van Diemen, R., Ferrat, M., Haughey, E., Luz, S., Neogi, S., Pathak, M., Petzold, J., Portugal Pereira, J., Vyas, P., Huntley, E., Kissick, K., Belkacemi, M., Malley, J. (Eds.), Climate Change and Land: An IPCC Special Report on Climate Change, Desertification, Land Degradation, Sustainable Land Management, Food Security, and Greenhouse Gas Fluxes in Terrestrial Ecosystems. pp. 3–36. https://doi.org/10.1017/9781009157988.001

Jacquemont, J., Houlbrèque, F., Tanvet, C., Rodolfo-Metalpa, R., 2022. Long-term exposure to an extreme environment induces species-specific responses in corals' photosynthesis and respiration rates. Mar. Biol. 169, 82. https://doi.org/10.1007/s00227-022-04063-6

Jeffrey, S.W., Humphrey, G.F., 1975. New spectrophotometric equations for determining chlorophylls a, b, c1 and c2 in higher plants, algae and natural phytoplankton. Biochem.

und Physiol. der Pflanz. 167, 191–194. https://doi.org/10.1016/S0015-3796(17)30778-3

Jeger, M.J., 2022. The impact of climate change on disease in wild plant populations and communities. Plant Pathol. 71, 111–130. https://doi.org/10.1111/ppa.13434

Jimenez, I.M., Kuḧl, M., Larkum, A.W.D., Ralph, P.J., 2011. Effects of flow and colony morphology on the thermal boundary layer of corals. J. R. Soc. Interface 8, 1785–1795. https://doi.org/10.1098/rsif.2011.0144

Johns, K.A., Emslie, Michael J, Hoey, Andrew S, Osborne, Kate, Jonker, Michelle J, Cheal, Alistair J, Johns, C.:, Emslie, M J, Hoey, A S, Osborne, K, Jonker, M J, Cheal, A J, 2018. Macroalgal feedbacks and substrate properties maintain a coral reef regime shift. Ecosphere 9, e02349. https://doi.org/10.1002/ecs2.2349

Johnson, M.E., Lustic, C., Bartels, E., Baums, I.B., Gilliam, D.S., Larson, L., Lirman, D., Miller, M.W., Nedimyer, K., Schopmeyer, S., 2011. Caribbean Acropora restoration guide: Best practices for propagation and population enhancement. Arlington, VA, USA.

Jokiel, P.L., Maragos, J., Franzisket, L., 1978. Coral growth: Buoyant weight technique, in: Stoddart, D.R., Johannes, R.E. (Eds.), Coral Reefs: Research Methods. UNESCO, Paris, France, pp. 529–541.

Kang, C.K., Choy, E.J., Son, Y., Lee, J.Y., Kim, J.K., Kim, Y., Lee, K.S., 2008. Food web structure of a restored macroalgal bed in the eastern Korean peninsula determined by C and N stable isotope analyses. Mar. Biol. 153, 1181–1198. https://doi.org/10.1007/s00227-007-0890-y

Kassambara, K., Mundt, F., 2020. factoextra: Extract and visualize the results of multivariate data analyses. R Packag. version 1.0.7.

Kavousi, J., Denis, V., Sharp, V., Reimer, J.D., Nakamura, T., Parkinson, J.E., 2020. Unique

combinations of coral host and algal symbiont genotypes reflect intraspecific variation in heat stress responses among colonies of the reef-building coral, Montipora digitata. Mar. Biol. 167, 23. https://doi.org/10.1007/s00227-019-3632-z

Kayitesi, N.M., Guzha, A.C., Mariethoz, G., 2022. Impacts of land use land cover change and climate change on river hydro-morphology- a review of research studies in tropical regions. J. Hydrol. 615, 128702. https://doi.org/10.1016/j.jhydrol.2022.128702

Kenkel, C.D., Goodbody-Gringley, G., Caillaud, D., Davies, S.W., Bartels, E., Matz, M. V., 2013. Evidence for a host role in thermotolerance divergence between populations of the mustard hill coral (Porites astreoides) from different reef environments. Mol. Ecol. 22, 4335–4348. https://doi.org/10.1111/mec.12391

Kenkel, C.D., Setta, S.P., Matz, M. V., 2015. Heritable differences in fitness-related traits among populations of the mustard hill coral, Porites astreoides. Heredity (Edinb). 115, 509–516. https://doi.org/10.1038/hdy.2015.52

Kenyon, T.M., Doropoulos, C., Dove, S., Webb, G.E., Newman, S.P., Sim, C.W.H., Arzan, M., Mumby, P.J., 2020. The effects of rubble mobilisation on coral fragment survival, partial mortality and growth. J. Exp. Mar. Bio. Ecol. 533, 151467. https://doi.org/10.1016/j.jembe.2020.151467

Kenyon, T.M., Doropoulos, C., Wolfe, K., Webb, G.E., Dove, S., Harris, D., Mumby, P.J., 2023. Coral rubble dynamics in the Anthropocene and implications for reef recovery. Limnol. Oceanogr. 68, 110–147. https://doi.org/10.1002/lno.12254

Khaled, R.A.H., Duru, M., Decruyenaere, V., Jouany, C., Cruz, P., 2006. Using leaf traits to rank native grasses according to their nutritive value. Rangel. Ecol. Manag. 59, 648–654. https://doi.org/10.2111/05-031R2.1

Kirk, N.L., Howells, E.J., Abrego, D., Burt, J.A., Meyer, E., 2018. Genomic and transcriptomic signals of thermal tolerance in heat-tolerant corals (Platygyra daedalea) of the Arabian/Persian Gulf. Mol. Ecol. 27, 5180–5194. https://doi.org/10.1111/mec.14934

Kitchen, S.A., Von Kuster, G., Kuntz, K.L.V., Reich, H.G., Miller, W., Griffin, S., Fogarty, N.D., Baums, I.B., 2020. STAGdb: a 30K SNP genotyping array and Science Gateway for Acropora corals and their dinoflagellate symbionts. Sci. Rep. 10, 12488. https://doi.org/10.1038/s41598-020-69101-z

Kleypas, J., Allemand, D., Anthony, K., Baker, A.C., Beck, M.W., Hale, L.Z., Hilmi, N., Hoegh-Guldberg, O., Hughes, T., Kaufman, L., Kayanne, H., Magnan, A.K., Mcleod, E., Mumby, P., Palumbi, S., Richmond, R.H., Rinkevich, B., Steneck, R.S., Voolstra, C.R., Wachenfeld, D., Gattuso, J.P., 2021. Designing a blueprint for coral reef survival. Biol. Conserv. 257, 109107. https://doi.org/10.1016/j.biocon.2021.109107

Kojis, B.L., Quinn, N.J., 2001. The importance of regional differences in hard coral recruitment rates for determining the need for coral restoration. Bull. Mar. Sci. 69, 967–974.

Kriefall, N.G., Kanke, M.R., Aglyamova, G. V, Davies, S.W., 2022. Reef environments shape microbial partners in a highly connected coral population. Proc. R. Soc. B 289, 20212459. https://doi.org/10.1098/rspb.2021.2459

Kropat, J., Gallaher, S.D., Urzica, E.I., Nakamoto, S.S., Strenkert, D., Tottey, S., Mason, A.Z., Merchant, S.S., 2015. Copper economy in Chlamydomonas: Prioritized allocation and eallocation of copper to respiration vs. Photosynthesis. Proc. Natl. Acad. Sci. 112, 2644–2651. https://doi.org/10.1073/pnas.1422492112

Kruczynski, W.L., Fletcher, P.J., 2012. Tropical Connections: South Florida's marine

environment. Cambridge, MD, USA.

Kuffner, I.B., Bartels, E., Stathakopoulos, A., Enochs, I.C., Kolodziej, • G, Toth, L.T., Manzello, D.P., 2017. Plasticity in skeletal characteristics of nursery-raised staghorn coral, Acropora cervicornis. Coral Reefs 36, 679–684. https://doi.org/10.1007/s00338-017-1560-2

Kunstler, G., Falster, D., Coomes, D.A., Hui, F., Kooyman, R.M., Laughlin, D.C., Poorter, L., Vanderwel, M., Vieilledent, G., Wright, S.J., Aiba, M., Baraloto, C., Caspersen, J., Cornelissen, J.H.C., Gourlet-Fleury, S., Hanewinkel, M., Herault, B., Kattge, J., Kurokawa, H., Onoda, Y., Peñuelas, J., Poorter, H., Uriarte, M., Richardson, S., Ruiz-Benito, P., Sun, I.F., Ståhl, G., Swenson, N.G., Thompson, J., Westerlund, B., Wirth, C., Zavala, M.A., Zeng, H., Zimmerman, J.K., Zimmermann, N.E., Westoby, M., 2016. Plant functional traits have globally consistent effects on competition. Nature 529, 204–207. https://doi.org/10.1038/nature16476

La Peyre, M., Furlong, J., Brown, L.A., Piazza, B.P., Brown, K., 2014. Oyster reef restoration in the northern Gulf of Mexico: Extent, methods and outcomes. Ocean Coast. Manag. 89, 20–28. https://doi.org/10.1016/j.ocecoaman.2013.12.002

Lachs, L., Humanes, A., Pygas, D.R., Bythell, J.C., Mumby, P.J., Ferrari, R., Figueira, W.F., Beauchamp, E., East, H.K., Edwards, A.J., Golbuu, Y., Martinez, H.M., Sommer, B., van der Steeg, E., Guest, J.R., 2023. No apparent trade-offs associated with heat tolerance in a reef-building coral. Commun. Biol. 6, 400. https://doi.org/10.1038/s42003-023-04758-6

Ladd, M.C., Burkepile, D.E., Shantz, A.A., 2019. Near-term impacts of coral restoration on target species, coral reef community structure, and ecological processes. Restor. Ecol. 27, 1166–1176. https://doi.org/10.1111/rec.12939

Ladd, M.C., Miller, M.W., Hunt, J.H., Sharp, W.C., Burkepile, D.E., 2018. Harnessing ecological processes to facilitate coral restoration. Front. Ecol. Environ. 16, 239–247. https://doi.org/10.1002/fee.1792

LaJeunesse, T.C., Parkinson, J.E., Gabrielson, P.W., Jeong, H.J., Reimer, J.D., Voolstra, C.R., Santos, S.R., 2018. Systematic Revision of Symbiodiniaceae Highlights the Antiquity and Diversity of Coral Endosymbionts. Curr. Biol. 28, 2570–2580. https://doi.org/10.1016/j.cub.2018.07.008

LaJeunesse, T.C., Wham, D.C., Pettay, D.T., Parkinson, J.E., Keshavmurthy, S., Chen, C.A., 2019. Ecologically differentiated stress-tolerant endosymbionts in the dinoflagellate genus Symbiodinium (Dinophyceae) Clade D are different species. Phycologia 53, 305–319. https://doi.org/10.2216/13-186.1

Lam, V.W.Y., Allison, E.H., Bell, J.D., Blythe, J., Cheung, W.W.L., Frölicher, T.L., Gasalla, M.A., Sumaila, U.R., 2020. Climate change, tropical fisheries and prospects for sustainable development. Nat. Rev. Earth Environ. 1, 440–454. https://doi.org/10.1038/s43017-020-0071-9

Lamarque, P., Lavorel, S., Mouchet, M., Quétier, F., 2014. Plant trait-based models identify direct and indirect effects of climate change on bundles of grassland ecosystem services. Proc. Natl. Acad. Sci. 111, 13751–13756. https://doi.org/10.1073/pnas.1216051111

Lamont, T.A.C., Williams, B., Chapuis, L., Prasetya, M.E., Seraphim, M.J., Harding, H.R., May, E.B., Janetski, N., Jompa, J., Smith, D.J., Radford, A.N., Simpson, S.D., 2022. The sound of recovery: Coral reef restoration success is detectable in the soundscape. J. Appl. Ecol. 59, 742–756. https://doi.org/10.1111/1365-2664.14089

Lange, I.D., Perry, C.T., 2019. Bleaching impacts on carbonate production in the Chagos Archipelago: influence of functional coral groups on carbonate budget trajectories. Coral

Reefs 38, 619–624. https://doi.org/10.1007/s00338-019-01784-x

Lange, I.D., Perry, C.T., Alvarez-Filip, L., 2020. Carbonate budgets as indicators of functional reef "health": A critical review of data underpinning census-based methods and current knowledge gaps. Ecol. Indic. 110, 105857. https://doi.org/10.1016/j.ecolind.2019.105857

Lavy, A., Eyal, G., Neal, B., Keren, R., Loya, Y., Ilan, M., 2015. A quick, easy and non-intrusive method for underwater volume and surface area evaluation of benthic organisms by 3D computer modelling. Methods Ecol. Evol. 6, 521–531. https://doi.org/10.1111/2041-210X.12331

Lê, S., Josse, J., Husson, F., 2008. FactoMineR: An R package for multivariate analysis. J. Stat. Softw. 25, 1–18. https://doi.org/10.18637/jss.v025.i01

Leggat, W.P., Camp, E.F., Suggett, D.J., Heron, S.F., Fordyce, A.J., Gardner, S., Deakin, L., Turner, M., Beeching, L.J., Kuzhiumparambil, U., Eakin, C.M., Ainsworth, T.D., 2019. Rapid Coral Decay Is Associated with Marine Heatwave Mortality Events on Reefs. Curr. Biol. 29, 2723–2730. https://doi.org/10.1016/j.cub.2019.06.077

Levy, G., Shaish, L., Haim, A., Rinkevich, B., 2010. Mid-water rope nursery—Testing design and performance of a novel reef restoration instrument. Ecol. Eng. 36, 560–569. https://doi.org/10.1016/j.ecoleng.2009.12.003

Levy, O., Dubinsky, Z., Achituv, Y., Erez, J., 2006. Diurnal polyp expansion behavior in stony corals may enhance carbon availability for symbionts photosynthesis. J. Exp. Mar. Bio. Ecol. 333, 1–11. https://doi.org/10.1016/j.jembe.2005.11.016

Lewis, R.E., Davy, S.K., Gardner, S.G., Rongo, T., David, ·, Suggett, J., Nitschke, M.R., 2022. Colony self-shading facilitates Symbiodiniaceae cohabitation in a South Pacific

coral community. Coral Reefs 41, 1433–1447. https://doi.org/10.1007/s00338-022-02292-1

Liddicoat, C., Krauss, S.L., Bissett, A., Borrett, R.J., Ducki, L.C., Peddle, S.D., Bullock, P., Dobrowolski, M.P., Grigg, A., Tibbett, M., Breed, M.F., 2022. Next generation restoration metrics: Using soil eDNA bacterial community data to measure trajectories towards rehabilitation targets. J. Environ. Manage. 310, 114748. https://doi.org/10.1016/j.jenvman.2022.114748

Liefer, J.D., Garg, A., Fyfe, M.H., Irwin, A.J., Benner, I., Brown, C.M., Follows, M.J., Omta, A.W., Finkel, Z. V., 2019. The macromolecular basis of phytoplankton C:N:P under nitrogen starvation. Front. Microbiol. 10, 763. https://doi.org/10.3389/fmicb.2019.00763

Lirman, D., 2000. Fragmentation in the branching coral Acropora palmata (Lamarck): Growth, survivorship, and reproduction of colonies and fragments. J. Exp. Mar. Bio. Ecol. 251, 41–57. https://doi.org/10.1016/S0022-0981(00)00205-7

Lirman, D., Schopmeyer, S., 2016. Ecological solutions to reef degradation: optimizing coral reef restoration in the Caribbean and Western Atlantic. PeerJ 4, e2597. https://doi.org/10.7717/peerj.2597

Lirman, D., Schopmeyer, S., Galvan, V., Drury, C., Baker, A.C., Baums, I.B., 2014. Growth dynamics of the threatened caribbean staghorn coral acropora cervicornis: Influence of host genotype, symbiont identity, colony size, and environmental setting. PLoS One 9, e107253. https://doi.org/10.1371/journal.pone.0107253

Lirman, D., Thyberg, T., Herlan, J., Hill, C., Young-Lahiff, C., Schopmeyer, S., Huntington, B., Santos, R., Drury, C., 2010. Propagation of the threatened staghorn coral Acropora cervicornis: Methods to minimize the impacts of fragment collection and maximize production. Coral Reefs 29, 729–735. https://doi.org/10.1007/s00338-010-0621-6

Lizcano-Sandoval, L.D., Londoño-Cruz, E., Zapata, F.A., 2018. Growth and survival of Pocillopora damicornis (Scleractinia: Pocilloporidae) coral fragments and their potential for coral reef restoration in the Tropical Eastern Pacific. Mar. Biol. Res. 14, 887–897. https://doi.org/10.1080/17451000.2018.1528011

Llases, M.E., Morgada, M.N., Vila, A.J., 2019. Biochemistry of Copper Site Assembly in Heme-Copper Oxidases: A Theme with Variations. Int. J. Mol. Sci. 20, 3830. https://doi.org/10.3390/ijms20153830

Löf, M., Madsen, P., Metslaid, M., Witzell, J., Jacobs, D.F., 2019. Restoring forests: regeneration and ecosystem function for the future. New For. 50, 139–151. https://doi.org/10.1007/s11056-019-09713-0

Lohr, K.E., Camp, E.F., Kuzhiumparambil, U., Lutz, A., Leggat, W., Patterson, J.T., Suggett, D.J., 2019. Resolving coral photoacclimation dynamics through coupled photophysiological and metabolomic profiling. J. Exp. Biol. 222, jeb195982. https://doi.org/10.1242/jeb.195982

Lohr, K.E., Patterson, J.T., 2017. Intraspecific variation in phenotype among nursery-reared staghorn coral Acropora cervicornis (Lamarck, 1816). J. Exp. Mar. Bio. Ecol. 486, 87–92. https://doi.org/10.1016/j.jembe.2016.10.005

Loya, Y., 1976. Skeletal regeneration in a Red Sea scleractinian coral population. Nature 261, 490–491. https://doi.org/10.1038/261490a0

Loya, Y., Sakai, K., Yamazato, K., Nakano, Y., Sambali, H., van Woesik, R., 2001. Coral bleaching: the winners and the losers. Ecol. Lett. 4, 122–131. https://doi.org/10.1046/j.1461-0248.2001.00203.x

Lundgren, P., Vera, J.C., Peplow, L., Manel, S., van Oppen, M.J.H., 2013. Genotype –

environment correlations in corals from the Great Barrier Reef. BMC Genet. 14, 9. https://doi.org/10.1186/1471-2156-14-9

MacNeil, M.A., Mellin, C., Matthews, S., Wolff, N.H., McClanahan, T.R., Devlin, M., Drovandi, C., Mengersen, K., Graham, N.A.J., 2019. Water quality mediates resilience on the Great Barrier Reef. Nat. Ecol. Evol. 3, 620–627. https://doi.org/10.1038/s41559-019-0832-3

Madani, N., Kimball, J.S., Ballantyne, A.P., Affleck, D.L.R., Van Bodegom, P.M., Reich, P.B., Kattge, J., Sala, A., Nazeri, M., Jones, M.O., Zhao, M., Running, S.W., 2018. Future global productivity will be affected by plant trait response to climate. Sci. Rep. 8, 2870. https://doi.org/10.1038/s41598-018-21172-9

Madin, J.S., Anderson, K.D., Andreasen, M.H., Bridge, T.C.L., Cairns, S.D., Connolly, S.R., Darling, E.S., Diaz, M., Falster, D.S., Franklin, E.C., Gates, R.D., Hoogenboom, M.O., Huang, D., Keith, S.A., Kosnik, M.A., Kuo, C., Lough, J.M., Lovelock, C.E., Luiz, O., Martinelli, J., Mizerek, T., Pandol, J.M., Pochon, X., Wallace, C.C., Widman, E., Baird, A.H., 2016a. The Coral Trait Database, a curated database of trait information for coral species from the global oceans. Sci. Data 3, 160017. https://doi.org/10.1038/sdata.2016.17

Madin, J.S., Hoogenboom, M.O., Connolly, S.R., Darling, E.S., Falster, D.S., Huang, D., Keith, S.A., Mizerek, T., Pandolfi, J.M., Putnam, H.M., Baird, A.H., 2016b. A Trait-Based Approach to Advance Coral Reef Science. Trends Ecol. Evol. 31, 419–428. https://doi.org/10.1016/j.tree.2016.02.012

Madin, J.S., McWilliam, M., Quigley, K., Bay, L.K., Bellwood, D., Doropoulos, C., Fernandes, L., Harrison, P., Hoey, A.S., Mumby, P.J., Ortiz, J.C., Richards, Z.T., Riginos, C., Schiettekatte, N.M.D., Suggett, D.J., van Oppen, M.J.H., 2023. Selecting

coral species for reef restoration. J. Appl. Ecol. 60, 1537–1544. https://doi.org/10.1111/1365-2664.14447

Main, T.M., Dobberfuhl, D.R., Elser, J.J., 1997. N:P stoichiometry and ontogeny of crustacean zooplankton: A test of the growth rate hypothesis. Limnol. Oceanogr. 42, 1474–1478. https://doi.org/10.4319/lo.1997.42.6.1474

Marshall, P.A., Baird, A.H., 2000. Bleaching of corals on the Great Barrier Reef: Differential susceptibilities among taxa. Coral Reefs 19, 155–163. https://doi.org/10.1007/s003380000086

Martell, H.A., 2023. Thermal priming and bleaching hormesis in the staghorn coral, Acropora cervicornis (Lamarck 1816). J. Exp. Mar. Bio. Ecol. 560, 151820. https://doi.org/10.1016/j.jembe.2022.151820

Martínez-Rendis, A., Acosta-González, G., Arias-González, J.E., 2020. A spatio-temporal long-term assessment on the ecological response of reef communities in a Caribbean marine protected area. Aquat. Conserv. Mar. Freshw. Ecosyst. 30, 273–289. https://doi.org/10.1002/aqc.3263

Matz, M. V., Treml, E.A., Aglyamova, G. V., Bay, L.K., 2018. Potential and limits for rapid genetic adaptation to warming in a Great Barrier Reef coral. PLoS Genet. 14, e1007220. https://doi.org/10.1371/journal.pgen.1007220

McClanahan, T., Maina, J., Pet-Soede, L., 2002. Effects of the 1998 coral morality event on Kenyan coral reefs and fisheries. Ambio 31, 543–550. https://doi.org/10.1579/0044-7447-31.7.543

McClanahan, T.R., 2004. The relationship between bleaching and mortality of common corals. Mar. Biol. 144, 1239–1245. https://doi.org/10.1007/s00227-003-1271-9

McCormick, M.I., 1994. Comparison of field methods for measuring surface tomography and their associations with a tropical reef fish assemblage. Mar. Ecol. Prog. Ser. 112, 87–96. https://doi.org/10.3354/meps112087

McCulloch, M.T., D'Olivo, J.P., Falter, J., Holcomb, M., Trotter, J.A., 2017. Coral calcification in a changing world and the interactive dynamics of pH and DIC upregulation. Nat. Commun. 8, 15686. https://doi.org/10.1038/ncomms15686

McFadden, I.R., Sendek, A., Brosse, M., Bach, P.M., Baity-Jesi, M., Bolliger, J., Bollmann, K., Brockerhoff, E.G., Donati, G., Gebert, F., Ghosh, S., Ho, H.-C., Khaliq, I., Lever, J.J., Logar, I., Moor, H., Odermatt, D., Pellissier, L., de Queiroz, L.J., Rixen, C., Schuwirth, N., Shipley, J.R., Twining, C.W., Vitasse, Y., Vorburger, C., Wong, M.K.L., Zimmermann, N.E., Seehausen, O., Gossner, M.M., Matthews, B., Graham, C.H., Altermatt, F., Narwani, A., 2023. Linking human impacts to community processes in terrestrial and freshwater ecosystems. Ecol. Lett. 26, 203–218. https://doi.org/10.1111/ele.14153

McLachlan, R.H., Price, J.T., Solomon, S.L., Grottoli, A.G., 2020. Thirty years of coral heat-stress experiments: a review of methods. Coral Reefs 39, 885–902. https://doi.org/10.1007/s00338-020-01931-9

McLeod, I.M., Hein, M.Y., Babcock, R., Bay, L., Bourne, D.G., Cook, N., Doropoulos, C., Gibbs, M., Harrison, P., Lockie, S., van Oppen, M.J.H., 2022. Coral restoration and adaptation in Australia: The first five years. PLoS One 17, e0273325. https://doi.org/10.1371/journal.pone.0273325

McWhorter, J.K., Halloran, P.R., Roff, G., Skirving, W.J., Mumby, P.J., 2022a. Climate refugia on the Great Barrier Reef fail when global warming exceeds 3°C. Glob. Chang. Biol. 28, 5768–5780. https://doi.org/10.1111/gcb.16323

McWhorter, J.K., Halloran, P.R., Roff, G., Skirving, W.J., Perry, C.T., Mumby, P.J., 2022b. The importance of 1.5°C warming for the Great Barrier Reef. Glob. Chang. Biol. 28, 1332–1341. https://doi.org/10.1111/gcb.15994

Mead, D., Lk, B., Anthony, K., Hussey, K., Taylor, B., Fidelman, P., Pj, M., Harrison, D., Mt, G., Daly, J., Bryan, S., 2019. Reef Restoration and Adaptation Program – Research and Development Program. A report provided to the Australian Government from the Reef Restoration and Adaptation Program.

Meesters, E.H., Noordeloos, M., Bak, R.P.M., 1994. Damage and regeneration: Links to growth in the reef-building coral Montastrea annularis. Mar. Ecol. Prog. Ser. 112, 119–128. https://doi.org/10.3354/meps112119

Merk, H.J., Prins, J.A., 1954. Thermal convection in laminar Boundary layers II. Appl. Sci. Res. Sect. A 4, 207–221. https://doi.org/10.1007/BF03184952

Merselis, D.G., Lirman, D., Rodriguez-Lanetty, M., 2018. Symbiotic immuno-suppression: Is disease susceptibility the price of bleaching resistance? PeerJ 6, e4494. https://doi.org/10.7717/peerj.4494

Mertz, E.M., McDonald, A., 2021. Ecosystem Pushing: Coral Restoration in Refugia as an Unexplored Answer to Climate Change Adaptation. IOP Conf. Ser. Earth Environ. Sci. 809, 012011. https://doi.org/10.1088/1755-1315/809/1/012011

Meyer, E., Davies, S., Wang, S., Willis, B.L., Abrego, D., Juenger, T.E., Matz, M. V., 2009. Genetic variation in responses to a settlement cue and elevated temperature in the reef-building coral Acropora millepora. Mar. Ecol. Prog. Ser. 392, 81–92. https://doi.org/10.3354/meps08208

Middlebrook, R., Anthony, K.R.N., Hoegh-Guldberg, O., Dove, S., 2010. Heating rate and

symbiont productivity are key factors determining thermal stress in the reef-building coral Acropora formosa. J. Exp. Biol. 213, 1026–1034. https://doi.org/10.1242/jeb.031633

Miller, M., Crabbe, J., Villamizar, E., Croquer, A., Banaszak, A., 2022. Acropora palmata. The IUCN Red List of Threatened Species [WWW Document]. URL https://www.iucnredlist.org/es/species/133006/165672016 (accessed 2.10.24).

Montefalcone, M., Morri, C., Bianchi, C.N., 2020. Influence of Local Pressures on Maldivian Coral Reef Resilience Following Repeated Bleaching Events, and Recovery Perspectives. Front. Mar. Sci. 7, 587. https://doi.org/10.3389/fmars.2020.00587

Moon, I.J., Kim, S.H., Chan, J.C.L., 2019. Climate change and tropical cyclone trend. Nature 570, E3–E5. https://doi.org/10.1038/s41586-019-1222-3

Morikawa, M.K., Palumbi, S.R., Baker, A.C., Kaufman, L., Knowlton, N., 2019. Using naturally occurring climate resilient corals to construct bleaching-resistant nurseries. Proc. Natl. Acad. Sci. 116, 10586–10591. https://doi.org/10.1073/pnas.1721415116

Muhando, C.A., Lanshammar, F., 2008. Ecological effects of the crown-of-thorns starfish removal programme on Chumbe Island Coral Park, Zanzibar, Tanzania, in: The 11th International Coral Reef Symposium. Ft. Lauderdale, Florida, 7-11 July 2008, pp. 1127–1131.

Muller, E.M., Bartels, E., Baums, I.B., 2018. Bleaching causes loss of disease resistance within the threatened coral species acropora cervicornis. Elife 7, e35066. https://doi.org/10.7554/eLife.35066

Naidoo, R., Gerkey, D., Hole, D., Pfaff, A., Ellis, A.M., Golden, C.D., Herrera, D., Johnson, K., Mulligan, M., Ricketts, T.H., Fisher, B., 2019. Evaluating the impacts of protected

areas on human well-being across the developing world. Sci. Adv. 5, eaav3006. https://doi.org/10.1126/sciadv.aav3006

Nakamura, T., Van Woesik, R., 2001. Water-flow rates and passive diffusion partially explain differential survival of corals during the 1998 bleaching event. Mar. Ecol. Prog. Ser. 212, 301–304. https://doi.org/10.3354/meps212301

Nedimyer, K., Gaines, K., Roach, S., 2011. Coral Tree Nursery©: An innovative approach to growing corals in an ocean-based field nursery. AACL Bioflux 4, 442–446.

Nelson, H.R., Kuempel, C.D., Altieri, A.H., 2016. The resilience of reef invertebrate biodiversity to coral mortality. Ecosphere 7, e01399. https://doi.org/10.1002/ecs2.1399

Nicholls, R.J., Lincke, D., Hinkel, J., Brown, S., Vafeidis, A.T., Meyssignac, B., Hanson, S.E., Merkens, J.L., Fang, J., 2021. A global analysis of subsidence, relative sea-level change and coastal flood exposure. Nat. Clim. Chang. 11, 338–342. https://doi.org/10.1038/s41558-021-00993-z

Nielsen, J.J.V., Matthews, G., Frith, K.R., Harrison, H.B., Marzonie, M.R., Slaughter, K.L., Suggett, D.J., Bay, L.K., 2022. Experimental considerations of acute heat stress assays to quantify coral thermal tolerance. Sci. Rep. 12, 16831. https://doi.org/10.1038/s41598-022-20138-2

Nishiguchi, S., Wada, N., Yamashiro, H., Ishibashi, H., Takeuchi, I., 2018. Continuous recordings of the coral bleaching process on Sesoko Island, Okinawa, Japan, over about 50 days using an underwater camera equipped with a lens wiper. Mar. Pollut. Bull. 131, 422–427. https://doi.org/10.1016/j.marpolbul.2018.04.020

Nithyanandan, M., Le Vay, L., Raja, D.K., Kesavan, R., Pereira, D., 2018. Coral nursery and transplantation of the staghorn coral, Acropora downingi in Sabah Al-Ahmad Sea City,

Kuwait, Arabian Gulf. Cogent Environ. Sci. 4, 1480334. https://doi.org/10.1080/23311843.2018.1480334

Nitschke, M.R., Gardner, S.G., Goyen, S., Fujise, L., Camp, E.F., Ralph, P.J., Suggett, D.J., 2018. Utility of Photochemical Traits as Diagnostics of Thermal Tolerance amongst Great Barrier Reef Corals. Front. Mar. Sci. 5, 45. https://doi.org/10.3389/fmars.2018.00045

Norici, A., Bazzoni, A.M., Pugnetti, A., Raven, J.A., Giordano, M., 2011. Impact of irradiance on the C allocation in the coastal marine diatom Skeletonema marinoi Sarno and Zingone. Plant. Cell Environ. 34, 1666–1677. https://doi.org/10.1111/j.1365-3040.2011.02362.x

Nuñez Lendo, C.I., Camp, E.F., Edmondson, J., Hughes, D.H., Kuzhiumparambil, U., Clases, D., Gonzalez de Vega, R., Suggett, D.J., 2023. Multiple trait approach to inform ecosystem service value of corals propagated for restoration on the Great Barrier Reef. Res. Sq. PREPRINT. https://doi.org/10.21203/rs.3.rs-2030847/v1

Nuñez Lendo, C.I., Suggett, D.J., Boote, C., McArdle, A., Nicholson, F., Fisher, E.E., Smith, D., Camp, E.F., 2024. Carbonate budgets induced by coral restoration of a Great Barrier Reef site following cyclone damage. Front. Mar. Sci. 10, 1298411. https://doi.org/10.3389/FMARS.2023.1298411

Nunez, S., Arets, E., Alkemade, R., Verwer, C., Leemans, R., 2019. Assessing the impacts of climate change on biodiversity: is below 2°C enough? Clim. Change 154, 351–365. https://doi.org/10.1007/s10584-019-02420-x

O'Donnell, K.E., Lohr, K.E., Bartels, E., Baums, I.B., Patterson, J.T., 2018. Acropora cervicornis genet performance and symbiont identity throughout the restoration process. Coral Reefs 37, 1109–1118. https://doi.org/10.1007/s00338-018-01743-y

O'Donnell, K.E., Lohr, K.E., Bartels, E., Patterson, J.T., 2017. Evaluation of staghorn coral (Acropora cervicornis, Lamarck 1816) production techniques in an ocean-based nursery with consideration of coral genotype. J. Exp. Mar. Bio. Ecol. 487, 53–58. https://doi.org/10.1016/j.jembe.2016.11.013

Oksanen, J., Kindt, R., Legendre, P., O'Hara, B., Simpson, G.L., Solymos, P.M., Stevens, M.H.H., & Wagner, H., 2008. The vegan package. Community Ecol. Packag. 10, 631–637.

Oliver, T.A., Palumbi, S.R., 2011. Do fluctuating temperature environments elevate coral thermal tolerance? Coral Reefs 30, 429–440. https://doi.org/10.1007/s00338-011-0721-y

Omori, M., 2019. Coral restoration research and technical developments: what we have learned so far. Mar. Biol. Res. 15, 377–409. https://doi.org/10.1080/17451000.2019.1662050

Omori, M., Iwao, K., Tamura, M., 2008. Growth of transplanted Acropora tenuis 2 years after egg culture. Coral Reefs 27, 165. https://doi.org/10.1007/s00338-007-0312-0

Ortiz, J.C., Pears, R.J., Beeden, R., Dryden, J., Wolff, N.H., Gomez Cabrera, M. del C., Mumby, P.J., 2021. Important ecosystem function, low redundancy and high vulnerability: The trifecta argument for protecting the Great Barrier Reef's tabular Acropora. Conserv. Lett. 14, e12817. https://doi.org/10.1111/conl.12817

Osman, E.O., Smith, D.J., Ziegler, M., Kürten, B., Conrad, C., El-Haddad, K.M., Voolstra, C.R., Suggett, D.J., 2018. Thermal refugia against coral bleaching throughout the northern Red Sea. Glob. Chang. Biol. 24, e474–e484. https://doi.org/10.1111/gcb.13895

Owen, D.P., Long, M.H., Fitt, W.K., Hopkinson, B.M., 2021. Taxon-specific primary production rates on coral reefs in the Florida Keys. Limnol. Oceanogr. 66, 625–638.

https://doi.org/10.1002/lno.11627

Padilla-Gamiño, J.L., Bidigare, R.R., Barshis, D.J., Alamaru, A., Hédouin, L., Hernández-Pech, X., Kandel, F., Leon Soon, S., Roth, M.S., Rodrigues, L.J., Grottoli, A.G., Portocarrero, C., Wagenhauser, S.A., Buttler, F., Gates, R.D., 2013. Are all eggs created equal? A case study from the Hawaiian reef-building coral Montipora capitata. Coral Reefs 32, 137–152. https://doi.org/10.1007/s00338-012-0957-1

Palumbi, Barshis, D., Traylor-Knowles, N., Bay, R., 2014. Mechanisms of reef coral resistance to future climate change. Science. 344, 895–898. https://doi.org/10.1126/science.1251336

Pandolfi, J.M., Bradbury, R.H., Sala, E., Hughes, T.P., Bjorndal, K.A., Cooke, R.G., McArdle, D., McClenachan, L., Newman, M.J.H., Paredes, G., Warner, R.R., Jackson, J.B.C., 2003. Global trajectories of the long-term decline of coral reef ecosystems. Science. 301, 955–958. https://doi.org/10.1126/science.1085706

Parkinson, J.E., Baker, A.C., Baums, I.B., Davies, S.W., Grottoli, A.G., Kitchen, S.A., Matz, M. V., Miller, M.W., Shantz, A.A., Kenkel, C.D., 2020. Molecular tools for coral reef restoration: Beyond biomarker discovery. Conserv. Lett. 13, e12687. https://doi.org/10.1111/conl.12687

Parkinson, J.E., Banaszak, A.T., Altman, N.S., LaJeunesse, T.C., Baums, I.B., 2015. Intraspecific diversity among partners drives functional variation in coral symbioses. Sci. Rep. 5, 15667. https://doi.org/10.1038/srep15667

Pawlik, J.R., Mcmurray, S.E., 2019. The Emerging Ecological and Biogeochemical Importance of Sponges on Coral Reefs. Ann. Rev. Mar. Sci. 12, 315–337. https://doi.org/10.1146/annurev-marine-010419-010807

Pecl, G.T., Araújo, M.B., Bell, J.D., Blanchard, J., Bonebrake, T.C., Chen, I.C., Clark, T.D., Colwell, R.K., Danielsen, F., Evengård, B., Falconi, L., Ferrier, S., Frusher, S., Garcia, R.A., Griffis, R.B., Hobday, A.J., Janion-Scheepers, C., Jarzyna, M.A., Jennings, S., Lenoir, J., Linnetved, H.I., Martin, V.Y., McCormack, P.C., McDonald, J., Mitchell, N.J., Mustonen, T., Pandolfi, J.M., Pettorelli, N., Popova, E., Robinson, S.A., Scheffers, B.R., Shaw, J.D., Sorte, C.J.B., Strugnell, J.M., Sunday, J.M., Tuanmu, M.N., Vergés, A., Villanueva, C., Wernberg, T., Wapstra, E., Williams, S.E., 2017. Biodiversity redistribution under climate change: Impacts on ecosystems and human well-being. Science. 355, eaai9214. https://doi.org/10.1126/science.aai9214

Pendleton, L.H., Hoegh-Guldberg, O., Langdon, C., Comte, A., 2016. Multiple stressors and ecological complexity require a new approach to coral reef research. Front. Mar. Sci. 3, 36. https://doi.org/10.3389/fmars.2016.00036

Peñuelas, J., Fernández-Martínez, M., Ciais, P., Jou, D., Piao, S., Obersteiner, M., Vicca, S., Janssens, I.A., Sardans, J., 2019. The bioelements, the elementome, and the biogeochemical niche. Ecology 100, e02652. https://doi.org/10.1002/ecy.2652

Perkins-Kirkpatrick, S.E., Stone, D.A., Mitchell, D.M., Rosier, S., King, A.D., Lo, Y.E., Pastor-Paz, J., Frame, D., Wehner, M., 2022. On the attribution of the impacts of extreme weather events to anthropogenic climate change. Environ. Res. Lett. 17, 024009. https://doi.org/10.1088/1748-9326/ac44c8

Perring, M.P., Erickson, T.E., Brancalion, P.H.S., 2018. Rocketing restoration: enabling the upscaling of ecological restoration in the Anthropocene. Restor. Ecol. 26, 1017–1023. https://doi.org/10.1111/rec.12871

Perry, C.T., Alvarez-Filip, L., Graham, N.A.J., Mumby, P.J., Wilson, S.K., Kench, P.S., Manzello, D.P., Morgan, K.M., Slangen, A.B.A., Thomson, D.P., Januchowski-Hartley,

F., Smithers, S.G., Steneck, R.S., Carlton, R., Edinger, E.N., Enochs, I.C., Estrada-Saldívar, N., Haywood, M.D.E., Kolodziej, G., Murphy, G.N., Pérez-Cervantes, E., Suchley, A., Valentino, L., Boenish, R., Wilson, M., MacDonald, C., 2018. Loss of coral reef growth capacity to track future increases in sea level. Nature 558, 396–400. https://doi.org/10.1038/s41586-018-0194-z

Perry, C.T., Edinger, E.N., Kench, P.S., Murphy, G.N., Smithers, S.G., Steneck, R.S., Mumby, P.J., 2012. Estimating rates of biologically driven coral reef framework production and erosion: A new census-based carbonate budget methodology and applications to the reefs of Bonaire. Coral Reefs 31, 853–868. https://doi.org/10.1007/s00338-012-0901-4

Perry, C.T., Hepburn, L.J., 2008. Syn-depositional alteration of coral reef framework through bioerosion, encrustation and cementation: Taphonomic signatures of reef accretion and reef depositional events. Earth-Science Rev. 86, 106–144. https://doi.org/10.1016/j.earscirev.2007.08.006

Perry, C.T., Morgan, K.M., 2017. Bleaching drives collapse in reef carbonate budgets and reef growth potential on southern Maldives reefs. Sci. Rep. 7, 40581. https://doi.org/10.1038/srep40581

Perry, C.T., Murphy, G.N., Kench, P.S., Smithers, S.G., Edinger, E.N., Steneck, R.S., Mumby, P.J., 2013. Caribbean-wide decline in carbonate production threatens coral reef growth. Nat. Commun. 4, 1402. https://doi.org/10.1038/ncomms2409

Peters, M.K., Hemp, A., Appelhans, T., Becker, J.N., Behler, C., Classen, A., Detsch, F., Ensslin, A., Ferger, S.W., Frederiksen, S.B., Gebert, F., Gerschlauer, F., Gütlein, A., Helbig-Bonitz, M., Hemp, C., Kindeketa, W.J., Kühnel, A., Mayr, A. V., Mwangomo, E., Ngereza, C., Njovu, H.K., Otte, I., Pabst, H., Renner, M., Röder, J., Rutten, G.,

Schellenberger Costa, D., Sierra-Cornejo, N., Vollstädt, M.G.R., Dulle, H.I., Eardley, C.D., Howell, K.M., Keller, A., Peters, R.S., Ssymank, A., Kakengi, V., Zhang, J., Bogner, C., Böhning-Gaese, K., Brandl, R., Hertel, D., Huwe, B., Kiese, R., Kleyer, M., Kuzyakov, Y., Nauss, T., Schleuning, M., Tschapka, M., Fischer, M., Steffan-Dewenter, I., 2019. Climate–land-use interactions shape tropical mountain biodiversity and ecosystem functions. Nature 568, 88–92. https://doi.org/10.1038/s41586-019-1048-z

Pettersson, R., Olsson, M., 1998. A nitric acid–hydrogen peroxide digestion method for trace element analysis of milligram amounts of plankton and periphyton by total-reflection X-ray fluorescence spectrometry. J. Anal. At. Spectrom. 13, 609–613. https://doi.org/10.1039/A708575C

Pomeroy, A.W.M., Ghisalberti, M., Peterson, M., Farooji, V.E., 2023. A framework to quantify flow through coral reefs of varying coral cover and morphology. PLoS One 18, e0279623. https://doi.org/10.1371/journal.pone.0279623

Pontes, L.D.S., Soussana, J.F., Louault, F., Andueza, D., Carrère, P., 2007. Leaf traits affect the above-ground productivity and quality of pasture grasses. Funct. Ecol. 21, 844–853. https://doi.org/10.1111/j.1365-2435.2007.01316.x

Powers, S.P., Peterson, C.H., Grabowski, J.H., Lenihan, H.S., 2009. Success of constructed oyster reefs in no-harvest sanctuaries: Implications for restoration. Mar. Ecol. Prog. Ser. 389, 159–170. https://doi.org/10.3354/meps08164

Pratchett, M.S., Heron, S.F., Mellin, C., Cumming, G.S., 2021. Recurrent Mass-Bleaching and the Potential for Ecosystem Collapse on Australia's Great Barrier Reef, in: Canadell, J.G., Jackson, R.B. (Eds.), Ecosystem Collapse and Climate Change. Ecological Studies, vol 241. Springer, Cham., pp. 265–289. https://doi.org/10.1007/978-3-030-71330-0_10

Pratchett, M.S., McCowan, D., Maynard, J.A., Heron, S.F., 2013. Changes in Bleaching Susceptibility among Corals Subject to Ocean Warming and Recurrent Bleaching in Moorea, French Polynesia. PLoS One 8, e70443. https://doi.org/10.1371/journal.pone.0070443

Ptacnik, R., Andersen, T., Tamminen, T., 2010. Performance of the Redfield Ratio and a Family of Nutrient Limitation Indicators as Thresholds for Phytoplankton N vs. P Limitation. Ecosystems 13, 1201–1214. https://doi.org/10.1007/s10021-010-9380-z

Pupier, C.A., Fine, M., Bednarz, V.N., Rottier, C., Grover, R., Ferrier-Pagès, C., 2019. Productivity and carbon fluxes depend on species and symbiont density in soft coral symbioses. Sci. Rep. 9, 17819. https://doi.org/10.1038/s41598-019-54209-8

Purcell, S., 1996. Quantifying organic content of material from coral reefs, in: The Great Barrier Reef, Science, Use and Management: A National Conference. James Cook University of North Queensland Townsville, Queensland, Australia, 25-29 November 1996, pp. 61–66.

Putchim, L., Thongtham, N., Hewett, A., Chansang, H., 2008. Survival and growth of Acropora spp . in mid-water nursery and after transplantation at Phi Phi Islands , Andaman Sea , Thailand, in: The 11th International Coral Reef Symposium. Ft. Lauderdale, Florida, 7-11 July 2008, pp. 1268–1261.

Quigley, K., Alvarez Roa, C., Raina, J.-B., Pernice, M., van Oppen, M.J.H., 2023. Heat-Evolved Microalgal Symbionts Increase Thermal Bleaching Tolerance of Coral Juveniles Without a Trade-Off Against Growth. Coral Reefs 42, 1227–1232. https://doi.org/10.1007/s00338-023-02426-z

Quigley, K.M., Alvarez Roa, C., Beltran, V.H., Leggat, B., Willis, B.L., 2021. Experimental evolution of the coral algal endosymbiont, Cladocopium goreaui: lessons learnt across a

decade of stress experiments to enhance coral heat tolerance. Restor. Ecol. 29, e13342. https://doi.org/10.1111/rec.13342

Quigley, K.M., Bay, L.K., van Oppen, M.J.H., 2020. Genome-wide SNP analysis reveals an increase in adaptive genetic variation through selective breeding of coral. Mol. Ecol. 29, 2176–2188. https://doi.org/10.1111/mec.15482

Rahav, O., Dubinsky, Z., Achituv, Y., Falkowski, P.G., 1989. Ammonium metabolism in the zooxanthellate coral, Stylophora pistillata. Proc. R. Soc. London B 236, 325–337. https://doi.org/10.1098/rspb.1989.0026

Randall, C.J., Negri, A.P., Quigley, K.M., Foster, T., Ricardo, G.F., Webster, N.S., Bay, L.K., Harrison, P.L., Babcock, R.C., Heyward, A.J., 2020. Sexual production of corals for reef restoration in the Anthropocene. Mar. Ecol. Prog. Ser. 635, 203–232. https://doi.org/10.3354/meps13206

Raymundo, L.J., Maypa, A.P., Gomez, E.D., Cadiz, P., 2007. Can dynamite-blasted reefs recover? A novel, low-tech approach to stimulating natural recovery in fish and coral populations. Mar. Pollut. Bull. 54, 1009–1019. https://doi.org/10.1016/j.marpolbul.2007.02.006

Razak, T.B., Boström-Einarsson, L., Alisa, C.A.G., Vida, R.T., Lamont, T.A.C., 2022. Coral reef restoration in Indonesia: A review of policies and projects. Mar. Policy 137, 104940. https://doi.org/10.1016/j.marpol.2021.104940

Reaka-Kudla, M.L., 2005. Biodiversity of Caribbean Coral Reefs, Caribbean Marine Biodiversity. Des Tech Publishers, Lancaster, PA.

Reaser, J.K., Pomerance, R., Thomas, P.O., 2000. Coral bleaching and global climate change: Scientific findings and policy recommendations. Conserv. Biol. 14, 1500–1511.

https://doi.org/10.1046/j.1523-1739.2000.99145.x

Redfield, A.C., 1934. On the proportions of organic derivatives in sea water and their relation to the composition of plankton. University Press of Liverpool.

Reef Restoration Foundation, 2020. Reef Restoration Foundation [WWW Document]. URL https://rrf.org.au/ (accessed 4.20.20).

Rees, S.A., Opdyke, B.N., Wilson, P.A., Henstock, T.J., 2007. Significance of Halimeda bioherms to the global carbonate budget based on a geological sediment budget for the Northern Great Barrier Reef, Australia. Coral Reefs 26, 177–188. https://doi.org/10.1007/s00338-006-0166-x

Riahi, K., van Vuuren, D.P., Kriegler, E., Edmonds, J., O'Neill, B.C., Fujimori, S., Bauer, N., Calvin, K., Dellink, R., Fricko, O., Lutz, W., Popp, A., Cuaresma, J.C., KC, S., Leimbach, M., Jiang, L., Kram, T., Rao, S., Emmerling, J., Ebi, K., Hasegawa, T., Havlik, P., Humpenöder, F., Da Silva, L.A., Smith, S., Stehfest, E., Bosetti, V., Eom, J., Gernaat, D., Masui, T., Rogelj, J., Strefler, J., Drouet, L., Krey, V., Luderer, G., Harmsen, M., Takahashi, K., Baumstark, L., Doelman, J.C., Kainuma, M., Klimont, Z., Marangoni, G., Lotze-Campen, H., Obersteiner, M., Tabeau, A., Tavoni, M., 2017. The Shared Socioeconomic Pathways and their energy, land use, and greenhouse gas emissions implications: An overview. Glob. Environ. Chang. 42, 153–168. https://doi.org/10.1016/j.gloenvcha.2016.05.009

Rice, M.M., Maher, R.L., Correa, A.M.S., Moeller, H. V., Lemoine, N.P., Shantz, A.A., Burkepile, D.E., Silbiger, N.J., 2020. Macroborer presence on corals increases with nutrient input and promotes parrotfish bioerosion. Coral Reefs 39, 409–418. https://doi.org/10.1007/s00338-020-01904-y

Richmond, R.H., 1997. Reproduction and Recruitment in Corals: Critical Links in the

Persistence of Reefs, in: (Birkeland, C. (Ed.), Life and Death of Coral Reefs. Chapman and Hall, New York, NY., pp. 175–197. https://doi.org/10.1007/978-1-4615-5995-5_8

Richmond, R.H., Tisthammer, K.H., Spies, N.P., 2018. The effects of anthropogenic stressors on reproduction and recruitment of corals and reef organisms. Front. Mar. Sci. 5, 226. https://doi.org/10.3389/fmars.2018.00226

Rinkevich, B., 2019. The active reef restoration toolbox is a vehicle for coral resilience and adaptation in a changing world. J. Mar. Sci. Eng. 7, 201. https://doi.org/10.3390/jmse7070201

Rinkevich, B., 2017. Rebutting the inclined analyses on the cost-effectiveness and feasibility of coral reef restoration. Ecol. Appl. 27, 1970–1973. https://doi.org/10.1002/eap.1559

Rinkevich, B., 2015. Climate Change and Active Reef Restoration—Ways of Constructing the "Reefs of Tomorrow." J. Mar. Sci. Eng. 3, 111–127. https://doi.org/10.3390/jmse3010111

Rinkevich, Baruch, 2015. Novel tradable instruments in the conservation of coral reefs, based on the coral gardening concept for reef restoration. J. Environ. Manage. 162, 199–205. https://doi.org/10.1016/j.jenvman.2015.07.028

Rinkevich, B., 2014. Rebuilding coral reefs: Does active reef restoration lead to sustainable reefs? Curr. Opin. Environ. Sustain. 7, 28–36. https://doi.org/10.1016/j.cosust.2013.11.018

Rinkevich, B., 2006. The Coral Gardening Concept and the Use of Underwater Nurseries: Lessons Learned from Silvics and Silviculture, in: Precht, W.F. (Ed.), Coral Reef Restoration Handbook. CRC Press, Boca Raton, FL, USA, pp. 291–301. https://doi.org/10.1201/9781420003796-21

Rinkevich, B., 2005. Conservation of coral reefs through active restoration measures: Recent approaches and last decade progress. Environ. Sci. Technol. 39, 4333–4342. https://doi.org/10.1021/es0482583

Rinkevich, B., 2000. Steps towards the evaluation of coral reef restoration by using small branch fragments. Mar. Biol. 136, 807–812. https://doi.org/10.1007/s002270000293

Rinkevich, B., 1995. Restoration strategies for coral reefs damaged by recreational activities: the use of sexual and asexual recruits. Restor. Ecol. 3, 241–251. https://doi.org/10.1111/j.1526-100X.1995.tb00091.x

Ritson-Williams, R., Gates, R.D., 2020. Coral community resilience to successive years of bleaching in Kāneʻohe Bay, Hawaiʻi. Coral Reefs 39, 757–769. https://doi.org/10.1007/s00338-020-01944-4

Rivera, H.E., Cohen, A.L., Thompson, J.R., Baums, I.B., Fox, M.D., Meyer-Kaiser, K.S., 2022. Palau's warmest reefs harbor thermally tolerant corals that thrive across different habitats. Commun. Biol. 5, 1394. https://doi.org/10.1038/s42003-022-04315-7

Rodrigues, L.J., Grottoli, A.G., 2007. Energy reserves and metabolism as indicators of coral recovery from bleaching. Limnol. Oceanogr. 52, 1874–1882. https://doi.org/10.4319/lo.2007.52.5.1874

Rodrigues, L.J., Padilla-Gamiño, J.L., 2022. Trophic provisioning and parental trade-offs lead to successful reproductive performance in corals after a bleaching event. Sci. Rep. 12, 18702. https://doi.org/10.1038/s41598-022-21998-4

Rogers, A., Blanchard, J.L., Mumby, P.J., 2018. Fisheries productivity under progressive coral reef degradation. J. Appl. Ecol. 55, 1041–1049. https://doi.org/10.1111/1365-2664.13051

Rogers, A., Blanchard, J.L., Mumby, P.J., 2014. Vulnerability of coral reef fisheries to a loss of structural complexity. Curr. Biol. 24, 1000–1005. https://doi.org/10.1016/j.cub.2014.03.026

Roper, C.D., Camp, E.F., Edmondson, J., Suggett, D.J., 2022. Combined impacts of natural recruitment and active propagation for coral population recovery on the Great Barrier Reef. Mar. Ecol. Prog. Ser. 700, 95–109. https://doi.org/10.3354/meps14184

Ruckelshaus, M.H., Jackson, S.T., Mooney, H.A., Jacobs, K.L., Kassam, K.A.S., Arroyo, M.T.K., Báldi, A., Bartuska, A.M., Boyd, J., Joppa, L.N., Kovács-Hostyánszki, A., Parsons, J.P., Scholes, R.J., Shogren, J.F., Ouyang, Z., 2020. The IPBES Global Assessment: Pathways to Action. Trends Ecol. Evol. 35, 407–414. https://doi.org/10.1016/j.tree.2020.01.009

Ruiz-Jaen, M.C., Aide, T.M., 2005. Restoration success: How is it being measured? Restor. Ecol. 13, 569–577. https://doi.org/10.1111/j.1526-100X.2005.00072.x

Santoso, P., Setiawan, F., Subhan, B., Arafat, D., Bengen, D.G., Iqbal Sani, L.M., Humphries, A.T., Madduppa, H., 2022. Influence of Coral Reef Rugosity on Fish Communities in Marine Reserves Around Lombok Island, Indonesia. Environ. Biol. Fishes 105, 105–117. https://doi.org/10.1007/s10641-021-01198-1

Scapin, L., Zucchetta, M., Facca, C., Sfriso, A., Franzoi, P., 2016. Using fish assemblage to identify success criteria for seagrass habitat restoration. Web Ecol. 16, 33–36. https://doi.org/10.5194/we-16-33-2016

Scheufen, T., Krämer, W.E., Iglesias-Prieto, R., Enríquez, S., 2017. Seasonal variation modulates coral sensibility to heat-stress and explains annual changes in coral productivity. Sci. Rep. 7, 4937. https://doi.org/10.1038/s41598-017-04927-8

Schleuning, M., Neuschulz, E.L., Albrecht, J., Bender, I.M.A., Bowler, D.E., Dehling, D.M., Fritz, S.A., Hof, C., Mueller, T., Nowak, L., Sorensen, M.C., Böhning-Gaese, K., Kissling, W.D., 2020. Trait-Based Assessments of Climate-Change Impacts on Interacting Species. Trends Ecol. Evol. 35, 319–328. https://doi.org/10.1016/j.tree.2019.12.010

Schoepf, V., Stat, M., Falter, J.L., McCulloch, M.T., 2015. Limits to the thermal tolerance of corals adapted to a highly fluctuating, naturally extreme temperature environment. Sci. Rep. 5, 17639. https://doi.org/10.1038/srep17639

Schopmeyer, S.A., Lirman, D., Bartels, E., Gilliam, D.S., Goergen, E.A., Griffin, S.P., Johnson, M.E., Lustic, C., Maxwell, K., Walter, C.S., 2017. Regional restoration benchmarks for Acropora cervicornis. Coral Reefs 36, 1047–1057. https://doi.org/10.1007/s00338-017-1596-3

Scoffin, T.P., 1992. Taphonomy of coral reefs: a review. Coral Reefs 11, 57–77. https://doi.org/10.1007/BF00357423

Scoffin, T.P., Stearn, C.W., Boucher, D., Frydl, P., Hawkins, C.M., Hunter, I.G., MacGeachy, J.K., 1980. Calcium Carbonate Budget of a Fringing Reef on the West Coast of Barbados. Part II—Erosion, Sediments and Internal Structure. Bull. Mar. Sci. 30, 475–508.

Seraphim, M.J., Sloman, K.A., Alexander, M.E., Janetski, N., Jompa, J., Ambo-Rappe, R., Snellgrove, D., Mars, F., Harborne, A.R., 2020. Interactions between coral restoration and fish assemblages: implications for reef management. J. Fish Biol. 97, 633–655. https://doi.org/10.1111/jfb.14440

Shafir, S., Rinkevich, B., 2010. Integrated long term mid-water coral nurseries: A management instrument evolving into a floating ecosystem. Univ. Mauritius Res. J. 16,

365–386.

Shafir, S., Rinkevich, B., 2008. The underwater silviculture approach for reef restoration: An emergent aquacultural theme, in: Schwartz, S.H. (Ed.), Aquaculture Research Trends. Nova Science Publishers, Inc., NewYork, NY, pp. 279–295.

Shafir, S., Van Rijn, J., Rinkevich, B., 2006. Steps in the construction of underwater coral nursery, an essential component in reef restoration acts. Mar. Biol. 149, 679–687. https://doi.org/10.1007/s00227-005-0236-6

Shaish, L., Levy, G., Gomez, E.D., Rinkevich, B., 2008. Fixed and suspended coral nurseries in the Philippines: Establishing the first step in the "gardening concept" of reef restoration. J. Exp. Mar. Bio. Ecol. 358, 86–97. https://doi.org/10.1016/j.jembe.2008.01.024

Shaish, L., Levy, G., Katzir, G., Rinkevich, B., 2010. Coral reef restoration (Bolinao, Philippines) in the face of frequent natural catastrophes. Restor. Ecol. 18, 285–299. https://doi.org/10.1111/j.1526-100X.2009.00647.x

Shapiro, S.S., Wilk, M.B., 1965. An analysis of variance test for normality. Biometrika 52, 591–611. https://doi.org/10.1093/biomet/52.3-4.591

Shaver, E.C., Burkepile, D.E., Silliman, B.R., 2018. Local management actions can increase coral resilience to thermally-induced bleaching. Nat. Ecol. Evol. 2, 1075–1079. https://doi.org/10.1038/s41559-018-0589-0

Shaver, E.C., Courtney, C.A., West, J.M., Maynard, J., Hein, M., Wagner, C., Philibotte, J., MacGowan, P., I, M., Boström-Einarsson, L., Bucchianeri, K., Johnston, L., Koss, J., 2020. A Manager's Guide for Coral Reef Restoration Planning and Design. NOAA Technical Memorandum CRCP. https://doi.org/10.25923/vht9-tv39

Shaver, E.C., McLeod, E., Hein, M.Y., Palumbi, S.R., Quigley, K., Vardi, T., Mumby, P.J., Smith, D., Montoya-Maya, P., Muller, E.M., Banaszak, A.T., McLeod, I.M., Wachenfeld, D., 2022. A roadmap to integrating resilience into the practice of coral reef restoration. Glob. Chang. Biol. 28, 4751–4764. https://doi.org/10.1111/gcb.16212

Shaver, E.C., Silliman, B.R., 2017. Time to cash in on positive interactions for coral restoration. PeerJ 5, e3499. https://doi.org/10.7717/peerj.3499

Shin, Y.J., Arneth, A., Chowdhury, R.R., Midgley, G.F., Alkemade, J.R.M., 2019. Plausible futures of nature, its contributions to people and their good quality of life, in: Brondízio, E.S., Settele, J., Diaz, S., Ngo, H.T. (Eds.), The Global Assessment Report on Biodiversity and Ecosystem Services. pp. 599–766. https://doi.org/10.5281/zenodo.3831673

Shlesinger, T., Loya, Y., 2019. Breakdown in spawning synchrony: A silent threat to coral persistence. Science. 365, 1002–1007. https://doi.org/10.1126/science.aax0110

Siebeck, U.E., Marshall, N.J., Klüter, A., Hoegh-Guldberg, O., 2006. Monitoring coral bleaching using a colour reference card. Coral Reefs 25, 453–460. https://doi.org/10.1007/s00338-006-0123-8

Silbiger, N.J., Nelson, C.E., Remple, K., Sevilla, J.K., Quinlan, Z.A., Putnam, H.M., Fox, M.D., Donahue, M.J., 2018. Nutrient pollution disrupts key ecosystem functions on coral reefs. Proc. R. Soc. B 285, 20172718. https://doi.org/10.1098/rspb.2017.2718

Sith, R., Watanabe, A., Nakamura, T., Yamamoto, T., Nadaoka, K., 2019. Assessment of water quality and evaluation of best management practices in a small agricultural watershed adjacent to Coral Reef area in Japan. Agric. Water Manag. 213, 659–673. https://doi.org/10.1016/j.agwat.2018.11.014

Smith, P.K., Krohn, R.I., Hermanson, G.T., Mallia, A.K., Gartner, F.H., Provenzano, M.D., Fujimoto, E.K., Goeke, N.M., Olson, B.J., Klenk, D.C., 1985. Measurement of protein using bicinchoninic acid. Anal. Biochem. 150, 76–85. https://doi.org/10.1016/0003-2697(85)90442-7

Smith, S. V., Key, G.S., 1975. Carbon dioxide and metabolism in marine environments. Limnol. Oceanogr. 3, 493–495. https://doi.org/10.4319/lo.1975.20.3.0493

Smith, S. V., Kinsey, D.W., 1976. Calcium carbonate production, coral reef growth, and sea level change. Science. 194, 937–939. https://doi.org/10.1126/science.194.4268.937

Soong, K., 1993. Colony size as a species character in massive reef corals. Coral Reefs 12, 77–83. https://doi.org/10.1007/BF00302106

Spalding, M., Burke, L., Wood, S.A., Ashpole, J., Hutchison, J., zu Ermgassen, P., 2017. Mapping the global value and distribution of coral reef tourism. Mar. Policy 82, 104–113. https://doi.org/10.1016/j.marpol.2017.05.014

Spencer Davies, P., 1989. Short-term growth measurements of corals using an accurate buoyant weighing technique. Mar. Biol. 101, 389–395. https://doi.org/10.1007/BF00428135

Staszak, L.A., Armitage, A.R., 2013. Evaluating salt marsh restoration success with an index of ecosystem integrity. J. Coast. Res. 29, 410–418. https://doi.org/10.2112/JCOASTRES-D-12-00075.1

Staudinger, M.D., Grimm, N.B., Staudt, A., Carter, S.L., Chapin III, F.S., Kareiva, P., Ruckelshaus, M., Stein, B.A., 2013. Impacts of Climate Change on Biodiversity, Ecosystems, and Ecosystem Services: Technical Input to the 2013 National Climate Assessment. Cooperative Report to the 2013 National Climate Assessment.

Stearn, C., Scoffin, T., Martindale, W., 1977. Calcium Carbonate Budget of a Fringing Reef on the West Coast of Barbados. Part I—Zonation and Productivity. Bull. Mar. Sci. 27, 479–510.

Stella, J.S., Wolfe, K., Roff, G., Rogers, A., Priest, M., Golbuu, Y., Mumby, P.J., 2022. Functional and phylogenetic responses of motile cryptofauna to habitat degradation. J. Anim. Ecol. 91, 2203–2219. https://doi.org/10.1111/1365-2656.13809

Steneck, R.S., Mumby, P.J., MacDonald, C., Rasher, D.B., Stoyle, G., 2018. Attenuating effects of ecosystem management on coral reefs. Sci. Adv. 4, eaao5493. https://doi.org/10.1126/sciadv.aao5493

Sterner, R.., Elser, J.., 2003. Ecological Stoichiometry: The Biology of Elements from Molecules to the Biosphere, Princeton University Press, Princeton, New Jersey, USA. Princeton: Princeton University Press. https://doi.org/10.1515/9781400885695

Stewart-Sinclair, P.J., Klein, C.J., Bateman, I.J., Lovelock, C.E., 2021. Spatial cost–benefit analysis of blue restoration and factors driving net benefits globally. Conserv. Biol. 35, 1850–1860. https://doi.org/10.1111/cobi.13742

Stimson, J., Kinzie, R.A., 1991. The temporal pattern and rate of release of zooxanthellae from the reef coral Pocillopora damicornis (Linnaeus) under nitrogen-enrichment and control conditions. J. Exp. Mar. Bio. Ecol. 153, 63–74. https://doi.org/10.1016/S0022-0981(05)80006-1

Storlazzi, C.D., Gingerich, S.B., Van Dongeren, A., Cheriton, O.M., Swarzenski, P.W., Quataert, E., Voss, C.I., Field, D.W., Annamalai, H., Piniak, G.A., McCall, R., 2018. Most atolls will be uninhabitable by the mid-21st century because of sea-level rise exacerbating wave-driven flooding. Sci. Adv. 4, eaap9741. https://doi.org/10.1126/sciadv.aap9741

Strahl, J., Stolz, I., Uthicke, S., Vogel, N., Noonan, S.H.C., Fabricius, K.E., 2015. Physiological and ecological performance differs in four coral taxa at a volcanic carbon dioxide seep. Comp. Biochem. Physiol. Part A Mol. Integr. Physiol. 184, 179–186. https://doi.org/10.1016/j.cbpa.2015.02.018

Strudwick, P., Seymour, J., Camp, E.F., Edmondson, J., Haydon, T., Howlett, L., Le Reun, N., Siboni, N., Suggett, D.J., 2022. Impacts of nursery-based propagation and out-planting on coral-associated bacterial communities. Coral Reefs 41, 95–112. https://doi.org/10.1007/s00338-021-02207-6

Stuart-Smith, R.D., Brown, C.J., Ceccarelli, D.M., Edgar, G.J., 2018. Ecosystem restructuring along the Great Barrier Reef following mass coral bleaching. Nature 560, 92–96. https://doi.org/10.1038/s41586-018-0359-9

Suding, K.N., 2011. Toward an Era of Restoration in Ecology: Successes, Failures, and Opportunities Ahead. Annu. Rev. Ecol. Evol. Syst. 42, 465–487. https://doi.org/10.1146/annurev-ecolsys-102710-145115

Suggett, D.J., Camp, E.F., Edmondson, J., Boström-Einarsson, L., Ramler, V., Lohr, K., Patterson, J.T., 2019. Optimizing return-on-effort for coral nursery and outplanting practices to aid restoration of the Great Barrier Reef. Restor. Ecol. 27, 683–693. https://doi.org/10.1111/rec.12916

Suggett, D.J., Edmondson, J., Howlett, L., Camp, E.F., 2020. Coralclip®: a low-cost solution for rapid and targeted out-planting of coral at scale. Restor. Ecol. 28, 289–296. https://doi.org/10.1111/rec.13070

Suggett, D.J., Goyen, S., Evenhuis, C., Szabó, M., Pettay, D.T., Warner, M.E., Ralph, P.J., 2015. Functional diversity of photobiological traits within the genus Symbiodinium appears to be governed by the interaction of cell size with cladal designation. New

Phytol. 208, 370–381. https://doi.org/10.1111/nph.13483

Suggett, D.J., Kikuchi, R.K.P., Oliveira, M.D.M., Spanó, S., Carvalho, R., Smith, D.J., 2012. Photobiology of corals from Brazil's near-shore marginal reefs of Abrolhos. Mar. Biol. 159, 1461–1473. https://doi.org/10.1007/s00227-012-1925-6

Suggett, D.J., Nitschke, M.R., Hughes, D.J., Bartels, N., Camp, E.F., Dilernia, N., Edmondson, J., Fitzgerald, S., Grima, A., Sage, A., Warner, M.E., 2022. Toward bio-optical phenotyping of reef-forming corals using Light-Induced Fluorescence Transient-Fast Repetition Rate fluorometry. Limnol. Oceanogr. Methods 20, 172–191. https://doi.org/10.1002/lom3.10479

Suggett, D.J., Smith, D.J., 2020. Coral bleaching patterns are the outcome of complex biological and environmental networking. Glob. Chang. Biol. 26, 68–79. https://doi.org/10.1111/gcb.14871

Suggett, D.J., Smith, D.J., 2011. Interpreting the sign of coral bleaching as friend vs. foe. Glob. Chang. Biol. 17, 45–55. https://doi.org/10.1111/j.1365-2486.2009.02155.x

Suggett, D.J., van Oppen, M.J.H., 2022. Horizon scan of rapidly advancing coral restoration approaches for 21st century reef management. Emerg. Top. Life Sci. 6, 125–136. https://doi.org/10.1042/ETLS20210240

Suggett, D.J., Warner, M.E., Leggat, W., 2017. Symbiotic dinoflagellate functional diversity mediates coral survival under ecological crisis. Trends Ecol. Evol. 32, 735–745. https://doi.org/10.1016/j.tree.2017.07.013

Sweatman, H., Delean, S., Syms, C., 2011. Assessing loss of coral cover on Australia's Great Barrier Reef over two decades, with implications for longer-term trends. Coral Reefs 30, 521–531. https://doi.org/10.1007/s00338-010-0715-1

Szmant-Froelieh, A., Pilson, M.E.Q., 1984. Effects of feeding frequency and symbiosis with zooxanthellae on nitrogen metabolism and respiration of the coral Astrangia danae. Mar. Biol. 81, 153–162. https://doi.org/10.1007/BF00393114

Szmant, A.M., Ferrer, L.M., FitzGerald, L.M., 1990. Nitrogen excretion and O:N ratios in reef corals: Evidence for conservation of nitrogen. Mar. Biol. 104, 119–127. https://doi.org/10.1007/BF01313165

Teh, L.S.L., Teh, L.C.L., Sumaila, U.R., 2013. A Global Estimate of the Number of Coral Reef Fishers. PLoS One 8, e65397. https://doi.org/10.1371/journal.pone.0065397

Thomas, L., Rose, N.H., Bay, R.A., López, E.H., Morikawa, M.K., Ruiz-Jones, L., Palumbi, S.R., 2018. Mechanisms of Thermal Tolerance in Reef-Building Corals across a Fine-Grained Environmental Mosaic: Lessons from Ofu, American Samoa. Front. Mar. Sci. 4, 434. https://doi.org/10.3389/fmars.2017.00434

Tiddy, I.C., Kaullysing, D., Bailey, D.M., Chumun, P.K., Killen, S.S., Le Vin, A., Bhagooli, R., 2021. Outplanting of branching Acropora enhances recolonization of a fish species and protects massive corals from predation. Coral Reefs 40, 1549–1561. https://doi.org/10.1007/s00338-021-02147-1

Tonk, L., Sampayo, E.M., Weeks, S., Magno-Canto, M., Hoegh-Guldberg, O., 2013. Host-Specific Interactions with Environmental Factors Shape the Distribution of Symbiodinium across the Great Barrier Reef. PLoS One 8, e68533. https://doi.org/10.1371/journal.pone.0068533

Topor, Z.M., Rasher, D.B., Duffy, J.E., Brandl, S.J., 2019. Marine protected areas enhance coral reef functioning by promoting fish biodiversity. Conserv. Lett. 12, e12638. https://doi.org/10.1111/conl.12638

Tortolero-Langarica, J.J.A., Rodríguez-Troncoso, A.P., Cupul-Magaña, A.L., Alarcón-Ortega, L.C., Santiago-Valentín, J.D., 2019. Accelerated recovery of calcium carbonate production in coral reefs using low-tech ecological restoration. Ecol. Eng. 128, 89–97. https://doi.org/10.1016/j.ecoleng.2019.01.002

Toth, L.T., Storlazzi, C.D., Kuffner, I.B., Quataert, E., Reyns, J., McCall, R., Stathakopoulos, A., Hillis-Starr, Z., Holloway, N.H., Ewen, K.A., Pollock, C.G., Code, T., Aronson, R.B., 2023. The potential for coral reef restoration to mitigate coastal flooding as sea levels rise. Nat. Commun. 14, 2313. https://doi.org/10.1038/s41467-023-37858-2

Trew, B.T., Maclean, I.M.D., 2021. Vulnerability of global biodiversity hotspots to climate change. Glob. Ecol. Biogeogr. 30, 768–783. https://doi.org/10.1111/geb.13272

Tribble, G.W., Sansone, F.J., Smith, S. V., 1990. Stoichiometric modeling of carbon diagenesis within a coral reef framework. Geochim. Cosmochim. Acta 54, 2439–2449. https://doi.org/10.1016/0016-7037(90)90231-9

Tribollet, A., Decherf, G., Hutchings, P.A., Peyrot-Clausade, M., 2002. Large-scale spatial variability in bioerosion of experimental coral substrates on the Great Barrier Reef (Australia): Importance of microborers. Coral Reefs 21, 424–432. https://doi.org/10.1007/s00338-002-0267-0

Tribollet, A., Golubic, S., 2005. Cross-shelf differences in the pattern and pace of bioerosion of experimental carbonate substrates exposed for 3 years on the northern Great Barrier Reef, Australia. Coral Reefs 24, 422–434. https://doi.org/10.1007/s00338-005-0003-7

Ulstrup, K.E., Berkelmans, R., Ralph, P.J., van Oppen, M.J.H., 2006. Variation in bleaching sensitivity of two coral species across a latitudinal gradient on the Great Barrier Reef: the role of zooxanthellae. Mar. Ecol. Prog. Ser. 314, 135–148. https://doi.org/10.3354/meps314135

UNEP-WCMC, 2006. In the front line: shoreline protection and other ecosystem services from mangroves and coral reefs. UNEP-WCMC Biodiversity Series 24, Cambridge, UK.

United Nations, 2020. Executive Summary: The UN Decade on Ecosystem Restoration.

van Oppen, M.J.H., Gates, R.D., Blackall, L.L., Cantin, N., Chakravarti, L.J., Chan, W.Y., Cormick, C., Crean, A., Damjanovic, K., Epstein, H., Harrison, P.L., Jones, T.A., Miller, M., Pears, R.J., Peplow, L.M., Raftos, D.A., Schaffelke, B., Stewart, K., Torda, G., Wachenfeld, D., Weeks, A.R., Putnam, H.M., 2017. Shifting paradigms in restoration of the world's coral reefs. Glob. Chang. Biol. 23, 3437–3448. https://doi.org/10.1111/gcb.13647

van Oppen, M.J.H., Oliver, J.K., Putnam, H.M., Gates, R.D., 2015. Building coral reef resilience through assisted evolution. Proc. Natl. Acad. Sci. 112, 2307–2313. https://doi.org/10.1073/pnas.1422301112

van Woesik, R., Banister, R.B., Bartels, E., Gilliam, D.S., Goergen, E.A., Lustic, C., Maxwell, K., Moura, A., Muller, E.M., Schopmeyer, S., Winters, R.S., Lirman, D., 2020. Differential survival of nursery-reared Acropora cervicornis outplants along the Florida reef tract. Restor. Ecol. 29, e13302. https://doi.org/10.1111/rec.13302

Vander Voort, G.F., 1999. Metallography, principles and practice. ASM International, Metals Park, OH. https://doi.org/10.31399/asm.tb.mpp.9781627082600

Vardi, T., Hoot, W.C., Levy, J., Shaver, E., Winters, R.S., Banaszak, A.T., Baums, I.B., Chamberland, V.F., Cook, N., Gulko, D., Hein, M.Y., Kaufman, L., Loewe, M., Lundgren, P., Lustic, C., Macgowan, P., Matz, M. V, Mcgonigle, M., Mcleod, I., Moore, J., Moore, T., Pivard, S., Pollock, F.J., Rinkevich, B., Suggett, D.J., Suleiman, S., Viehman, T.S., Villalobos, T., Weis, V.M., Wolke, C., Montoya-Maya, P.H., 2021. Six priorities to advance the science and practice of coral reef restoration worldwide. Restor.

Ecol. 29, e13498. https://doi.org/10.1111/rec.13498

Veal, C.J., Carmi, M., Fine, M., Hoegh-Guldberg, O., 2010. Increasing the accuracy of surface area estimation using single wax dipping of coral fragments. Coral Reefs 29, 893–897. https://doi.org/10.1007/s00338-010-0647-9

Venn, A.A., Quinn, J., Jones, R., Bodnar, A., 2009. P-glycoprotein (multi-xenobiotic resistance) and heat shock protein gene expression in the reef coral Montastraea franksi in response to environmental toxicants. Aquat. Toxicol. 93, 188–195. https://doi.org/10.1016/j.aquatox.2009.05.003

Viehman, T.S., Hench, J.L., Griffin, S.P., Malhotra, A., Egan, K., Halpin, P.N., 2018. Understanding differential patterns in coral reef recovery: chronic hydrodynamic disturbance as a limiting mechanism for coral colonization. Mar. Ecol. Prog. Ser. 605, 135–150. https://doi.org/10.3354/meps12714

Villanueva, R.D., Baria, M.V.B., dela Cruz, D.W., 2012. Growth and survivorship of juvenile corals outplanted to degraded reef areas in Bolinao-Anda Reef Complex, Philippines. Mar. Biol. Res. 8, 877–884. https://doi.org/10.1080/17451000.2012.682582

Vollmer, S. V., Palumbi, S.R., 2007. Restricted gene flow in the Caribbean staghorn coral Acropora cervicornis: Implications for the recovery of endangered reefs. J. Hered. 98, 40–50. https://doi.org/10.1093/jhered/esl057

Voolstra, C.R., Buitrago-López, C., Perna, G., Cárdenas, A., Hume, B.C.C., Rädecker, N., Barshis, D.J., 2020. Standardized short-term acute heat stress assays resolve historical differences in coral thermotolerance across microhabitat reef sites. Glob. Chang. Biol. 26, 4328–4343. https://doi.org/10.1111/gcb.15148

Voolstra, C.R., GIGA Community of Scientists (COS), Wörheide, G., Lopez, J. V., 2017.

Corrigendum to: Advancing genomics through the Global Invertebrate Genomics Alliance (GIGA). Invertebr. Syst. 31, 231. https://doi.org/10.1071/IS16059_CO

Voolstra, C.R., Suggett, D.J., Peixoto, R.S., Parkinson, J.E., Quigley, K.M., Silveira, C.B., Sweet, M., Muller, E.M., Barshis, D.J., Bourne, D.G., Aranda, M., 2021a. Extending the natural adaptive capacity of coral holobionts. Nat. Rev. Earth Environ. 2, 747–762. https://doi.org/10.1038/s43017-021-00214-3

Voolstra, C.R., Valenzuela, J.J., Turkarslan, S., Cárdenas, A., Hume, B.C.C., Perna, G., Buitrago-López, C., Rowe, K., Orellana, M. V., Baliga, N.S., Paranjape, S., Banc-Prandi, G., Bellworthy, J., Fine, M., Frias-Torres, S., Barshis, D.J., 2021b. Contrasting heat stress response patterns of coral holobionts across the Red Sea suggest distinct mechanisms of thermal tolerance. Mol. Ecol. 30, 4466–4480. https://doi.org/10.1111/mec.16064

Waltham, N.J., Elliott, M., Lee, S.Y., Lovelock, C., Duarte, C.M., Buelow, C., Simenstad, C., Nagelkerken, I., Claassens, L., Wen, C.K.C., Barletta, M., Connolly, R.M., Gillies, C., Mitsch, W.J., Ogburn, M.B., Purandare, J., Possingham, H., Sheaves, M., 2020. UN Decade on Ecosystem Restoration 2021-2030—What Chance for Success in Restoring Coastal Ecosystems? Front. Mar. Sci. 7, 71. https://doi.org/10.3389/fmars.2020.00071

Ward, S., Harrison, P., Hoegh-guldberg, O., 2000. Coral bleaching reduces reproduction of scleractinian corals and increases susceptibility to future stress, in: The 9th International Coral Reef Symposium. Bali, 23-27 October 2000, Vol. 2, pp. 1123–1128.

Ware, M., Garfield, E.N., Nedimyer, K., Levy, J., Kaufman, L., Precht, W., Scott Winters, R., Miller, S.L., 2020. Survivorship and growth in staghorn coral (Acropora cervicornis) outplanting projects in the Florida Keys National Marine Sanctuary. PLoS One 15, e0231817. https://doi.org/10.1371/journal.pone.0231817

Warne, D.J., Crossman, K.A., Jin, W., Mengersen, K., Osborne, K., Simpson, M.J., Thompson, A.A., Wu, P., Ortiz, J.-C., 2022. Identification of two-phase recovery for interpretation of coral reef monitoring data. J. Appl. Ecol. 59, 153–164. https://doi.org/10.1111/1365-2664.14039

Warner, M.E., Suggett, D.J., 2016. The Photobiology of Symbiodinium spp.: Linking Physiological Diversity to the Implications of Stress and Resilience, in: Goffredo, S., Dubinsky, Z. (Eds.), The Cnidaria, Past, Present and Future. Springer, Cham., pp. 489–509. https://doi.org/10.1007/978-3-319-31305-4_30

Webb, A.E., Enochs, I.C., van Hooidonk, R., van Westen, R.M., Besemer, N., Kolodziej, G., Viehman, T.S., Manzello, D.P., 2023. Restoration and coral adaptation delay, but do not prevent, climate-driven reef framework erosion of an inshore site in the Florida Keys. Sci. Rep. 13, 258. https://doi.org/10.1038/s41598-022-26930-4

Wegley, L., Edwards, R., Rodriguez-Brito, B., Liu, H., Rohwer, F., 2007. Metagenomic analysis of the microbial community associated with the coral Porites astreoides. Environ. Microbiol. 9, 2707–2719. https://doi.org/10.1111/j.1462-2920.2007.01383.x

Weiskopf, S.R., Rubenstein, M.A., Crozier, L.G., Gaichas, S., Griffis, R., Halofsky, J.E., Hyde, K.J.W., Morelli, T.L., Morisette, J.T., Muñoz, R.C., Pershing, A.J., Peterson, D.L., Poudel, R., Staudinger, M.D., Sutton-Grier, A.E., Thompson, L., Vose, J., Weltzin, J.F., Whyte, K.P., 2020. Climate change effects on biodiversity, ecosystems, ecosystem services, and natural resource management in the United States. Sci. Total Environ. 733, 137782. https://doi.org/10.1016/j.scitotenv.2020.137782

West, J.M., Salm, R. V., 2003. Resistance and Resilience to Coral Bleaching: Implications for Coral Reef Conservation and Management. Conserv. Biol. 17, 956–967. https://doi.org/10.1046/j.1523-1739.2003.02055.x

Westcott, D.A., Fletcher, C.S., Kroon, F.J., Babcock, R.C., Plagányi, E.E., Pratchett, M.S., Bonin, M.C., 2020. Relative efficacy of three approaches to mitigate Crown-of-Thorns Starfish outbreaks on Australia's Great Barrier Reef. Sci. Rep. 10, 12594. https://doi.org/10.1038/s41598-020-69466-1

Westoby, M., 1998. A leaf-height-seed (LHS) plant ecology strategy scheme. Plant Soil 199, 213–227. https://doi.org/10.1023/A:1004327224729

White, E.P., Ernest, S.K.M., Kerkhoff, A.J., Enquist, B.J., 2007. Relationships between body size and abundance in ecology. Trends Ecol. Evol. 22, 323–330. https://doi.org/10.1016/j.tree.2007.03.007

Wild, C., Huettel, M., Klueter, A., Kremb, S.G., Rasheed, M.Y.M., Jørgensen, B.B., 2004. Coral mucus functions as an energy carrier and particle trap in the reef ecosystem. Nature 428, 66–70. https://doi.org/10.1038/nature02344

Williams, G.J., Graham, N.A.J., 2019. Rethinking coral reef functional futures. Funct. Ecol. 33, 942–947. https://doi.org/10.1111/1365-2435.13374

Williams, S.L., Ambo-Rappe, R., Sur, C., Abbott, J.M., Limbong, S.R., 2017. Species richness accelerates marine ecosystem restoration in the Coral Triangle. Proc. Natl. Acad. Sci. 114, 11986–11991. https://doi.org/10.1073/pnas.1707962114

Williams, S.L., Sur, C., Janetski, N., Hollarsmith, J.A., Rapi, S., Barron, L., Heatwole, S.J., Yusuf, A.M., Yusuf, S., Jompa, J., Mars, F., 2019. Large-scale coral reef rehabilitation after blast fishing in Indonesia. Restor. Ecol. 27, 447–456. https://doi.org/10.1111/rec.12866

Wilson, S.K., Graham, N.A.J., Pratchett, M.S., Jones, G.P., Polunin, N.V.C., 2006. Multiple disturbances and the global degradation of coral reefs: are reef fishes at risk or resilient?

Glob. Chang. Biol. 12, 2220–2234. https://doi.org/10.1111/j.1365-2486.2006.01252.x

Winters, G., Holzman, R., Blekhman, A., Beer, S., Loya, Y., 2009. Photographic assessment of coral chlorophyll contents: Implications for ecophysiological studies and coral monitoring. J. Exp. Mar. Bio. Ecol. 380, 25–35. https://doi.org/10.1016/j.jembe.2009.09.004

Wolfe, K., Kenyon, T.M., Desbiens, A., de la Motte, K., Mumby, P.J., 2023. Hierarchical Drivers of Cryptic Biodiversity on Coral Reefs. Ecol. Monogr. 93, e1586. https://doi.org/10.1002/ecm.1586

Woodhead, A.J., Williams, G.J., Hicks, C.C., Norström, A. V., Graham, N.A.J.J., Williams, G.J., Graham, N.A.J.J., 2019. Coral reef ecosystem services in the Anthropocene. Funct. Ecol. 33, 1023–1034. https://doi.org/10.1111/1365-2435.13331

Woodward, G., Ebenman, B., Emmerson, M., Montoya, J.M., Olesen, J.M., Valido, A., Warren, P.H., 2005. Body size in ecological networks. Trends Ecol. Evol. 20, 402–409. https://doi.org/10.1016/j.tree.2005.04.005

Wooldridge, S.A., 2014. Formalising a mechanistic linkage between heterotrophic feeding and thermal bleaching resistance. Coral Reefs 33, 1131–1136. https://doi.org/10.1007/s00338-014-1193-7

Wright, I.J., Reich, P.B., Westoby, M., Ackerly, D.D., Baruch, Z., Bongers, F., Cavender-Bares, J., Chapin, T., Cornellssen, J.H.C., Diemer, M., Flexas, J., Garnier, E., Groom, P.K., Gulias, J., Hikosaka, K., Lamont, B.B., Lee, T., Lee, W., Lusk, C., Midgley, J.J., Navas, M.L., Niinemets, Ü., Oleksyn, J., Osada, H., Poorter, H., Pool, P., Prior, L., Pyankov, V.I., Roumet, C., Thomas, S.C., Tjoelker, M.G., Veneklaas, E.J., Villar, R., 2004. The worldwide leaf economics spectrum. Nature 428, 821–827. https://doi.org/10.1038/nature02403

Wright, R.M., Mera, H., Kenkel, C.D., Nayfa, M., Bay, L.K., Matz, M. V., 2019. Positive genetic associations among fitness traits support evolvability of a reef-building coral under multiple stressors. Glob. Chang. Biol. 25, 3294–3304. https://doi.org/10.1111/gcb.14764

www.coralnurtureprogram.org, n.d. Activity to date [WWW Document]. URL https://www.coralnurtureprogram.org/activity-to-date (accessed 2.25.24).

www.ipbes.net, n.d. Intergovernmental Platform on Biodiversity and Ecosystem Services (IPBES) [WWW Document]. URL https://www.ipbes.net/global-assessment (accessed 2.25.24).

www.un.org, n.d. Sustainable Development Goals [WWW Document]. URL https://www.un.org/sustainabledevelopment/sustainable-development-goals/ (accessed 2.25.24).

Xin, L.H., Adzis, K.A.A., Hyde, J., Cob, Z.C., 2016. Growth performance of Acropora formosa in natural reefs and coral nurseries for reef restoration. AACL Bioflux 9, 1090–1100.

Yanovski, R., Nelson, P.A., Abelson, A., 2017. Structural complexity in coral reefs: Examination of a novel evaluation tool on different spatial scales. Front. Ecol. Evol. 5, 27. https://doi.org/10.3389/fevo.2017.00027

Yates, K.K., Zawada, D.G., Smiley, N.A., Tiling-Range, G., 2017. Divergence of seafloor elevation and sea level rise in coral reef ecosystems. Biogeosciences 14, 1739–1772. https://doi.org/10.5194/bg-14-1739-2017

Young, C.N., Schopmeyer, S.A., Lirman, D., 2012. A Review of Reef Restoration and Coral Propagation Using the Threatened Genus Acropora in the Caribbean and Western

Atlantic. Bull. Mar. Sci. 88, 1075–1098. https://doi.org/10.5343/bms.2011.1143

Young, M.A.L., Bellwood, D.R., 2011. Diel patterns in sea urchin activity and predation on sea urchins on the Great Barrier Reef. Coral Reefs 30, 729–736. https://doi.org/10.1007/s00338-011-0754-2

Zakai, D., Levy, O., Chadwick-Furman, N.E., 2000. Experimental fragmentation reduces sexual reproductive output by the reef-building coral Pocillopora damicornis. Coral Reefs 19, 185–188. https://doi.org/10.1007/s003380000091

Zhao, Q., Bai, J., Huang, L., Gu, B., Lu, Q., Gao, Z., 2016. A review of methodologies and success indicators for coastal wetland restoration. Ecol. Indic. 60, 442–452. https://doi.org/10.1016/j.ecolind.2015.07.003